

Navid Saeidi

---

# Improving adsorption of perfluoroalkyl acids by tailoring surface chemistry of activated carbon and electric potentials

# **Improving adsorption of perfluoroalkyl acids by tailoring surface chemistry of activated carbon and electric potentials**

Von der Fakultät für Chemie und Mineralogie

der Universität Leipzig

genehmigte

D I S S E R T A T I O N

zur Erlangung des akademischen Grades

DOCTOR RERUM NATURALIUM

(Dr. rer. nat.)

vorgelegt

von M. Sc. (Chemieingenieur) Navid Saeidi

geboren am 02.04.1985 in Teheran (Iran)

Angenommen aufgrund der Gutachten von:

Prof. Frank-Dieter Kopinke  
Prof. Peter Grathwohl

Tag der Verleihung: 22.06.2021



The present study was accomplished in the period between December 2016 and December 2020 in the Helmholtz Centre for Environmental Research - UFZ in the Department of Environmental Engineering, under the supervision of Dr. Anett Georgi and Prof. Dr. Frank-Dieter Kopinke.



Bibliographic description

Navid Saeidi

## **Improving adsorption of perfluoroalkyl acids by tailoring surface chemistry of activated carbon and electric potentials**

Leipzig University, dissertation

174 pages, 57 figures, 21 tables and 241 references

### **Compendium / Kurzzreferat**

The subject of the present thesis is enhancing adsorption of perfluoroalkyl acids (PFAAs) from water on activated carbon (AC) and developing an approach for on-site regeneration of the AC saturated with the compounds. Adsorption of PFAAs on AC is the most common technology for remediation of water contaminated with these compounds. However, there are some drawbacks, e.g. largely differing adsorption performances of various ACs for PFAAs, very low adsorption affinity of short-chain PFAAs and lack of on-site techniques for regeneration of exhausted AC, which reduce the overall efficiency of this technique. In addition, adsorption of PFAAs must be considered as a relocation of the pollutants, not yet their final elimination. With the aim of mitigating the problems mentioned above, this thesis has focused on (i) understanding the effect of AC properties on adsorption of PFAAs, (ii) modifying AC with targeted functional groups for enhancing its affinity towards short- and long-chain PFAAs, (iii) a deeper insight into adsorption mechanism of PFAAs on AC and (iv) developing an electrochemical-based approach for controlling adsorption/desorption of PFAAs on AC. Adsorption of PFAAs was correlated with physical and surface chemical properties of well characterised activated carbon felts (ACFs). The surface chemical properties which were crucial for very high adsorption affinity of ACFs were identified. Targeted modifications were applied to develop the desired surface chemistry on ACF. The modified ACF exposes very high affinity and capacity for short- and long-chain PFAAs even in presence of competitive organic and inorganic ions and in a wide range of pH values. A deeper mechanistic study was performed by a direct comparison between adsorption behaviour of PFAAs with phenanthrene as a nonionic adsorbate and octanoic acid as F-free analogon of perfluorooctanoic acid (PFOA). External electrical potential was applied to control adsorption of PFAAs on various ACFs, enabling not only to improve adsorption of PFAAs but also to desorb

PFAAs from saturated ACFs. A long-term (around 1000 h) electrosorption/electrodesorption of PFOA with negligible loss of performance of the operational cell was obtained. On account of this, we consider the present study as a significant step forward toward enhancement of adsorption technologies in removal of PFAAs from water.

Die vorliegende Arbeit behandelt die Adsorption von Perfluoralkansäuren (PFAAs) an Aktivkohlen (AK). Die Adsorption der Stoffe durch AK ist die gebräuchlichste Technologie zur Entfernung dieser Stoffe aus kontaminiertem Wasser. Diese Technologie ist jedoch mit einer Reihe von Problemen behaftet, einschließlich stark variierender Adsorptionsleistungen von verschiedenen AK-Produkten für die Stoffklasse der PFAAs und fehlender On-site-Regenerierungsmethoden für erschöpfte AK, die insgesamt die Effizienz dieser Reinigungstechnologie verringern. Hinzu kommt, dass die adsorptive Entfernung der PFAAs aus dem Wasser zunächst nur eine Schadstoffverlagerung, noch keine finale Eliminierung darstellt. Mit dem Ziel, diese Probleme zu mildern und die Technologie weiterzuentwickeln, setzt diese Dissertation ihre Schwerpunkte auf (i) die Untersuchung des Einflusses von Oberflächeneigenschaften von AK auf die Adsorption der PFAAs, (ii) die Modifizierung von AK zur Verbesserung ihrer Affinität für kurz- und langkettige PFAAs, (iii) einen tieferen Einblick in den Mechanismus der Adsorption von PFAAs und (iv) die Entwicklung eines elektrochemischen Ansatzes zur Steuerung der Adsorption von PFAAs an AK. Die Adsorption von PFAAs wurde mit den physikalischen und chemischen Oberflächeneigenschaften der charakterisierten AK korreliert. Die chemischen Oberflächeneigenschaften, die entscheidend für eine außergewöhnlich starke Adsorption von PFAAs sind, wurden identifiziert und zur gezielten Modifizierung einer AK genutzt. Die modifizierte AK weist sehr hohe Adsorptionskapazitäten und -affinitäten für sowohl kurzkettige als auch langkettige PFAAs auf. Beide Eigenschaften wurden durch die Anwesenheit von konkurrierenden organischen und anorganischen Ionen nur wenig beeinflusst. Externes elektrisches Potenzial wurde schließlich verwendet, um die Adsorption und Desorption der PFAAs an bzw. von AK zu steuern. Es wurde ein Langzeit-Adsorptions-Desorptions-Versuch über ca. 1000 Betriebsstunden durchgeführt, ohne dass die Prozessleistung signifikant beeinträchtigt wurde.

## Contents

<b>1. Introduction</b> .....	9
<b>2. Theoretical part</b> .....	13
<b>2.1. Perfluoroalkyl acids</b> .....	13
<b>2.1.1. History, properties and regulations</b> .....	13
<b>2.1.2. Occurrence in water</b> .....	14
<b>2.1.3. Treatment technologies</b> .....	16
<b>2.2. Adsorption on activated carbon</b> .....	19
<b>2.4. Electrosorption on activated carbon</b> .....	24
<b>3. Practical part - Results and discussion</b> .....	29
<b>3.1. Understanding the effect of carbon surface chemistry on adsorption of perfluorinated alkyl substances</b> .....	33
<b>3.2. What is specific in adsorption of perfluoroalkyl acids on carbon materials</b> .....	69
<b>3.3. Controlling adsorption of perfluoroalkyl acids on activated carbon felt by means of electrical potentials</b> .....	111
<b>4. Summary</b> .....	143
<b>5. Conclusion and outlook</b> .....	153
<b>References</b> .....	159
<b>Acknowledgements</b> .....	169
<b>Curriculum vitae</b> .....	171
<b>List of publications</b> .....	173





## 1. Introduction

Emerging organic micropollutants (EOP) which are found in the mg/L or ng/L concentration range in natural water, soil and wastewater are considered to be potential threats to environmental ecosystems (Petrie et al., 2015). Plenty of research work and scientific efforts have been contributed to these substances in the past decade, with the aims of gaining more awareness from the public and asking for government actions to establish guidelines for better environmental protection. Three kinds of targets can be generally defined as EOP in scientific research, including (i) new compounds and molecules recently appeared that were not known before, (ii) existed contaminants with undiscovered environmental issues or emerging interests, (iii) new information on their environmental risks challenging our understanding of some legacy contaminants (Sauvé and Desrosiers, 2014).

Perfluoroalkyl acids (PFAAs) are a class of EOP that consist of a fully fluorinated hydrophobic alkyl chain attached to a hydrophilic end group (Arvaniti and Stasinakis, 2015). For over 50 years, the eight-carbon chain products, i.e. perfluorooctanoic acid (PFOA) and perfluorooctylsulfonic acid (PFOS), have been widely used in several industrial and household applications due to their unique physicochemical properties such as thermal stability (i.e., bond dissociation energy (BDE) in  $\text{C}_2\text{F}_5\text{--F} = 127 \text{ kcal/mol}$  vs.  $\text{BDE}_{\text{C}_2\text{H}_5\text{--H}} = 101 \text{ kcal/mol}$ , and  $\text{BDE}_{\text{CF}_3\text{--CF}_3} = 99 \text{ kcal/mol}$  vs.  $\text{BDE}_{\text{CH}_3\text{--CH}_3} = 89 \text{ kcal/mol}$ ) and oxidative resistance (i.e., standard reduction potential for  $\text{F} + \text{e}^- \rightarrow \text{F}^-$ ,  $E^0 = 3.6 \text{ V}$ ) (Vecitis et al., 2009). These properties make perfluorinated compounds highly resistant to biodegradation and - together with their partition properties - bioaccumulative. They are the focus of current attenuation because of their detection in various sources of water and a rapid increase in evidence for their adverse health effects including tumor induction, hepatotoxicity, developmental toxicity, immunotoxicity, endocrine disruption, and neurotoxicity (Hurley et al., 2016; Post et al., 2017; Phong Vo et al., 2020). PFOS (in 2009) and PFOA (in 2019) were added to Annex B of the Stockholm Convention on Persistent Organic Pollutants (Higgins and Field, 2017). Since June 2013, PFOA and its ammonium salt have been identified as chemicals of “very high concern” and added to the candidate list of European Chemicals Agency (ECHA) (Sznajder-Katarzyńska et al., 2019). Thereafter, shorter-chain perfluorocarboxylic (<C7) and perfluorosulfonic acids (<C6) are increasingly used by industry as alternatives or result as degradation products from alternative precursor compounds and thus are detected in the water cycle (Post et al., 2013; Higgins and Field, 2017). Nevertheless, also these compounds are

persistent, still bioaccumulative (though at a lesser extent), have a higher mobility in soil and their toxicity is less well understood (Lau, 2012; Scheringer et al., 2014). Therefore, the wide distribution, bioaccumulation, and toxicity of PFAAs make it important and urgent to develop treatment methods to remove PFAAs from various sources of water. Several studies showed that conventional wastewater treatment methods such as trickling filtration, activated sludge, anaerobic digestion and chlorination have a limited efficiency in removing PFAAs from aqueous waste streams (Boulanger et al., 2005; Vecitis et al., 2009; Phong Vo et al., 2020). Thus, these compounds are either accumulated in sludge or released to receiving waters via wastewater treatment plant effluents in Switzerland (Huset et al., 2008), Hong Kong (Ma and Shih, 2010), USA (Hu et al., 2016), Thailand (Kunacheva et al., 2011), China (Pan et al., 2011), Netherlands (Kwadijk et al., 2010), Denmark (Bossi et al., 2008), Spain (Campo et al., 2014), Japan (Shivakoti et al., 2010), Australia (Thompson et al., 2011b), Korea (Kim et al., 2012), Greece (Stasinakis et al., 2013), Canada (D'eon et al., 2009), Taiwan (Lin et al., 2010) and Germany (Ahrens et al., 2009).

Remediation of soil and groundwater with PFAAs contamination is extremely challenging (Arias Espana et al., 2015; Phong Vo et al., 2020). So far, there are no in-situ remediation technologies available. The most common treatment technology is pump-and-treat with subsequent treatment of the PFAAs contaminated water by adsorption onto activated carbon (AC) (Arias Espana et al., 2015; Deng et al., 2015; Phong Vo et al., 2020). There is a wide variability in adsorption performance among various AC products, i.e. maximum adsorption capacities calculated by Langmuir equation from 16 mg/g to 435 mg/g for adsorption of PFOA on commercial ACs while from 72 mg/g to 714 mg/g for PFOS (Ochoa-Herrera and Sierra-Alvarez, 2008; Qu et al., 2009; Yu et al., 2009; Punyapalakul et al., 2013; Zhang et al., 2016a; Söregård et al., 2020). Competitive sorption by dissolved natural organic matter (DNOM) has led to highly variable removal efficiencies of PFAAs (Kothawala et al., 2017; Gagliano et al., 2020) and early breakthrough of PFAAs in AC treatment systems (Rahman et al., 2014; Gagliano et al., 2020). In particular, the use of shorter-chain PFAAs replacement products has resulted in serious problems in water treatment (Rahman et al., 2014; Phong Vo et al., 2020). For instance, early breakthrough and/or almost no removal of perfluorobutanoic acid (PFBA) were observed in granular activated carbon (GAC) filtration systems (Eschauzier et al., 2012; Rahman et al., 2014; Phong Vo et al., 2020). A message from these studies is the need for a better understanding of structure-property correlations

for selection and targeted modification of ACs for PFAAs adsorption from water with various salt matrices and DNOM. Zhi and Liu (Zhi and Liu, 2015) have studied the effect of surface chemistry on adsorption affinity of PFOA and PFOS. Correlations between individual adsorbent properties and adsorption coefficients of PFOA and PFOS were, however, generally weak. Adsorption of PFAAs on a set of well characterised ACs is needed to study more precisely the adsorption mechanism of PFAAs on ACs. The hydrophobic effect and electrostatic interactions have been discussed as two main driving forces for adsorption of PFOA and PFOS on AC (Yu et al., 2009; Du et al., 2014; Zhi and Liu, 2015). On the other hand, other mechanisms which are involved in adsorption of ionizable organic compounds (IOCs), e.g. formation of charge-assisted hydrogen bonds, i.e. (+/-) or (-)CAHBs (Kah et al., 2017), respectively, should be considered. A better understanding of mechanism of adsorption of PFAAs on AC enables one to optimize AC with respect to high affinity towards PFAAs. In particular, modifying an AC with high affinity for short-chain PFAAs is of vital importance as these compounds have in general very low affinities for adsorption on ACs (Eschauzier et al., 2012; Rahman et al., 2014; Phong Vo et al., 2020). On top of it, understanding and prediction of sorption phenomena for organic compounds is of great general importance in environmental science and engineering. For non-ionic organic compounds polyparameter linear free energy relationships (PP-LFER) were successfully developed (Endo and Goss, 2014). However, there is still a lack of prediction tools for sorption of ionic compounds (Endo and Goss, 2014; Sigmund et al., 2020). Since PFAAs adsorption data were not considered yet even in the most recent models (Sigmund et al., 2020), a direct comparison between adsorption of PFAAs with adsorption of neutral and charged organic compounds on well characterised ACs can help broaden the training set for this type of predicting models.

On the other hand, regeneration of exhausted ACs with PFAAs is extremely challenging (Du et al., 2014). Frequent regeneration of exhausted adsorbents because of fast breakthrough of PFAAs has been recently addressed as one of the biggest challenge in remediation of water contaminated with that compound class (Gagliano et al., 2020). PFAAs-saturated adsorbents can be regenerated using hot water, solutions of sodium salts and alcohols (Gagliano et al., 2020). Hot water (80 °C) could regenerate AC saturated with PFOS by 50% (Deng et al., 2015). Due to the lower solubility of PFAAs in media with high ionic strength, ‘conventional’ solutions of sodium salts were ineffective (Conte et al., 2015; Deng et al., 2015). In some published works, it was tried to regenerate the adsorbent saturated with PFOA and PFOS by extraction with methanol and

ethanol. For instance, 87% recovery of AC fibers saturated with PFOS by means of pure ethanol (Chen et al., 2017) and 67% recovery of GAC exhausted with PFOA by means of pure methanol (Chularueangksorn et al., 2014) were reported. So far, on-site regeneration of AC adsorbers is not state of the art. Instead, PFAAs-loaded AC is incinerated or regeneration is done thermally ( $T > 800^{\circ}\text{C}$ ) in specialized plants with high-temperature post-treatment of exhaust gases (Schultz et al., 2003). This, however, requires long-distance transportation of tons of adsorbent material. Controlling adsorption of anionic PFAAs on AC by means of external electric potential is a promising approach for not only improving adsorption of PFAAs on AC but also for their desorption from saturated AC. This so called electrosorption method involves sorption of anionic PFAAs on positively charged AC surface and desorption of PFAAs from negatively charged AC surface by external potential. A detailed investigation on process parameters such as required potentials and optimal electrode materials is so far missing. Another issue for using the electrosorption is difficulty for prolongation of this process as AC properties are changed under both anodic and cathodic potentials.

Nevertheless, remediation of water contaminated with PFAAs is still problematic and finding efficient and effective solutions to mitigate the above mentioned problems is in hot debate. The aim of this thesis is (i) to investigate deeply the adsorption behaviour and mechanism of PFAAs on AC, (ii) to modify AC to an adsorbent with high affinity for short- and long-chain PFAAs and (iii) to develop an electrochemistry-based approach for a long term adsorption-desorption operation. The thesis is therefore tripartite with emphasis on:

1. Investigation of adsorption of PFAAs on well characterised ACs from water with various salt matrices and NOM to understand adsorption mechanism of these compounds on AC.
2. Modification of AC to produce one adsorbent with exceptionally high adsorption affinity to short- and long-chain PFAAs and addressing what is specific in adsorption behaviour of PFAAs on carbon materials.
3. Control of PFAAs adsorption on AC by means of external potential: development of an on-site approach to regenerate adsorbents exhausted with PFAAs.

## **2. Theoretical part**

### **2.1. Perfluoroalkyl acids**

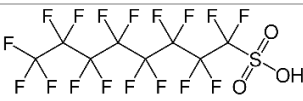

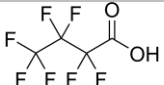
#### **2.1.1. History, properties and regulations**

“Fluorinated substances” is a general, nonspecific name that describes a universe of organic and inorganic substances that contain at least one F atom, with vastly different physical, chemical, and biological properties (Banks et al., 1994). Synonyms include “fluorochemicals” and “fluorinated chemicals”. A subset of fully fluorinated substances is fully fluorinated aliphatic substances that contain one or more C atoms on which all the H substituents (present in the nonfluorinated analogues) have been replaced by F atoms, in such a manner that they contain the perfluoroalkyl moiety  $C_nF_{2n+1}-$  (Buck et al., 2011). When the perfluoroalkyl chain is connected to an acidic group such as carboxyl or sulfonyl, these compounds are hereafter referred to “perfluoroalkyl acids” and denoted by the acronym PFAAs. PFAAs have been used extensively in a variety of products and industries due to their particular chemical characteristics and resistance to degradation (Lau, 2012). PFAAs are used for surface treatment of textiles because they repel both water and oil (Chen et al., 2009). Their use is widespread and routine for the formulation of Aqueous Film Forming Foams (AFFFs). AFFFs are commonly used for combating hydrocarbon fires because they act as low-viscosity vapour sealants to inhibit combustion of jet fuel (Kishi and Arai, 2008). Among the PFAAs, perfluorooctylsulfonic acid (PFOS) and perfluorooctanoic acid (PFOA), the eight-carbon chain products, have received the most attention in recent years due to their persistence, bioaccumulation and toxicity. PFOA, PFOS and short-chain PFAAs, e.g. perfluorobutanoic acid (PFBA), have been made by two major manufacturing methods, electrochemical fluorination (ECF) and telomerization (Buck et al., 2011; Lindstrom et al., 2011). Table 1 lists the structures and some important environmental properties of PFOA, PFOS and PFBA, which are target compounds in this thesis.

Substantial changes in the management model of PFAAs were launched in 2000, when 3M Company, the main large-scale manufacturer of PFOS, in agreement with the US Environmental Protection Agency (USEPA), started the voluntary phasing out of C8-based production and replacing PFOS with perfluorobutane sulphonate (PFBS, C4) and shorter chain PFAAs (Sznajder-Katarzyńska et al., 2019). The first government stewardship program, “2010/15 PFOA Stewardship Program”, involving a risk reduction strategy for manufacturers and downstream users of PFAAs was implemented in 2006 by USEPA in collaboration with eight dominant PFAAs producers: Arkema, Asahi, Ciba (now BASF), Clariant (now Archroma), Daikin, DuPont, 3M, and Solvay

Solexis (Sznajder-Katarzyńska et al., 2019). Thereafter, many different research programs implemented in the United States, Canada, Asia, Australia, and the European Union are focused on the distribution, toxicity, production hazards, processing, and use of PFAAs and are intended to minimize this risk. Despite their restricted use, and concerns about the effects of PFOS and PFOA on the environment and human health, they are still used by industries, especially those that manufacture semiconductors (ISMI, 2019).

Table 1. Structure and physico-chemical properties of PFOS, PFOA and PFBA.

Compound	Structure	MW (g/mol) <sup>a</sup>	Water solubility (g/L)	Vapor pressure at 25°C (Pa) <sup>d</sup>	Critical micelle concentration (g/L) <sup>f</sup>	pK <sub>a</sub>	Log K <sub>ow</sub>
PFOS		500.1	0.57 <sup>b</sup>	$3.31 \times 10^{-4}$ <sup>b</sup>	4.6	-3.27 <sup>g</sup>	5.25 <sup>j</sup>
PFOA		414.1	4.3 <sup>c</sup>	4.17 <sup>d</sup>	15.7	0-1 <sup>h</sup>	4.30 <sup>j</sup>
PFBA		214.1	high	131 <sup>e</sup>	-	0.7 <sup>i</sup>	2.43 <sup>a</sup>

<sup>a</sup> <http://www.chemspider.com/>, Log K<sub>ow</sub> of PFBA is a predicted value

<sup>b</sup> Potassium salt, (Stock et al., 2009)

<sup>c</sup> (Kaiser et al., 2006)

<sup>d</sup> Experimental value from (Bhatarai and Gramatica, 2011)

<sup>e</sup> Predicted value from (Bhatarai and Gramatica, 2011)

<sup>f</sup> In solution with sodium ion as the dominant counterion, (Kissa, 2001)

<sup>g</sup> (Brooke et al., 2004)

<sup>h</sup> Predicted values from (Goss, 2008; Cheng et al., 2009; Baggioli et al., 2018)

<sup>i</sup> Predicted value from (Goss, 2008)

<sup>j</sup> Predicted values for anionic molecules from (Arp et al., 2006)

### 2.1.2. Occurrence in water

Giesy and Kannan (2001) were among the first to report the widespread distribution of PFAAs, which are released in the environment during their industrial production and application, and also as a result of leaching from, and degradation of, consumer products (Giesy and Kannan, 2001). Eventually, PFAAs enter wastewater treatment plants (WWTPs) and as such WWTPs have been suggested as one of the major point sources of PFAAs to surface waters (Boulanger et al., 2005; Xiao et al., 2012) and the atmosphere (Ahrens et al., 2011). In addition, discharge of PFAAs contained in industrial waste or biosolids has been reported to contaminate surface and groundwater (Hölzer et al., 2008). Although about 40 different PFAAs have been detected in water

(Ahrens, 2011), most studies have targeted PFOS and PFOA since, in many cases where several PFAAs were monitored in water, PFOS and PFOA were detected more frequently and at the highest concentrations (Ahrens et al., 2010; Ahrens, 2011; Thompson et al., 2011a). PFBS and PFBA, two possible short-chain replacement compounds for PFOS and PFOA, respectively, were found to be the dominant PFAAs in recent studies (Ahrens et al., 2010; Brendel et al., 2018; Phong Vo et al., 2020). These two compounds have been detected in surface waters of some European countries including Germany (Shafique et al., 2017) and Spain (Lorenzo et al., 2016). Typical PFAAs concentrations in water range from pg/L to ng/L. However, higher concentrations ( $\mu\text{g/L}$  to even  $\text{mg/L}$ ) have been detected in surface and groundwater following firefighting activities or explosions (Rumsby et al., 2009), and in some waters adjacent to fluorochemical manufacturing facilities (Hoffman et al., 2011).

PFAAs, in particular PFOA and PFOS, have been also detected in treated drinking/tap water worldwide. Typical concentrations in drinking water in different countries are quite comparable ( $<50$  ng/L PFOS;  $<100$  ng/L PFOA) (Figure 1), except for the point source contamination scenarios in Germany, the United States, and the United Kingdom (Emmett et al., 2006; Exner and Färber, 2006; Arvaniti and Stasinakis, 2015). PFBA and PFBS have been detected in tap water in Germany (Gellrich et al., 2013), France (Schwanz et al., 2016) and Spain (Llorca et al., 2012).

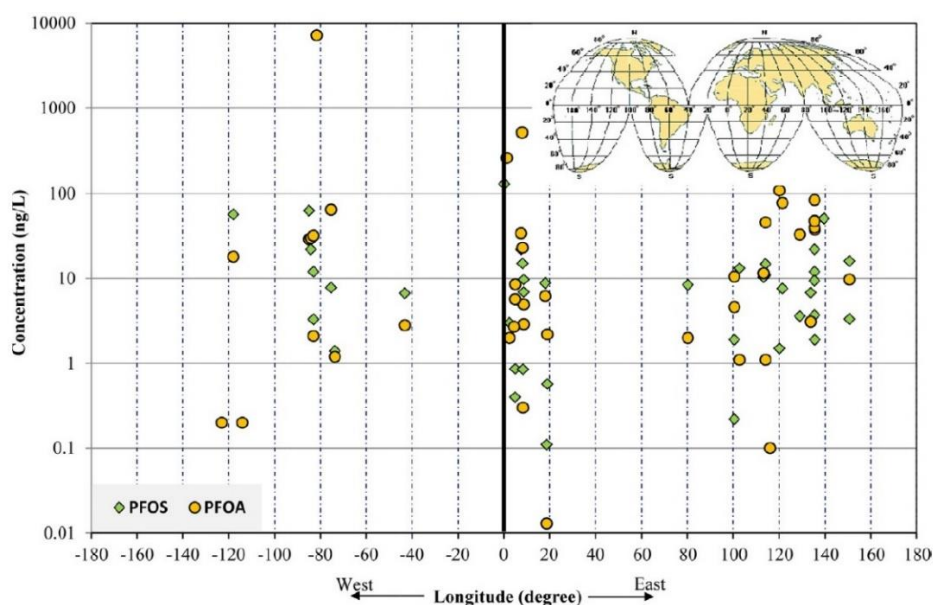


Figure 1. Reported global concentrations of PFOA and PFOS in drinking water (Rahman et al., 2014).



### 2.1.3. Treatment technologies

As mentioned earlier, remediation and treatment of PFAAs contaminated water are extremely challenging (Boulanger et al., 2005; Vecitis et al., 2009; Phong Vo et al., 2020). Conventional wastewater treatment techniques such as trickling filtration, activated sludge, anaerobic digestion and chlorination have been reported to have little effect on PFOA and PFOS mass flows (Schultz et al., 2006; Rahman et al., 2014). Microbial communities cannot metabolize PFOS and PFOA (Key et al., 1998; Hollingsworth et al., 2005). In some cases, PFOS and PFOA concentrations were greater in the WWTP effluent as compared to those in the influent (Schultz et al., 2006; Sinclair and Kannan, 2006). It suggests microbial transformation of fluorosulfonamides to PFOS (Boulanger et al., 2005), fluorotelomer alcohols to PFOA, or release of residual PFOA and PFOS from disposed products (Boulanger et al., 2005). Tertiary water treatment technologies such as adsorption (Du et al., 2014), ion-exchange (Lampert et al., 2007), and reverse osmosis (Tang et al., 2006) have been shown to be effective in removal of PFOA and PFOS from water. However, removal of short-chain PFAAs using such technologies is not that effective (Eschauzier et al., 2012; Rahman et al., 2014; Phong Vo et al., 2020). In all tertiary treatment cases, a subsequent destruction step such as incineration is required for complete perfluorochemicals elimination.

The most common remediation technology for water contaminated with PFOS and PFOA is based on their adsorption onto AC (Arias Espana et al., 2015; Deng et al., 2015; Phong Vo et al., 2020). However, there is a wide variability in adsorption performance among various AC products, i.e. adsorption capacities from 16 mg/g to 435 mg/g for adsorption of PFOA on commercial ACs while from 72 mg/g to 714 mg/g for PFOS (Ochoa-Herrera and Sierra-Alvarez, 2008; Qu et al., 2009; Yu et al., 2009; Punyapalakul et al., 2013; Zhang et al., 2016a; Söregård et al., 2020). Furthermore, some studies showed that presence of dissolved natural organic matter (DNOM) decreases considerably adsorption of PFAAs due to competition (Kothawala et al., 2017) then resulting in early breakthrough of PFAAs in AC treatment systems (Rahman et al., 2014). In particular, presence of shorter-chain PFAAs such as PFBA in water resulted in serious drawbacks for effective and efficient removal of these compounds from water (Eschauzier et al., 2012; Rahman et al., 2014). A very rapid breakthrough of PFOA was also reported in a pilot-scale adsorption plant at the 3M Cottage Grove Facility, USA, where GAC was used as an adsorbent (Minnesota Pollution Control Agency, 2009). In addition to ACs, other adsorbents have been applied for adsorption of PFAAs, e.g. mineral materials (Zhou et al., 2010; Punyapalakul et al.,

2013; Zhou et al., 2013), polyaniline nanotubes (Xu et al., 2015), carbon nanotubes (Li et al., 2011b), ionic fluorogels (Kumarasamy et al., 2020), resins (Carter and Farrell, 2010; Deng et al., 2010), biomaterials (Deng et al., 2013) and molecularly imprinted polymers (Karoyo and Wilson, 2013).

PFAAs resist oxidation due to the complete substitution of reactive C-H bonds by more stable C-F bonds. Fluorine will resist oxidation because it is the most electronegative element. It is also the most powerful inorganic oxidant known with a reduction potential of 3.6 V (Wardman, 1989) and therefore it is thermodynamically unfavourable when attempting to create fluorine atoms with any other one-electron oxidant. Most Advanced Oxidation Processes (AOPs) which frequently utilize the hydroxyl radical (Andreozzi et al., 1999) are not successful (Schröder and Meesters, 2005). In order to overcome these difficulties, a number of reagents have been used in order to adjust some degradation processes including: activated persulfate (Chen and Zhang, 2006), Fenton's agent (da Silva-Rackov et al., 2016; Santos et al., 2016), subcritical water (Hori et al., 2006), zero-valent metals (Lee et al., 2010), and/or combinations of at least two of the above (Tang et al., 2012). Degradation of PFOS and PFOA at the mg/L level has been ineffective for AOPs such as ozone, O<sub>3</sub>/UV, O<sub>3</sub>/H<sub>2</sub>O<sub>2</sub>, and Fenton's reagent (Schröder and Meesters, 2005). Reported kinetic data have suggested low reaction rates at relatively low temperatures, e.g. 40 °C, and activation at higher temperatures is required to accelerate the reaction (Hori et al., 2008). Chemical oxidation or UV irradiation require relatively high temperatures (70–90 °C) or energy-consuming irradiation to proceed successfully (Lee et al., 2012). Electrochemical oxidation was also applied to degrade PFOA and PFOS. The Ti/SnO<sub>2</sub>–Sb–Bi anode was adopted to degrade PFOA, where the decarboxylation of PFOA was supposed to be the first step of decomposition (Zhuo et al., 2011). The boron-doped diamond electrode (BDD) has the ability to degrade PFOS with trifluoroacetic acid as intermediate and S<sub>4</sub><sup>2-</sup> and F<sup>-</sup> as mineralization products (Carter and Farrell, 2008). In the same way, PFOA can be oxidized on BDD to F<sup>-</sup> and CO<sub>2</sub> (Zhuo et al., 2012). The step to large-scale application of these methods is however very expensive (Radjenovic and Sedlak, 2015). Moreover, due to the recalcitrance of PFAAs their electrochemical degradation is slow (Niu et al., 2016). Filtration by means of reverse osmosis (Tang et al., 2006) and nano-filtration (Steinle-Darling and Reinhard, 2008) have been demonstrated for removal of PFOA and PFOS. This kind of processes requires water pre-treatment, e.g. adsorption, in order to enhance efficiency (Baudequin et al., 2011). Nano-filtration and ultra-filtration are severely limited in total processing

capacity (Wang et al., 2015). Sonochemistry refers to the use of an acoustic field to generate chemical reactions in a solution. Sound waves are used to collapse any bubbles in the solution. As a result, high vapour temperatures are generated which causes pyrolysis and combustion of chemicals. This technique has been utilized for the decomposition of contaminants in aqueous media, including PFAAs, which decompose at the bubble/water interface due to pyrolysis (Moriwaki et al., 2005). Ultrasonic degradation was carried out in moderately dilute aqueous solutions ( $<1\ \mu\text{M}$ ) of perfluorochemicals including PFOS and PFOA, which are not representative of field concentrations. Extensive research is required before it can be applied in the field (Arias Espana et al., 2015). Combustion is the most common thermal treatment of waste. Incineration, a combustion based process, is one of the oldest chemical destruction techniques (Vecitis et al., 2009). Laboratory scale studies have shown PFOS and perfluorosulfonamides to be more than 99% mineralized at  $600\ ^\circ\text{C}$ . Gas-phase NMR studies have determined the more than 99% destruction temperature for various PFOA salts to be in the range of  $300\ ^\circ\text{C}$ – $350\ ^\circ\text{C}$  during a few hours residence time (Krusic et al., 2005). Incineration is most energy efficient for solid wastes, since all the heat will go into destroying the contaminant in question. Highly concentrated aqueous fluorochemical solutions and fluorochemicals adsorbed to a solid matrix could also be incinerated, however, energy will be wasted on destroying the matrix (Vecitis et al., 2009).

The costs of different remediation technologies for PFOS and PFOA contaminated materials vary significantly depending on several factors including the type of equipment used, the materials, inlet concentrations, flow rates and capacity and location of the treatment plant. Keller et al. (1999) (Keller et al., 1999) calculated the operating cost of a number of AOP techniques for water treatment for different reactor sizes, flow rates and inlet concentrations for methyl tert-butyl ether (MTBE) contaminated wastewater (Keller et al., 1999). These authors reported a cost ranges \$0.29 - \$5.78, \$0.67 - \$7.25, and \$0.62 - \$4.06 per 1000 gal (about  $4.5\ \text{m}^3$ ) of water treated for ozone alone, GAC + ozone, and UV/ $\text{H}_2\text{O}_2$  treatments, respectively. In general, electrooxidation on BDD electrodes is a very expensive process as the price of conductive diamond is currently in the range  $12,000$ – $18,000\ \text{€ m}^{-2}$  (Jia and Zhang, 2016). Filtration processes have high operational costs, which range between \$3.1 and \$3.32 per 1000 gal of water treated (Arias Espana et al., 2015). On the other hand, among the reviewed technologies the adsorption with AC has the lowest operating costs ranging between \$0.17 and \$0.59 per 1000 gal of water treated (Keller et al., 1999).

## 2.2. Adsorption on activated carbon

Activated carbon (AC) is the oldest kind of adsorbent in human history, from normal carbonized wood in the ancient Egyptian periods over 5700 years ago, until AC fibers used in the present days (Streat et al., 1995; Marsh and Rodríguez-Reinoso, 2006b). As it can efficiently remove a broad spectrum of substances, both organic and inorganic, from air, liquids, and solids (e.g., from soil) by adsorption, it has been used in various fields, such as chemical engineering, the environment, purification, food and beverage applications (Marsh and Rodríguez-Reinoso, 2006b, a).

AC can be produced from nearly all carbon-containing organic materials, mainly wood, sawdust, nutshells, fruit stones, peat, lignite, coal, petroleum coke, straw and automobile tires (Streat et al., 1995; Marsh and Rodríguez-Reinoso, 2006b). Furthermore, AC fibers and felts are commercially prepared from rayon, polyacrylonitrile (PAN), phenolic resins, petroleum and coal tar pitch. The use of a suitable precursor is mainly based on the following criteria: (i) low in inorganic matter; (ii) availability and cost; (iii) low degradation upon storage; and (iv) ease of activation (calcined coke is a difficult material while wood char is easily activated) (Marsh and Rodríguez-Reinoso, 2006b). The production of AC involves 2 steps, the carbonization process, at temperatures lower than 800 °C in the absence of oxygen, and the activation process, which plays an important role in the development of the surface area and pore volume of AC. The activation process can be divided into 2 different methods; physical activation, such as being activated by a heated stream of carbon dioxide or steam, and chemical activation, which uses chemicals, such as  $\text{ZnCl}_2$ ,  $\text{HNO}_3$ ,  $\text{NaOH}$ , and  $\text{KOH}$ , in the processing (Marsh and Rodríguez-Reinoso, 2006b). All this makes AC relatively cheap, environmentally friendly and available in mass quantities. Furthermore, it can be regenerated, which can reduce the cost of products (Marsh and Rodríguez-Reinoso, 2006b). One significant limitation of AC in water cleaning processes consists in its incompatibility with strong oxidants such that exhausted AC cannot be smoothly regenerated by chemical oxidation.

Adsorption arises as a result of the unsaturated and unbalanced molecular forces that are present on every solid surface. Thus, when a solid surface is brought into contact with a liquid or gas, there is an interaction between the fields of forces of the surface and that of the liquid or the gas. The solid surface tends to satisfy these residual forces by attracting and retaining on its surface the molecules, atoms, or ions of the gas or liquid. This results in a greater concentration of the gas or liquid in the near vicinity of the solid surface than in the bulk gas or vapor phase, despite the nature of the gas or vapor. The process by which this surface excess is caused is called adsorption (Bansal

and Goyal, 2005). Adsorption can be divided in two types: physical adsorption and chemisorption. In the case of physical adsorption, the adsorbate is bound to the surface by relatively weak van der Waals forces, which are similar to the molecular forces of cohesion and are involved in the condensation of vapors into liquids. Chemisorption, on the other hand, involves exchange or sharing of electrons between the adsorbate molecules and the surface of the adsorbent resulting in a chemical reaction. The bond formed between the adsorbate and the adsorbent is essentially a chemical bond and is thus much stronger than in the physisorption (Saha and Grappe, 2017). Adsorption of organic and inorganic compounds from water comprises several aspects, such as the effects of solution pH and ionic strength, isotherms, thermodynamics and kinetics, desorption and adsorbent regeneration. Some basic adsorption terms are summarized in Figure 2.

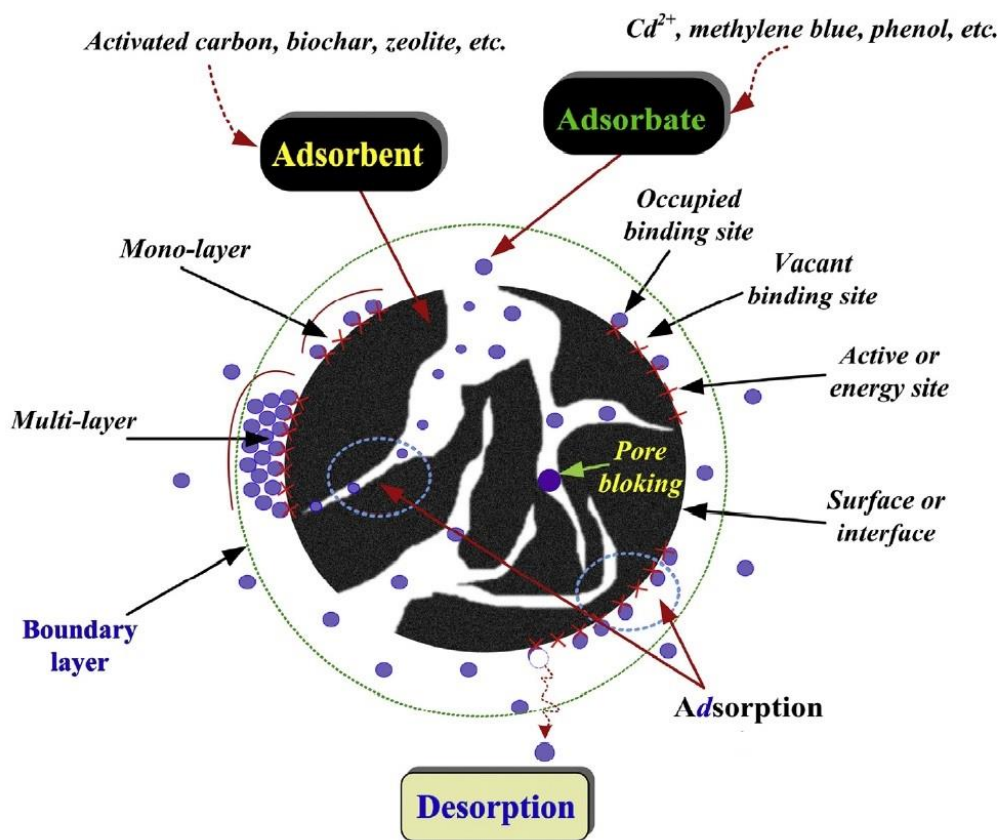


Figure 2. Some basic terms used in adsorption science and technology (Tran et al., 2017).

As mentioned earlier, adsorption of emerging organic pollutants from water on AC has been posed as a promising technique for removal of such compounds from water. Several extensive literature reviews have summarized the knowledge available on the sorption behaviour of AC (Hilber and

Bucheli, 2010) and other carbonaceous adsorbents (Koelmans et al., 2006). These studies mainly covered the sorption of noncharged compounds, which is now relatively well understood. A number of relationships have been established, including: (i) the positive correlations between sorption affinity and the sorbate's hydrophobicity (Koelmans et al., 2006), (ii) the dual-mode sorption behaviour (Cornelissen et al., 2005), and (iii) the  $\pi$ - $\pi$  electron donor-acceptor interactions (Pan and Xing, 2008). Until recently, little attention had been paid to the sorption of ionic or ionizable organic compounds (IOCs) including PFAAs, compared to that of neutral compounds (Kah et al., 2017).

The spectrum of interaction mechanisms for IOCs on carbonaceous adsorbents was discussed, including hydrophobicity (van der Waals interactions), H-bonds, electron donor-acceptor interactions, electrostatic interactions, ligand exchange, Lewis acid-base reactions, covalent bond formation and oxidative coupling as well as formation of charge-assisted hydrogen bonds, i.e. (+) or (-)CAHBs, respectively (Kah et al., 2017). In adsorption of PFAAs on AC, the hydrophobic effect and electrostatic interactions have been discussed as two main driving forces (Yu et al., 2009; Du et al., 2014; Zhi and Liu, 2015). According to the  $pK_a$  values of PFOS (-3.27 (Brooke D., 2004)) and PFOA (around 0 to 1 (Goss, 2008; Cheng et al., 2009; Baggioli et al., 2018)), under relevant pH conditions they fully dissociate in water. Thus, it is to be expected that electrostatic interactions between the anionic head group and charged surface groups of AC influence their adsorption process. Hydrophobicity also plays a role in adsorption of PFOA and PFOS (Yu et al., 2009; Du et al., 2014). Nevertheless, more study is required to understand better the adsorption behaviour of PFAAs on AC. For instance, Yu et al. (Yu et al., 2009) and Deng et al. (Deng et al., 2015) reported that decreasing solution pH from pH 7 to pH 3 has a stronger increasing effect on adsorption of PFOA than on that of PFOS on the same AC. It could be caused by formation of (-)CAHBs in adsorption of PFOA. (-)CAHBs can be formed between the carboxyl group of an adsorbate molecule and surface carboxyl or hydroxyl groups of the adsorbent when the two functional groups have similar  $pK_a$  values (Gilli and Gilli, 2000), as suggested for e.g. adsorption of benzoic acid (Li et al., 2013) and sulfamethazine (Teixidó et al., 2011) to AC. A range of  $\Delta pK_a = pK_{a, \text{proton donor group}} - pK_{a, \text{proton acceptor group}} < 5$  logarithmic units was considered as relevant for establishment of (-)CAHBs. PFOS with  $pK_a$  -3.27 does not meet the stated condition for formation of (-)CAHBs: its acidity is too strong. A literature review of the published studies shows that maximum loadings of PFOA on commercial AC products vary from 16 mg/g to 435 mg/g

while for PFOS they range from 72 mg/g to 714 mg/g. Furthermore, adsorption affinity of PFOA and PFOS can extremely differ among various AC products, i.e. by up to 4 orders of magnitude in sorption coefficients under the same experimental conditions (Ochoa-Herrera and Sierra-Alvarez, 2008; Qu et al., 2009; Yu et al., 2009; Punyapalakul et al., 2013; Zhang et al., 2016a; Söregård et al., 2020). Such a huge diversity in adsorption performance of various ACs to components of a substance class have been rarely observed. Zhi and Liu (Zhi and Liu, 2015) have studied the effect of surface chemistry on adsorption affinity of PFOA and PFOS. They concluded that adsorbent surface chemistry overwhelmed physical properties in controlling the extent of uptake. Correlations between individual carbon properties and adsorption coefficients of PFOA and PFOS were, however, generally weak. On the other hand, it has been reported that coexisting inorganic anions and cations have different effects on adsorption of PFOA and PFOS on various adsorbents (Du et al., 2014). DNOM as ubiquitous component of surface and groundwater needs to be considered as relevant competitor for PFAAs adsorption (Gagliano et al., 2020). Indeed, a reduction in PFAAs adsorption in the presence of moderate DNOM concentrations (1.5 to 8 mg/L) on AC was reported (Appleman et al., 2013) which was ascribed to occupation of pore space or sorption sites. Nevertheless, in a study the response was variable based on the type of DNOM and the PFAAs chain length (Kothawala et al., 2017). Adsorption of PFAAs on well characterised ACs from water with various salt matrices and containing DNOM can help for better understanding the adsorption behaviour and mechanism of PFAAs. On top of it, it can help for a proper selection of AC for an efficient adsorption of short- and long-chain PFAAs. A better understanding of adsorption behaviour and mechanism of PFAAs on AC addresses the most influencing characteristics of AC for high adsorption affinity to PFAAs. Thus, such characteristics can be developed on AC by targeted modifications. It is especially important for adsorption of short-chain PFAAs as these compounds have generally very low affinity for adsorption on AC (Eschauzier et al., 2012; Rahman et al., 2014). Previously, Zhi and Liu (Zhi and Liu, 2016) have tried to increase adsorption affinity of some ACs for PFOA and PFOS by removing oxygen-containing groups from AC under temperatures  $\geq 800$  °C. In fact, they wanted to develop basic sites on AC which may expose electrostatic attractions with PFAAs. However, as mentioned by Zhi and Liu (Zhi and Liu, 2016) this kind of treatment was not effective in producing long-term active sites. Thermal defunctionalisation leaves some unsaturated radicals at the edges of the basal planes, which are susceptible to re-oxidation even at room temperature in ambient atmosphere (Menéndez et al.,

1996). Therefore, the desired characteristics should be developed by means of appropriate modification techniques.

For non-ionic organic compounds polyparameter linear free energy relationships (PP-LFER) were successfully developed and applied for prediction of absorption and, with some limitations, even for adsorption equilibria (Endo and Goss, 2014). However, there is still a lack of prediction tools for sorption of ionic compounds (Endo and Goss, 2014; Sigmund et al., 2020). Sigmund et al. (2020) have very recently reported a model to predict Freundlich isotherm parameters for adsorption of ionizable compounds to carbonaceous adsorbents using a deep learning neural network approach (Sigmund et al., 2020). However, PFAAs were not included in their training data set and the required molecule parameters for this compound class are not available. A direct comparison between adsorption of PFAAs with adsorption of other ionic and nonionic organic compounds on well characterised ACs can address what is special in adsorption of PFAAs on AC. This also helps for understanding and prediction of sorption phenomena for organic compounds. Phenanthrene and octanoic acid are two good candidates for this comparison. Phenanthrene as a neutral molecule is a representative of the 3-ring polycyclic aromatic hydrocarbons (PAHs) with high hydrophobicity ( $\log K_{ow} = 4.57$  (Karickhoff, 1981)) and thus high adsorption affinity on AC (Walters and Luthy, 1984). Octanoic acid is the F-free structural analogue to PFOA. It has, however, a much weaker acid group ( $pK_a = 4.9$  (Wellen et al., 2017)).

Adsorption is a dynamic process, where solute continuously adsorbs onto and desorbs from AC. When the amount adsorbed equals the amount desorbed, the system is at equilibrium. This equilibrium depends on the solute concentration and water temperature. The amount solute adsorbed by the adsorbent can be calculated from the differences between the initial concentration of the solute in the solution and its final concentration in the aqueous supernatant after a certain time interval according to Eq. 1:

$$q_e = \frac{V(C_0 - C_e)}{m} \quad (1)$$

where  $q_e$  (mg/g) is the concentration of adsorbed solute at equilibrium,  $C_0$  and  $C_e$  (mg/L) are the initial and equilibrium concentrations of the solute respectively,  $V$  (L) is the volume of the solution and  $m$  (g) is the mass of adsorbent. The single point adsorption coefficient  $K_d$  (L/g) of the adsorbate on the adsorbent can be calculated by means of Eq. (2):



$$K_d = \frac{q_e}{C_e} \quad (2)$$

The Freundlich and Langmuir equations are often used to describe adsorption isotherms, i.e., the relation between aqueous solute concentration ( $C_e$ ) versus adsorbed solute quantity, or AC loading ( $q_e$ ), at equilibrium and at a specific temperature. In the Langmuir model, it is assumed that (i) the surface is homogeneous with respect to the energy of adsorption, (ii) there is no interaction between adsorbed species, (iii) adsorption sites are equally available to all species and (iv) the adsorbed layer is a monolayer (Langmuir, 1918). Eq. 3 is a linearized form of Langmuir equation:

$$\frac{C_e}{q_e} = \frac{C_e}{q_m} + \frac{1}{q_m K_L} \quad (3)$$

with  $C_e$  (mg/L) and  $q_e$  (mg/g) as defined above, and  $q_m$  (mg/g) as the maximum (monolayer) adsorption capacity of the adsorbent.  $K_L \times 1000$  (L/g) is a constant related to the affinity between the adsorbate and the adsorbent. For a good adsorbent, a high adsorption capacity  $q_m$  and a steep initial sorption isotherm slope (high  $K_L$ ) are desirable (Kratochvil and Volesky, 1998).

The Freundlich equation assumes heterogeneity of adsorption sites, and is considered as an empirical equation which can only be used up to moderate sorbent loadings, as the equation doesn't include a maximum adsorption capacity (Pikaar et al., 2006). Eq. 4 is a linearized form of Freundlich equation:

$$\log q_e = n \times \log C_e + \log K_F \quad (4)$$

where  $K_F$  ((mg/g)/(mg/L)<sup>n</sup>) is the Freundlich constant related to the affinity between adsorbent and adsorbate, and  $n$  (dimensionless) is the Freundlich exponent.

## 2.4. Electrosorption on activated carbon

In general, electrosorption is defined as a current or polarization potential-induced adsorption phenomenon on the surface of the charged electrodes (Han et al., 2006b). Specifically, when an external electrostatic field is imposed to the surface of the electrodes immersed in an aqueous

electrolyte solution, charged ions are forced to move towards the oppositely charged electrodes, allowing the occurrence of charge separation across the interface, resulting in the formation of strong electrical double layers (EDL) near the high conductivity and large surface areas (Oren, 2008) (Figure 3a). The charge on the electrode surface is compensated for ionic countercharges at the electrolyte side of the interface as well. This compensation can occur by adsorption of ions with opposite sign to the fixed charges on the electrode (Ban et al., 1998) and/or by an accumulation of counter ions in the outer Helmholtz plane and the diffuse (Gouy-Chapman) layer (Zou et al., 2008). The water dipoles then tend to align with the electrical field (Ban et al., 1998). Theoretically, at any interface between an electronic conductor (a solid electrode or an immiscible liquid phase) and electrolyte solution, there exist some regions where the two sides of the interface are carrying an excess of opposite electrical charges, while the whole interfacial system is electrically neutral, defined by the term of EDL (Figure 3b) (Foo and Hameed, 2009). To obtain a large ion adsorption capacity, it is important that a large surface area is created and thus typically materials such as ACs are used that have internal surface areas of the order of  $10^3$  m<sup>2</sup>/g (Biesheuvel et al., 2009). Often, the carbon pores are modeled as having a bimodal distribution of macropores and micropores. The solution within macropores is assumed to be net neutral, and macropores are dominantly responsible for transport of ions. Ions are assumed to be stored in the EDLs within (overlapping) micropores which dominate charge storage (Biesheuvel et al., 2014). Capacitive deionization (CDI) is a fastly expanding research field that utilizes these phenomena for the desalination of water. There is no doubt that salt removal of a CDI cell relies strongly on the physical and chemical properties of the carbon electrodes (Porada et al., 2013b). For example, Porada et al. comprehensively studied the physical structure of carbon electrodes and concluded that the salt adsorption capacity could be dramatically improved with an increase in the carbon electrode's microporosity (Porada et al., 2013a).

Very recently it has been reported that an important property of AC that enhances its performance in CDI applications is chemical surface charge functionalization (Gao et al., 2015; Gao et al., 2016). An important implication of surface charge is that the porous material can electrostatically adsorb salt ions from the solution within micropores, sustaining micropore electroneutrality by altering the pH. Notably, this adsorption can occur with no externally applied electric potential. This fixed charge changes the degree of charging of the EDLs and so fundamentally changes the relationship between charge efficiency and applied potential. For

example, applied electrical potentials of a sign opposite to the fixed charge first expels ions of charge opposite to the fixed charge before reaching the potential at which the net charge on the electrode is balanced, i.e. potential of zero charge ( $E_{PZC}$ ).

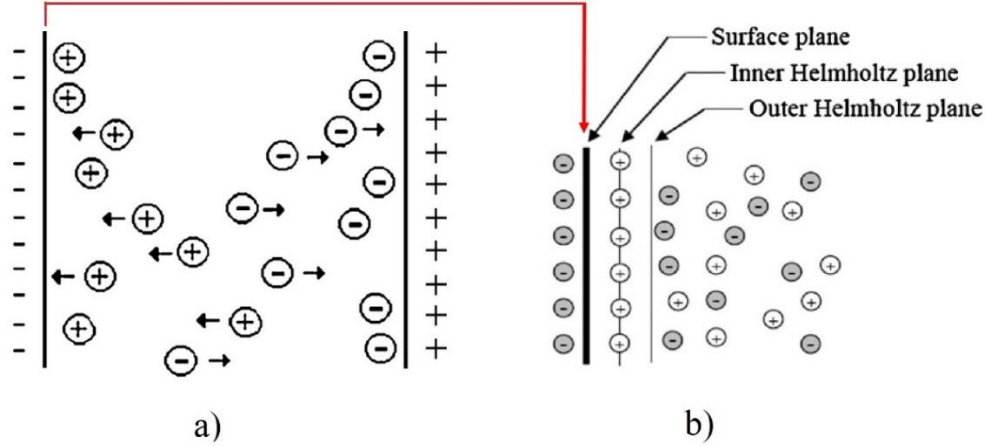


Figure 3. Electrosorption deionization operating principle (a) (Zou et al., 2008), the schematic diagram of the electrical double layer (b) (Foo and Hameed, 2009).

Only after crossing the  $E_{PZC}$ , can electric charges effectively accumulate net charge of the same sign as the fixed charge (Gao et al., 2015). Figure 4 shows a sketch of EDL inside a micropore in AC in a CDI cell.

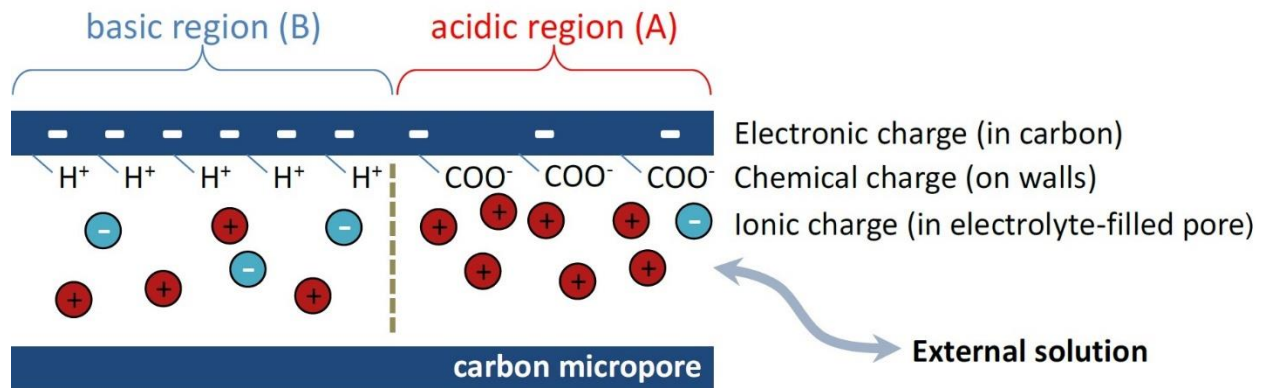


Figure 4. Sketch of EDL structure inside a micropore in AC in a CDI cell. On the scale of nanometers or less, regions influenced by adsorbed protons (basic, “B”) are distinguished from regions influenced by carboxylic groups (acid, “A”). The electronic charge in the carbon can differ between the two regions, as well as the ionic composition in the aqueous phase. Both types of regions are in equilibrium with the external solution outside the micropore (Biesheuvel, 2015).

In comparison to CDI, electrosorption of organic ions should include a superposition of electrostatic and non-electrostatic interactions. Some studies have investigated reversible electrosorption of organic ionizable molecules such as ionizable antibiotics (Wang et al., 2018), phenol (Han et al., 2006b), herbicide (Ania and Béguin, 2007), pyridine (Niu and Conway, 2002), aniline (Han et al., 2006a) and aromatic basic dyes (Bayram and Ayranci, 2010) on polarized porous electrodes from water. However, none of them has comprehensively studied the effect of AC properties on electrosorption of these compounds.

The electrosorption of PFOA and PFOS on electrodes composed of carbon nanotubes and graphene has been described in three previous publications (Li et al., 2011a; Wang et al., 2014; Niu et al., 2017). The factors influencing the process, e.g., the presence of competitive inorganic and organic ions, the surface chemistry of the adsorbent, cyclability of the process and more importantly regeneration of the adsorbent by converting potential, were not investigated in these studies even though such information would be useful for practical treatment of water by electrosorption. In addition, they used carbon nanotube and graphene as adsorbents, which limited production scales and recycling technology restrict their practical applications in water purification and wastewater treatment (Li et al., 2011a). On the other hand, mechanism behind the influence of potential on electrosorption of ionizable organic compounds on AC still is not clear. Fischer (Fischer, 2001) developed a model based on Gouy-Chapman model for predicting the electrosorption of organic compounds on AC versus potential. His model predicts a bell shape dependence of adsorption with applied potential. The maximum of the bell (maximum adsorption coefficient or loading) can shift to positive or negative potentials due to specific orientation adsorption or charges of the adsorbing pollutant molecule. However, he mentioned that the model didn't fit well with the few available experimental data from literature. The reason was that the data was of poor quality and usually only one potential branch was reported.

Regeneration of AC saturated with PFAAs is performed off-site with a thermal process under  $T > 800\text{ }^{\circ}\text{C}$  in specialized plants with post-treatment of exhaust gases (Schultz et al., 2003). This, however, requires long-distance transportation of tons of adsorbent material. Controlling adsorption of PFAAs on AC by means of external potential is a promising approach for on-site regeneration of AC exhausted with PFAAs. One of the problems for using carbon-based materials, in particular AC, as electrodes in electrosorption/electrodesorption of organic compounds and/or inorganic compounds is attrition of the electrodes by direct and/or indirect oxidation and reduction

under potential (Bayram and Ayranci, 2011; Tabti et al., 2014; Gineys et al., 2017). It is well-known that such changes in carbon electrode properties lead to performance degradation of CDI cells after a prolonged polarization time (Anderson et al., 2010; Villar et al., 2010; Wang et al., 2013; Biesheuvel et al., 2014). In recent years, it has been tried to improve the performance stability for long-term CDI operation (Cohen et al., 2013; Gao et al., 2015). As electrosorption of ionizable organic compounds is a younger research field than CDI, no studies are available on improvement of the performance of such a process for long times of polarization.

### 3. Practical part - Results and discussion

This thesis contributes to mitigate the above mentioned problems by understanding better adsorption mechanism of PFAAs on AC, modifying AC to have high affinity towards both short- and long-chain PFAAs and finally developing an electrochemical-based approach (electrosorption) for long-term adsorption-desorption of PFAAs. In this chapter, the results of the dissertation are presented and discussed as three scientific publications, which were published in the scientific journals stated below. The related Supporting Information (abbreviated as “SI” in the text) can be found after each section. The topics discussed in this chapter are the following:

1. Understanding the effect of carbon surface chemistry on adsorption of perfluorinated alkyl substances. The study was published in *Chemical Engineering Journal* (Saeidi et al., 2020a)
2. What is specific in adsorption of perfluoroalkyl acids on carbon materials? The study was published in *Chemosphere* (Saeidi et al., 2020b).
3. Controlling adsorption of perfluoroalkyl acids on activated carbon felt by means of electrical potentials. The study was published in *Chemical Engineering Journal* (Saeidi et al., 2021)

1. Very diverse adsorption affinities and capacities of PFAAs on various ACs have been reported (Ochoa-Herrera and Sierra-Alvarez, 2008; Qu et al., 2009; Yu et al., 2009; Punyapalakul et al., 2013; Zhang et al., 2016a; Söregård et al., 2020). It means that adsorption affinity and capacity of PFAAs on AC depend strongly on properties of AC. In addition, it has been reported that inorganic anions and cations as well as DNOM have different effects on adsorption of PFAAs on AC (Du et al., 2014; Gagliano et al., 2020). On account of this, section 3.1 investigates the adsorption behaviour of PFOA and PFOS on well characterised ACFs and in various water matrices. It was shown that the different extent of the PFAAs uptake is not controlled by textural properties of the applied ACFs. Instead, a good correlation between cation and anion exchange capacities (CEC and AEC, respectively) of the ACFs at pH 7, as well as their point of zero net proton charges (PZC) with adsorption capacities and affinities of PFOA and PFOS are demonstrated for the first time. More importantly, a deeper understanding of the adsorption behaviour of the PFAAs on AC is achieved by observing that maximum loadings of the PFAAs

are in all cases equal to or lower than the AEC of the ACFs. The superposition of hydrophobic interactions and electrostatic attractions between PFOA and PFOS anions and positively charged sites of ACF leads to exceptionally high adsorption affinity ( $K_d$  up to  $10^8$  L/kg). These findings for the first time clarify that C-centered positive charges which are created by proton adsorption to  $\pi$ -electron-rich regions on the basal plane of AC are more important than basic oxygen-containing groups for high adsorption affinity and capacity of AC to the PFAAs. Another achievement of this section is the finding that the effect of inorganic ions on the PFAAs adsorption at circumneutral pH depends on the surface chemistry of the AC. Furthermore, DNOM does not significantly affect the PFAAs adsorption most likely due to size exclusion exerted by the micropores of the ACFs. Finally, the study of adsorption behaviour of the PFAAs on well characterised ACFs addresses ideal AC adsorbents for removal of PFOA and PFOS: they should have low heteroatom content, leading to a low surface polarity and sufficient density of carbon-based positive charges at circumneutral pH. Please see chapter 4 for the detailed list of achievements.

2. Section 3.2 works on (i) addressing differences between adsorption behaviour of PFAAs and phenanthrene (as nonionic organic compound) as well as octanoic acid (as PFOA fluorine-free analogon) and (ii) developing targeted modification of ACF for increasing its affinity towards short- and long-chain PFAAs. For this purpose, the commercial ACF (CACF) with the lowest affinity and capacity toward PFOA and PFOS from section 3.1 (Saeidi et al., 2020a) was selected for further modifications. For the first time, amino-functionalisation of AC, without any pretreatment but using directly its native content of carboxylic groups for amidation was used to create basic amine groups on CACF. Thermal treatment under pure hydrogen was applied to create stable  $\pi$ -electron-rich basic sites on CACF. The CACF, defunctionalised (DeCACF) and amino-functionalised (CACFNH<sub>2</sub>) ACFs were applied for adsorption of PFOA, PFOS, PFBA, phenanthrene and octanoic acid from water containing various salt matrices and DNOM. The first achievement of this section is the enhancement of adsorption affinity based on single point adsorption coefficient ( $K_d$ ) of the CACF for PFOA, PFOS and PFBA up to 3 orders of magnitude by the defunctionalisation approach. Such a substantial enhancement in adsorption affinity as observed here for the defunctionalised carbon, has been rarely reported before. In contrast, amidation of CACF showed a minor improvement in adsorption of the target compounds only. Sensitivity of PFAAs adsorption to competition by DNOM depends on modification type and was

negligible in case of DeCACF. DeCACF keeps its high affinity towards PFOA ( $K_d$  up to  $10^7$  L/kg) and PFBA ( $K_d$  up to  $10^5$  L/kg) within 5 adsorption cycles with intermittent extractive regeneration. It proves that the preparation of an AC with very stable basic sites was successful. The comparison between adsorption affinities of PFOA, octanoic acid and phenanthrene on the ACFs reveals that the two acids are much more affected by surface chemistry than phenanthrene, whereby PFOA reacts with the highest sensitivity. Electrostatic interactions and charge compensation provided by positively charged surface sites (quantified by their anion exchange capacity) are obviously more crucial for PFAAs than for common organic acids (such as the tested octanoic acid). A possible reason is their exceptionally strong acidity with  $pK_a < 1$ . In particular, the results of this section contribute to a targeted design of optimized carbon-based adsorbents for efficient removal of PFAAs from water. In addition, this section helps for understanding and prediction of sorption phenomena for organic compounds. Please refer to chapter 4 for the detailed list of achievements.

3. So far, on-site regeneration of AC adsorbers is not state of the art (Gagliano et al., 2020). Controlling adsorption of PFAAs on AC by means of external potential (electrosorption) can be applied for not only increasing adsorption of PFAAs but also for desorption of PFAAs from saturated AC. Previously, three published studies have tried to enhance adsorption of PFOA and PFOS on electrodes made of carbon nanotube (Li et al., 2011a; Wang et al., 2014) and a composition of graphene/carbon nanotube (Niu et al., 2017). However, these works haven't studied precisely the factors influencing the process. In addition, they haven't considered possibility of regenerating the electrodes by external potential after loading with the compounds. Section 3.3 is aimed at a proof-of-principle of electrosorption of PFOA and PFBA by investigating the effects of applied direct electrical potentials on their sorption behaviour on activated carbon felt (ACF) in water containing DNOM and various salt matrices. This section reveals that the electrosorption of PFOA and PFBA was influenced by the state of fixed net charge on the ACFs (studied by potential of zero charge ( $E_{PZC}$ ) of the ACFs) as well as applied potential. Thus, electrosorption of PFOA and PFBA on the ACFs (based on  $K_d$  values at environmentally relevant concentrations of the compounds) at various potentials resulted in bell-shape curves with peaks (maximum electrosorption) at potentials higher than  $E_{PZC}$  of the ACFs. These results indicate that before selecting a carbon electrode for electrosorption of such organic compounds, its surface chemistry and  $E_{PZC}$  should be taken into account.  $K_d$  value in electrosorption of environmentally relevant concentrations of PFOA at peak potential and that at negative potentials are 650,000 L/kg



versus 14,800 L/kg, respectively, i.e. a difference around 44 times. This difference is a factor of about 100 in case of PFBA. Based on electroadsorption and electrodesorption isotherms of PFOA, a first estimation of the concentration factor that is achievable in a fixed-bed electroadsorption/electrodesorption unit is 130. This concentration factor is much higher than that reported in reverse osmosis processes of PFAAs compounds, which is 6.7 (Appleman et al., 2014). Information on  $E_{PZC}$  of carbon electrodes is also useful for protecting carbon electrodes against possible attritions caused by applying harsh potentials. ElectroadSORPTION of PFOA at +500 mV and electrodesorption of it at -1000 mV showed a significant decline in electrosorption of PFOA over 5 electroadsorption and electrodesorption cycles. Selection of milder potentials based on  $E_{PZC}$  of the ACF used as adsorbent (electrodesorption at -100 mV <  $E_{PZC}$  = +75mV < electroadsorption at +300 mV) resulted in electroadsorption and electrodesorption of PFOA with almost stable performance over 10 cycles (1000 h). A quiet stable performance in the cell over 10 cycles was obtained while adsorption was performed without potential and electrodesorption was carried out at -100 mV.

The presence of coexisting inorganic ions and DNOM as well as changing pH of solution have negligible effects on performance of electroadsorption and electrodesorption of PFAAs. Accordingly, this process can be applied for remediation of various sources of water contaminated with PFAAs. Chapter 4 shows the corresponding achievement list.

### 3.1. Understanding the effect of carbon surface chemistry on adsorption of perfluorinated alkyl substances

Navid Saeidi, Frank-Dieter Kopinke, Anett Georgi \*

*Helmholtz Centre for Environmental Research – UFZ, Department of Environmental Engineering,  
D-04318 Leipzig, Germany*

#### **Abstract**

The adsorption of perfluorooctanoic acid (PFOA) and perfluorooctylsulfonic acid (PFOS) on various activated carbon felts (ACFs) was studied and related to their surface characteristics. The adsorption isotherms of the ACFs studied differ widely in terms of adsorption affinities as well as maximum loadings. Cation and anion exchange capacities (CEC and AEC) at pH 7, as well as point of zero net proton charge (PZC), were identified as good indicators for understanding of each adsorbent's behavior towards the perfluorinated alkyl substances (PFAS) in their anionic state. Maximum loadings of the two PFAS are in all cases equal to or lower than the AEC of the ACFs. The superposition of hydrophobic interactions and electrostatic attraction between PFAS anions and positively charged sites of ACF leads to exceptionally high adsorption affinity ( $K_d$  up to  $10^8$  L/kg). In this respect, positive charges created by proton adsorption to  $\pi$ -electron-rich regions on the basal plane of carbon are more important than basic oxygen-containing groups. The effect of inorganic ions on adsorption of PFAS is variable and is also influenced by the surface chemistry of the ACFs. Dissolved natural organic matter did not significantly affect PFAS adsorption most likely due to size exclusion exerted by the micropores of the ACFs.

#### **Keywords:**

PFOA; PFOS; Activated Carbon Felts; Anion Exchange Capacity; Surface Chemistry.

---

\* Corresponding author e-mail: anett.georgi@ufz.de

<b>Nomenclature</b>			
AC	activated carbon	$q_e$	equilibrium concentration of adsorbed solute on adsorbent
ACF	activated carbon felt	$q_m$	Langmuir maximum
AEC	anion exchange capacity		adsorption capacity of adsorbent
$C_0$	initial concentration of solute in solution	SRNOM	Suwannee River natural organic matter
(-)CAHB	negative charge-assisted hydrogen bonds	TPD	temperature-programmed desorption
CEC	cation exchange capacity	$V$	volume of solution
$C_e$	equilibrium concentration of solute in solution		
EDL	electrical double layer		
EfOM	effluent organic matter		
IOC	ionizable organic compounds		
IS	ionic strength		
$K_F$	Freundlich coefficient		
$K_L$	Langmuir coefficient		
$K_d$	single point adsorption coefficient		
$m$	mass of activated carbon felt		
$n$	Freundlich exponent constant		
NOM	natural organic matter		
PFAS	perfluorinated alkyl substances		
PFOA	perfluorooctanoic acid		
PFOS	perfluorooctylsulfonic acid		
PZC	point of zero net proton charge		

## 1. Introduction

Perfluorinated alkyl substances (PFAS) are characterized by a fully fluorinated carbon backbone. This renders these compounds highly resistant to both chemical and biological degradation (Fujii et al., 2007; Schuricht et al., 2017). The eight-carbon chain compounds PFOA and PFOS were two of the most widely used PFAS in the last 60 years which nowadays are frequently detected in wastewater, surface water, groundwater and even tap water throughout the world (Fujii et al., 2007; Arvaniti and Stasinakis, 2015). Regarding toxicity of PFAS for humans, medical research has associated PFAS with adverse effects on growth, as well as implications in birth weight, fertility disorders, phenomena of early menopause in women, carcinogenesis and thyroid malfunction (Rahman et al., 2014). Therefore, it is necessary to work on efficient techniques for removal of PFAS from water.

Adsorption on activated carbon (AC) is the most widely applied technique for removal of PFOA and PFOS from water (Deng et al., 2015; Chen et al., 2017). However, there are strong differences in performance among various AC types. A review of the available literature reveals that reported

maximum loadings of PFOA on commercial AC products vary from 16 mg/g to 435 mg/g while for PFOS they range from 72 mg/g to 714 mg/g (Ochoa-Herrera and Sierra-Alvarez, 2008; Qu et al., 2009; Yu et al., 2009; Punyapalakul et al., 2013; Zhang et al., 2016a). One message from these studies is the need for a better understanding of structure-property correlations for selection and targeted modification of ACs for PFAS adsorption.

The hydrophobic effect and electrostatic interactions have been discussed as two main driving forces for adsorption of PFOA and PFOS on AC (Yu et al., 2009; Du et al., 2014; Zhi and Liu, 2015). According to the  $pK_a$  values of PFOS (-3.27 (Brooke D., 2004)) and PFOA (around 0 to 1 (Goss, 2008; Cheng et al., 2009; Baggioli et al., 2018)), under relevant pH conditions they fully dissociate in water. Thus, it is to be expected that electrostatic interactions between the anionic head group and charged surface groups of AC influence their adsorption process. Hydrophobicity also plays a role in adsorption of PFOA and PFOS (Yu et al., 2009; Du et al., 2014). It has been reported (Yu et al., 2009; Deng et al., 2015; Chen et al., 2017) that its impact is more pronounced for PFOS due to the longer perfluorinated carbon chain. Octanol-water partition coefficients were calculated for the acids in their protonated forms as  $\log K_{ow, PFOA} = 4.30$  vs.  $\log K_{ow, PFOS} = 5.25$  (Arp et al., 2006). However, they cannot simply be applied for estimation of sorption effects because the anions rather than the neutral molecules are the relevant species in aqueous solution. Due to the complex sorption mechanism, the surface chemistry of AC is crucial in determining adsorption affinity of PFOA and PFOS. Zhi and Liu (Zhi and Liu, 2015) have studied the effect of surface chemistry on adsorption affinity of PFOA and PFOS. They concluded that adsorbent surface chemistry overwhelmed physical properties in controlling the extent of uptake. Correlations between individual carbon properties and adsorption coefficients of PFOA and PFOS were, however, generally weak. Carbon surface polarity or hydrophobicity, as indicated by oxygen content or total surface acidity, were evaluated as less important, although surface basicity of AC, providing anion exchange sites, showed the strongest positive effect on affinity of PFOA and PFOS. The authors noted that studies with carbon materials having very similar physical properties but differences in surface chemistry are needed in order to confirm these findings. Furthermore, three ACFs belonged to the best adsorbents in their study, but a lack of literature data on PFOA and PFOS adsorption to ACFs hinders further comparison of the observed phenomena (Zhi and Liu, 2015).

The total basicity of AC was linked to AEC and determined as being the factor most influencing higher uptake of PFOA and PFOS on AC (Zhi and Liu, 2015). The conventional method to determine the surface basicity of AC is the determination of total proton consumption upon immersion in HCl solution (Boehm, 1966). However, this type of titration method only provides an upper limit for the AEC, as the end-point is typically  $\leq$  pH 3. AC contains various basic and acidic groups having a broad range of  $pK_a$  values. Therefore, at pH 7 the AEC of AC can be different from that at pH 3. In order to determine AEC and CEC originating from all protonated and deprotonated sites on AC at the relevant pH, we propose to apply a standard method established for soils which has also been used for AC (Oen et al., 2012; Hsieh and Pignatello, 2017). While AEC provides information on electrostatic attraction between AC and PFOA or PFOS anions, the CEC of AC gives information about electrostatic repulsion due to negatively charged surface sites at a certain pH. In addition, based upon knowledge of the CEC, the impact of ionic strength on PFOA and PFOS adsorption can be evaluated more precisely.

In a recent review, the spectrum of interaction mechanisms for ionic and ionizable organic compounds (IOCs) on carbonaceous adsorbents was discussed, including hydrophobicity (van der Waals interactions), H-bonds, electron donor-acceptor interactions, electrostatic interactions, ligand exchange, Lewis acid-base reactions, covalent bond formation and oxidative coupling as well as formation of positive or negative charge-assisted hydrogen bonds, i.e. (+) or (-)CAHBs, respectively (Kah et al., 2017). Among all these types of interactions, (-)CAHBs might be relevant for PFAS adsorption in addition to the previously discussed hydrophobic and electrostatic interactions but have so far not been considered. (-)CAHBs can be formed between the carboxyl group of an adsorbate molecule and surface carboxyl or hydroxyl groups of the adsorbent when the two functional groups have similar  $pK_a$  values (Gilli and Gilli, 2000), as suggested for e.g. adsorption of benzoic acid (Li et al., 2013) and sulfamethazine (Teixidó et al., 2011) to AC. The strength of such H-bonds is determined by the difference in proton affinities of the H-donor and H-acceptor atoms, i.e. the difference in  $pK_a$  between the proton donor group ( $pK_{a, DH}$ ) and proton acceptor group ( $pK_{a, AH^+}$ ). The lower the difference, the stronger the CAHB, exceeding the bond strength of ordinary H-bonds (Gilli and Gilli, 2000; Gilli et al., 2009). A range of  $\Delta pK_a = pK_{a, DH} - pK_{a, AH^+} < 5$  was considered as relevant for establishment of CAHBs. PFOS with  $pK_a$  -3.27 does not meet the stated condition for formation of (-)CAHBs: its acidity is too strong. However, the relevance of (-)CAHB in adsorption of PFOA ( $pK_a \sim 1$ ) on AC will be discussed in

this study. Furthermore, Cheng et al. (Cheng et al., 2009) observed the formation of remarkably stable  $(\text{PFOA})_2\text{H}^-$  dimers in electrospray ionization at  $\text{pH} \leq 4$  and micromolar PFOA concentrations. The authors explained this phenomenon by intermolecular hydrogen bond formation between two PFOA anions, which does not occur in the case of PFOS molecules. The possible effect of the formation of such structures upon adsorption of PFOA on AC will also be discussed here.

It has been reported that coexisting inorganic anions and cations have different effects on adsorption of PFOA and PFOS on various adsorbents (Du et al., 2014). In addition to the salting-out effect, which slightly increases adsorption of hydrophobic compounds at high ionic strength (IS) ( $\geq 0.1 \text{ M}$ ) (Higgins and Luthy, 2006; Yu et al., 2008), the presence of inorganic ions leads to a compression of the electrical double layer (EDL) at charged surface sites of the adsorbents. The latter effect is believed to affect the affinity between adsorbent surfaces and the adsorbate anions (Wang and Shih, 2011; Kwon et al., 2012; Du et al., 2015). On the other hand, competitive ion binding might occur at low salt concentrations. For example, Zhang et al. (Zhang et al., 2011) reported that  $\text{SO}_4^{2-}$  (1 mM) slightly reduced adsorption capacity for PFOS anions on crosslinked chitosan beads which were positively charged under the applied conditions. Therefore, it can be expected that ACs with various surface chemistries show different responses in adsorption of PFOA and PFOS with respect to varying concentrations of inorganic ions.

Natural organic matter (NOM) as ubiquitous component of surface and groundwater needs to be considered as relevant competitor for PFAS adsorption. Indeed, in some studies with granular AC a reduction in PFAS adsorption in the presence of low NOM concentrations (1.5 to 8 mg/l) was reported [33, 34] which was ascribed to occupation of pore space or sorption sites. Nevertheless, in one study the response was variable based on the type of NOM and the PFAS chain length. Hydrophobic interactions between PFAS and NOM prior to adsorption were addressed as probable reason for improved PFAS removal in presence of DOM [34]. Considering the surface chemistry of AC in terms of NOM effects can help to further elucidate the underlying mechanisms.

This work is aimed at studying the effect of AC properties upon adsorption affinity of PFOA and PFOS with a strong focus on carbon surface chemistry. For this purpose a series of commercially available ACFs having distinct surface chemical properties were applied. These ACFs differ widely in adsorption capacities for PFOA and PFOS. Structure-property correlations were derived based on detailed characterization of surface chemistry and porosity of the ACFs. The adsorption

behavior of PFOA and PFOS on ACFs at various pH values and in aqueous solutions with various salt matrices was studied. Specifically, the effect of the surface chemistry of AC upon the adsorption affinity of PFOA and PFOS from water containing natural organic matter (NOM) and with high ionic strength is reported upon for the first time. In addition, two recently discussed interaction mechanisms, i.e. formation of (–)CAHBs and (PFOA)<sub>2</sub>H<sup>–</sup> dimers are evaluated in terms of their potential involvement in the adsorption mechanism of PFOA.

## **2. Materials and Methods**

### *2.1. Materials*

#### *2.1.1. Chemicals*

PFOA and PFOS were purchased from Sigma-Aldrich (96% and 98% purity, respectively). HCl (fuming 37%), NaOH (99%), NaHCO<sub>3</sub> (>99%), KCl (>99%), NaNO<sub>3</sub> (>99%), MgSO<sub>4</sub> (>98%), CH<sub>3</sub>COONH<sub>4</sub> (98%), Na<sub>2</sub>CO<sub>3</sub> (>99%) and Na<sub>2</sub>SO<sub>4</sub> (99%) were obtained from Merck. Methanol (99.9%) was purchased from CHEMSOLUTE. In this work, Suwannee River natural organic matter (SRNOM, reference number: 2R101N), which is a reference material of the International Humic Substances Society (IHSS), was used as NOM. Characterization of SRNOM has been performed by Driver and Perdue (Driver and Perdue, 2014).

#### *2.1.2. Activated carbon felts*

The ACFs were purchased from Jacobi CARBONS, Sweden. The commercial names of these ACFs are ACTITEX VS19, ACTITEX FC 1501, ACTITEX FC 1001 and ACTITEX WK L20, which are hereafter addressed by the abbreviated names of VS, FC15, FC10 and WK, respectively. According to the company information, these ACFs are all made from synthetic rayon-based viscose fiber as precursor. The ACFs were pretreated before use. In brief, the ACFs were washed with methanol (20 mL per 10 cm<sup>2</sup> of the felt) and then rinsed 5 times with 20 mL of distilled water. Each time the samples were shaken for 1 h. Finally, the ACFs were dried overnight at 80 °C and kept in a desiccator for further use.

### *2.2. Characterization of the activated carbon felts*

The fiber diameters of the ACFs were measured by means of a digital light microscope equipped with a high-resolution zoom lens (KEYENCE VH-Z500). The specific surface area, pore size

distribution of the mesopores (pore width > 2 nm) and pore volume of the ACFs were determined by means of nitrogen adsorption/desorption at  $-196^{\circ}\text{C}$  using a Belsorp MINI (BEL Japan, Ltd.). The BJH method was used to analyze mesopores. The pore size distribution in the micropore range (pore width < 2 nm) was determined by means of adsorption of  $\text{CO}_2$  at  $0^{\circ}\text{C}$  using a magnetic suspension balance (Rubotherm, Germany) and analyzed by NLDFT using the software package Pore analyser (Porotec GmbH, Germany).

The PZC of the ACFs was determined by means of the immersion method as follows (Babić et al., 1999): a sample of each ACF (0.05 g) was put into 10 mL electrolyte solution (10 mM  $\text{Na}_2\text{SO}_4$ ) and agitated for 48 h in glass vessels by a reciprocal shaker (HS 260 basic – IKA) at 120 swivel motions per minute (spm). Initial pH values were adjusted with 0.1 M HCl and NaOH solutions. The point in which the initial pH is equal to the final pH was considered as PZC. The acidic surface functional groups of the ACFs were determined according to the Boehm titration method (Fidel et al., 2013). Briefly, 0.5 g samples of the ACFs were shaken with 25 mL of each of the three alkaline 0.05 M Boehm reactants  $\text{NaHCO}_3$ ,  $\text{Na}_2\text{CO}_3$ , and NaOH for 24 h at room temperature. The equilibrated Boehm reactants were separated from the ACFs and kept in a refrigerator for the next step. Afterwards, 0.05 M HCl was added at a 2:1 volume ratio to the  $\text{NaHCO}_3$  and NaOH extracts and at a 3:1 volume ratio to the  $\text{Na}_2\text{CO}_3$  extract. In order to remove  $\text{CO}_2$ , the acidified samples were sparged with  $\text{N}_2$  for 2 h in glass vials before titration. All treated extracts were titrated with 0.01 M NaOH to an endpoint of pH  $\sim 8.2$ , using phenolphthalein as indicator.

AEC and CEC were measured by means of a standard method established for soils, which has also been used for AC (Oen et al., 2012; Hsieh and Pignatello, 2017). In brief, the ACF (0.5 g) was first shaken with 1 M KCl solution (10 mL) for 24 h, followed by washing five times with 0.01 M KCl (10 mL). After the final washing, the mixture was adjusted to pH  $7 \pm 0.2$  with 0.1 M NaOH and HCl, and allowed to equilibrate for 8 h. The decanted supernatant phase was then analyzed for  $\text{K}^+$  and  $\text{Cl}^-$  by means of ICP-OES (SPECTRO Analytical Instruments) and Ion Chromatography (ICDX 500 system, Dionex), respectively. It is assumed that the concentration of the entrained  $\text{K}^+$  and  $\text{Cl}^-$  are equal to those of the final washing solution. The sample was then washed four times with 0.5 M  $\text{NaNO}_3$  solution (8 mL) in order to displace the adsorbed  $\text{K}^+$  and  $\text{Cl}^-$ . The exchanged solutions were combined and  $\text{K}^+$  and  $\text{Cl}^-$  concentrations were determined in the decanted liquid. The AEC and CEC were calculated on the basis of the difference between exchanged  $\text{Cl}^-$  and  $\text{K}^+$ , corrected by the initially entrained  $\text{Cl}^-$  and  $\text{K}^+$  before the exchange process, respectively.



Temperature-programmed desorption (TPD) was performed using a BELCAT-B chemisorption analyzer (BEL Japan, Osaka) connected with a mass spectrometer (MKS Cirrus 2). The samples were first pretreated at 150 °C for 30 min in an argon atmosphere. They were then heated up from 150 °C to 1100 °C in a helium flow (50 mL/min) with a heating rate of 10 K/min, whereby the evolved gases, CO<sub>2</sub> and CO, were determined. X-ray photoelectron spectroscopy (XPS) was performed with an Axis Ultra photoelectron spectrometer (Kratos, Manchester, UK) using monochromatized Al K $\alpha$  radiation ( $h\nu = 1486.6$  eV).

### 2.3. Analytical methods

Analysis of PFOA and PFOS were performed using a liquid chromatography system coupled to a single-stage quadrupole mass spectrometer with electrospray ionization (LCMS-2020; SHIMADZU Corporation). Aliquots of 3  $\mu$ L of the solution containing the target compounds were injected onto a 100 mm  $\times$  2 mm Gemini C6-Phenyl column filled with fully porous organo-silica having 110 Å pore size and 3  $\mu$ m particle size (Phenomenex Company). The mobile phase was a combination of solvent A, consisting of 5 mM ammonium acetate dissolved in 90% deionized water and 10% methanol, and solvent B, consisting of 5 mM ammonium acetate dissolved in 90% methanol and 10% water. A combination of 30% of solvent A and 70% of solvent B was delivered at a flow rate of 3 mL/min by the LC pump. The column temperature was maintained at 40 °C and the total run time was 10 min. The correlation coefficients ( $R^2$ ) of the calibration curves for PFOA and PFOS were  $> 0.99$  for sample concentrations less than 1 mg/L.

### 2.4. Adsorption experiments

Batch adsorption experiments with PFOA and PFOS were carried out in 25 mL vessels containing 10 mL solution. Certain amounts of the ACFs were added into the vessels containing a certain background electrolyte solution; the pH of the system was then adjusted to the desired value by adding 0.1 M HCl or NaOH solution. In general, the concentration of Na<sup>+</sup> in all solutions increased due to pH adjustment by  $(60 \pm 30)$   $\mu$ M, which is negligible compared to 10 mM Na<sub>2</sub>SO<sub>4</sub> background electrolyte. The vessels were then shaken overnight by the reciprocal shaker at 120 spm. The pH of the solutions containing adsorbent was checked and adjusted again to the desired value; certain concentrations of PFOA and PFOS in the solution were then prepared by adding

specific volumes of their 200 mg/L aqueous stock solutions. In the case of NOM experiments, 100 mg/L stock solutions of NOM in 10 mM Na<sub>2</sub>SO<sub>4</sub> adjusted to pH 7 were prepared and used.

The amount of PFOA and PFOS adsorbed by the ACFs (adsorbate loading) was calculated from the differences between the initial concentration of the solutes in the solution and their final concentration in the aqueous supernatant after a certain time interval according to Eq. 1:

$$q_e = \frac{V(C_0 - C_e)}{m} \quad (1)$$

where  $q_e$  (mg/g) is the concentration of adsorbed solute at equilibrium,  $C_0$  and  $C_e$  (mg/L) are the initial concentration and concentration of the solute in the solution at equilibrium, respectively,  $V$  (L) is the volume of the solution and  $m$  (g) is the mass of ACF.

The single point adsorption coefficient  $K_d$  (L/g) of the adsorbates on the ACFs was calculated by means of Eq. (2):

$$K_d = \frac{q_e}{C_e} \quad (2)$$

where  $q_e$  (mg/g) and  $C_e$  (mg/L) are the equilibrium concentrations of adsorbed and freely dissolved solute, respectively. Equilibrium was considered to be reached after 2 d, as the aqueous phase concentration of the solutes did not change significantly ( $\leq 5\%$ ) with further prolonged contact time.

#### 2.4.1. Adsorption isotherms

The experimental data were fitted with a linear form of the Langmuir equation (Eq. 3) (Langmuir, 1918):

$$\frac{C_e}{q_e} = \frac{C_e}{q_m} + \frac{1}{q_m K_L} \quad (3)$$

with  $C_e$  (mg/L) and  $q_e$  (mg/g) as defined above, and  $q_m$  (mg/g) as the maximum (monolayer) adsorption capacity of the adsorbent.  $K_L$  (L/mg) is a constant related to the affinity between the

adsorbate and the adsorbent. For a good adsorbent, a high adsorption capacity  $q_m$  and a steep initial sorption isotherm slope (high  $K_L$ ) are desirable (Kratochvil and Volesky, 1998).

In addition, the empirical Freundlich equation in its linear form (Eq. 4) was applied:

$$\log q_e = n \log C_e + \log K_F \quad (4)$$

where  $K_F$  (mg/g)/(mg/L)<sup>n</sup> is the Freundlich constant related to the affinity between adsorbent and adsorbate, and  $n$  (dimensionless) is the Freundlich exponent.

### 3. Results and discussion

#### 3.1. Characteristics of ACFs

Table 1 shows the physical properties of the ACFs.

The adsorption results were calculated and reported based on normalization to specific surface area of the ACFs. Pore size distributions in pore width range  $> 2$  nm were studied by means of N<sub>2</sub> adsorption/desorption results and the BJH method and compared also to a commercial powder AC (CHEMVIRON) (Figure 1Sa). This comparison illustrates that the pore size distribution of the ACFs is narrower, i.e. almost exclusively covering the micropore range. In order to further elucidate the pore size distribution in the micropore range CO<sub>2</sub> adsorption (0° C) and NLDFT analysis were applied (Figure 1Sb). The results show that there is a bimodal distribution of pore widths which is similar for all four ACFs, but their relative proportion (pore volume) is different. In the 1 to 2 nm pore width range, VS has the highest pore volume, followed by FC15, FC10 and WK. In contrast, WK has the highest proportion of pores in the  $< 1$  nm pore width range.

Table 1. Physical properties of the ACFs.

Sample	BET surface area (m <sup>2</sup> /g) <sup>a</sup>	Total pore volume (cm <sup>3</sup> /g) <sup>a</sup>	Pore volume (1-2 nm pore width) <sup>b</sup>	Pore volume ( $< 1$ nm pore width) <sup>b</sup>	Fiber Diameter (μm) <sup>c</sup>
VS	2100	0.99	0.575	0.229	10 ± 1
FC15	1600	0.74	0.474	0.128	10 ± 2
FC10	1400	0.62	0.341	0.209	12 ± 1
WK	1100	0.53	0.136	0.229	12 ± 1

<sup>a</sup> determined by means of N<sub>2</sub> adsorption/desorption, <sup>b</sup> determined by means of CO<sub>2</sub> adsorption,

<sup>c</sup> each diameter is an average of 10 measurements.

Table 2 lists the results of Boehm titration, TPD and PZC. These characterizations of the functional groups of the ACFs reveal that the ACFs contain various surface functional groups. According to the Boehm titration results, WK contains the highest concentration of carboxylic ( $1.12 \mu\text{mol}/\text{m}^2$ ) and total acidic groups ( $2.10 \mu\text{mol}/\text{m}^2$ ), followed by FC10, FC15 and VS. The difference in total acidity between VS ( $0.23 \mu\text{mol}/\text{m}^2$ ) and WK is large: nearly a factor of 9. ACFs contain negatively charged sites at pH 7 due to the deprotonation of carboxylic acid groups.

At pH 3, these groups are largely protonated. In addition, the concentrations of weakly acidic groups, i.e. phenolics, lactones and lactols, were obtained and are reported in Table 2. Phenolic groups do not deprotonate under the conditions of our adsorption experiments (pH 3 and pH 7) as their  $pK_a$  is in the range of 10 to 13 (Jacquesy et al., 1988). Lactones and lactols have  $pK_a$  values in the range of 6 to 10 (Olah and Ku, 1970; Gómez-Bombarelli et al., 2013a).

Table 2. Characteristics of the functional groups of the ACFs.

Sample	Boehm Titration				TPD			N-content <sup>b</sup>	PZC
	$pK_a \sim 3-6$	$pK_a \sim 6-10$	$pK_a \sim 10-13$	$pK_a \sim 3-13$	CO	CO <sub>2</sub>	O-content <sup>a</sup>		
	Carboxylic acids	Lactons and lactols	Phenols	Total acidity					
	( $\mu\text{mol}/\text{m}^2$ )	( $\mu\text{mol}/\text{m}^2$ )	( $\mu\text{mol}/\text{m}^2$ )	( $\mu\text{mol}/\text{m}^2$ )	( $\mu\text{mol}/\text{m}^2$ )	( $\mu\text{mol}/\text{m}^2$ )	(wt%)	(wt%)	
VS	0.0386	0.124	0.0667	0.229	0.338	0.192	2.5	0.2	$7.3 \pm 0.1$
FC15	0.0687	0.0750	0.287	0.431	1.19	0.169	3.9	0.5	$7.1 \pm 0.1$
FC10	0.298	0.0992	0.695	1.09	4.22	1.13	15.9	0.6	$6.5 \pm 0.2$
WK	1.12	0.321	0.643	2.08	3.39	2.14	13.7	0.5	$5.9 \pm 0.2$

<sup>a</sup> calculated from released CO and CO<sub>2</sub>, <sup>b</sup> determined by means of XPS.

TPD profiles of the ACFs are shown in Figure 2S. The oxygen content of the ACFs was calculated based upon the amount of CO<sub>2</sub> and CO released in TPD (see Table 2). The results proved that FC10 (15.9 wt%) and WK (13.7 wt%) contain a higher quantity of oxygen than FC15 (3.9 wt%) and VS (2.5 wt%), revealing that WK and FC10 are more hydrophilic than VS and FC15. As can be seen in Table 2, acidic groups (CO<sub>2</sub>-releasing groups (Papirer et al., 1991)) represent 1/3 of the total O-content in FC10 but 1/2 of the total O in WK. That means that the surface of WK is not only hydrophilic due to the O-content, but also more negatively charged at pH 7; this is also reflected in its low PZC. For all other ACFs, the PZC values are closer to pH 7, i.e. there is a balance of positive and negative charges at circumneutral pH, with a slight dominance of positive

charges for FC15 and VS and of negative charges for FC10, respectively. At pH 3, the net charge on all ACFs is positive.

Positively charged sites on ACs can also be formed by nitrogen-containing functional groups, which can be introduced through either reaction with nitrogen-containing reagents (such as  $\text{NH}_3$ , nitric acid, and amines) or activation with nitrogen-containing precursors (Pittman et al., 1997; Carrott et al., 2001). N-contents of the ACFs are similar and very low (Table 2). Consequently, nitrogen sites do not contribute significantly to surface basicity of the ACFs.

In addition to heteroatom-related charges, the carbon structure itself can create positively charged sites. These sites are located in  $\pi$ -electron-rich regions on the basal plane of carbon crystallites which are of Lewis type and thus can bind protons from solution. These sites are typical for ACs with low oxygen content (Boehm, 1994). Their presence can be supported by removing acidic and other electron-withdrawing groups from AC by means of specific thermal treatments (Shafeeyan et al., 2010).

Positively or negatively charged sites on the surface are involved in the uptake of inorganic anions or cations, respectively, by ion-exchange or electrostatic interactions. Table 3 lists AEC and CEC values of the ACFs at circumneutral pH. Figure 3S confirms the hypothesis that AEC and CEC are inversely related: VS has the highest AEC, followed by FC15, FC10 and WK, while CEC follows the opposite trend. As the CEC of ACFs was determined at pH 7, only the acidic groups with  $\text{p}K_{\text{a}} \leq 7$  (carboxylic acid groups as well as some lactones and lactols) played a role. As Figure 4S shows, there is a good agreement between the sequence of carboxylic acid group content from Boehm titration and the CEC of the ACFs. In addition, the AEC of the ACFs originates not only from basic oxygen-containing groups but also from positively charged sites created by protons on  $\pi$ -electron-rich regions. In addition, it should be noted that there is also a positive correlation between AEC and micropore volume in the range of 1-2 nm pores (Figure 5S).

Table 3. Anion and cation exchange capacity of the investigated ACFs.

Sample	Anion exchange capacity ( $\mu\text{mol}/\text{m}^2$ )	Cation exchange capacity ( $\mu\text{mol}/\text{m}^2$ )
VS	0.148	0.0714
FC15	0.137	0.131
FC10	0.0922	0.418
WK	0.0536	0.795

As the various ACFs according to the supplier are derived from the same starting material, the different carbonization/activation procedures could result in defunctionalization (removal of O-containing groups) and widening of pores at the same time. Taking into account the importance of the AEC for PFAS adsorption, the correlation between the pore volume parameter and  $q_m$  (Figure 2) could also be indirect (cross-correlation).

### 3.2. Adsorption Experiments

#### 3.2.1. Adsorption of PFOA and PFOS

Adsorption isotherms of PFOA and PFOS on the ACFs at pH 7 were determined and are shown in Figure 6S. Figure 1 shows the isotherms fitted with Freundlich and Langmuir equations. The isotherm parameters normalized to the specific surface area of the ACFs were listed in Table 4. Table 1S lists the same parameters in terms of mass unit. Obviously, there are large differences in the uptakes of PFOA by the various ACFs. Note that the Freundlich equation can only be applied within a certain PFOA concentration range, i.e. below the vicinity of the maximum loading on the individual ACFs (Figure 1a and c). Judging from the regression coefficients  $R^2$ , both Freundlich and Langmuir equations fit the isotherms well for PFOA (Table 4). The Langmuir model, which is based on the assumption of monolayer coverage, can be applied to the whole concentration range. Maximum monolayer adsorption loadings ( $q_m$ ) of PFOA on ACFs are  $0.065 \mu\text{mol}/\text{m}^2$  (56.8 mg/g) >  $0.055 \mu\text{mol}/\text{m}^2$  (36.2 mg/g) >  $0.0175 \mu\text{mol}/\text{m}^2$  (10.20 mg/g) >  $0.00445 \mu\text{mol}/\text{m}^2$  (2.08 mg/g), referring to VS > FC15 > FC10 > WK, respectively. The adsorption affinity of PFOA based on Freundlich constants ( $K_F$ ) or Langmuir constants ( $K_L$ ) confirms that VS has the highest affinity for PFOA, followed by FC15, FC10 and WK (Table 4).

Also for PFOS there are large differences in adsorption properties between the various ACFs and the order of the maximum adsorption capacities ( $q_m$ ) and adsorption affinities ( $K_F$  and  $K_L$ ) of PFOS is the same as that of PFOA (Figure 1 and Table 4). It has been reported in several studies that the adsorption affinity and capacity of PFOS is higher than that of PFOA on the same AC and under the same experimental condition (Yu et al., 2009; Deng et al., 2015; Zhi and Liu, 2015; Chen et al., 2017). Our data are in conformity with these findings except for WK (same  $q_m$ ). However, the fitting of PFOS adsorption on WK according to the Langmuir model was not as good for WK as for the other ACFs, as the maximum loading is not reached in the concentration range studied. This order of capacities and affinities for adsorption of PFOA and PFOS is correlated with both,

the porosity and the surface chemical characteristics of the ACFs and their relative importance is discussed in detail in the following sections.

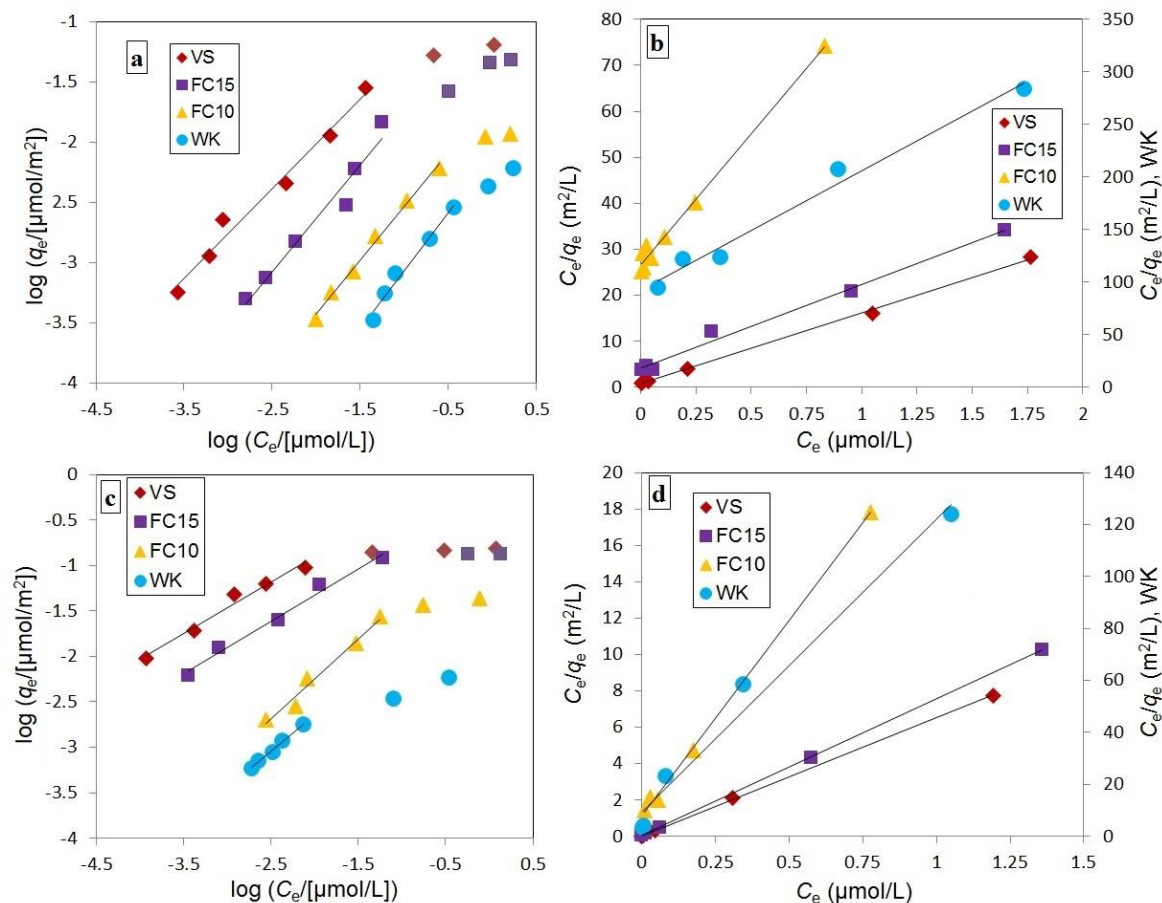


Figure 1. Experimental adsorption data on the ACFs at pH 7: adsorption of PFOA fitted with Freundlich (a) and Langmuir (b) equations; adsorption of PFOS fitted with Freundlich (c) and Langmuir (d) equations.

### 3.2.1.1. Effect of Micropore Size Distribution

Figure 2 shows the effect of micropore size distribution on maximum loading of PFOA and PFOS on the ACFs. There is a correlation between the adsorption capacity of PFOA and PFOS on the ACFs and the volume of pores with 1-2 nm width (Figure 2a). In contrast, the adsorption capacities do not correlate with the volume of pores with < 1 nm width (Figure 2b). Therefore, the availability of pores with width < 1 nm is obviously not a crucial factor for PFAS adsorption. In addition, even though the ACFs differ in the available pore volume in the 1-2 nm range (i.e. by a factor < 5), these differences by far cannot explain the differences in adsorption capacities (up to a factor of

30 between VS and WK). Furthermore, one can estimate the degree of pore filling reached at the highest maximum loading achieved, i.e. for PFOS on VS as best adsorbing ACF.

Table 4. Freundlich and Langmuir parameters for adsorption of PFOA and PFOS.<sup>a</sup>

ACF adsorbent	Adsorbate	Freundlich			Langmuir		
		$K_F$ ( $\mu\text{mol}/\text{m}^2$ )/( $\mu\text{mol}/\text{L}$ ) <sup>n</sup>	$n$	$R^2$	$q_m$ ( $\mu\text{mol}/\text{m}^2$ )	$K_L$ ( $\text{L}/\mu\text{mol}$ )	$R^2$
VS	PFOA	0.309	0.74	0.975	0.0649	0.0198	0.998
VS	PFOS	1.72	0.57	0.986	0.154	0.187	0.999
FC15	PFOA	0.139	0.88	0.961	0.0546	0.00450	0.990
FC15	PFOS	0.676	0.58	0.985	0.134	0.0971	0.999
FC10	PFOA	0.0234	0.89	0.994	0.0175	0.00214	0.990
FC10	PFOS	0.332	0.88	0.976	0.0465	0.0185	0.998
WK	PFOA	0.0100	0.98	0.969	0.00445	0.00482	0.986
WK	PFOS	0.0871	0.79	0.991	0.00885	0.0124	0.979

<sup>a</sup> table 1S lists these parameters in terms of mass units.

Based on a molar volume of PFOS of about 270 mL/mol, the maximum volumetric loading of 0.085 mL PFOS/g results in a filling degree of 1-2 nm pores (0.58 mL/g) of only 15%. It means the *volume* of this micropore fraction will most likely not be the limiting factor in PFAS adsorption. In conclusion, the availability of pores in a certain size range cannot explain the vastly different adsorption properties of the ACFs and surface chemistry obviously plays a major role.

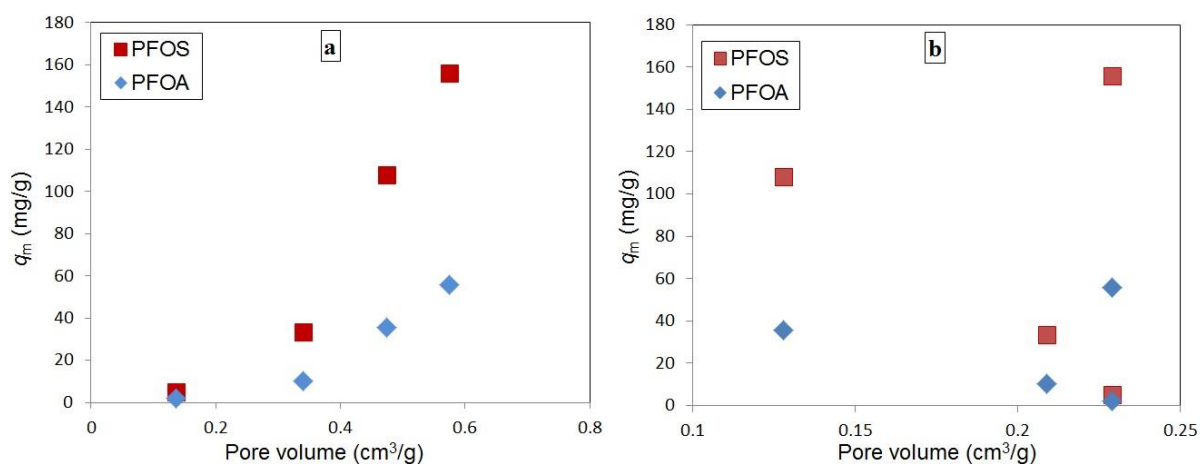


Figure 2. Effect of micropore size distribution of the ACFs on adsorption of PFOA and PFOS: (a) maximum loading versus volume of pores with 1-2 nm width and (b) maximum loading versus pore volume of pores with width < 1 nm.



### 3.2.1.2. Effect of Surface Chemistry

Figure 3 correlates the adsorption behavior of PFOA and PFOS on the ACFs with parameters characterizing their surface chemistry (AEC, CEC, PZC and oxygen content). In order to compare the adsorption *affinity* of PFOA and PFOS on the ACFs, beside  $q_m$  also single point adsorption coefficients ( $K_d$ ) were calculated from isotherms at a constant equilibrium aqueous phase concentration of  $C_{e, \text{PFOA}} = 20 \text{ } \mu\text{g/L}$  ( $0.05 \text{ } \mu\text{mol/L}$ ) and  $C_{e, \text{PFOS}} = 8 \text{ } \mu\text{g/L}$  ( $0.016 \text{ } \mu\text{mol/L}$ ). Adsorption parameters in Figure 3 were normalized to the BET surface area of the ACFs. In addition, Figure 7S shows these correlations with normalization of adsorption parameters to pore volume in the width range of 1-2 nm. Again, even after these normalizations large differences in  $K_d$  and  $q_m$  values remain pointing to the importance of the differences in surface chemistry. As can be seen in Figure 3a, the maximum loading of PFOA and PFOS on the ACFs correlates positively with AEC, meaning the higher the AEC, the higher the adsorption capacity, although CEC has an inverse correlation with the maximum loading of PFOA and PFOS on the ACFs (Figure 3b). AECs of all ACFs are higher than the maximum loading with PFOA. In contrast, for PFOS,  $q_m$  and AEC are comparable, especially for VS and FC15. The finding that maximum loadings of PFOA and PFOS are in any case equal to or lower than the AEC of the ACF is important as it indicates that the anions of these molecules can be adsorbed favorably by a combination of hydrophobic and electrostatic interactions if sufficient charge-balancing cationic sites are available at the ACF surface.

VS, as the best adsorbent among the four ACFs, reaches  $K_d$  values in the range of  $K_d = 0.66 \text{ L/m}^2$  or  $1.4 \times 10^6 \text{ L/kg}$  for PFOA and  $1.01 \text{ L/m}^2$  or  $2.2 \times 10^7 \text{ L/kg}$  for PFOS. These values reflect a very high adsorption affinity, which is even higher than that of very hydrophobic compounds such as polycyclic aromatic hydrocarbons at AC. For instance, single point adsorption coefficients for anthracene at an aqueous phase concentration of  $10 \text{ } \mu\text{g/L}$  onto AC are in the order of  $10^6 \text{ L/kg}$  (Dobbs, 1980; Walters and Luthy, 1984), which is an order of magnitude lower than for PFOS.

Figure 3c and d show plots of  $\log K_d$  versus AEC and CEC, respectively. As already observed for monolayer adsorption capacities, there is a positive correlation of  $\log K_d$  with AEC, whereas it is inversely correlated with CEC. PZC of WK is 5.9, meaning that at pH 7 the net charge on WK is negative. The same is true for FC10 (PZC 6.5). This can be a reason for the relatively low adsorption affinity of PFOA and PFOS on WK at pH 7. It suggests that adsorption affinity of PFOA and PFOS on WK and FC10 increases if pH is lower than 5.9 and 6.5, respectively; this

will be discussed later in detail. As can be seen in Figure 3e, PZC, as a measure of the ratio between number of positive and negative charges at pH 7, also correlates well with adsorption affinity of the two PFAS as expressed by  $\log K_d$ . Oxygen content, on the other hand, can be considered as a general measure for surface polarity and thus as an inverse measure of hydrophobicity.

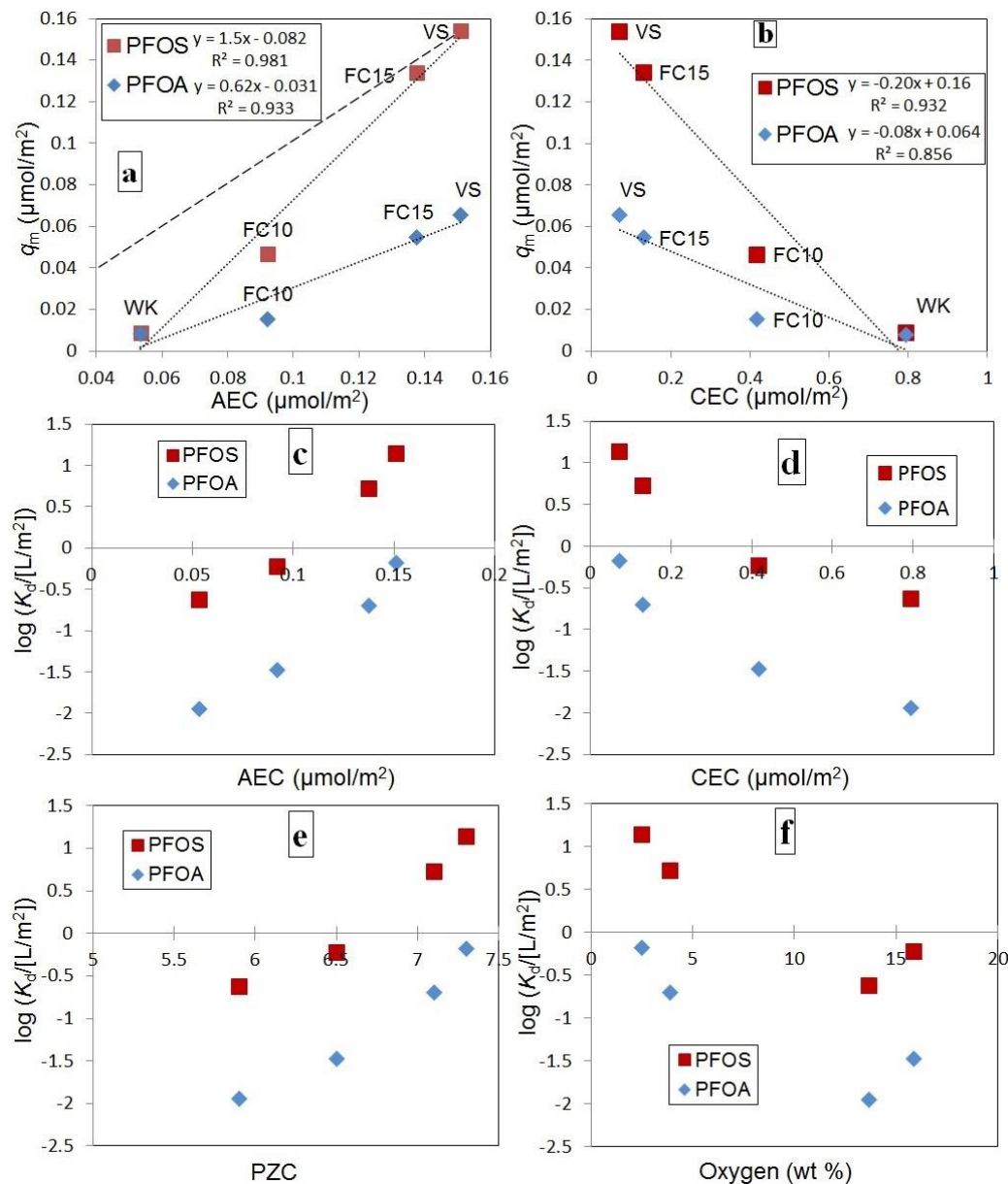


Figure 3. Correlation between maximum loading  $q_m$  ( $\mu\text{mol}/\text{m}^2$ ) versus AEC (a), CEC (b) and between single point adsorption coefficient  $\log(K_d)$  [L/m<sup>2</sup>] and AEC (c), CEC (d), PZC (e) and oxygen content (f) at pH 7.  $K_d$ s are calculated for  $C_{e, \text{PFOA}} = 20 \mu\text{g}/\text{L}$  ( $0.05 \mu\text{mol}/\text{L}$ ) and  $C_{e, \text{PFOS}} = 8 \mu\text{g}/\text{L}$  ( $0.016 \mu\text{mol}/\text{L}$ ). Dashed line in (a) represents the hypothetical case of  $q_m = \text{AEC}$ .

Figure 3f shows that the adsorbents with low oxygen content (VS and FC15) expose a high adsorption affinity of PFOA and PFOS. However, the difference in adsorption by FC10 and WK is not well predicted. As mentioned earlier, oxygen content in WK is to a higher extent related to acidic groups than in FC10 (1/2 vs. 1/3 of the total O), which leads to a lower PZC and lower AEC in the case of WK. Obviously, electrostatic interactions overwhelm general surface hydrophobicity/hydrophilicity in their effect on adsorption of PFOA and PFOS on AC, as has also been observed by Zhi and Liu (Zhi and Liu, 2015).

The results point out that AEC showed the strongest positive correlation with adsorption affinity of PFOA and PFOS. As mentioned earlier, basicity of the ACFs originates from oxygen-free carbon sites and/or oxygen-containing basic groups. The latter are included in the CO-releasing groups in TPD, which in general comprise weakly acidic oxygen-containing groups such as ether groups (Shafeeyan et al., 2010) as well as basic oxygen-containing groups including pyrone and chromene type structures (Papirer et al., 1987; Zielke et al., 1996). The functional groups of WK and FC10 released  $4.2 \mu\text{mol}/\text{m}^2$  and  $3.4 \mu\text{mol}/\text{m}^2$  CO and their oxygen contents are 13.7 and 15.9 wt%, respectively.

In contrast, VS and FC15 have as low as 2.5 wt% and 3.9 wt% oxygen and their CO release in TPD is only  $0.34 \mu\text{mol}/\text{m}^2$  and  $1.2 \mu\text{mol}/\text{m}^2$ , respectively. Thus, it can be concluded that the ACFs with highest affinity for PFAS, i.e. VS and FC15, create positive charges by proton adsorption to electron-rich carbon sites rather than by basic oxygen-containing groups. It is obvious from Figure 8S that AEC and CEC themselves are strongly correlated with each other, which is in accordance with the hypothesis that this  $\pi$ -electron basicity of the graphene layers is favorably formed if electron-withdrawing substituents (e.g. carboxylic groups responsible for CEC) are missing. Overall, these results give clear indications on the optimal surface chemistry of ACs for achieving high performance in removal of PFOA and PFOS. Building upon this knowledge additional studies including targeted surface modification of AC are currently conducted in our group.

### *3.2.2. Effect of Inorganic and Organic Ions*

#### *3.2.2.1. Inorganic Ions*

Figure 4 illustrates single point adsorption coefficients of PFOA and PFOS on the ACFs in adsorption experiments from water containing 10 mM, 50 mM and 200 mM  $\text{Na}_2\text{SO}_4$ . The various ACFs show opposite trends in their response to the increasing salt content. The adsorption

affinities of PFOA and PFOS on VS and FC15, which have a higher density of positively charged sites at pH 7 (according to  $PZC \geq 7$  and  $AEC > CEC$  at pH 7), slightly decrease with an increase of  $Na_2SO_4$  concentration.

A stronger and opposite trend is observed for WK and FC10, which have a higher density of negative surface charges ( $PZC \leq 7$ ,  $CEC > AEC$  at pH 7). In this case  $K_d$  values increase by 1 to 1.5 orders of magnitude, with the strongest effect for WK, having the highest CEC. This illustrates that electrostatic attraction and repulsion of the two PFAS towards cationic and anionic surface sites play a significant role in their adsorption. However, repulsive interactions are obviously more affected by IS effects. Attractive electrostatic interactions involved in adsorption of organic ions are short-range interactions as the adsorbate comes into direct contact with the bare surface. In this case, the EDL compression effect at increased IS is not relevant, as the EDL is beyond the interaction distance. Thus, the effect of the salt addition on adsorption affinity of PFOA and PFOS on the ACFs (see Figure 4) is rather due to a weak competition of sulfate ions (in mM concentrations) and the PFAS anions (in  $\mu M$  concentration). In this respect, PFOA and PFOS behave similarly, indicating that it is the superposition of hydrophobic interactions and electrostatic attraction that leads to strong adsorption, which cannot be easily outcompeted by inorganic ions.

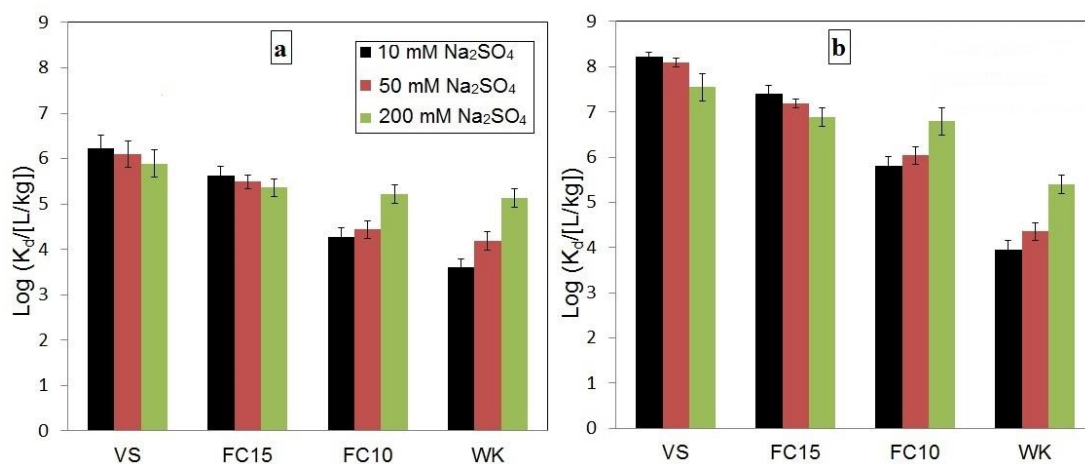


Figure 4. Single point adsorption coefficient  $K_d$  of PFOA (a) and PFOS (b) on four ACFs from water containing different concentrations of  $Na_2SO_4$ . Experimental conditions:  $C_0 = 1$  mg/L PFOA or PFOS in x mM  $Na_2SO_4$ ; adsorbent dosage: 0.1 g/L; pH = 7). The error bars are the maximum deviation of single values from the mean value of 3 experiments.

Electrostatic repulsion can be a longer-distance interaction, i.e. in this case shielding of anionic sites by the compressed EDL at high IS comes into play. This is observed in the case of the ACFs bearing a high density of negative charges at pH 7, i.e. FC10 and WK. Consequently, the various ACFs have comparable adsorption affinities for PFOA and PFOS from solutions containing 200 mM Na<sub>2</sub>SO<sub>4</sub>, although in 10 mM Na<sub>2</sub>SO<sub>4</sub> they differ significantly. Note that the loading of the PFAS on the ACFs in adsorption experiments from solutions having various IS concentrations (Figure 4) is still below the AEC of the ACFs in all cases. These results deliver two messages: I) the effect of ionic strength upon adsorption of PFOA and PFOS on AC depends upon the surface chemistry of the adsorbent, and II) electrostatic repulsion appears to be the main reason for a low adsorption affinity of some ACs for PFOA and PFOS, at least at low loadings.

#### 3.2.2.2. Organic Ions

As NOM is a ubiquitous component of surface and ground water, it is important to consider its potential effects on PFAS adsorption. For this purpose, a standard material representative for surface water NOM, Suwannee River natural organic matter (SRNOM) (W. et al., 2015), was used. NOM consists of refractory macromolecules with aromatic and aliphatic regions bearing acidic functional groups such as carboxylic acid groups (Rosario-Ortiz, 2014) and thus carry negative charges at neutral pH. Figure 5 shows adsorption of PFOA and PFOS on ACFs in presence of 5 mg/L SRNOM at pH 7 and pH 3. It was expected that SRNOM containing organic anionic molecules would compete with adsorption of PFOA and PFOS anions. However, no considerable decrease was observed in adsorption affinity of PFOA and PFOS on all ACFs in presence of 5 to 20 mg/L NOM at pH 7 as well as at pH 3 (data not presented here).

Yu et al. (Yu et al., 2012) reported that effluent organic matters (EfOM) with low-molecular-weight compounds (molecular weight < 1 kDa) significantly reduce the adsorption of PFOA and PFOS on a microporous powder AC (mean pore diameter 1.3 nm), although they reported that the effect of large-molecular-weight compounds of EfOM (molecular weight > 30 kDa) was much lower. Taking an average molar mass of about 24,000 g/mol (24 kDa) for SRNOM (Wagoner et al., 1997), the microporous ACF materials probably exert a size exclusion effect on NOM sufficient to prevent surface coverage and pore blockage. Obviously, the nature of NOM is an important factor for its effect on AC adsorption performance.

### 3.2.3. Adsorption as a Function of pH

Increasing adsorption of PFOA and PFOS on various kinds of ACs when pH falls below their PZC values has been reported previously (Yu et al., 2009; Deng et al., 2015; Chen et al., 2017). This was attributed to the increasing density of positively charged sites on AC, and thus stronger electrostatic attractions towards the anions of PFOA and PFOS. Figure 6 shows single point adsorption coefficients at pH 8, 7, 3 and 1.5, respectively, illustrating that adsorption affinity of PFOA and PFOS on ACFs increases with decreasing pH from pH 8 to pH 1.5.

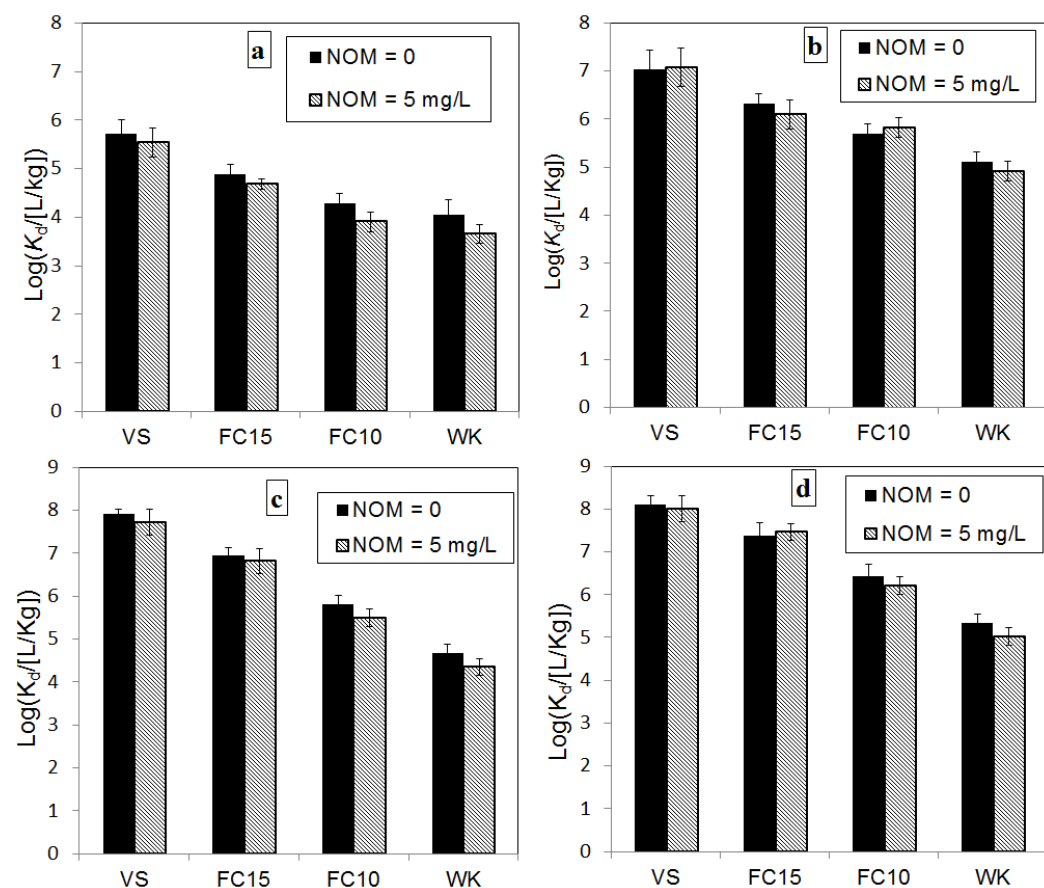


Figure 5. Single point adsorption coefficient  $K_d$  of PFOA (a and b) and PFOS (c and d) on the ACFs at pH 7 (a and c) and pH 3 (b and d). Experimental conditions:  $C_0 = 1$  mg/L PFOA or PFOS in 10 mM  $\text{Na}_2\text{SO}_4$  with and without SRNOM; adsorbent dosage: 0.02 g/L for VS and FC15, 0.1 for FC10 and 0.5 g/L for WK. The error bars are the maximum deviation of single values from the mean value of 3 experiments.

Interestingly, by decreasing pH from 8 to 1.5 adsorption of PFOA increased significantly more than that of PFOS (see Figure 6). Yu et al. (Yu et al., 2009) and Deng et al. (Deng et al., 2015) also reported that decreasing solution pH from pH 7 to pH 3 has a stronger effect on adsorption of

PFOA than on that of PFOS. They considered a  $pK_a$  of PFOA of 2.5 and claimed that at pH 3, PFOA is partly present in a protonated, neutral form having a higher hydrophobicity than that of the anion. However, more recent studies agree on a  $pK_a$  of PFOA  $\leq 1$ . Therefore, other effects should play a role in this regard. The fact that PFOA and PFOS react similarly towards changes in ionic strength but that PFOA is more sensitive to pH changes might point to specific interactions involving the carboxylate group.

Cheng et al. (Cheng et al., 2009) observed the formation of remarkably stable  $(PFOA)_2H^-$  dimers in electrospray ionization at a solution pH below  $\sim 4$  and micromolar PFOA concentrations. The resulting dimers are not only larger but also their charge density is significantly reduced in comparison with the free PFOA anions, which would lead to improved adsorption affinity. This type of interaction can be understood as a  $(-)$ CAHB between two PFOA molecules.

On the other hand, formation of exceptionally strong  $(-)$ CAHB between weak acids and functional groups of carbon-based adsorbents can enhance the uptake of weak acids (Teixidó et al., 2011; Li et al., 2013; Pignatello et al., 2017). In fact, it was revealed that  $(-)$ CAHB can be formed between a carboxyl group of an ionizable organic compound as adsorbate and a surface carboxyl or hydroxyl group of the adsorbent having a comparable  $pK_a$ . However, only solute–surface H-bonds that are much stronger than solute–water and water–surface H-bonds can contribute substantially to overall adsorption. The  $pK_a$  of carboxylic groups on carbonaceous adsorbents are in the range of 3-6 (Strelko et al., 2002). If the  $pK_a$  of PFOA is considered to be between 0 and 1, then the requirement of  $\Delta pK_a = pK_{a, DH} - pK_{a, AH^+} < 5$  is probably met and  $(-)$ CAHBs can be formed. However, PFOS with  $pK_a$  -3.5 does not meet the stated condition for formation of  $(-)$ CAHB.

These types of  $(-)$ CAHB are supported by increasing proton concentrations, thus, they might be an explanation for increasing PFOA adsorption at lower pH. However, at pH 7 the contribution to the overall PFOA adsorption is probably low. This is substantiated by the following findings: I) PFOS, which is unlikely to form such bonds, is adsorbed more preferably at all ACFs studied; II) PFOA adsorption correlates with the density of positive charges, whereas it is inversely correlated with the density of carboxylic groups on the surface of the ACFs; and III) in adsorbate/adsorbent systems where  $(-)$ CAHB were discussed to be relevant, the increase of ionic strength up to 0.1 M generally had only minor effects on the extent of adsorption. In contrast, we found a strong ionic strength impact for O-rich ACFs, which is similar for PFOA and PFOS. Thus,

we conclude that electrostatic repulsion plays a stronger role than (–)CAHB formation in the interaction of the two PFAS with carboxylic groups of the ACFs.

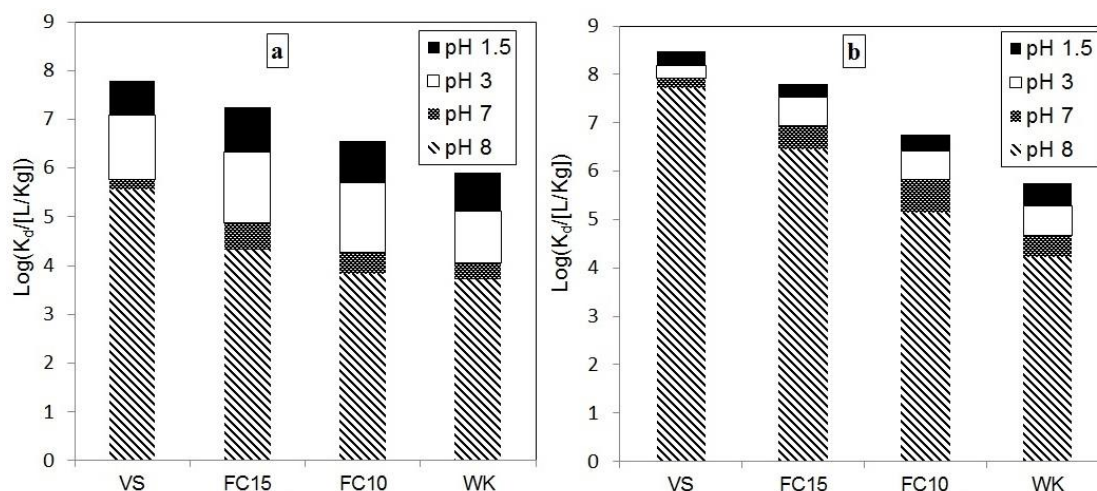


Figure 6. Single point adsorption coefficients  $K_d$  of PFOA (a) and PFOS (b) on the ACFs at pH 8, pH 7, pH 3 and pH 1.5. Experimental conditions:  $C_0 = 1$  mg/L PFOA or PFOS in 10 mM  $\text{Na}_2\text{SO}_4$ ; adsorbent dosage: 0.02 g/L for VS and FC15, 0.1 g/L for FC10 and 0.5 g/L for WK.

### 3.2.4. Adsorption from Real Groundwater

Our results from adsorption of PFOA and PFOS show very high adsorption affinities of the compounds towards two of the ACFs, namely VS and FC15. Furthermore, the results prove that this high adsorption affinity is not significantly influenced by potential competitive effects of organic and inorganic ions. Therefore, adsorption affinities of PFOA and PFOS on the ACFs from a real groundwater should be comparable with what we observed earlier in adsorption of PFOA and PFOS from synthetic water. Leuna is a former refinery site near Merseburg in the eastern part of Germany. It has been a center of chemical production for about 100 years. Groundwater sampled from a well with a PFOS content of 4.6  $\mu\text{g/L}$  was used for adsorption experiments with FC15. In addition to PFOS, this water contains other organic compounds, including benzene (3.5 mg/L) and methyl tert-butyl ether (MTBE) (1.9 mg/L). The  $K_d$  in adsorption of PFOS from this groundwater (pH  $\sim 7.6$ ) on FC15 at  $C_e = 1$   $\mu\text{g/L}$  is  $6.5 \times 10^6$  L/kg (see adsorption isotherms in Figure 9S and Table 2S). This  $K_d$  falls between the  $K_d$  values in adsorption of PFOS at pH 7 and pH 8 ( $7.9 \times 10^6$  and  $2.5 \times 10^6$  L/kg, respectively) in synthetic water reported in Figure 6 for the nearly the same



$C_e$ . Thus, the high adsorption affinity of this ACF for PFOS also applies for a real groundwater matrix.

#### **4. Conclusions**

Microporous ACFs with optimal surface properties allow excellent adsorption of PFOA and PFOS with only minor competition by NOM, presumably due to size-exclusion of these anionic macromolecules. A correlation between adsorption of PFOA and PFOS and the presence of a narrow micropore fraction (width of 1-2 nm) was found. However, neither the differences in total BET surface area nor available pore volume in a certain size range can explain the vastly different adsorption of PFAS on the various ACFs. Thus, we conclude that surface chemistry plays the major role. AEC at pH 7 and PZC are good indicators of chemical surface properties suitable for adsorption of anionic PFAS. The maximum molar loading of PFOS on the best adsorbing ACF reaches the molar anion exchange capacity of this carbon. At the same time it corresponds to a pore filling degree of only 15% (considering the pore volume in the 1-2 nm pore size range). This demonstrates the importance of charge-balancing sites on the AC surface for adsorption of PFAS anions. Clearly, the superposition of hydrophobic interactions and electrostatic attraction between PFAS anions and positively charged sites of AC leads to exceptionally high adsorption affinities. Sorption equilibria of such interactions cannot be predicted by conventional approaches, e.g. based on octanol-water partition coefficients. The effect of inorganic ions on PFAS adsorption at circumneutral pH depends on the surface chemistry of the AC. Adsorption is only slightly suppressed by inorganic ions for ACFs with  $PZC > 7$  and  $CEC < AEC$  due to minor competition effects for anion binding. In contrast, ACFs with  $PZC < 7$  and  $CEC > AEC$  benefit from high ionic strength due to suppression of electrostatic repulsion.

Ideal AC adsorbents for removal of organic anions such as PFOA and PFOS should have a low heteroatom content, leading to a low surface polarity and sufficient density of carbon-based positive charges at circumneutral pH.

#### **Acknowledgements**

Dr. Hans Uhlig (Institut für Nichtklassische Chemie e.V.) is acknowledged for conducting the microporosity analysis.

## References

- [1] S. Fujii, C. Polprasert, S. Tanaka, N.P. Hong Lien, Y. Qiu, New POPs in the water environment: distribution, bioaccumulation and treatment of perfluorinated compounds – a review paper, *J. Water Supply Res. T.* 56 (2007) 313-326.
- [2] F. Schuricht, E.S. Borovinskaya, W. Reschetilowski, Removal of perfluorinated surfactants from wastewater by adsorption and ion exchange — Influence of material properties, sorption mechanism and modeling, *J. Environ. Sci.* 54 (2017) 160-170.
- [3] O.S. Arvaniti, A.S. Stasinakis, Review on the occurrence, fate and removal of perfluorinated compounds during wastewater treatment, *Sci. Total Environ.* 524-525 (2015) 81-92.
- [4] M.F. Rahman, S. Peldszus, W.B. Anderson, Behaviour and fate of perfluoroalkyl and polyfluoroalkyl substances (PFASs) in drinking water treatment: A review, *Water Res.* 50 (2014) 318-340.
- [5] W. Chen, X. Zhang, M. Mamadiev, Z. Wang, Sorption of perfluorooctane sulfonate and perfluorooctanoate on polyacrylonitrile fiber-derived activated carbon fibers: in comparison with activated carbon, *RSC Adv.* 7 (2017) 927-938.
- [6] S. Deng, Y. Nie, Z. Du, Q. Huang, P. Meng, B. Wang, J. Huang, G. Yu, Enhanced adsorption of perfluorooctane sulfonate and perfluorooctanoate by bamboo-derived granular activated carbon, *J. Hazard. Mater.* 282 (2015) 150-157.
- [7] D. Zhang, Q. Luo, B. Gao, S.-Y.D. Chiang, D. Woodward, Q. Huang, Sorption of perfluorooctanoic acid, perfluorooctane sulfonate and perfluoroheptanoic acid on granular activated carbon, *Chemosphere* 144 (2016) 2336-2342.
- [8] Y. Qu, C. Zhang, F. Li, X. Bo, G. Liu, Q. Zhou, Equilibrium and kinetics study on the adsorption of perfluorooctanoic acid from aqueous solution onto powdered activated carbon, *J. Hazard. Mater.* 169 (2009) 146-152.
- [9] V. Ochoa-Herrera, R. Sierra-Alvarez, Removal of perfluorinated surfactants by sorption onto granular activated carbon, zeolite and sludge, *Chemosphere* 72 (2008) 1588-1593.
- [10] P. Punyapalakul, K. Suksomboon, P. Prarat, S. Khaodhiar, Effects of Surface Functional Groups and Porous Structures on Adsorption and Recovery of Perfluorinated Compounds by Inorganic Porous Silicas, *Sep. Sci. Technol.* 48 (2013) 775-788.
- [11] Q. Yu, R. Zhang, S. Deng, J. Huang, G. Yu, Sorption of perfluorooctane sulfonate and perfluorooctanoate on activated carbons and resin: Kinetic and isotherm study, *Water Res.* 43 (2009) 1150-1158.
- [12] Z. Du, S. Deng, Y. Bei, Q. Huang, B. Wang, J. Huang, G. Yu, Adsorption behavior and mechanism of perfluorinated compounds on various adsorbents—A review, *J. Hazard. Mater.* 274 (2014) 443-454.
- [13] Y. Zhi, J. Liu, Adsorption of perfluoroalkyl acids by carbonaceous adsorbents: Effect of carbon surface chemistry, *Environ. Pollut.* 202 (2015) 168-176.
- [14] F.A. Brooke D., Nwaogu TA., Environmental Risk Evaluation Report: Perfluorooctane Sulfonate (PFOS), UK Environment Agency (2004).
- [15] K.-U. Goss, The pKa Values of PFOA and Other Highly Fluorinated Carboxylic Acids, *Environ. Sci. Technol.* 42 (2008) 456-458.
- [16] A. Baggioli, M. Sansotera, W. Navarrini, Thermodynamics of aqueous perfluorooctanoic acid (PFOA) and 4,8-dioxa-3H-perfluorononanoic acid (DONA) from DFT calculations: Insights into degradation initiation, *Chemosphere* 193 (2018) 1063-1070.
- [17] J. Cheng, E. Psillakis, M.R. Hoffmann, A.J. Colussi, Acid Dissociation versus Molecular Association of Perfluoroalkyl Oxoacids: Environmental Implications, *J. Phys. Chem. A* 113 (2009) 8152-8156.
- [18] H.P.H. Arp, C. Niederer, K.-U. Goss, Predicting the Partitioning Behavior of Various Highly Fluorinated Compounds, *Environ. Sci. Technol.* 40 (2006) 7298-7304.
- [19] H.P. Boehm, Chemical Identification of Surface Groups, in: D.D. Eley, H. Pines, P.B. Weisz (Eds.) *Advances in Catalysis*, Academic Press 1966, pp. 179-274.
- [20] A.M.P. Oen, B. Beckingham, U. Ghosh, M.E. Kruså, R.G. Luthy, T. Hartnik, T. Henriksen, G. Cornelissen, Sorption of Organic Compounds to Fresh and Field-Aged Activated Carbons in Soils and Sediments, *Environ. Sci. Technol.* 46 (2012) 810-817.
- [21] H.-S. Hsieh, J.J. Pignatello, Activated carbon-mediated base hydrolysis of alkyl bromides, *Appl. Catal. B* 211 (2017) 68-78.
- [22] M. Kah, G. Sigmund, F. Xiao, T. Hofmann, Sorption of ionizable and ionic organic compounds to biochar, activated carbon and other carbonaceous materials, *Water Res.* 124 (2017) 673-692.
- [23] G. Gilli, P. Gilli, Towards an unified hydrogen-bond theory, *J. Mol. Struct.* 552 (2000) 1-15.

- [24] X. Li, J.J. Pignatello, Y. Wang, B. Xing, New Insight into Adsorption Mechanism of Ionizable Compounds on Carbon Nanotubes, *Environ. Sci. Technol.* 47 (2013) 8334-8341.
- [25] M. Teixidó, J.J. Pignatello, J.L. Beltrán, M. Granados, J. Peccia, Speciation of the Ionizable Antibiotic Sulfamethazine on Black Carbon (Biochar), *Environ. Sci. Technol.* 45 (2011) 10020-10027.
- [26] P. Gilli, L. Pretto, V. Bertolasi, G. Gilli, Predicting Hydrogen-Bond Strengths from Acid-Base Molecular Properties. The  $pK_a$  Slide Rule: Toward the Solution of a Long-Lasting Problem, *Acc. Chem. Res.* 42 (2009) 33-44.
- [27] Q. Yu, S. Deng, G. Yu, Selective removal of perfluorooctane sulfonate from aqueous solution using chitosan-based molecularly imprinted polymer adsorbents, *Water Res.* 42 (2008) 3089-3097.
- [28] C.P. Higgins, R.G. Luthy, Sorption of Perfluorinated Surfactants on Sediments, *Environ. Sci. Technol.* 40 (2006) 7251-7256.
- [29] F. Wang, K. Shih, Adsorption of perfluorooctanesulfonate (PFOS) and perfluorooctanoate (PFOA) on alumina: Influence of solution pH and cations, *Water Res.* 45 (2011) 2925-2930.
- [30] Y.-N. Kwon, K. Shih, C. Tang, J.O. Leckie, Adsorption of perfluorinated compounds on thin-film composite polyamide membranes, *J. Appl. Polym. Sci.* 124 (2012) 1042-1049.
- [31] Z. Du, S. Deng, Y. Chen, B. Wang, J. Huang, Y. Wang, G. Yu, Removal of perfluorinated carboxylates from washing wastewater of perfluorooctanesulfonyl fluoride using activated carbons and resins, *J. Hazard. Mater.* 286 (2015) 136-143.
- [32] Q. Zhang, S. Deng, G. Yu, J. Huang, Removal of perfluorooctane sulfonate from aqueous solution by crosslinked chitosan beads: Sorption kinetics and uptake mechanism, *Bioresour. Technol.* 102 (2011) 2265-2271.
- [33] T.D. Appleman, E.R.V. Dickenson, C. Bellona, C.P. Higgins, Nanofiltration and granular activated carbon treatment of perfluoroalkyl acids, *J. Hazard. Mater.* 260 (2013) 740-746.
- [34] D.N. Kothawala, S.J. Köhler, A. Östlund, K. Wiberg, L. Ahrens, Influence of dissolved organic matter concentration and composition on the removal efficiency of perfluoroalkyl substances (PFASs) during drinking water treatment, *Water Res.* 121 (2017) 320-328.
- [35] Y. Matsui, Y. Fukuda, T. Inoue, T. Matsushita, Effect of natural organic matter on powdered activated carbon adsorption of trace contaminants: characteristics and mechanism of competitive adsorption, *Water Res.* 37 (2003) 4413-4424.
- [36] Y. Matsui, D.R.U. Knappe, R. Takagi, Pesticide Adsorption by Granular Activated Carbon Adsorbers. 1. Effect of Natural Organic Matter Preloading on Removal Rates and Model Simplification, *Environ. Sci. Technol.* 36 (2002) 3426-3431.
- [37] J.E. Kilduff, T. Karanfil, W.J. Weber, Competitive Effects of Nondisplaceable Organic Compounds on Trichloroethylene Uptake by Activated Carbon. I. Thermodynamic Predictions and Model Sensitivity Analyses, *J. Colloid Interface Sci.* 205 (1998) 271-279.
- [38] M.S. Shafeeyan, W.M.A.W. Daud, A. Houshmand, A. Shamiri, A review on surface modification of activated carbon for carbon dioxide adsorption, *J. Anal. Appl. Pyrol.* 89 (2010) 143-151.
- [39] P.J.M. Carrott, J.M.V. Nabais, M.M.L. Ribeiro Carrott, J.A. Pajares, Preparation of activated carbon fibres from acrylic textile fibres, *Carbon* 39 (2001) 1543-1555.
- [40] C.U. Pittman, G.R. He, B. Wu, S.D. Gardner, Chemical modification of carbon fiber surfaces by nitric acid oxidation followed by reaction with tetraethylenepentamine, *Carbon* 35 (1997) 317-331.
- [41] S.J. Driver, E.M. Perdue, Acidic Functional Groups of Suwannee River Natural Organic Matter, Humic Acids, and Fulvic Acids, *Advances in the Physicochemical Characterization of Dissolved Organic Matter: Impact on Natural and Engineered Systems*, American Chemical Society 2014, pp. 75-86.
- [42] B.M. Babić, S.K. Milonjić, M.J. Polovina, B.V. Kaludierović, Point of zero charge and intrinsic equilibrium constants of activated carbon cloth, *Carbon* 37 (1999) 477-481.
- [43] R.B. Fidel, D.A. Laird, M.L. Thompson, Evaluation of Modified Boehm Titration Methods for Use with Biochars, *J. Environ. Qual.* 42 (2013) 1771-1778.
- [44] I. Langmuir, THE ADSORPTION OF GASES ON PLANE SURFACES OF GLASS, MICA AND PLATINUM, *J. Am. Chem. Soc.* 40 (1918) 1361-1403.
- [45] D. Kratochvil, B. Volesky, Advances in the biosorption of heavy metals, *Trends Biotechnol.* 16 (1998) 291-300.
- [46] J.-C. Jacquesy, J.-P. Gesson, M.-P. Jouannetaud, Protonated Phenol Derivatives as Reactive Species, *Rev. Chem. Intermed.* 9 (1988) 1-26.
- [47] R. Gómez-Bombarelli, E. Calle, J. Casado, Mechanisms of Lactone Hydrolysis in Acidic Conditions, *J. Org. Chem.* 78 (2013) 6880-6889.
- [48] G.A. Olah, A.T. Ku, Stable carbonium ions. CVIII. Protonated lactones and their cleavage reactions in fluorosulfuric acid-antimony pentafluoride solution, *J. Org. Chem.* 35 (1970) 3916-3922.

- [49] E. Papirer, J. Dentzer, S. Li, J.B. Donnet, Surface groups on nitric acid oxidized carbon black samples determined by chemical and thermodesorption analyses, *Carbon* 29 (1991) 69-72.
- [50] H.P. Boehm, Some aspects of the surface chemistry of carbon blacks and other carbons, *Carbon* 32 (1994) 759-769.
- [51] R.W. Walters, R.G. Luthy, Equilibrium adsorption of polycyclic aromatic hydrocarbons from water onto activated carbon, *Environ. Sci. Technol.* 18 (1984) 395-403.
- [52] R.A. Dobbs, Cohen, J. M., Carbon Adsorption Isotherms For Toxic Organics, U.S. EPA Cincinnati, OH, 1980.
- [53] E. Papirer, S. Li, J.-B. Donnet, Contribution to the study of basic surface groups on carbons, *Carbon* 25 (1987) 243-247.
- [54] U. Zielke, K.J. Hüttinger, W.P. Hoffman, Surface-oxidized carbon fibers: I. Surface structure and chemistry, *Carbon* 34 (1996) 983-998.
- [55] G.N. W., M. Daniel, H. Norbert, M.P. A., P.E. Michael, Suwannee River Natural Organic Matter: Isolation of the 2R101N Reference Sample by Reverse Osmosis, *Environ. Eng. Sci.* 32 (2015) 38-44.
- [56] F. Rosario-Ortiz, Advances in the Physicochemical Characterization of Dissolved Organic Matter: Impact on Natural and Engineered Systems, ACS Symposium Series, American Chemical Society, 2014, pp. 0.
- [57] J. Yu, L. Lv, P. Lan, S. Zhang, B. Pan, W. Zhang, Effect of effluent organic matter on the adsorption of perfluorinated compounds onto activated carbon, *J. Hazard. Mater.* 225-226 (2012) 99-106.
- [58] D.B. Wagoner, R.F. Christman, G. Cauchon, R. Paulson, Molar Mass and Size of Suwannee River Natural Organic Matter Using Multi-Angle Laser Light Scattering, *Environ. Sci. Technol.* 31 (1997) 937-941.
- [59] J.J. Pignatello, W.A. Mitch, W. Xu, Activity and Reactivity of Pyrogenic Carbonaceous Matter toward Organic Compounds, *Environ. Sci. Technol.* 51 (2017) 8893-8908.
- [60] V. Strelko, D.J. Malik, M. Streat, Characterisation of the surface of oxidised carbon adsorbents, *Carbon* 40 (2002) 95-104.



Appendix: supporting information to

**Understanding the effect of carbon surface chemistry on adsorption of perfluorinated alkyl substances**

Navid Saeidi, Frank-Dieter Kopinke, Anett Georgi

*Helmholtz Centre for Environmental Research – UFZ, Department of Environmental Engineering,  
D-04318 Leipzig, Germany*

(10 Pages, 2 Tables and 9 Figures)

**Figure 1Sa** shows a comparison between pore size distributions of the ACFs and that of a coal-derived commercial powder AC (Chemviron) obtained by  $N_2$  adsorption at  $-196\text{ }^{\circ}\text{C}$ . The results show that the pore size distributions of the ACFs are predominantly in the micropore range, whereas Chemviron AC exposes a broader distribution, including micro-, meso- and macropores. Figure 1Sb illustrates the micropore size distribution of the ACFs obtained by  $CO_2$  adsorption at  $0\text{ }^{\circ}\text{C}$ .

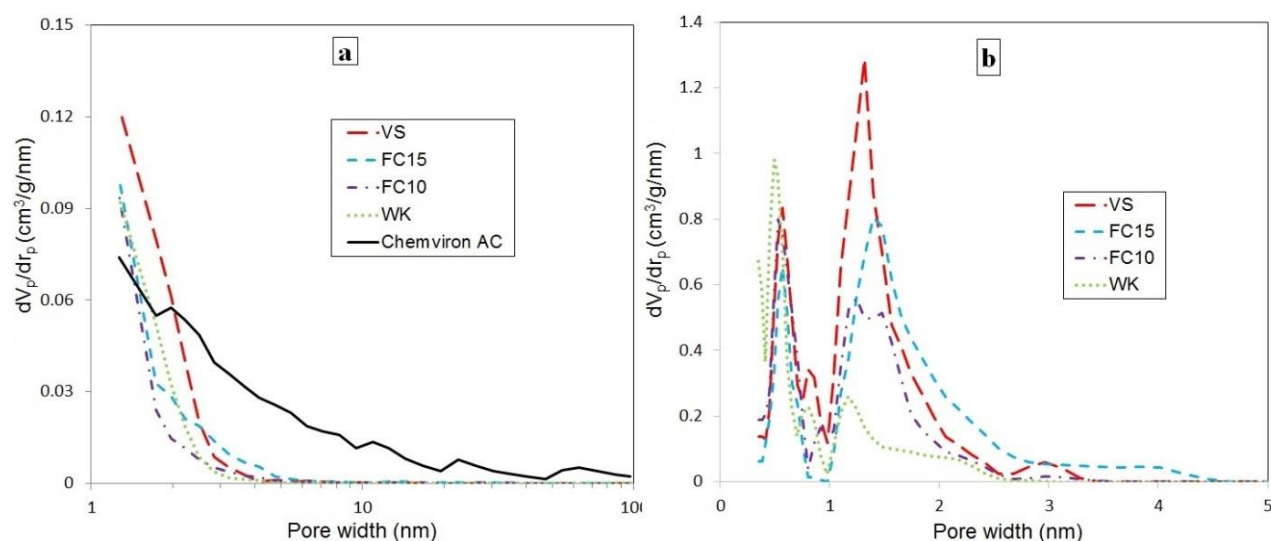


Figure 1S. Pore size distributions of the ACFs and Chemviron powder AC: a) analysis of mesopores by means of  $N_2$  adsorption/desorption results and BJH method; b) analysis of micropores by means of  $CO_2$  adsorption results and NLDFT analysis.

**Figure 2S** shows TPD profiles of the ACFs. From the thermograms it is obvious that WK released the highest amount of CO<sub>2</sub>, whereas VS released low amounts of both CO and CO<sub>2</sub> compared to the others.

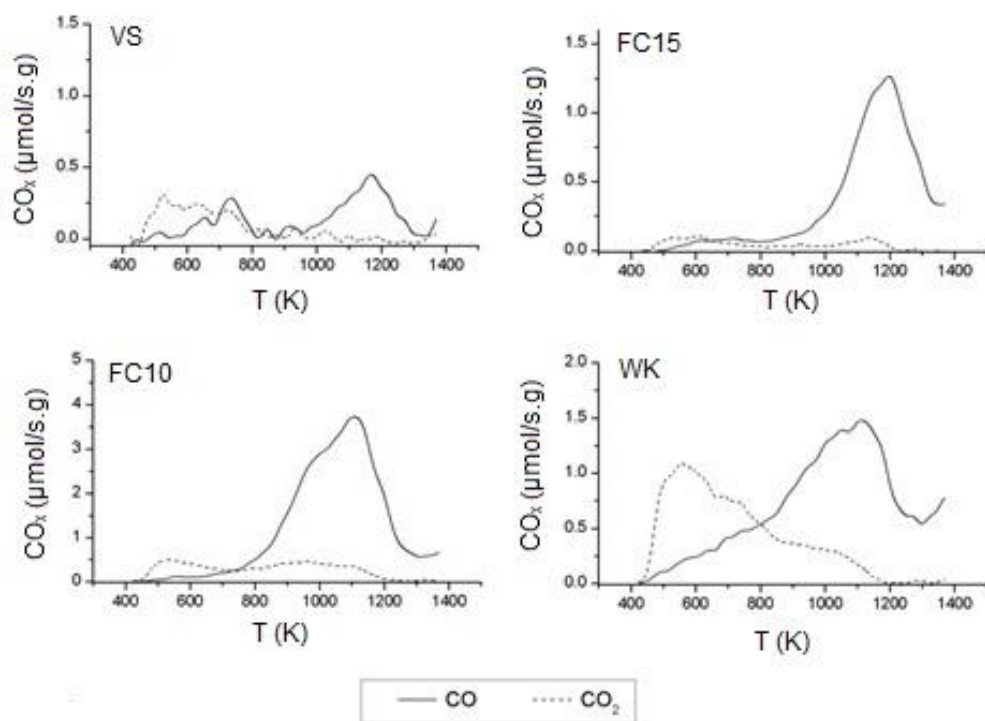


Figure 2S. TPD profiles of the ACFs (heating rate 10 K/min). The dashed lines represent the release of CO<sub>2</sub> and solid lines represent release of CO.

**Figure 3S** shows that AEC and CEC follow opposite trends, meaning that the ACF with the highest AEC has the lowest CEC (VS), and the ACF with the lowest AEC has the highest CEC (WK).

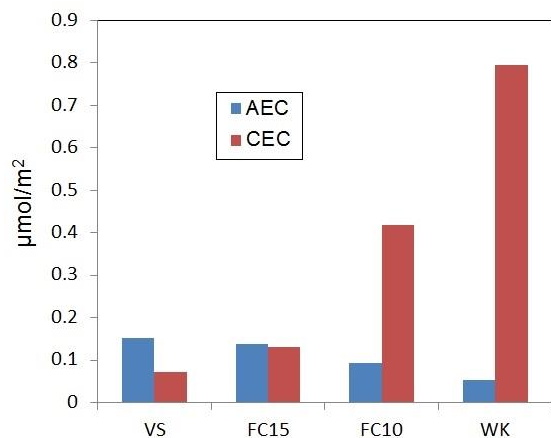


Figure 3S. Comparison between anion (AEC) and cation (CEC) exchange capacities of the ACFs used.



**Figure 4S** compares CEC and carboxylic groups' concentration of the ACFs.

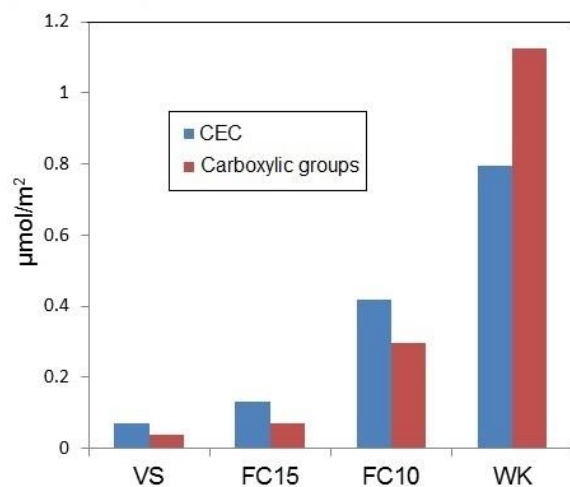


Figure 4S. Comparison between CEC and concentration of carboxylic groups of the ACFs.

**Figure 5S** shows the positive correlation between AEC of the ACFs and micropore volume in the range of 1-2 nm pores.

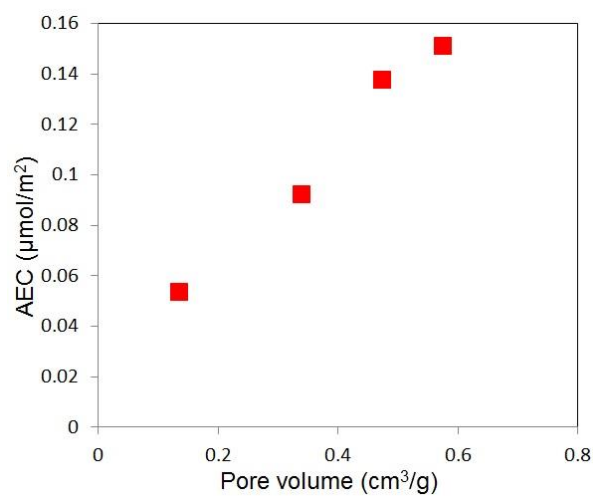


Figure 5S. Correlation between AEC of the ACFs and micropore volume of 1-2 nm pores.

**Figure 6S** shows a plot of  $C_e$  against  $q_e$  from adsorption of PFOA and PFOS on the ACFs.

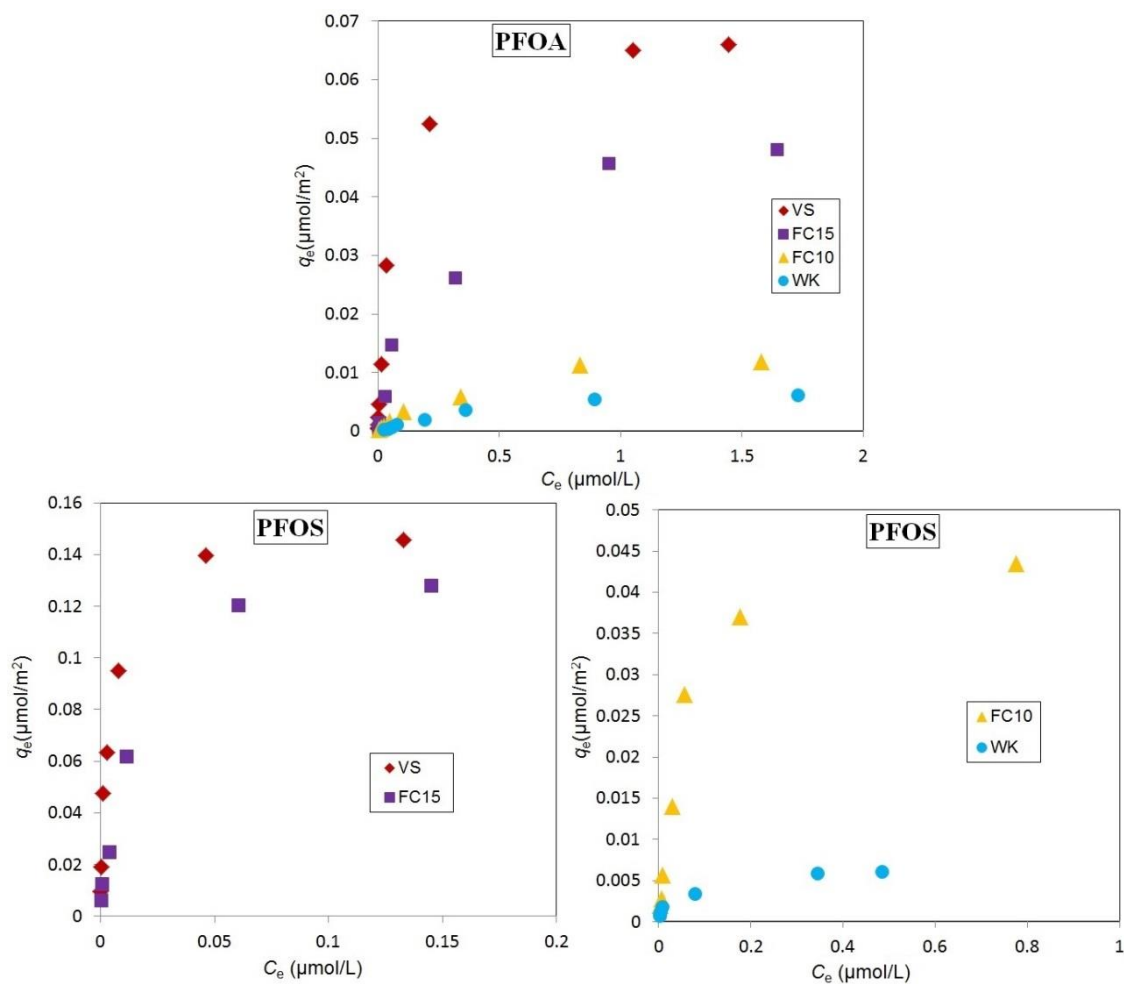


Figure 6S. Experimental adsorption data on the ACFs at pH 7.

**Table 1S** lists the isotherm parameters collected in Table 4 in terms of mass units.

Table 1S. Freundlich and Langmuir parameters for adsorption of PFOA and PFOS.

ACF adsorbent	Adsorbate	Freundlich			Langmuir		
		Log ( $K_F/[ (mg/g)/(mg/L)^n ]$ )	$n$	$R^2$	$q_m$ (mg/g)	Log ( $K_L/[L/g]$ )	$R^2$
VS	PFOA	2.70	0.74	0.975	55.6	4.69	0.998
VS	PFOS	3.43	0.57	0.976	156	5.59	0.999
FC15	PFOA	2.30	0.88	0.961	35.7	4.05	0.990
FC15	PFOS	2.91	0.58	0.985	108	5.29	0.999
FC10	PFOA	1.49	0.89	0.994	10.20	3.71	0.990
FC10	PFOS	2.63	0.88	0.976	33.3	4.56	0.998
WK	PFOA	1.00	0.98	0.977	2.08	4.06	0.986
WK	PFOS	1.92	0.79	0.991	5.00	4.39	0.979

**Figure 7S** shows correlations between adsorption parameters normalized to volume of pores with width 1-2 nm and surface properties of the ACFs.

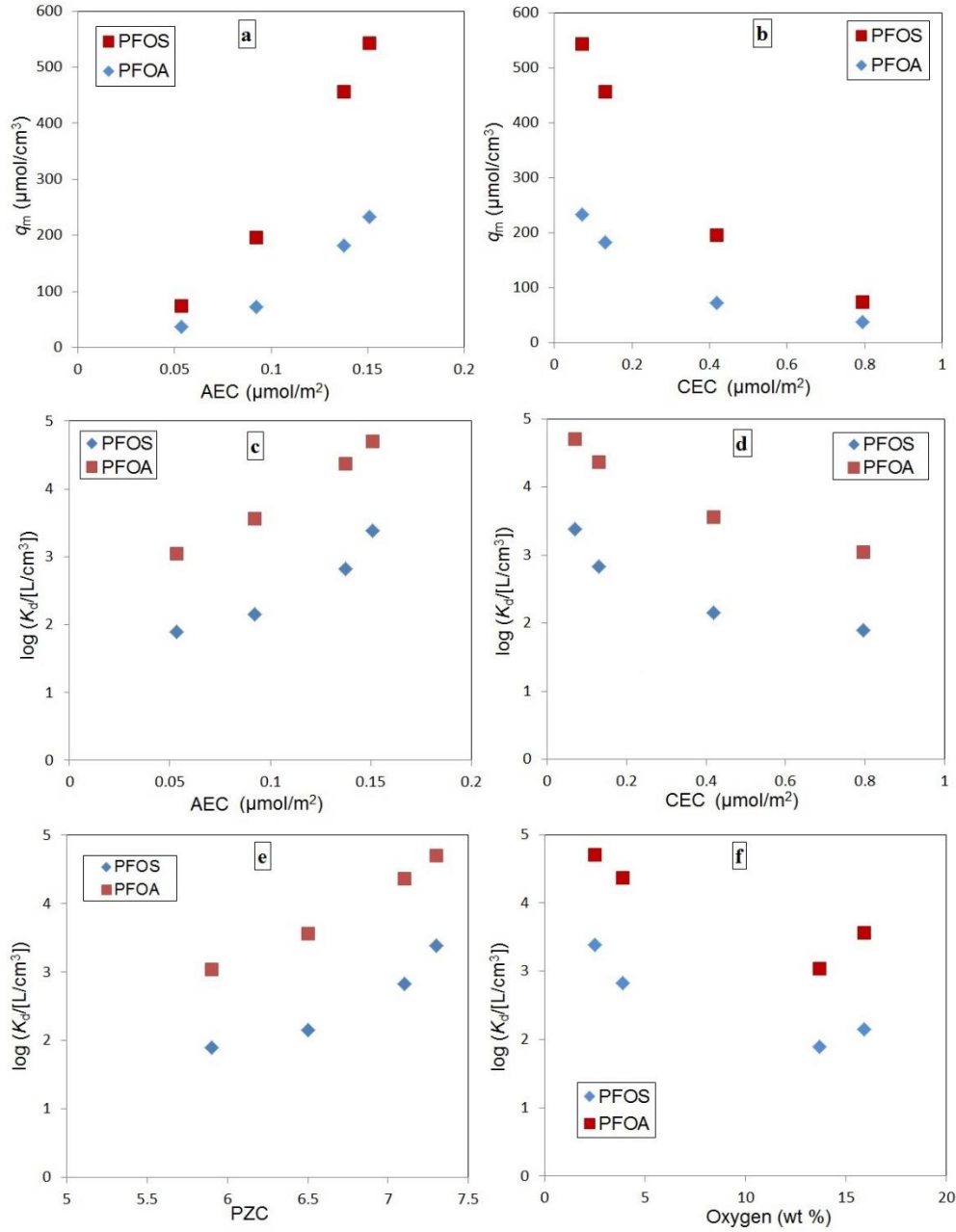


Figure 7S. Correlation between maximum loading  $q_m$  and  $K_d$  values, both normalized to pore volume in the pore width range of 1-2 nm, versus surface chemistry parameters of the ACFs:  $q_m$  vs. AEC (a) and CEC (b) and  $\log(K_d)$  ( $[\text{L}/\text{cm}^3]$ ) vs. AEC (c), CEC (d), PZC (e) and oxygen content (f) at pH 7.  $K_d$  values are calculated for  $C_{e, \text{PFOA}} = 20 \mu\text{g}/\text{L}$  ( $0.05 \mu\text{mol}/\text{L}$ ) and  $C_{e, \text{PFOS}} = 8 \mu\text{g}/\text{L}$  ( $0.016 \mu\text{mol}/\text{L}$ ).

**Figure 8S** illustrates the correlation between AEC and CEC.

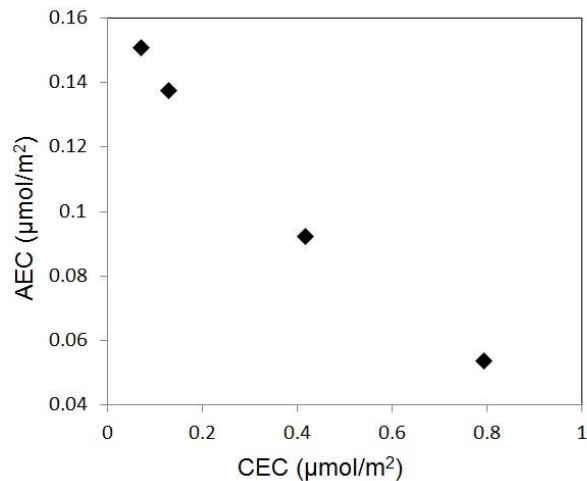


Figure 8S. Correlation between AEC and CEC of four ACFs.

**Figure 9S** shows the adsorption isotherms of PFOS from real groundwater on FC15.

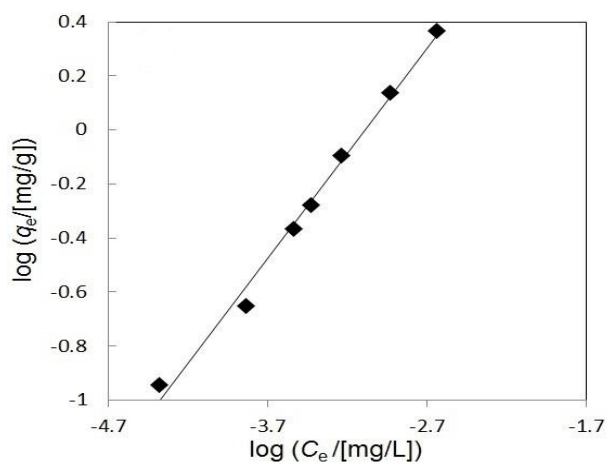


Figure 9S. Experimental data in adsorption of PFOS from real groundwater on FC15 fitted with Freundlich equation.

**Table 2S** lists the corresponding adsorption parameters.

Table 2S. Freundlich parameters for adsorption of PFOS from Leuna groundwater.

ACF adsorbent	Adsorbate	Log (K <sub>F</sub> /[(mg/g)/(mg/L) <sup>n</sup> ])	n	R <sup>2</sup>
FC15	PFOS	2.40	0.77	0.991



### 3.2. What is specific in adsorption of perfluoroalkyl acids on carbon materials

Navid Saeidi, Frank-Dieter Kopinke, Anett Georgi \*

*Helmholtz Centre for Environmental Research – UFZ, Department of Environmental Engineering,  
D-04318 Leipzig, Germany*

#### **Abstract**

Various activated carbon products show wide variability in adsorption performance towards perfluoroalkyl acids (PFAAs) and predictive tools are largely missing. In order to gain a better understanding on the adsorption mechanisms of PFAAs, perfluorooctanoic acid (PFOA) was compared with its fluorine-free analogon octanoic acid (OCA) as well as phenanthrene (nonionic) in terms of their response towards changes in carbon surface chemistry. For this approach, a commercial activated carbon felt (ACF) with high content of acidic surface groups was modified by amino-functionalisation as well as thermal defunctionalisation in  $H_2$  (yielding DeCACF). While improvement by amino-functionalisation was moderate, defunctionalisation drastically enhanced adsorption of PFOA and other PFAAs. In comparison, OCA and phenanthrene were much less affected. Electrostatic interactions and charge compensation provided by positively charged surface sites (quantified by their anion exchange capacity) are obviously more crucial for PFAAs than for common organic acids (such as the tested OCA). A possible reason is their exceptionally strong acidity with  $pK_a < 1$ . Nevertheless, at the best modified ACF material (DeCACF) the sorption coefficients ( $K_d$ ) for PFOA and perfluorooctylsulfonic acid (PFOS) at environmentally relevant concentrations reach the range of  $10^7$  L/kg which is outstanding. DeCACF provides a surface with overall low polarity (low O-content), low density of acidic sites causing electrostatic repulsion, but nevertheless a sufficient density of charge-balancing sites for organic anions. The results of the present study contribute to an optimised selection of adsorbents for PFAA adsorption from water considering also various salt matrices and the presence of natural organic matter.

#### **Keywords:**

PFOA; PFOS; PFBA; Octanoic acid; Activated carbon; Adsorption mechanism.

---

\* Corresponding author e-mail: anett.georgi@ufz.de

<b>Nomenclature</b>			
AC	activated carbon	PFBA	perfluorobutanoic acid
ACF	activated carbon felt	PFOA	perfluorooctanoic acid
AEC	anion exchange capacity	PFOS	perfluorooctylsulfonic acid
CACF	commercial activated carbon felt	PHE	phenanthrene
CACFNH <sub>2</sub>	amino-functionalised activated carbon felt	PSD	pore size distribution
$C_0$	initial concentration of solute in solution	PZC	point of zero net proton charge
$C_e$	equilibrium concentration of solute in solution	$pK_a$	negative logarithm of the acid dissociation constant
CEC	cation exchange capacity	$q_e$	equilibrium concentration of adsorbed solute on adsorbent
DeCACF	defunctionalised activated carbon felt	$q_m$	Langmuir maximum adsorption capacity of adsorbent
$K_F$	Freundlich adsorption coefficient	$R^2$	correlation coefficient
$K_L$	Langmuir adsorption coefficient	SRNOM	Suwannee River natural organic matter
$K_d$	single-point adsorption coefficient	$t$	time
$K_{ow}$	octanol-water partitioning coefficient	TPD	temperature-programmed decomposition
$m$	mass of activated carbon felt	$V$	volume of solution
$n$	Freundlich exponent	$V_p$	pore volume
NOM	natural organic matter	$V_{total}$	total pore volume
OCA	octanoic acid	XPS	X-ray photoelectron spectroscopy
PFAAs	perfluoroalkyl acids		

## 1. Introduction

Perfluoroalkyl acids (PFAAs) are a class of fully fluorinated hydrocarbons. In the last 60 years these compounds have been used for producing non-stick, waterproof and stain-resistant coatings for various products (Teaf et al., 2019). They are the focus of current attention because of their detection in various sources of water and a rapid increase in evidence for their adverse health effects, including tumour induction, hepatotoxicity, developmental toxicity, immunotoxicity, endocrine disruption and neurotoxicity (Sznajder-Katarzyńska et al., 2019).

The compounds with eight carbon atoms, perfluorooctanoic acid (PFOA) and perfluorooctylsulfonic acid (PFOS), are the most studied PFAAs, although recent research has also revealed the occurrence of shorter-chain PFAAs in drinking water (Brendel et al., 2018; Phong Vo et al., 2020). PFOS (in 2009) and PFOA (in 2019) were added to Annex B of the Stockholm Convention on Persistent Organic Pollutants (Higgins and Field, 2017). Since June 2013, PFOA and its ammonium salt are considered as chemicals of “very high concern” by the European Chemicals Agency (T. Pancras, 2016). Thereafter, shorter-chain PFAAs and polyfluorinated compounds with smaller perfluoroalkyl structural elements have increasingly been developed as replacement compounds (Higgins and Field, 2017). Despite of some shorter-chain fluorinated

alternatives being less bioaccumulative, these compounds or their perfluorinated degradation products are still persistent in the environment (Higgins and Field, 2017; Phong Vo et al., 2020). In addition, due to the lower efficiency of the shorter-chain PFAAs, larger amounts might be needed for obtaining the same performance (Brendel et al., 2018).

Remediation of sites with PFAAs soil and groundwater contamination is extremely challenging (Arias Espana et al., 2015; Gagliano et al., 2020). So far, there are no *in-situ* remediation technologies available. The most common treatment technology is pump-and-treat with subsequent treatment of the PFAAs contaminated water by adsorption onto activated carbon (AC) (Gagliano et al., 2020). However, there are some drawbacks which reduce the performance of PFAAs adsorption, i.e. highly variable removal efficiencies due to competitive adsorption by natural organic matter (NOM) (Rahman et al., 2014; Gagliano et al., 2020) and the use of shorter-chain PFAA replacement products such as perfluorobutanoic acid (PFBA) which has resulted in serious problems in water treatment (McCleaf et al., 2017). More importantly, although a number of studies have considered the mechanism of PFAAs adsorption on AC, some of the observed phenomena still provoke questions. Adsorption affinities of PFOA and PFOS, for instance, can differ extremely between various AC products, i.e. by up to 4 orders of magnitude in sorption coefficients under the same experimental conditions (Deng et al., 2015; Zhi and Liu, 2016; Saeidi et al., 2020a; Söregård et al., 2020). To our knowledge, such huge differences in adsorption affinity on various ACs have rarely been observed for other organic compounds.

Understanding and prediction of sorption phenomena for organic compounds is of great importance in environmental science and engineering. For non-ionic organic compounds, polyparameter linear free energy relationships (PP-LFER) were successfully developed and applied for prediction of absorption and, with some limitations, even for adsorption equilibria (Endo and Goss, 2014). However, there is still a lack of prediction tools for sorption of ionic compounds (Endo and Goss, 2014; Sigmund et al., 2020). Sigmund et al. (Sigmund et al., 2020) have very recently reported a model to predict Freundlich isotherm parameters for adsorption of ionisable compounds to carbonaceous adsorbents using a deep learning neural network approach. However, PFAAs were not included in their training data set and the required molecule parameters for this compound class are not available. Improved mechanistic understanding and identification of decisive adsorbent properties is required as basis for development of predictive tools but also targeted adsorbent optimization.



We believe that a direct comparison of the adsorption behaviour of PFAAs and other model compounds, i.e. octanoic acid (OCA) and phenanthrene (PHE), for a set of well-characterised ACs can help to explain what is so special about adsorption of PFAAs on AC. OCA is the non-fluorinated structural analogue to PFOA. It has, however, a much weaker acid group ( $pK_a = 4.9$  (Wellen et al., 2017)). PHE, as a neutral molecule, is a representative of the 3-ring polycyclic aromatic hydrocarbons with high hydrophobicity ( $\log K_{OW, PHE} = 4.57$  (Karickhoff, 1981)) and thus high adsorption affinity on AC (Walters and Luthy, 1984).

Furthermore, there is still discussion on what characteristic of AC can be considered as a good indicator of PFAAs' adsorption performance. Electrostatic interactions or anion exchange between protonated sites on ACs and anions of PFOA ( $pK_a$  between 0 and 1 (Goss, 2008)) and PFOS ( $pK_a = -3.27$  (Brooke D., 2004)) have been considered as important contributions for adsorption of PFAAs (Zhi and Liu, 2015). In our previous work, we studied four commercial activated carbon felts (ACFs) and correlated the uptake of PFOA and PFOS by the adsorbents with various surface properties (Saeidi et al., 2020a). Samples with low content of oxygen and high anion exchange capacity (AEC) provided excellent adsorption which was assigned to the interplay of hydrophobic and electrostatic interactions between PFAA anions and positively charged sites of the ACFs (Saeidi et al., 2020a). Alternatively, point of zero net proton charge (PZC) has been addressed as an indicator for adsorption behaviour of various adsorbents towards PFAAs: the higher the PZC, the higher the sorption affinity (Du et al., 2014; Inyang and Dickenson, 2017; Hassan et al., 2020). Zhi and Liu (Zhi and Liu, 2015, 2016) have, however, reported that this hypothesis is not always true for uptake of PFOA and PFOS on AC. Thus, in this study we considered various parameters for description of surface properties of AC, including beside porosity and PZC also cation exchange capacity (CEC), AEC, O-content, N-content and content of various acidic groups. The set of AC used for these correlations builds upon as-received AC materials (data from our previous study, Saeidi et al., 2020) but is extended in this study by targeted modification for obtaining improved adsorption. These modifications were done with the rationale to further decrease the density of repulsive anionic and increase the number of charge-balancing cationic surface sites for PFAA anion adsorption while maintaining an overall rather non-polar carbon surface. Thermal defunctionalisation to remove acidic oxygen-containing groups from AC and to increase the  $\pi$ -electron-based basicity (Shafeeyan et al., 2010) and amino-functionalisation to create net positive surface charge at near-neutral pH (Cai and Larese-Casanova, 2016; Zhang et al., 2016b) were

selected as modification strategies. Amino-functionalised sorbents, e.g. chitosan-based polymers (Long et al., 2019), poly(ethylenimine)-functionalised cellulose (Ateia et al., 2018) and amino-functionalised covalent organic framework (Ji et al., 2018), have recently emerged as novel materials with effective performance in PFAAs removal (Phong Vo et al., 2020). Amino-functionalised cellulose has shown promising potential for being an effective adsorbent for PFAAs in a wide range of pH (from 4.5 to its PZC=10.9) and in presence of competitive inorganic and organic compounds (Ateia et al., 2018). The authors suggested to also apply amino-functionalisation strategies for enhancing performance of other conventional adsorbents towards PFAAs.

To follow the above mentioned goals, a commercial microporous ACF (CACF) with comparably high content of acidic groups, was used for preparation of amino-functionalised ACF (CACFNH<sub>2</sub>) and defunctionalised ACF (DeCACF). In particular, this work addresses the questions of what is specific in adsorption of PFAAs on carbon materials and which type of basic groups on the AC increases uptake of long-chain and short-chain PFAAs from water.

## **2. Materials and Methods**

### *2.1. Materials*

PFOA, PFOS and PFBA (96%, 98% and 98% purity, respectively) as well as PHE (98%) and octanoic-d<sub>15</sub> acid were purchased from Sigma-Aldrich (USA). HCl (fuming 37%), NaOH, NaHCO<sub>3</sub>, KCl, NaNO<sub>3</sub>, MgSO<sub>4</sub>, CH<sub>3</sub>COONH<sub>4</sub>, Na<sub>2</sub>CO<sub>3</sub> and Na<sub>2</sub>SO<sub>4</sub> (all in highest available purity) were obtained from Merck (Germany). Thionyl chloride (98% for synthesis), ethylenediamine (99.5% for synthesis) and OCA (>99% for synthesis) were obtained from CARL ROTH (Germany). Tetrahydrofuran (THF) (pure) was purchased from Applichem (Germany). Methanol of HPLC grade was bought from Th. Geyer (Germany). Suwannee River natural organic matter (SRNOM, reference number: 2R101N) was obtained from International Humic Substances Society (IHSS).

### *2.2. Activated carbon felt*

The ACF was provided by Jacobi CARBONS, Sweden. The commercial name of the ACF is ACTITEX WK L20 (CACF). The CACF was rinsed first with pure methanol and then deionized water before usage.

### 2.2.1. Amino-functionalisation and defunctionalisation of ACF

CACF was functionalised using ethylenediamine by a procedure reported elsewhere (Qiu et al., 2013; Zhang et al., 2016b) with some alterations. Ethylenediamine is connected to the AC surface through an amide bond between one of its amine groups and a surface carboxyl group, whereby the other amine group is able to provide a positive surface charge (as  $-\text{NH}_3^+$ ) when  $\text{pH} < \text{pK}_{\text{a1}}$  (Cai and Larese-Casanova, 2016). In our previous work, we determined the concentration of carboxylic groups of CACF by Boehm titration as 1.26 mmol/g or  $1.12 \mu\text{mol}/\text{m}^2$ , which is quite high. Therefore, we used it as received without any modification for creating carboxylic groups on it. In brief, 150 mg of CACF was dried at  $60^\circ\text{C}$  overnight and then stirred in 30 mL of thionyl chloride ( $\text{SOCl}_2$ ) at  $75^\circ\text{C}$  for 24 h. After the acyl chlorination ( $-\text{COOH} \rightarrow -\text{COCl}$ ), the ACF was washed with anhydrous THF five times and dried at  $50^\circ\text{C}$  for 1 h. The acyl-chlorinated CACF was reacted with 50 mL ethylenediamine at  $100^\circ\text{C}$  for 2 days. After cooling to room temperature, the amino-functionalised product ( $-\text{CONH}-\text{CH}_2-\text{CH}_2-\text{NH}_2$ , named  $\text{CACFNH}_2$ ) was washed with methanol five times and then with deionised water in order to remove excess diamine. Finally, the  $\text{CACFNH}_2$  was dried at  $50^\circ\text{C}$  overnight and kept in a desiccator for further use.

In addition, CACF was treated thermally under pure hydrogen in order to remove oxygen-containing groups from the ACF and saturate any active sites produced. The procedure reported in (Menéndez et al., 1996) was applied with some modifications. In brief, a certain amount of CACF was placed in a tube furnace, purged with nitrogen for 1 h and then with hydrogen for 30 min at ambient temperature, heated with a ramp of  $50 \text{ K}/\text{min}$  up to  $900^\circ\text{C}$  and kept at  $900^\circ\text{C}$  for 2 h. Finally, the sample cooled down to ambient temperature under a flow of hydrogen.

### 2.2.2. Characterisation of the activated carbon felts

The physical properties of the adsorbents, e.g. fiber diameter, specific surface area, pore volume and pore size distribution (PSD), were determined by procedures reported in detail in our previous work (Saeidi et al., 2020a).

Characterisation of surface chemistry of the ACFs was done by determination of PZC, acidic surface functional groups by Boehm titration, AEC and CEC of the ACFs as well as temperature-programmed decomposition (TPD) as also described in our previous work (Saeidi et al., 2020a). X-ray photoelectron spectroscopy (XPS) was performed using an Axis Ultra photoelectron spectrometer (Kratos, Manchester, UK) using monochromatised Al  $\text{K}\alpha$  radiation ( $h\nu = 1486.6 \text{ eV}$ ).

### 2.3. Analytical methods

Concentration of PFOA, PFOS, PFBA and OCA in solution was measured using a liquid chromatography system coupled to a single-stage quadrupole mass spectrometer with electrospray ionisation (LCMS-2020; Shimadzu, Japan). To analyse the concentration of the PFAAs in solutions, aliquots of 3  $\mu$ L of the samples were injected into a 100 mm  $\times$  2 mm Gemini C6-Phenyl column filled with fully porous organo-silica having 110 Å pore size and 3  $\mu$ m particle size (Phenomenex, USA). A combination of solvent A, consisting of 5 mM ammonium acetate dissolved in 90% deionized water and 10% methanol, and solvent B, consisting of 5 mM ammonium acetate dissolved in 90% methanol and 10% water was used as mobile phase. The LC pump delivered a mix of solvent A (30%) and solvent B (70%) at a flow rate of 3 mL/min. The column temperature was kept at 40 °C during the run which was 10 min. For concentrations < 1 mg/L the correlation coefficients ( $R^2$ ) of the calibration curves for the PFAAs were > 0.99 and the standard deviations for 5 measurements were around 5%. The detection limit for PFAAs were 0.05  $\mu$ g/L.

Since the detection limit of the LCMS for OCA was around 100  $\mu$ g/L, after adsorption experiments the solutions were concentrated by a factor of about 50 using Strata<sup>TM</sup>-X cartridges (Phenomenex, USA). Octanoic-d<sub>15</sub> acid was used as internal standard and added into the solutions before the preconcentration procedure. The correlation coefficients ( $R^2$ ) of the calibration curves for OCA and octanoic-d<sub>15</sub> acid for concentrations less than 3 mg/L were > 0.99.

PHE was analysed by means of HPLC with fluorescence detection ( $\lambda_{\text{ex}}$  = 244 nm,  $\lambda_{\text{em}}$  = 440 nm, Hewlett-Packard Series 1100, Agilent, Germany) using a Lichrospher 60 RP-C18 column (5  $\mu$ m, Merck, Germany). The mobile phase consisted of acetonitrile/water (65:35) delivered at a flow rate of 0.5 mL/min (25 °C).

### 2.4. Adsorption experiments

Adsorption of the target compounds on the adsorbents was performed in 25 mL glass vessels. To simulate the ionic strength of tap water, 10 mM Na<sub>2</sub>SO<sub>4</sub> was used as background electrolyte. In the case of OCA adsorption, 100 mL vessels filled with 100 mL electrolyte solution were used. The ACFs were weighted and added to the vessels. 0.1 M HCl or NaOH solutions were used to provide the desired solution pH. After 24 h shaking, the pH of the suspensions was adjusted back to the desired values. Certain concentrations of the target solutes were then spiked from stock solutions.

To study the effect of NOM on adsorption of the target solutes, 5 mg/L NOM was spiked from 100 mg/L NOM stock solutions.

The loading of the target adsorbates on the adsorbents was obtained as follows:

$$q_e = \frac{V \times (C_0 - C_e)}{m} \quad (1)$$

here  $q_e$  ( $\mu\text{mol/kg}$  or  $\mu\text{mol/m}^2$  if normalized by specific surface area of the adsorbent, as determined e.g. by BET analysis) denotes loading of adsorbate on the adsorbent at equilibrium. The initial concentration and concentration of adsorbate in solution at equilibrium are addressed by  $C_0$  and  $C_e$  ( $\mu\text{mol/L}$ ), respectively.  $V$  denotes the volume of solution in L and  $m$  is the mass of the adsorbent in kg.

The single-point adsorption coefficient  $K_d$  ( $\text{L/kg}$  or  $\text{L/m}^2$ ) of the solutes on the adsorbents can be calculated by Eq. (2):

$$K_d = \frac{q_e}{C_e} \quad (2)$$

where the loading  $q_e$  is divided by the concentration of the solute in solution at equilibrium  $C_e$ .

Equilibrium was considered to be approached after 2 d, as no significant changes in the aqueous phase solute concentrations were observed ( $\leq 5\%$ ) at further prolonged contact time.

#### 2.4.1. Adsorption isotherms

Adsorption isotherms were obtained by fitting experimental data with a linearised form of the Langmuir equation (Eq. 3):

$$\frac{C_e}{q_e} = \frac{C_e}{q_m} + \frac{1}{q_m \times K_L} \quad (3)$$

In Eq. 3,  $q_m$  ( $\mu\text{mol/m}^2$ ) is the maximum monolayer loading of the adsorbate on the ACF and  $K_L$  ( $\text{L}/\mu\text{mol}$ ) is the Langmuir constant which denotes the adsorption affinity of the solute on the adsorbent.

The data were also fitted with a linearised form of the empirical Freundlich equation (Eq. 4):

$$\log q_e = n \times \log C_e + \log K_F \quad (4)$$

In Eq. 4,  $K_F$  ( $(\mu\text{mol}/\text{m}^2)/(\mu\text{mol}/\text{L})^n$ ) is the Freundlich constant which denotes the adsorption affinity, while  $n$  is the Freundlich exponent (dimensionless).

### 3. Results and discussion

#### 3.1. Properties of ACFs

Total pore volume ( $V_{\text{total}}$ ), pore volume ( $V_p$ ) in certain ranges of pore widths and fiber diameters of the ACFs are listed in Table 1. Figure 1S shows PSD of the ACFs. A detailed discussion on physical properties of the ACFs and the effect of surface modification of the ACFs on their PSDs can be found in Supporting Information.

Table 1. Physical properties of the investigated activated carbon felts.

Sample	BET surface area ( $\text{m}^2/\text{g}$ ) <sup>a</sup>	$V_{\text{total}}$ ( $\text{cm}^3/\text{g}$ ) <sup>a</sup>	$V_p$ in 1-2 nm pore width ( $\text{cm}^3/\text{g}$ ) <sup>b</sup>	$V_p$ in pore width < 1 nm ( $\text{cm}^3/\text{g}$ ) <sup>b</sup>	Fiber Diameter ( $\mu\text{m}$ ) <sup>c</sup>
CACF	1100	0.53	0.14	0.23	$12 \pm 1$
CACFNH <sub>2</sub>	720	0.30	0.084	0.13	$12 \pm 2$
DeCACF	1000	0.46	0.16	0.15	$6.5 \pm 1$

<sup>a</sup> obtained using N<sub>2</sub> adsorption/desorption, <sup>b</sup> obtained using CO<sub>2</sub> adsorption,

<sup>c</sup> an average of 10 measurements was reported.

The surface chemical properties of the ACFs are shown in Table 2. The ACFs differ significantly in their surface functional groups. CACF owns the highest concentrations of carboxylic ( $1.12 \mu\text{mol}/\text{m}^2$ ) and total acidic groups ( $2.08 \mu\text{mol}/\text{m}^2$ ) among the ACFs. Amino-functionalisation by amidation reduced the concentration of free carboxylic groups (causing negative charge at near-neutral pH) by about 45%. All types of acidic groups were affected by the thermal defunctionalisation, resulting in a decrease in total acidity and concentration of carboxylic groups by one order of magnitude.

The results from TPD measurements (Figure 1) confirm that the concentration of remaining carboxylic groups (CO<sub>2</sub>-releasing groups) is the lowest for DeCACF, together with a very low concentration of CO-releasing groups, e.g. pyrone- and chromene-type structures which have a basic character. TPD profiles of CACFNH<sub>2</sub> show a peak related to NH<sub>3</sub>-releasing groups in the

temperature range of 425 K to 830 K. For CACF and DeCACF, however, this peak was not detected. Accordingly, the nitrogen content of CACF $\text{NH}_2$  was calculated as 1.1 wt%. XPS results also show that CACF $\text{NH}_2$  contains a higher nitrogen content (2.6 wt%) than CACF and DeCACF (< 0.5 wt%) and verify ethylenediamine binding to the surface as discussed in Supporting Information.

Table 2. Chemical surface characteristics of the activated carbon felts.

Sample	Boehm titration				TPD					XPS	PZC
	$\text{p}K_{\text{a}} \sim 3\text{-}6$	$\text{p}K_{\text{a}} \sim 6\text{-}10$	$\text{p}K_{\text{a}} \sim 10\text{-}13$	$\text{p}K_{\text{a}} \sim 3\text{-}13$							
	Carboxylic acids	Lactones and lactols	Phenols	Total acidity	CO	CO <sub>2</sub>	NH <sub>3</sub>	O <sup>a</sup>	N <sup>b</sup>	N	
	$\mu\text{mol}/\text{m}^2$							wt%			
CACF	1.12	0.321	0.643	2.08	3.39	2.14	-	13.7	-	0.47	
CACFNH <sub>2</sub>	0.611	0.264	0.710	1.58	3.33	1.66	1.0	7.90	1.1	2.6	$7.3 \pm 0.1$
DeCACF	0.0233	0.130	0.0670	0.220	0.550	0.0840	-	1.10	-	0.33	$9.3 \pm 0.1$

<sup>a</sup> calculated from released CO and  $\text{CO}_2$ ,

<sup>b</sup> calculated from released  $\text{NH}_3$ .

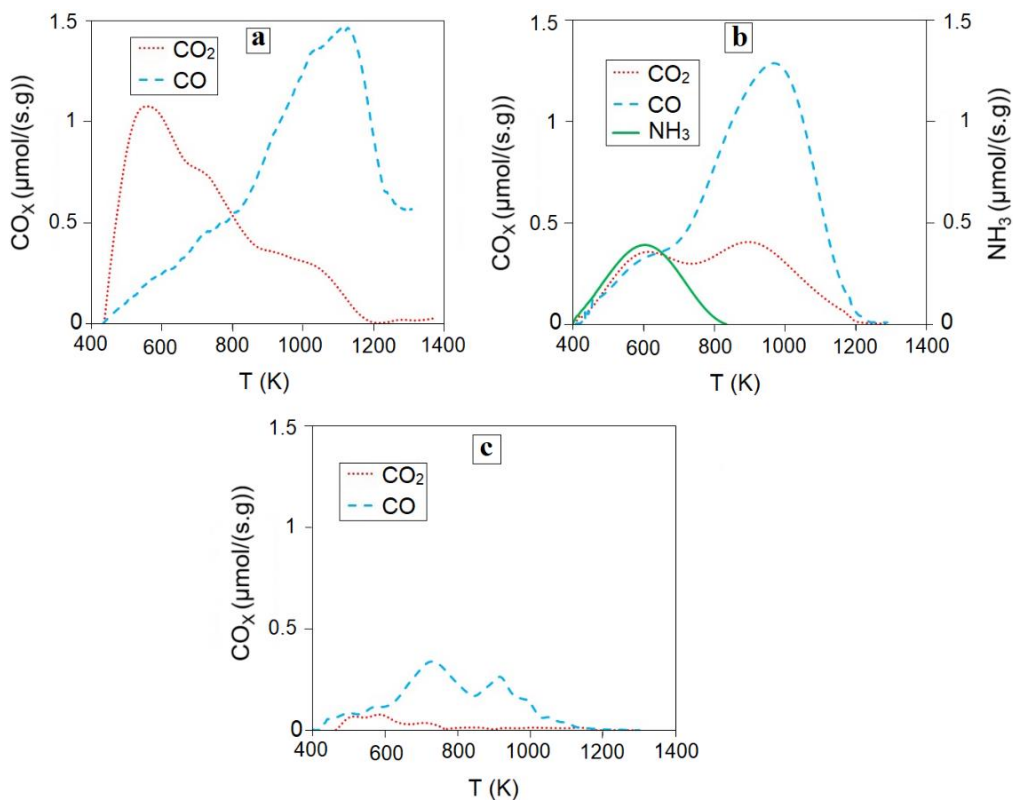


Figure 1. TPD profiles of the activated carbon felts CACF (a), CACF $\text{NH}_2$  (b) and DeCACF (c); heating rate 10 K/min.

In addition, XPS results confirm that the defunctionalisation affected most strongly the carboxylic groups of CACF, however, the content of phenolic and ether units was also reduced (see Figure 2S and related discussion in Supporting Information). Overall, DeCACF has the lowest ratio of carbon attached to oxygen per total carbon, i.e. 0.63 vs. 1.1 (CACF) and 0.93 (CACFNH<sub>2</sub>) (see Table 1S).

The charge-compensating capacity of the carbon surface in adsorption of organic anions or cations can be derived from AEC and CEC, which are shown in Table 3. Amino-functionalisation slightly lowered CEC, whereas thermal defunctionalisation nearly eliminated it. At the same time, these modifications increased AEC by a factor of 2 and 4, respectively. A good correlation exists between the content of carboxylic groups (Boehm titration) and CEC which was determined at pH 7 (Figure 3S). It reveals that carboxylic groups are most relevant for CEC of the ACFs at neutral pH. We refer the readers to Supporting Information for a more detailed discussion on surface chemical characteristics of the ACFs.

Table 3. Charge-compensation capacity of the ACFs.

Sample	Anion exchange capacity ( $\mu\text{mol}/\text{m}^2$ )	Cation exchange capacity ( $\mu\text{mol}/\text{m}^2$ )
CACF	0.054	0.79
CACFNH <sub>2</sub>	0.13	0.51
DeCACF	0.20	0.021

### 3.2. Adsorption Experiments

#### 3.2.1. Adsorption of PFOA, PFOS and PFBA

Adsorption isotherms of PFOA, PFOS and PFBA on the ACFs at pH 7 were determined and are shown in Figure 4S together with Freundlich and Langmuir plots in Figure 2. Table 4 lists the corresponding isotherm parameters normalised to specific surface areas of the adsorbents. The isotherm parameters were also calculated in terms of mass units and listed in Table 2S. Obviously, the adsorbents expose vastly different capacities for uptake of PFOA (Figure 2a and b). Maximum monolayer adsorption capacities ( $q_m$ ) of PFOA increase significantly from 0.0044  $\mu\text{mol}/\text{m}^2$  (2.1 mg/g) on CACF to 0.18  $\mu\text{mol}/\text{m}^2$  (80 mg/g) on DeCACF. Such a substantial enhancement in adsorption capacity as observed here for the defunctionalised carbon (factor of 40) has been rarely reported before. The adsorption affinities expressed by  $K_F$  and  $K_L$  also confirm a strong improvement in adsorption of PFOA on DeCACF. Furthermore, as can be seen in Table 4, the



order of the maximum loadings ( $q_m$ ) and affinities ( $K_F$  and  $K_L$ ) for PFOS and PFBA is the same as for PFOA: DeCACF  $\gg$  CACFNH<sub>2</sub> > CACF. All these results indicate that the defunctionalisation procedure yields an adsorbent with exceptionally high affinity for uptake of both long-chain and short-chain PFAAs. This high adsorption affinity was maintained by DeCACF for at least 5 adsorption/desorption cycles of PFOA and PFBA with intermittent regeneration by methanol extraction (see the Supporting information and Figure 5S for more details). In comparison, amidation of CACF showed only a minor improvement in adsorption of the PFAAs.

As mentioned earlier, amino-functionalisation and thermal defunctionalisation changed to some extent also the physical properties, i.e. specific surface area and PSD of CACF. Note that adsorption performance was already compared by normalizing PFAA equilibrium loadings to carbon surface area (Figure 2). Figure 6S shows a plot of maximum loadings of the PFAAs versus  $V_p$  in the pore size ranges of 1-2 nm width (Figure 6Sa) and < 1 nm (Figure 6Sb). The order of maximum loadings is in agreement with neither order of available  $V_p$  in 1-2 nm width nor  $V_p$  in < 1 nm width. It seems that available  $V_p$  in a certain size fraction doesn't control the different adsorption properties of the various ACFs. An estimation of the degree of pore filling reached at the highest maximum loading gained, i.e. for PFOS on DeCACF as the best adsorbent, underlines that. According to a molar volume of PFOS (around 270 mL/mol), the maximum volumetric loading of 0.054 mL PFOS/g leads to a filling degree of 1-2 nm pores (0.16 mL/g) of only 33% at maximum (as the < 1 nm pores can also contribute to PFOS uptake).

Table 4. Parameters of Freundlich and Langmuir isotherms for adsorption of PFAAs on the activate carbon felts at pH 7. <sup>a</sup>

ACF adsorbent	Adsorbate	Freundlich			Langmuir		
		$K_F$ ( $\mu\text{mol}/\text{m}^2$ )/( $\mu\text{mol}/\text{L}$ ) <sup>n</sup>	n	R <sup>2</sup>	$q_m$ ( $\mu\text{mol}/\text{m}^2$ )	$K_L$ (L/ $\mu\text{mol}$ )	R <sup>2</sup>
CACF	PFOA	0.010	0.98	0.969	0.0044	0.0048	0.986
CACF	PFOS	0.087	0.79	0.991	0.0088	0.012	0.979
CACF	PFBA	0.00038	0.58	0.989	0.0012	0.00048	0.963
CACFNH <sub>2</sub>	PFOA	0.010	0.52	0.981	0.013	0.0053	0.994
CACFNH <sub>2</sub>	PFOS	0.066	0.63	0.994	0.025	0.018	0.997
CACFNH <sub>2</sub>	PFBA	0.0010	0.62	0.992	0.0032	0.00051	0.986
DeCACF	PFOA	0.98	0.64	0.982	0.18	0.035	0.981
DeCACF	PFOS	5.5	0.76	0.992	0.20	0.21	0.999
DeCACF	PFBA	0.031	0.70	0.987	0.024	0.0039	0.997

<sup>a</sup> the isotherm parameters in mass units are listed in Table 1S.

This finding clarifies that the *volume* of this micropore fraction will unlikely be the limiting factor in PFAAs adsorption. Thus, it can be concluded that the availability of pores in a certain size range cannot justify the strong difference in adsorption behaviors of the ACFs and surface chemistry is the determining factor.

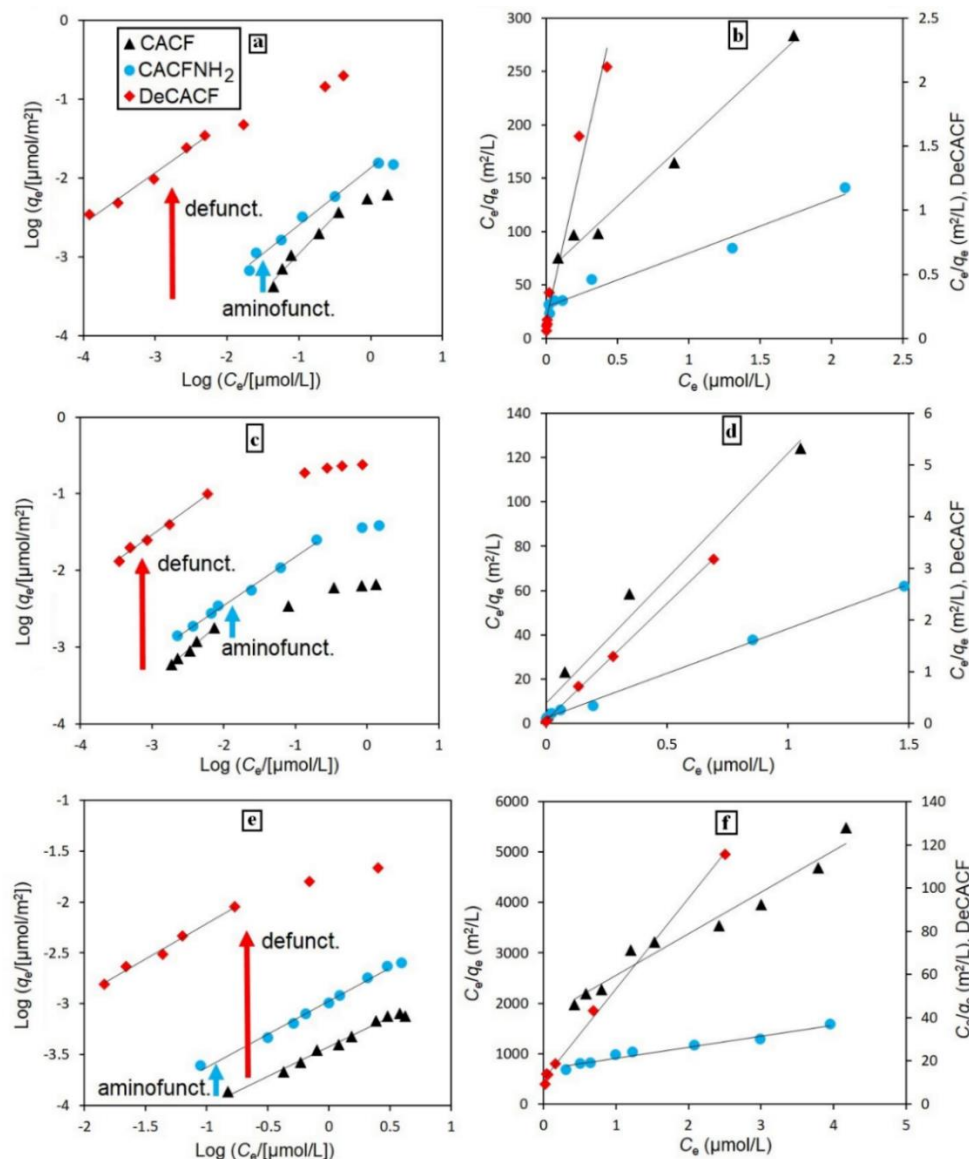


Figure 2. Experimental data on adsorption of various PFAAs on the ACFs in 10 mM Na<sub>2</sub>SO<sub>4</sub> at pH 7: Freundlich and Langmuir plots (left and right, respectively) for PFOA (a and b); PFOS (c and d) and PFBA (e and f).

We observed in a previous study (Saeidi et al., 2020a) considerable differences in adsorption loadings and affinities of PFOA and PFOS on 4 commercial ACFs, namely VS, FC15, FC10 and WK, which was subject to modification in the present study (note that WK in (Saeidi et al., 2020a)

= CACF). Figures 3a and b show the maximum loadings of the PFAAs on CACF, CACF $\text{NH}_2$  and DeCACF versus AEC and CEC and include also data for the other three commercial ACFs from (Saeidi et al., 2020a) (for ease of comparison, their characterisation data are included in the Supporting information (Tables 3S and 4S)).

It is a common feature for all investigated ACFs (including those investigated in (Saeidi et al., 2020a)) that the three PFAAs are adsorbed according to PFOS > PFOA > PFBA. This ranking is in accordance with the general trend of higher adsorption tendency of PFAAs with increasing chain-length as reported e.g. for adsorption on fluorinated graphene sheets (Li et al., 2017), metal-organic frame- works (Liu et al., 2015), amino-functionalised cellulose (Ateia et al., 2018) and AC (Zhi and Liu, 2016).

$K_d$  values were calculated from isotherms at the same aqueous phase concentration of  $C_{e, \text{PFOA}} = 20 \text{ } \mu\text{g/L}$  ( $0.048 \text{ } \mu\text{mol/L}$ ),  $C_{e, \text{PFOS}} = 8 \text{ } \mu\text{g/L}$  ( $0.016 \text{ } \mu\text{mol/L}$ ) and  $C_{e, \text{PFBA}} = 30 \text{ } \mu\text{g/L}$  ( $0.140 \text{ } \mu\text{mol/L}$ ) and plotted as surface-normalised  $K_d$  values against AEC and PZC of the ACFs in Figures 3c and 3d, respectively. It is obvious that defunctionalisation turned the worst among the commercial ACFs into the best adsorbent for the PFAAs. DeCACF as the sample with the highest AEC and PZC but lowest CEC and O-content shows the highest  $q_m$  and  $K_d$  values among all ACFs, with  $K_d = 2.9 \text{ L/m}^2$  ( $2.9 \times 10^6 \text{ L/kg}$ ) for PFOA,  $12 \text{ L/m}^2$  ( $1.2 \times 10^7 \text{ L/kg}$ ) for PFOS and  $0.074 \text{ L/m}^2$  ( $7.4 \times 10^4 \text{ L/kg}$ ) for PFBA at the above listed  $C_e$  values. This means an enhancement in adsorption affinity of the PFAAs by up to 3 orders of magnitude in comparison with the ACF as received (CACF). Table 5S shows a comparison between adsorption coefficients of PFAAs on DeCACF and those on various adsorbents including AC materials extracted from very recent studies. This comparison proves that DeCACF has an outstanding performance in adsorption of both short- and long-chain PFAAs compared to various commercial and lab-synthesized adsorbent materials (including Fe-based minerals, N-functionalised polymers, biochar and various activated carbon products).

Note that due to the non-linear isotherms observed for DeCACF with Freundlich  $n$  values < 1, adsorption performance increases with decreasing aqueous phase concentrations of the PFAAs. The  $K_d$  values at  $C_e = 0.3 \text{ } \mu\text{g/L}$  which is within the environmentally relevant range reach values as high as  $1.0 \times 10^7 \text{ L/kg}$  and  $3.5 \times 10^7 \text{ L/kg}$  for PFOA and PFOS, respectively.

In contrast, the increased AEC of CACF $\text{NH}_2$  is not translated equivalently into increased  $q_m$  and  $K_d$  values for adsorption of the PFAAs, as this adsorbent falls out of the otherwise rather

continuous correlation curves in Figures 3a and 3c. In general, adsorption of PFAAs on amino-functionalised adsorbents involves three combined factors, i.e. electrostatic interactions with functional groups of the adsorbent, hydrophobic interactions with the sorbent and sorbent morphology (Ateia et al., 2019). Possible reasons for the adsorption behaviour of PFAAs on CACF $\text{NH}_2$  are: I) Even though PZC is shifted to  $> 7$ , CACF $\text{NH}_2$  still keeps a significant density of negatively charged and thus repulsive sites for the PFAAs anions, as it still has the second-highest CEC at pH 7.

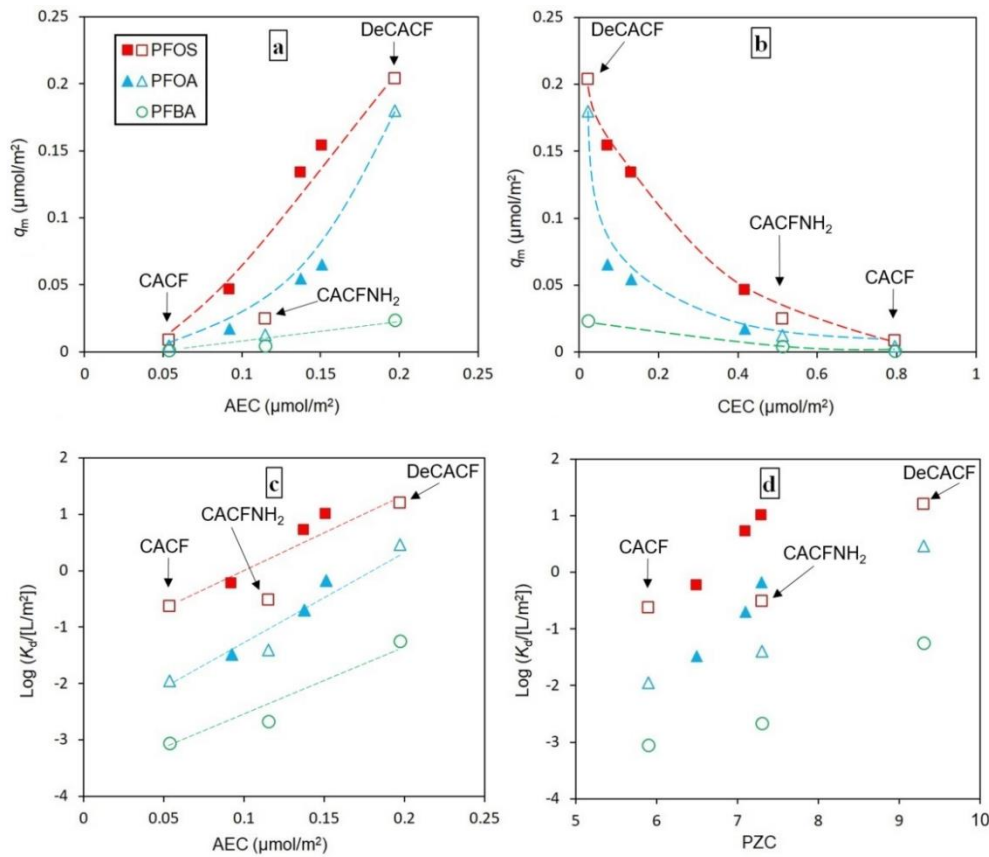


Figure 3. Correlations between maximum loadings  $q_m$  ( $\mu\text{mol}/\text{m}^2$ ) against AEC (a), CEC (b) and between single-point adsorption coefficients  $\log(K_d$  [ $\text{L}/\text{m}^2$ ]) against AEC (c) and PZC (d) for sorption of PFOA, PFOS and PFBA at pH 7.  $K_d$  values are obtained for  $C_{e, \text{PFOA}} = 20 \mu\text{g}/\text{L}$  ( $0.05 \mu\text{mol}/\text{L}$ ),  $C_{e, \text{PFOS}} = 8 \mu\text{g}/\text{L}$  ( $0.016 \mu\text{mol}/\text{L}$ ) and  $C_{e, \text{PFBA}} = 30 \mu\text{g}/\text{L}$  ( $0.140 \mu\text{mol}/\text{L}$ ). Filled symbols denote data from our previous study (Saeidi et al., 2020a). Lines were added as guide to the eye.

Therefore, in adsorption of PFAAs on amino-functionalised AC the density of negatively charged sites on the adsorbent should be considered as a determining factor in adsorption performance of the adsorbent. II) Amino-functionalisation creates a positive charge (at near neutral pH) in a rather

polar microenvironment, i.e. by units of surface  $\text{CO-NH-CH}_2\text{-CH}_2\text{-NH}_3^+$ . Even though they provide charge compensation for the anionic head group of PFAAs, such sites might be a less suitable micro-environment for adsorption of the hydrophobic perfluoroalkyl chain.

In this respect, carbon-centred positive charges resulting from proton adsorption to  $\pi$ -electron systems in DeCACF might be preferable. III) Amino-functionalisation, in addition, might hinder access of PFAAs to some of the pores, as the available pore opening space can be reduced in the derivatisation. Such size exclusion is not taken into account by normalisation to BET surface areas determined from adsorption/desorption of small gas molecules ( $\text{N}_2$ ,  $\text{CO}_2$ ). Interestingly,  $q_m \leq \text{AEC}$  holds for all ACFs and PFAAs studied. For DeCACF as best adsorbent, AEC is comparable with the maximum uptake capacity for PFOA and PFOS in terms of molar units. These results confirm the finding of our previous work indicating that the PFOA and PFOS anions can be adsorbed favourably by the interplay of hydrophobic and electrostatic interactions when charge-balancing cationic sites are sufficiently available at the ACF surface. At the same time, the increase in  $q_m$  is much higher than the actual increase in AEC between the worst and the defunctionalised ACF as best adsorbent, which also highlights the importance of reduced repulsive interactions (decrease in CEC as shown in Figure 3b). Correlations between  $\log K_d$  and PZC are shown in Figure 3d. The PZC values are 5.9 for CACF versus 7.3 for CACF $\text{NH}_2$  and 9.3 for DeCACF. PZC has been reported as a scale for the nature of electrostatic interactions between surface groups of carbon materials and PFAAs (Chen et al., 2011; Li et al., 2011a; Deng et al., 2015; Chen et al., 2017): it has been stated that if  $\text{pH} < \text{PZC}$  there are electrostatic attractions between positively charged sites of the adsorbent and PFAAs, and *vice versa*. Furthermore, a review paper (Kah et al., 2017) has recently extended this evaluation to all ionisable organic compounds, including dyes (Calvete et al., 2009; Machado et al., 2011), benzoic acid (Ayranci et al., 2005) and salicylic acid (Ayranci and Duman, 2006). However, AC in general contains a wide range of functional groups having various  $\text{pK}_a$  values. For such heterogeneous surfaces, PZC cannot have the same meaning as for more homogeneous surfaces such as e.g. metal oxides or synthetic polymers with one type of functional groups (amino-functionalised polymers). In the case of a distribution of  $\text{pK}_a$  values of surface groups, a significant portion of local positive and negative charges can remain simultaneously far above and below PZC, respectively.

It can be seen from Figure 3d that even though CACF $\text{NH}_2$  has the second highest PZC among the carbon materials tested, it is still among the worst adsorbents. AEC and CEC might be more

conclusive indicators of the charge density of the AC surface, as they quantify the density of charged sites at a certain relevant solution pH. Indeed, CACF $\text{NH}_2$  has the second-highest CEC at pH 7, meaning that it has still a high density of repulsive charges which are detrimental for PFAAs anion adsorption. Correlations of  $q_m$  values with CEC yield rather continuous curves which apparently become steeper in the range of the lowest CEC values. It is obvious that a reduced density of repulsive charges should be beneficial for adsorption. However, there is also a potential cross-correlation between CEC and AEC (see Figure 7S) as C-centred basic sites are favoured (high AEC) at carbon surfaces with low density of electron-withdrawing (e.g. carboxylic) groups (low CEC).

### 3.2.2. Adsorption of PFOA, octanoic acid and phenanthrene

Adsorption capacities and affinities of OCA and PHE on the ACFs were determined and compared with adsorption of PFOA. Figure 8S and Tables 6S and 7S show adsorption isotherms of PHE and OCA on the ACFs and the corresponding Freundlich and Langmuir parameters. The  $K_d$  values for adsorption of the model compounds were calculated using the respective isotherm equations at  $C_e = 10\text{--}20\text{ }\mu\text{g/L}$ , i.e. for the low loading range where capacity limitations are negligible.

Figure 4 shows correlations between maximum loadings  $q_m$  and single point adsorption coefficients  $K_d$  in adsorption of PFOA, OCA and PHE with AEC of the ACFs. Figure 9S shows correlations of single point adsorption coefficients  $K_d$  in adsorption of the compounds with CEC, PZC and oxygen content of the ACFs. It is obvious that the three adsorbates react with different sensitivity to the changes in AC surface chemistry. PHE is rather insensitive as it shows only a slight increase in  $q_m$  for the defunctionalised carbon and nearly no change in  $K_d$ . This substantiates that changes in physical characteristics due to the modification of the carbon were of minor importance. For PHE as representative of neutral hydrophobic compounds a low surface polarity of the carbon might offer beneficial interactions; however, the overall impact of surface chemistry is low. This is also in line with experience gathered for activated carbon adsorption of “contaminants of the past”, including e.g. BTEX, halogenated hydrocarbons or PAHs, where AC performance was mainly related to porosity aspects leading to a high surface area for adsorption. In contrast, many emerging contaminants carry acidic or basic groups and are charged in the relevant pH range. PFOA and OCA (used as non-fluorinated structural analogue) are both anions at pH 7. However, they differ largely in their acid strength, with  $\text{p}K_{a, \text{OCA}} = 4.9$  (Wellen et al., 2017)

and  $pK_{a, \text{PFOA}} = 0.1$  (Goss, 2008; Cheng et al., 2009; Baggioli et al., 2018). Both acids are much more sensitive regarding changes in surface chemistry of the ACF than PHE. In fact, PFOA reacts most strongly, i.e. with an increase in  $K_d$  by more than 2 orders of magnitude after the defunctionalisation of the ACF, whereas for OCA this enhancement is only by a factor of 4 (see Figure 4b). The maximum loading shows a similar difference: 40-fold increase for PFOA but only 3-fold increase for OCA (see Figure 4a). Thus, the question arises what is causing this stronger sensitivity of PFOA and other PFAAs towards surface chemistry of AC? While sorptive interactions of neutral molecules include mainly non-specific van der Waals interactions, H-bonding and  $\pi$ - $\pi$  interactions, charged molecules are also subject to attractive and repulsive electrostatic interactions. Beyond that, removal of an ionic organic compound from the water phase into an adsorbent requires charge compensation in order to maintain phase neutrality. Likewise, adsorption of PFOA anions to the carbon surface requires either I) existence of positive charges at the surface and displacement of counter anions into the solution, or II) uptake of PFOA into the pore space together with cations to balance the pore charges. Interestingly, for all ACFs, the maximum loading for PFOA/PFOS is less than or equal to their AEC for inorganic anions. Thus, it appears that positively charged sites at the carbon surface play the major role for charge balancing at least for the tested microporous activated carbon materials.

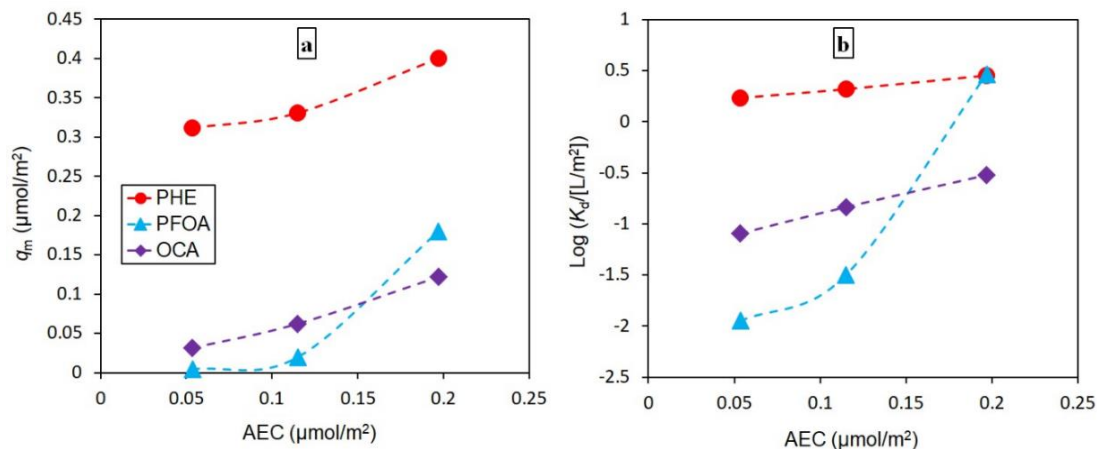


Figure 4. Correlations between maximum loadings  $q_m$  (a) and single point adsorption coefficients  $K_d$  (b) against AEC of the activated carbon felts in sorption of PFOA, OCA and PHE from 10 mM  $\text{Na}_2\text{SO}_4$  at pH 7.  $K_d$  values are reported for  $C_{e, \text{PFOA}} = 20 \mu\text{g/L}$  ( $0.048 \mu\text{mol/L}$ ),  $C_{e, \text{PHE}} = 10 \mu\text{g/L}$  ( $0.056 \mu\text{mol/L}$ ) and  $C_{e, \text{OCA}} = 10 \mu\text{g/L}$  ( $0.069 \mu\text{mol/L}$ ). Lines were added as guide to the eye.

In contrast to PFOA, OCA, due to its weaker acidity ( $pK_{a, \text{OCA}} = 4.9$ ), has alternative options for obtaining charge neutrality in adsorption:

- The  $pK_a$  of OCA is closer to 7, thus a mild shift in local pH and/or  $pK_a$  close to the surface and in narrow pores (i.e. within the electric double layer) may lead to OCA protonation and finally adsorption as a neutral molecule. Nanoconfinement effects in carbon adsorbents are discussed e.g. in (Pignatello et al., 2017).
- Charge-assisted hydrogen bonding (CAHB) was suggested as an important mechanism for adsorption of organic acids/bases (Gilli and Gilli, 2000). Formation of CAHB between the carboxyl group of a solute and surface carboxyl or hydroxyl groups of the adsorbent is possible if the  $pK_a$  values of the two functional groups are comparable:  $\text{surface-COO}^- + \text{H}^+ + \text{R-COO}^- \leftrightarrow (\text{surface-COO}^- \dots \text{H}^+ \dots \text{OOC-R})^-$  (Gilli and Gilli, 2000). CAHB can be understood as a charge neutralisation option, with an increase in the  $pK_a$  of the complex compared to the free acid ( $\text{R-COO}^-$ ) due to a tighter constriction of the proton shared by two carboxylic groups (Pignatello et al., 2017).

By means of these mechanisms, OCA could adapt more easily than PFOA even to unfavourable negatively charged surfaces. However, if sufficient positively charged sites at a surface with an overall rather low polarity are available, as in the case of DeCACF, then OCA is outcompeted in adsorption by PFOA (and PFOS). Their sorption coefficients reach a value of PHE which is considered as well adsorbable by activated carbons. In order to understand the better adsorption of PFOA compared to OCA at DeCACF as best adsorbent, it is also interesting to compare the hydrophobicity of the two anions. Such a comparison is usually done based on octanol-water partition coefficients. However, for ionised organic compounds such as PFOA and OCA (at neutral pH), experimental values are hardly available and calculated values obtainable from the various available software tools frequently differ vastly (Kah and Brown, 2008). Note that also in case of partitioning charge neutrality of phases must be kept so that the type of counterions in the two phases and ionic strength are relevant. Thus, octanol-water partitioning coefficients are probably less applicable predictors for adsorption of ionised compounds than known from neutral compounds. Nevertheless, based on the molecule structures one could expect a higher hydrophobicity for PFOA compared to OCA, as perfluoroalkane chains are more hydrophobic/lipophilic than alkanes as illustrated by  $\log K_{\text{OW, perfluoropentane}} = 4.40$  (C. Hansch, 1995) vs.  $\log K_{\text{OW, pentane}} = 3.39$  (Sangster, 1989). In contrast, Jing et al. suggested that the higher



hydrophobicity of PFAAs is not caused by higher hydrophobicity of the fluorinated alkyl chain. Rather it results from a lower charge density at the anionic head groups (carboxylate or sulfonate) due to the strong electron withdrawing effect of the fluorinated substituent (Jing et al., 2009). Both reasons can explain the observed *partitioning* behaviour of PFAAs, but they have different consequences for interpretation and modelling of *adsorptive* interactions. The stronger effect of the surface charge in adsorption for PFOA compared to OCA observed in this study rather speaks for a hard base head group.

To sum up, the specific importance of activated carbon surface chemistry for adsorption of PFAAs might result from their extremely low  $pK_a$  values (high acid strength) which strongly limits charge neutralization options in adsorption. In this case, positively charged surface groups in a rather non-polar environment are detrimental for providing both, charge-balancing for PFAA anionic head groups and hydrophobic interactions of the tail.

### 3.2.3. Effect of Competitive Ions

#### 3.2.3.1. Inorganic Ions

Figure 5a shows  $K_d$  values for PFOA adsorption from solutions containing certain concentrations of  $Na_2SO_4$  at circumneutral pH. Figure 10S illustrates the  $K_d$  values for adsorption of PFOS and PFBA. An increase in  $Na_2SO_4$  concentration from 10 mM to 200 mM enhanced adsorption affinities of the PFAAs on CACF and CACF $NH_2$ , whereas a slight decrease was found for DeCACF. It is known that an increase in the ionic strength of the electrolyte solution causes a compression of the electric double layer at charged surfaces, resulting in a shorter range of electrostatic repulsion or attraction forces. Thus an increase in ionic strength enhances adsorption of the PFAAs on the ACFs with  $CEC > AEC$  at pH 7 (CACF and CACF $NH_2$ ), where the decrease in repulsive electrostatic interactions is dominating. At the same time, a weaker and opposite trend occurs for DeCACF with  $CEC < AEC$  at pH 7, as in this case the decrease in attractive interactions is dominating. The rather small influence of high sulphate concentrations on PFOA adsorption by DeCACF speaks against a competition effect. These results confirm the view that inorganic ions cannot easily compete with strong uptake of the PFAAs exposed by the superposition of electrostatic attraction and hydrophobic interactions.

### 3.2.3.2. Natural organic matter

Surface coverage and pore blockage exposed by NOM were discussed as the main reasons that reduce adsorption of PFAAs on AC in natural water (Yu et al., 2012). In our previous study, however, we did not observe negative effects of NOM on adsorption of PFOA and PFOS on microporous ACFs at solution pH of 3 and 7. We attributed this to a size exclusion effect preventing the bulky NOM molecules from surface coverage and pore blockage (Saeidi et al., 2020a). Figure 5b shows adsorption of PFOA on the ACFs at pH 7 from solution containing 5 mg/L NOM, while Figure 11S shows the results for PFOS and PFBA. In contrast to minor effects for CACF and DeCACF, CACF $\text{NH}_2$  experienced a strong reduction in PFAA adsorption in the presence of NOM. As shown in Table 1 and Figures 1Sa and 1Sb, all ACFs have comparable micropore size distributions. CACF $\text{NH}_2$  contains surface- $\text{CONHCH}_2\text{-CH}_2\text{-NH}_3^+$  units at pH 7, which obviously offer more favourable interactions with negatively charged NOM molecules (also having a moderate polarity) than the carbon-centred positive charges in DeCACF.

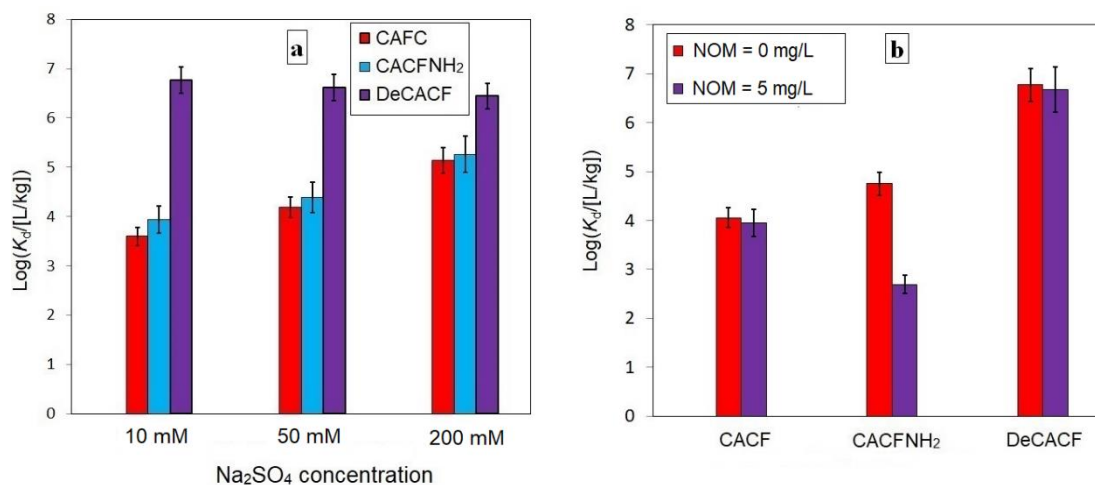


Figure 5. Effect of inorganic ions (a) and NOM (b) on sorption of PFOA. The experiments were carried out at pH 7 with  $C_0 = 1$  mg/L PFOA. In (a) the adsorbent dosage of all ACFs were 0.1 g/L. In (b) the experiments were performed in 10 mM  $\text{Na}_2\text{SO}_4$  with and without NOM and adsorbent dosage 0.5 g/L CACF and CACF $\text{NH}_2$  and 0.1 g/L DeCACF. The maximum deviation of single values from the mean value of 3 experiments is reported as error bars.

Steric effects could also play a role if amino-functionalisation affects pore entrances more than the inner micropore surfaces. Furthermore, considerable adsorption competition between negatively charged organic compounds and NOM has also been reported for amino-functionalised graphene oxide (Cai and Larese-Casanova, 2016). Irrespective of mechanistic interpretations, these results

show that the applied defunctionalisation of the ACF improves adsorption while maintaining a high selectivity for PFAAs over NOM, even for the less hydrophobic PFBA.

### 3.2.4. Effect of pH value

Figure 6 shows adsorption affinities of PFOA on the ACFs at pH values 3, 7 and 9 (for all PFAAs see Figure 12S). It is obvious that adsorption affinity of DeCACF is less sensitive to changes in pH (less than a factor of 10 in  $K_d$ ) than CACF and CACF $\text{NH}_2$ , where  $K_d$  increased by up to 2 orders of magnitude with decreasing pH. As O-containing groups were largely removed in DeCACF, protonation/deprotonation of carboxylic (mainly within pH 3-5) and phenolic groups (mainly within pH 10-13) is of only minor importance. The Lewis base sites on DeCAF are obviously only mildly affected by an increase in pH to 9 ( $\text{p}K_a \geq 9$ ). Therefore, adsorption affinity of the PFAAs on DeCACF is rather independent of solution pH in the range of 3 to 9. The improvement in  $K_d$  for CACF $\text{NH}_2$  compared to CACF mainly holds for pH 7, where amino-functionalisation leads to a reduced density of  $\text{COO}^-$  and the presence of  $\text{NH}_3^+$  groups. At pH 3, carboxylic groups are protonated anyway, and at pH 9, the positive charges of the amino groups are at least partly lost.

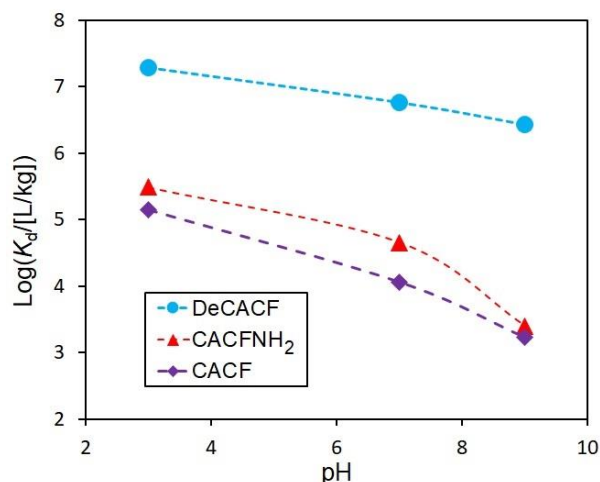


Figure 6. Effect of pH on sorption of PFOA on DeCACF, CACF and CACF $\text{NH}_2$ . The experiments were carried out with  $C_0 = 1$  mg/L of the adsorbate in 10 mM  $\text{Na}_2\text{SO}_4$  with the following adsorbent concentrations: 0.02 g/L for DeCACF and 0.5 g/L for CACF and CACF $\text{NH}_2$ . Lines were added as guide to the eye.

#### 4. Conclusions

The comparison of adsorption affinities on various ACFs showed that the order in sensitivity to carbon surface chemistry is PFOA >> octanoic acid > phenanthrene. On the other hand,  $K_d$  and  $q_m$  for PFOA adsorption strongly correlate with the anion exchange capacity of various AC materials. Thus, charge compensation in uptake of organic ions from water into a porous adsorbents must be taken into account. Our results indicate that charge compensation provided by carbon-centered positively charged surface sites is most beneficial for PFAA anions. The extremely low  $pK_a$  of PFAAs ( $pK_a < 1$ ) rules out other charge-compensation options such as a shift in protonation/deprotonation equilibria in adsorbent pores or charge-assisted hydrogen bonding which could be relevant for organic acids with typical  $pK_a$  values in the range of 4 to 5.

Defunctionalisation of a commercial ACF at 900 °C under hydrogen was shown to substantially enhance adsorption affinities of PFOA, PFOS and PFBA, i.e. by 3 orders of magnitude in  $K_d$ . This high adsorption affinity is rather insensitive to changes in pH as well as competition by inorganic ions and NOM. It was maintained for at least 5 adsorption/desorption cycles of PFOA and PFBA with intermittent regeneration by methanol extraction. Activated carbon treatment by thermal defunctionalisation in presence of  $H_2$  was shown to create a stable, basic surface nearly free of oxygen, which is obviously well suited for PFAA adsorption. It will be further optimized in future studies in terms of the balance between targeted surface modification and carbon consumption as well as the usage of forming gas (5%  $H_2$  in  $N_2$ ) for safety reasons. Defunctionalised ACF as the best adsorbent for all studied compounds exposes a superposition of electrostatic attractions and hydrophobic interactions for the organic anions. At this carbon surface, PFOA and PFOS reach the same affinity ( $K_d$  in low loading range) as phenanthrene, known as a well-adsorbing contaminant.

In contrast, amino-functionalisation by amidation of CACF increased the anion exchange capacity by only a factor of two. The improvement in PFAA adsorption was only moderate, and strongly affected by competition with NOM. Obviously, not only the presence but also the nature of basicity should be taken into account in selection of activated carbons for a highly efficient adsorption of both short- and long-chain perfluoroalkyl acids.

## References

- W. Shen, Z. Li, Y. Liu, Surface chemical functional groups modification of porous carbon, *Recent Patents on Chemical Engineering*, 1 (2008) 27–40.
- Arias Espana, V.A., Mallavarapu, M., Naidu, R., 2015. Treatment technologies for aqueous perfluorooctanesulfonate (PFOS) and perfluorooctanoate (PFOA): A critical review with an emphasis on field testing. *Environmental Technology & Innovation* 4, 168-181.
- Ateia, M., Alsbaiee, A., Karanfil, T., Dichtel, W., 2019. Efficient PFAS Removal by Amine-Functionalized Sorbents: Critical Review of the Current Literature. *Environmental Science & Technology Letters* 6, 688-695.
- Ateia, M., Attia, M.F., Maroli, A., Tharayil, N., Alexis, F., Whitehead, D.C., Karanfil, T., 2018. Rapid Removal of Poly- and Perfluorinated Alkyl Substances by Poly(ethylenimine)-Functionalized Cellulose Microcrystals at Environmentally Relevant Conditions. *Environmental Science & Technology Letters* 5, 764-769.
- Ayranci, E., Duman, O., 2006. Adsorption of aromatic organic acids onto high area activated carbon cloth in relation to wastewater purification. *Journal of Hazardous Materials* 136, 542-552.
- Ayranci, E., Hoda, N., Bayram, E., 2005. Adsorption of benzoic acid onto high specific area activated carbon cloth. *Journal of Colloid and Interface Science* 284, 83-88.
- Baggioli, A., Sansotera, M., Navarrini, W., 2018. Thermodynamics of aqueous perfluorooctanoic acid (PFOA) and 4,8-dioxo-3H-perfluorononanoic acid (DONA) from DFT calculations: Insights into degradation initiation. *Chemosphere* 193, 1063-1070.
- Brendel, S., Fetter, É., Staude, C., Vierke, L., Biegel-Engler, A., 2018. Short-chain perfluoroalkyl acids: environmental concerns and a regulatory strategy under REACH. *Environmental Sciences Europe* 30, 9.
- Brooke D., F.A., Nwaogu T.A., 2004. Environmental Risk Evaluation Report: Perfluorooctane Sulfonate (PFOS). UK Environment Agency.
- C. Hansch, A.L., and D. Hoek-man, 1995. Exploring QSAR, hydrophobic, electronic, and steric constants. American Chemical Society, Washington, DC.
- Cai, N., Larese-Casanova, P., 2016. Application of positively-charged ethylenediamine-functionalized graphene for the sorption of anionic organic contaminants from water. *Journal of Environmental Chemical Engineering* 4, 2941-2951.
- Calvete, T., Lima, E.C., Cardoso, N.F., Dias, S.L.P., Pavan, F.A., 2009. Application of carbon adsorbents prepared from the Brazilian pine-fruit-shell for the removal of Procion Red MX 3B from aqueous solution—Kinetic, equilibrium, and thermodynamic studies. *Chemical Engineering Journal* 155, 627-636.
- Chen, W., Zhang, X., Mamadiev, M., Wang, Z., 2017. Sorption of perfluorooctane sulfonate and perfluorooctanoate on polyacrylonitrile fiber-derived activated carbon fibers: in comparison with activated carbon. *RSC Advances* 7, 927-938.
- Chen, X., Xia, X., Wang, X., Qiao, J., Chen, H., 2011. A comparative study on sorption of perfluorooctane sulfonate (PFOS) by chars, ash and carbon nanotubes. *Chemosphere* 83, 1313-1319.
- Cheng, J., Psillakis, E., Hoffmann, M.R., Colussi, A.J., 2009. Acid Dissociation versus Molecular Association of Perfluoroalkyl Oxoacids: Environmental Implications. *The Journal of Physical Chemistry A* 113, 8152-8156.
- Deng, S., Nie, Y., Du, Z., Huang, Q., Meng, P., Wang, B., Huang, J., Yu, G., 2015. Enhanced adsorption of perfluorooctane sulfonate and perfluorooctanoate by bamboo-derived granular activated carbon. *Journal of Hazardous Materials* 282, 150-157.
- Du, Z., Deng, S., Bei, Y., Huang, Q., Wang, B., Huang, J., Yu, G., 2014. Adsorption behavior and mechanism of perfluorinated compounds on various adsorbents—A review. *Journal of Hazardous Materials* 274, 443-454.
- Endo, S., Goss, K.-U., 2014. Applications of Polyparameter Linear Free Energy Relationships in Environmental Chemistry. *Environmental Science & Technology* 48, 12477-12491.
- Gagliano, E., Sgroi, M., Falciglia, P.P., Vagliasindi, F.G.A., Roccaro, P., 2020. Removal of poly- and perfluoroalkyl substances (PFAS) from water by adsorption: Role of PFAS chain length, effect of organic matter and challenges in adsorbent regeneration. *Water Research* 171, 115381.
- Gilli, G., Gilli, P., 2000. Towards an unified hydrogen-bond theory. *Journal of Molecular Structure* 552, 1-15.
- Goss, K.-U., 2008. The pKa Values of PFOA and Other Highly Fluorinated Carboxylic Acids. *Environmental Science & Technology* 42, 456-458.
- Hassan, M., Liu, Y., Naidu, R., Du, J., Qi, F., 2020. Adsorption of Perfluorooctane sulfonate (PFOS) onto metal oxides modified biochar. *Environmental Technology & Innovation* 19, 100816.
- Higgins, C.P., Field, J.A., 2017. Our Stainfree Future? A Virtual Issue on Poly- and Perfluoroalkyl Substances. *Environmental Science & Technology* 51, 5859-5860.

Inyang, M., Dickenson, E.R.V., 2017. The use of carbon adsorbents for the removal of perfluoroalkyl acids from potable reuse systems. *Chemosphere* 184, 168-175.

Ji, W., Xiao, L., Ling, Y., Ching, C., Matsumoto, M., Bisbey, R.P., Helbling, D.E., Dichtel, W.R., 2018. Removal of GenX and Perfluorinated Alkyl Substances from Water by Amine-Functionalized Covalent Organic Frameworks. *Journal of the American Chemical Society* 140, 12677-12681.

Jing, P., Rodgers, P.J., Amemiya, S., 2009. High Lipophilicity of Perfluoroalkyl Carboxylate and Sulfonate: Implications for Their Membrane Permeability. *Journal of the American Chemical Society* 131, 2290-2296.

Kah, M., Brown, C.D., 2008. LogD: Lipophilicity for ionisable compounds. *Chemosphere* 72, 1401-1408.

Kah, M., Sigmund, G., Xiao, F., Hofmann, T., 2017. Sorption of ionizable and ionic organic compounds to biochar, activated carbon and other carbonaceous materials. *Water Research* 124, 673-692.

Karickhoff, S.W., 1981. Semi-empirical estimation of sorption of hydrophobic pollutants on natural sediments and soils. *Chemosphere* 10, 833-846.

Li, F., Wei, W., Gao, D., Xia, Z., 2017. The adsorption behavior and mechanism of perfluorochemicals on oxidized fluorinated graphene sheets supported on silica. *Analytical Methods* 9, 6645-6652.

Li, X., Chen, S., Quan, X., Zhang, Y., 2011. Enhanced Adsorption of PFOA and PFOS on Multiwalled Carbon Nanotubes under Electrochemical Assistance. *Environmental Science & Technology* 45, 8498-8505.

Liu, K., Zhang, S., Hu, X., Zhang, K., Roy, A., Yu, G., 2015. Understanding the Adsorption of PFOA on MIL-101(Cr)-Based Anionic-Exchange Metal-Organic Frameworks: Comparing DFT Calculations with Aqueous Sorption Experiments. *Environmental Science & Technology* 49, 8657-8665.

Long, L., Hu, X., Yan, J., Zeng, Y., Zhang, J., Xue, Y., 2019. Novel chitosan-ethylene glycol hydrogel for the removal of aqueous perfluorooctanoic acid. *Journal of Environmental Sciences* 84, 21-28.

Machado, F.M., Bergmann, C.P., Fernandes, T.H.M., Lima, E.C., Royer, B., Calvete, T., Fagan, S.B., 2011. Adsorption of Reactive Red M-2BE dye from water solutions by multi-walled carbon nanotubes and activated carbon. *Journal of Hazardous Materials* 192, 1122-1131.

McCleaf, P., Englund, S., Östlund, A., Lindegren, K., Wiberg, K., Ahrens, L., 2017. Removal efficiency of multiple poly- and perfluoroalkyl substances (PFASs) in drinking water using granular activated carbon (GAC) and anion exchange (AE) column tests. *Water Research* 120, 77-87.

Menéndez, J.A., Phillips, J., Xia, B., Radovic, L.R., 1996. On the Modification and Characterization of Chemical Surface Properties of Activated Carbon: In the Search of Carbons with Stable Basic Properties. *Langmuir* 12, 4404-4410.

Phong Vo, H.N., Ngo, H.H., Guo, W., Hong Nguyen, T.M., Li, J., Liang, H., Deng, L., Chen, Z., Hang Nguyen, T.A., 2020. Poly-and perfluoroalkyl substances in water and wastewater: A comprehensive review from sources to remediation. *Journal of Water Process Engineering* 36, 101393.

Pignatello, J.J., Mitch, W.A., Xu, W., 2017. Activity and Reactivity of Pyrogenic Carbonaceous Matter toward Organic Compounds. *Environmental Science & Technology* 51, 8893-8908.

Qiu, L., Chen, Y., Yang, Y., Xu, L., Liu, X., 2013. A Study of Surface Modifications of Carbon Nanotubes on the Properties of Polyamide 66/Multiwalled Carbon Nanotube Composites. *Journal of Nanomaterials* 2013, 8.

Rahman, M.F., Peldszus, S., Anderson, W.B., 2014. Behaviour and fate of perfluoroalkyl and polyfluoroalkyl substances (PFASs) in drinking water treatment: A review. *Water Research* 50, 318-340.

Saeidi, N., Kopinke, F.-D., Georgi, A., 2020. Understanding the effect of carbon surface chemistry on adsorption of perfluorinated alkyl substances. *Chemical Engineering Journal* 381, 122689.

Sangster, J., 1989. Octanol-Water Partition Coefficients of Simple Organic Compounds. *Journal of Physical and Chemical Reference Data* 18, 1111-1229.

Shafeeyan, M.S., Daud, W.M.A.W., Houshmand, A., Shamiri, A., 2010. A review on surface modification of activated carbon for carbon dioxide adsorption. *Journal of Analytical and Applied Pyrolysis* 89, 143-151.

Sigmund, G., Gharasoo, M., Hüffer, T., Hofmann, T., 2020. Deep Learning Neural Network Approach for Predicting the Sorption of Ionizable and Polar Organic Pollutants to a Wide Range of Carbonaceous Materials. *Environmental Science & Technology* 54, 4583-4591.

Söregård, M., Östblom, E., Köhler, S., Ahrens, L., 2020. Adsorption behavior of per- and polyfluoroalkyl substances (PFASs) to 44 inorganic and organic sorbents and use of dyes as proxies for PFAS sorption. *Journal of Environmental Chemical Engineering* 8, 103744.

Sznajder-Katarzyńska, K., Surma, M., Cieślík, I., 2019. A Review of Perfluoroalkyl Acids (PFAAs) in terms of Sources, Applications, Human Exposure, Dietary Intake, Toxicity, Legal Regulation, and Methods of Determination. *Journal of Chemistry* 2019, 2717528.

T. Pancras, G.S., T. Held, K. Baker, I. Ross, H. Slenders, M.J. Spence, 2016. Environmental fate and effects of polyand perfluoroalkyl substances (PFAS). ARCADIS, Brussels.

Teaf, C.M., Garber, M.M., Covert, D.J., Tuovila, B.J., 2019. Perfluorooctanoic Acid (PFOA): Environmental Sources, Chemistry, Toxicology, and Potential Risks. *Soil and Sediment Contamination: An International Journal* 28, 258-273.

Walters, R.W., Luthy, R.G., 1984. Equilibrium adsorption of polycyclic aromatic hydrocarbons from water onto activated carbon. *Environmental Science & Technology* 18, 395-403.

Wellen, B.A., Lach, E.A., Allen, H.C., 2017. Surface pKa of octanoic, nonanoic, and decanoic fatty acids at the air–water interface: applications to atmospheric aerosol chemistry. *Physical Chemistry Chemical Physics* 19, 26551-26558.

Yu, J., Lv, L., Lan, P., Zhang, S., Pan, B., Zhang, W., 2012. Effect of effluent organic matter on the adsorption of perfluorinated compounds onto activated carbon. *Journal of Hazardous Materials* 225-226, 99-106.

Zhang, J., Zhang, Y., Yu, S., Tang, Y., 2016. Sorption characteristics of tetrabromobisphenol A by oxidized and ethylenediamine-functionalized multi-walled carbon nanotubes. *Desalination and Water Treatment* 57, 17343-17354.

Zhi, Y., Liu, J., 2015. Adsorption of perfluoroalkyl acids by carbonaceous adsorbents: Effect of carbon surface chemistry. *Environmental Pollution* 202, 168-176.

Zhi, Y., Liu, J., 2016. Surface modification of activated carbon for enhanced adsorption of perfluoroalkyl acids from aqueous solutions. *Chemosphere* 144, 1224-1232.

## Appendix: supporting information to

### **What is specific in adsorption of perfluoroalkyl acids on carbon materials?**

Navid Saeidi, Frank-Dieter Kopinke, Anett Georgi \*

*Helmholtz Centre for Environmental Research – UFZ, Department of Environmental Engineering,  
D-04318 Leipzig, Germany*

Corresponding author contact information: Tel.: +49 341 235 1760; Fax: +49 341 235 1471; E-mail:  
anett.georgi@ufz.de

(19 Pages, 7 Tables and 12 Figures)



### Discussion on physical properties of the ACFs:

**Figure 1Sa** shows a comparison between pore size distributions (PSD) of the ACFs and that of a coal-derived commercial powder AC (Chemviron). The results show that the pores of CACF, CACF $\text{NH}_2$  and DeCACF are predominantly in the micropore range, whereas Chemviron AC exposes a broader distribution, including micro-, meso- and macropores. **Figure 1Sb** illustrates the PSD of the activated carbon felts obtained by  $\text{CO}_2$  sorption at 0 °C.

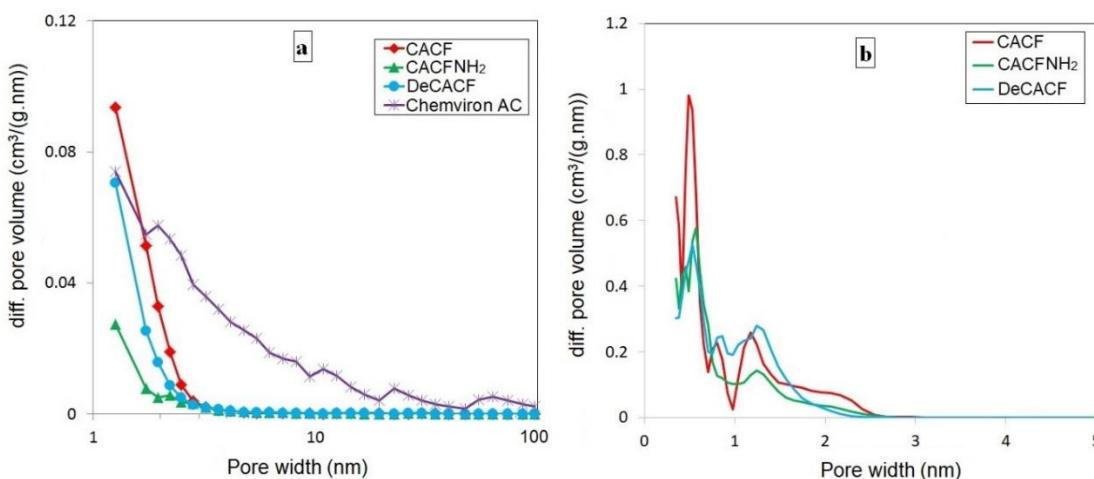


Figure 1S. Pore size distributions of the ACFs and Chemviron powder AC: a) analysis of mesopores obtained from  $\text{N}_2$  sorption data and BJH model; b) analysis of micropores obtained from  $\text{CO}_2$  sorption data and NLDFT analysis.

In general, amino-functionalisation reduced the total pore volume by 40% whereas defunctionalisation of the ACF led to only 15% loss (see Table 1). The decrease in the fibre diameter from 12 to 6.5  $\mu\text{m}$  reveals that the thermal defunctionalisation is inherently accompanied by a significant loss of AC material. The ACFs are mostly microporous in contrast to a commercial powder AC which has a wider PSD (Figure 1Sa). Figure 1Sb shows the PSD of the ACFs in the micropore range. All ACFs have a comparable bimodal PSD in the micropore range. However, the respective proportions of  $V_p$  are different. CACF has a 60/40 distribution of  $V_p$  in the two size ranges,  $< 1$  nm and 1-2 nm. Defunctionalisation mainly widened the most narrow pores  $< 1$  nm, whereas amino-functionalisation reduced the  $V_p$  in both size ranges, thus leading to about 30% decrease in specific surface area.

The missing share of larger pores in ACFs could be considered as a potential disadvantage with respect to a slower sorption kinetics. However, it is partly compensated for by the small fibre thickness, which means that the diffusion distances can be kept short.

### **Discussion on chemical surface properties of the ACFs:**

As it can be seen in Table 2, amino-functionalisation didn't affect significantly the content of weakly acidic groups (phenols, lactones and lactols). Due to the high  $pK_a$  (10 to 13 (Bandosz et al., 1993)), phenols do not play a role for surface net charge at near-neutral pH. On the other hand, protonation/deprotonation equilibria of lactones and lactols ( $pK_a$  in the range of 6 to 10 (Gómez-Bombarelli et al., 2013b)) can be relevant for surface net charge under the conditions applied in our experiments (pH 3 to 7).

**Figure 2S** shows C 1s XPS spectra of the various ACFs as well as the N 1s spectrum for ACFNH<sub>2</sub>. For CACF and DeCACF, five forms of carbon occurring on the surface were considered in the deconvolution of the C 1s XPS spectra (**Figure 2Sa** and **b**), although one additional type originating from C–N structures was recorded solely for CACFNH<sub>2</sub> (**Figure 2Sc**). Bands characteristic for carbon occurring in graphite (284.2-284.9 eV (Polovina et al., 1997)), phenols, ethers or alcohols (285.4-286.3 eV (Polovina et al., 1997)), carbonyls or quinones (287.2-287.9 eV (Polovina et al., 1997)), bonded to nitrogen structures (286.3-287.5 eV (Polovina et al., 1997)), carboxylic groups or esters (288.7-289.3 eV (Polovina et al., 1997)) are detected (see **Table 1S**). Furthermore, the band in the range 290.2 to 290.8 eV was contributed to carbonates, occluded CO or  $\pi$ -electrons in aromatic rings (Hontoria-Lucas et al., 1995).

The band of surface-bound ethylenediamine in XPS spectra can be deconvoluted with three peaks as observed for ethylenediamine-functionalised carbon nanotubes (Keen et al., 2006) and graphene oxide (Cai and Larese-Casanova, 2016); this also applies to CACFNH<sub>2</sub> (**Figure 2Sd**). In particular, the terminal C–NH<sub>2</sub> group (peak at 399.3 eV), and the amide group HN–C=O (peak at 400 eV) formed with the carbon surface can be observed. From the ethylenediamine structure it was expectable that the ratio of these peak areas is around 1:1 (Keen et al., 2006; Cai and Larese-Casanova, 2016). The amide formation reduces the carboxylic surface group concentration on CACFNH<sub>2</sub> compared to CACF (see results from Boehm titration and C 1s XPS). A third smaller peak in the N 1s spectrum occurs (at 401.7 eV). Keen et al. (Keen et al., 2006) reported that this peak is caused by ion pair formation between protonated ethylenediamine and carboxylate groups.

Obviously, some noncovalently bound ethylenediamine stays within the adsorbent even after exhaustive washing.

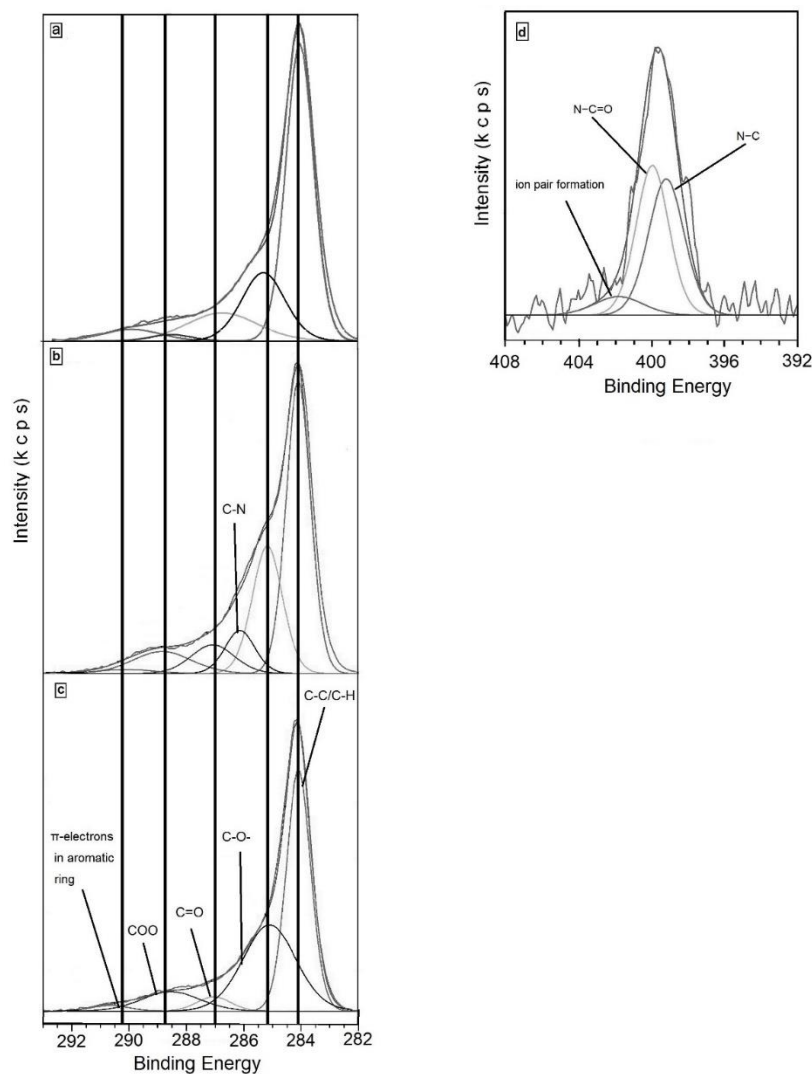


Figure 2S. Deconvoluted C 1s XPS spectra of CACF (a), CACFNH<sub>2</sub> (b) and DeCACF (c) as well as N 1s XPS spectrum of CACFNH<sub>2</sub> (d). Results are given in Table 1S.

Table 1S. Fraction of functional groups in C 1s and N 1s XPS spectra of activated carbon felts.

Sample	C <sup>a</sup> <sub>ox</sub> /C <sub>total</sub>	C 1s peak (relative area %)						N 1s peak (relative area %)		
		C in graphite	Phenol / ether	C-N	Carbonyl / quinone	Carboxyl	Others	Amine	Amide	Ion pair formation
CACF	1.1	48.0	37.0	-	4.0	9.0	2.0	-	-	-
CACFNH <sub>2</sub>	0.93	47.0	34.6	6.2	4.1	6.1	2.0	45.5	46.0	8.5
DeCACF	0.63	61.2	20.8	-	9.0	1.9	6.9	-	-	-

<sup>a</sup> carbon attached to oxygen.

The original CACF has a PZC as low as 5.9, thus at pH 7 its net surface charge is negative. Amino-functionalisation shifted the PZC to 7.3 whereas defunctionalisation caused a stronger shift to 9.3. A very low concentration of acidic groups coupled with a high concentration of C-centred basic sites provide DeCACF with this high PZC. The amidation procedure binds ethylenediamine to carboxylic groups; however, it is obviously incomplete as around 55% of carboxylic groups are remaining (based on Boehm titration results). Thus, the basic sites created (free amine group of ethylenediamine with  $pK_{a1} = 9.9$ ) just balance the remaining carboxylic groups, resulting in a PZC close to 7.

The high PZC and thus basic character of DeCACF combined with its low O content, as confirmed by the characterisation methods described above, highlights the role of basicity related to the carbon backbone itself, i.e.  $\pi$ -electron-rich sites. In fact, we supported the presence of these sites on DeCACF by removing acidic groups and saturating any resulting reactive radical sites with hydrogen.

**Figure 3S** compares CEC and carboxylic groups' concentrations (determined by Boehm titration) of the ACFs.

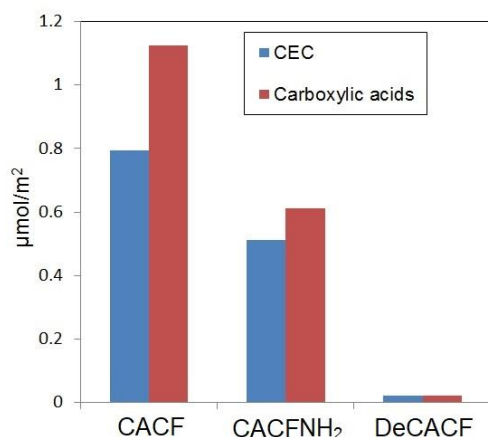


Figure 3S. Comparison between CEC and concentrations of carboxylic groups of the ACFs.

### Adsorption of PFOA, PFOS and PFBA:

**Figure 4S** shows experimental adsorption isotherms of PFOA, PFOS and PFBA on the ACFs at pH 7.

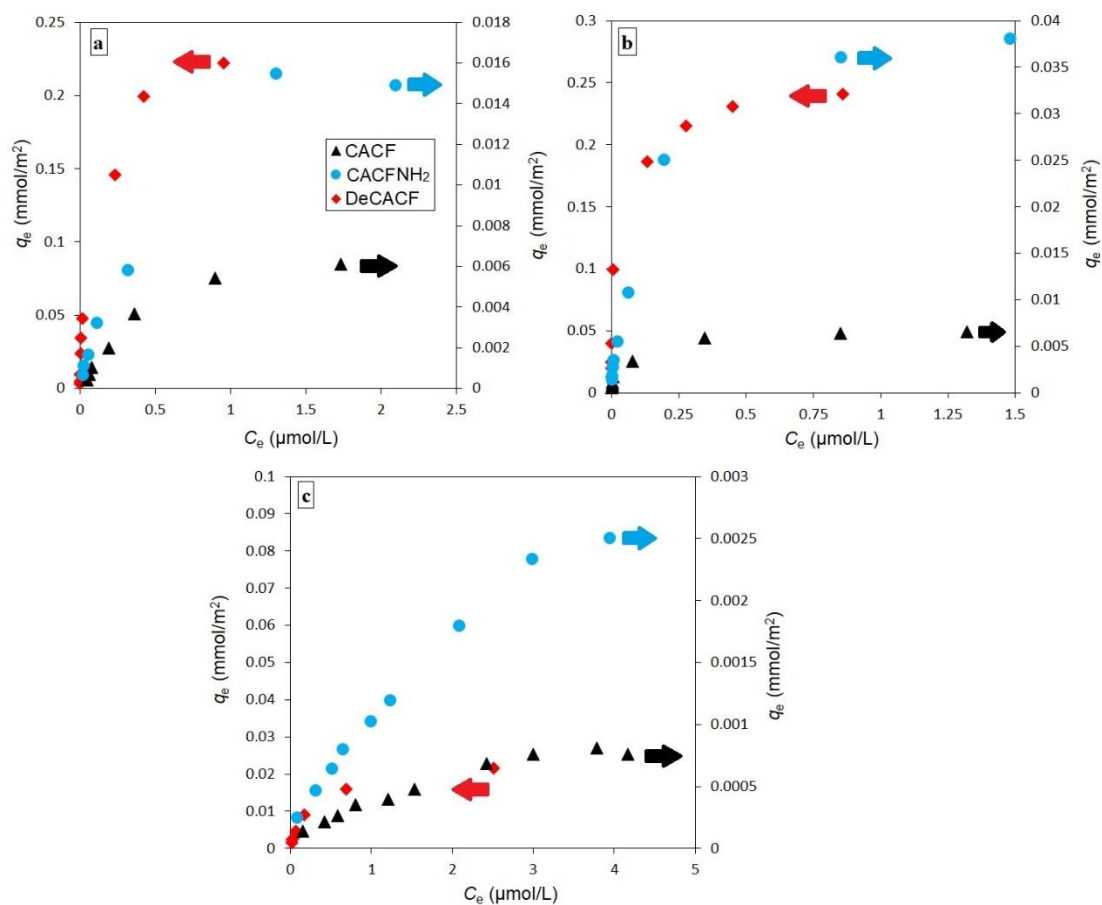


Figure 4S. Experimental data on adsorption of PFOA (a), PFOS (b) and PFBA (c) on the ACFs in 10 mM Na<sub>2</sub>SO<sub>4</sub> at pH 7.

**Table 2S** shows the isotherm parameters collected in Table 5 of the main part in terms of mass units.

Table 2S. Isotherm parameters of Freundlich and Langmuir for sorption of PFOA, PFOS and PFBA in terms of mass units.

ACF adsorbent	Adsorbate	Freundlich			Langmuir		
		$K_F$ (mg/g)/(mg/L) <sup>n</sup>	$n$	$R^2$	$q_m$ (mg/g)	$K_L$ (L/g)	$R^2$
CACF	PFOA	1.00	0.98	0.977	2.1	11,500	0.986
CACF	PFOS	83	0.79	0.991	5.0	25,000	0.979
CACF	PFBA	0.22	0.58	0.989	0.29	2,200	0.963
CACFNH <sub>2</sub>	PFOA	4.90	0.52	0.981	3.70	12,300	0.994
CACFNH <sub>2</sub>	PFOS	37	0.63	0.994	8.9	36,000	0.997
CACFNH <sub>2</sub>	PFBA	0.41	0.62	0.992	0.49	2,400	0.989
DeCACF	PFOA	710	0.64	0.983	80	79,000	0.981
DeCACF	PFOS	4,700	0.76	0.992	103	420,000	0.999
DeCACF	PFBA	19	0.70	0.987	5.1	17,200	0.997

**Figure 5S** shows adsorption of PFOA and PFBA on DeCACF in 5 successive adsorption-regeneration cycles. In brief, after the first adsorption step, the adsorbent (DeCACF) was immersed in pure methanol (1 g DeCACF in 1 L methanol) and shaken for 2 days. Then, the adsorbent was separated from methanol and dried. After that, the second adsorption cycle was performed by preparing the same adsorption condition as the first step, e.g. 0.1 g/L of adsorbent dosage for PFOA and 0.5 g/L for PFBA in 10 mM Na<sub>2</sub>SO<sub>4</sub> at pH around 7 plus 1 mg/L of adsorbates for 2 days. It is worth pointing out that desorption percentage, which was calculated by  $C_e$  of PFOA (or PFBA) after adsorption and  $C_e$  of PFOA (or PFBA) after desorption at the same cycle, was for all cycles > 90%, i.e. adsorption was largely reversible.

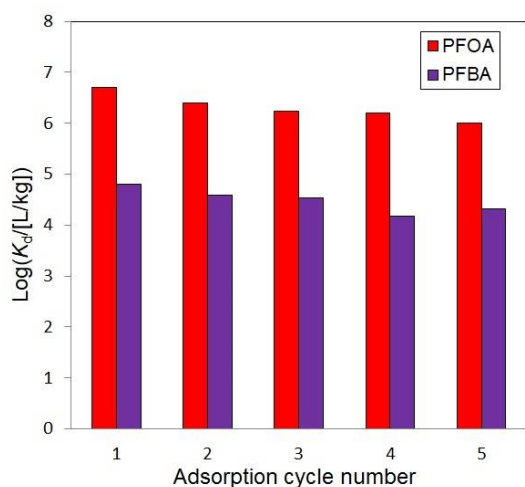


Figure 5S. Adsorption of PFOA and PFBA on DeCACF in 5 cycles. Experimental condition: adsorbent dosage: 0.1 g/L for PFOA and 0.5 g/L for PFBA;  $C_0 = 1$  mg/L, electrolyte: 10 mM Na<sub>2</sub>SO<sub>4</sub> at pH = 6.8 ± 0.4.

**Figure 6S** shows the effect of PSD on adsorption capacities of PFAAs on the ACFs.

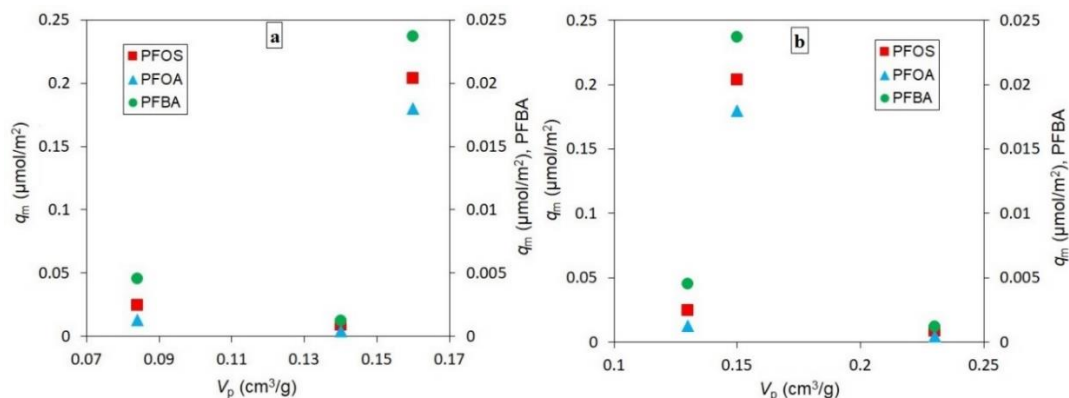


Figure 6S. Maximum loadings in adsorption of PFAAs versus volume of pores with (a) 1-2 nm width and (b) width < 1 nm.

**Tables 3S** and **4S** list physical properties and surface chemical properties of three commercial ACFs which were applied for sorption of PFOA and PFOS in our previous study (Saeidi et al., 2020a).

Table 3S. Physical properties of the commercial ACFs from our previous study (Saeidi et al., 2020a).

Sample	BET surface area (m <sup>2</sup> /g) <sup>a</sup>	Total pore volume (cm <sup>3</sup> /g) <sup>a</sup>	Pore volume (1-2 nm pore width) <sup>b</sup>	Pore volume (< 1 nm pore width) <sup>b</sup>	Fiber diameter (μm) <sup>c</sup>
VS	2100	0.99	0.57	0.23	10 ± 1
FC15	1600	0.74	0.47	0.13	10 ± 2
FC10	1400	0.62	0.34	0.21	12 ± 1

<sup>a</sup> obtained from nitrogen adsorption/desorption, <sup>b</sup> obtained from CO<sub>2</sub> sorption,

<sup>c</sup> an average of 10 measurements was reported.

Table 4S. Surface chemical properties of the commercial ACFs from our previous study (Saeidi et al., 2020a).

Sample	Boehm Titration				TPD			N-content <sup>b</sup>	PZC	AEC	CEC
	pK <sub>a</sub> ~ 3-6	pK <sub>a</sub> ~ 6-10	pK <sub>a</sub> ~ 10-13	pK <sub>a</sub> ~ 3-13	CO	CO <sub>2</sub>	O-content <sup>a</sup>				
	Carboxylic acids	Lactons and lactols	Phenols	Total acidity							
	(μmol/m <sup>2</sup> )				(wt%)					(μmol/m <sup>2</sup> )	
VS	0.0386	0.124	0.0667	0.229	0.338	0.192	2.5	0.2	7.3	0.148	0.0714
FC15	0.0687	0.0750	0.287	0.431	1.19	0.169	3.9	0.5	7.1	0.137	0.131
FC10	0.298	0.0992	0.695	1.09	4.22	1.13	15.9	0.6	6.5	0.0922	0.418

<sup>a</sup> obtained from released CO and CO<sub>2</sub>, <sup>b</sup> determined by means of XPS analysis.

**Table 5S** compares performance of DeCACF in adsorption of PFAAs with adsorption performance of various adsorbents including AC materials from very recently published studies. This comparison is based on single-point adsorption coefficients ( $K_d$ ) at a certain equilibrium aqueous phase concentration ( $C_e$ ) of the PFAAs. We calculated the  $K_d$  values from isotherm plots and Freundlich isotherm parameters reported in the respective studies. Sörensård et al. didn't report adsorption isotherms but  $K_d$  values in their adsorption experiments. From  $K_d$  values and other information provided by the authors, e.g. initial concentration of the adsorbates, adsorbent dosage and solution volume, we calculated  $C_e$  for the corresponding  $K_d$  values. Data were selected in order to provide comparable  $C_e$  for the various adsorbents for each solute, i.e. PFOA, PFOS and PFBA.

Table 5S. A comparison between single-point adsorption coefficients ( $K_d$ ) of PFAAs on DeCACF with those on various adsorbents reported very recently in literature.

Adsorbent	PFAAs	$K_d$ (L/kg)	$C_e$ (μg/L)	pH	Reference
DeCACF	PFOA	$2.9 \times 10^6$	20	7	This work
poly(ethylenimine)-functionalised cellulose	PFOA	$6.3 \times 10^5$	20	6.5	(Ateia et al., 2018)
GAC <sup>a</sup>	PFOA	$1.3 \times 10^5$	30	7	(Zhang et al., 2019)
Biochar <sup>b</sup>	PFOA	$8.2 \times 10^4$	40	7	(Zhang et al., 2019)
Powder AC <sup>c,*</sup>	PFOA	$5.6 \times 10^3$	6.7	7.5	(Söregård et al., 2020)
GAC <sup>d,*</sup>	PFOA	$3.1 \times 10^4$	1.3	7.5	(Söregård et al., 2020)
Nanoscale zerovalent iron	PFOA	$1.8 \times 10^3$	20	8.3	(Zhang et al., 2018)
DeCACF	PFOS	$1.2 \times 10^7$	8	7	This work
GAC <sup>a</sup>	PFOS	$5.1 \times 10^5$	10	7	(Zhang et al., 2019)
Biochar <sup>b</sup>	PFOS	$4.3 \times 10^5$	10	7	(Zhang et al., 2019)
Powder AC <sup>c,*</sup>	PFOS	$1.0 \times 10^4$	3.8	7.5	(Söregård et al., 2020)
GAC <sup>d,*</sup>	PFOS	$1.0 \times 10^4$	4	7.5	(Söregård et al., 2020)
Nanoscale zerovalent iron (nZVI)	PFOS	$8.7 \times 10^4$	2.5	8.6	(Zhang et al., 2018)
Sulfidated nZVI	PFOS	$5.9 \times 10^4$	2.5	8.3	(Zhang et al., 2018)
γ-FeOOH	PFOS	$8.3 \times 10^4$	2.5	7.4	(Zhang et al., 2018)
DeCACF	PFBA	$7.4 \times 10^4$	30	7	This work
GAC <sup>a</sup>	PFBA	$5.5 \times 10^3$	150	7	(Zhang et al., 2019)
Biochar <sup>b</sup>	PFBA	$6.9 \times 10^3$	150	7	(Zhang et al., 2019)
Powder AC <sup>c,*</sup>	PFBA	$9.1 \times 10^1$	82	7.5	(Söregård et al., 2020)
GAC <sup>d,*</sup>	PFBA	$1.3 \times 10^3$	23	7.5	(Söregård et al., 2020)

<sup>a</sup> Fisher Scientific (USA), <sup>b</sup> Biochar Supreme Inc. (USA), <sup>c</sup> NORIT® A ULTRA E 153 (Sweden), <sup>d</sup> Calgon Carbon (Sweden). \* The two best-performing adsorbent materials in terms of PFOA adsorption (named GAC 2 and PAC 2 there) were selected for comparison from a study of 44 sorbent materials (Söregård et al., 2020). Adsorption was performed from a mix of per- and polyfluoroalkyl substances (PFAS) (n=17). The total adsorbent loadings with PFAS are < 0.04 mg/g (1.7 mg/L total PFAS and 2.5 g/L adsorbent applied = 0.68 mg/g = 0.068 wt%). Due to this extremely low loading, adsorption competition unlikely plays a determining role in these experiments.

**Figure 7S** shows a plot of anion exchange capacities (AEC) and cation exchange capacities (CEC) versus point of zero net proton charges (PZC).

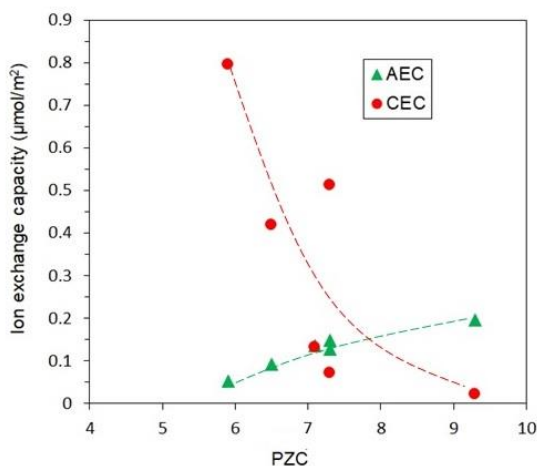


Figure 7S. AEC and CEC (μmol/m²) versus PZC of the ACFs. Lines were added as guide to the eye.



### Adsorption of PHE and OCA:

**Figure 8S** shows the experimental data in adsorption of PHE and OCA on CACF, CACF $\text{NH}_2$  and DeCACF fitted with Langmuir and Freundlich equations.

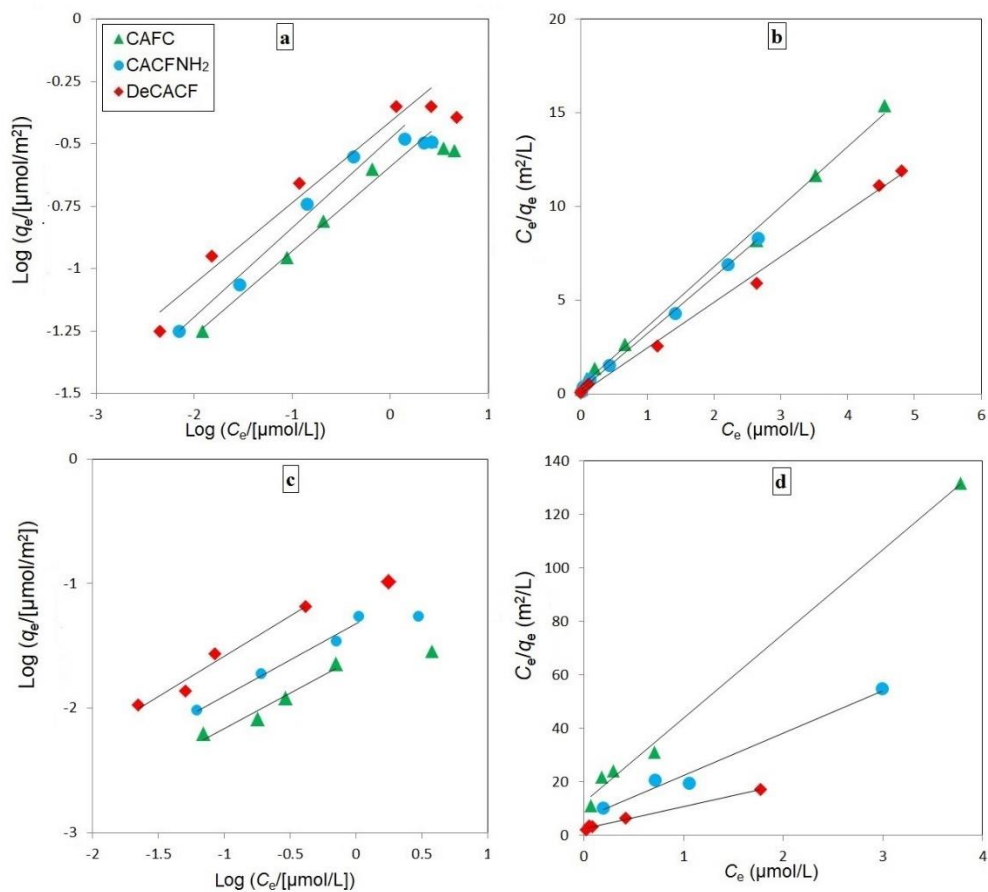


Figure 8S. Sorption isotherms for PHE on the ACFs fitted by Freundlich (a) and Langmuir (b) and for OCA fitted by Freundlich (c) and Langmuir (d) equations.

**Tables 6S and 7S** list the isotherm parameters based on specific surface areas and in mass units of the ACFs, respectively.

Table 6S. Isotherm parameters in sorption of PHE and OCA normalized to specific surface areas.

ACF adsorbent	Adsorbate	Freundlich			Langmuir		
		$K_F$ ( $\mu\text{mol}/\text{m}^2$ )/( $\mu\text{mol}/\text{L}$ ) <sup>n</sup>	$n$	$R^2$	$q_m$ ( $\mu\text{mol}/\text{m}^2$ )	$K_L$ ( $\text{L}/\mu\text{mol}$ )	$R^2$
CACF	PHE	0.26	0.34	0.987	0.31	0.0081	0.996
CACF $\text{NH}_2$	PHE	0.33	0.35	0.978	0.33	0.014	0.998
DeCACF	PHE	0.45	0.36	0.983	0.43	0.030	0.997
CACF	OCA	0.026	0.56	0.950	0.032	0.0026	0.995
CACF $\text{NH}_2$	OCA	0.048	0.58	0.984	0.062	0.0028	0.983
DeCACF	OCA	0.12	0.64	0.965	0.12	0.0031	0.992

Table 7S. Isotherm parameters in sorption of PHE and OCA in terms of mass units.

ACF adsorbent	Adsorbate	Freundlich			Langmuir		
		Log ( $K_F/[(\text{mg}/\text{g})/(\text{mg}/\text{L})^n]$ )	$n$	$R^2$	$q_m$ ( $\text{mg}/\text{g}$ )	Log ( $K_L/[\text{L}/\text{g}]$ )	$R^2$
CACF	PHE	1.9	0.34	0.987	56	4.7	0.996
CACF $\text{NH}_2$	PHE	2.0	0.35	0.978	59	4.8	0.998
DeCACF	PHE	2.2	0.36	0.983	77	5.2	0.997
CACF	OCA	1.0	0.56	0.950	5.3	4.2	0.995
CACF $\text{NH}_2$	OCA	1.2	0.58	0.984	6.5	4.3	0.983
DeCACF	OCA	1.8	0.64	0.965	17	4.4	0.992

**Figure 9S** shows correlations between single point adsorption coefficients of PFOA, OCA and PHE with surface chemical properties of the corresponding ACFs.

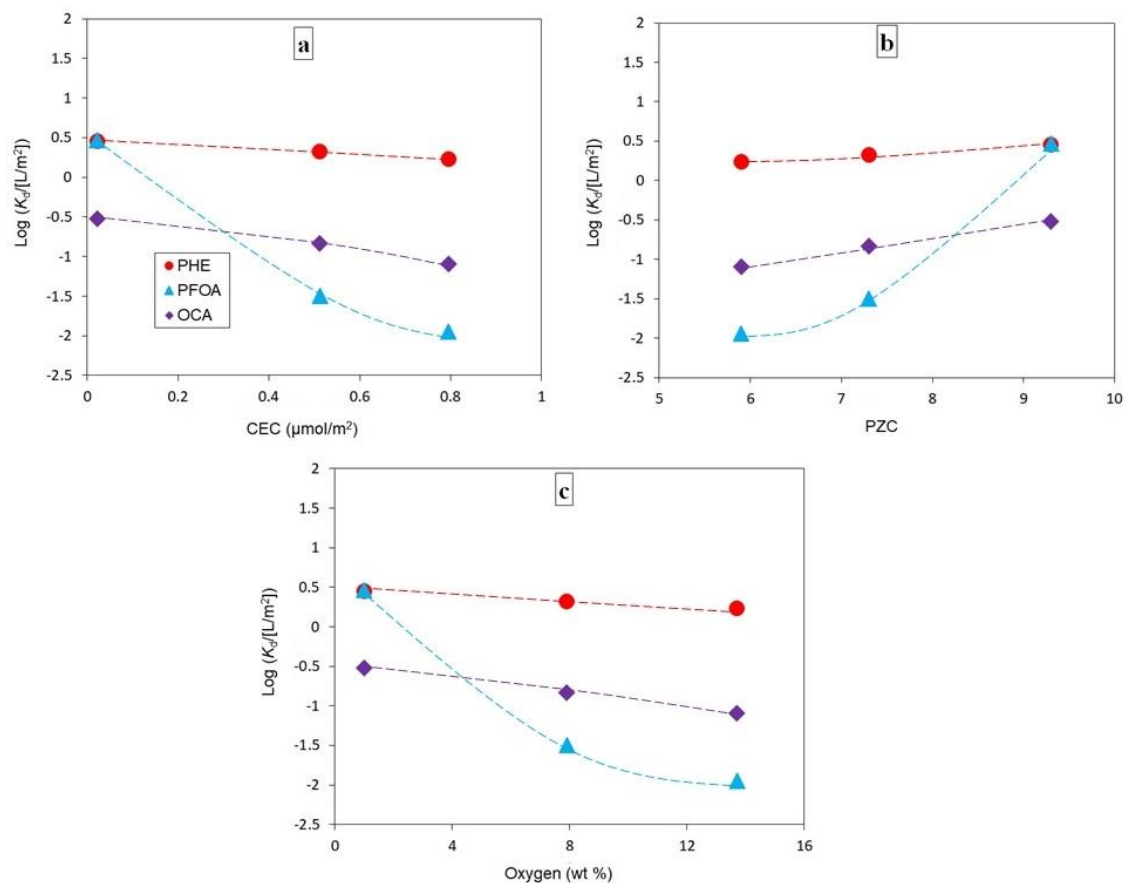


Figure 9S. Correlation between single point adsorption coefficients  $K_d$  and CEC (a), PZC (b) and oxygen content (c) of the ACFs in adsorption of PFOA, OCA and PHE from 10 mM  $\text{Na}_2\text{SO}_4$  at pH 7.  $K_d$  values are obtained at  $C_{e, \text{PFOA}} = 20 \mu\text{g}/\text{L}$  ( $0.048 \mu\text{mol}/\text{L}$ ),  $C_{e, \text{PHE}} = 10 \mu\text{g}/\text{L}$  ( $0.056 \mu\text{mol}/\text{L}$ ) and  $C_{e, \text{OCA}} = 10 \mu\text{g}/\text{L}$  ( $0.069 \mu\text{mol}/\text{L}$ ). Lines were added as guide to the eye.

### Effect of (in)organic ions on adsorption of PFOS and PFBA:

**Figure 10S** shows effect of inorganic ions on adsorption of PFOS and PFBA on the ACFs.

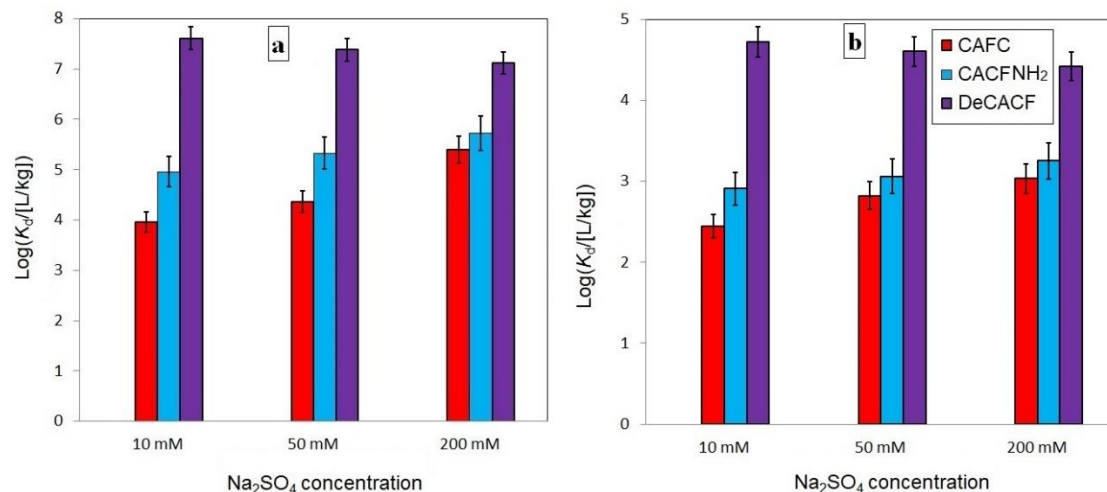


Figure 10S. Effect of inorganic ions on sorption of PFOS (a) and PFBA (b) on the ACFs. The experiments were carried out at pH 7 with  $C_0 = 1$  mg/L PFOS or PFBA and adsorbent dosage 0.1 g/L for sorption of PFOS on all ACFs, 2 g/L for PFBA on CACF and CACFNH<sub>2</sub> and 0.5 g/L for PFBA on DeCACF. The maximum deviation of single values from the mean value of 3 experiments is reported as error bars.

**Figure 11S** illustrates effect of NOM on adsorption of PFOS and PFBA.

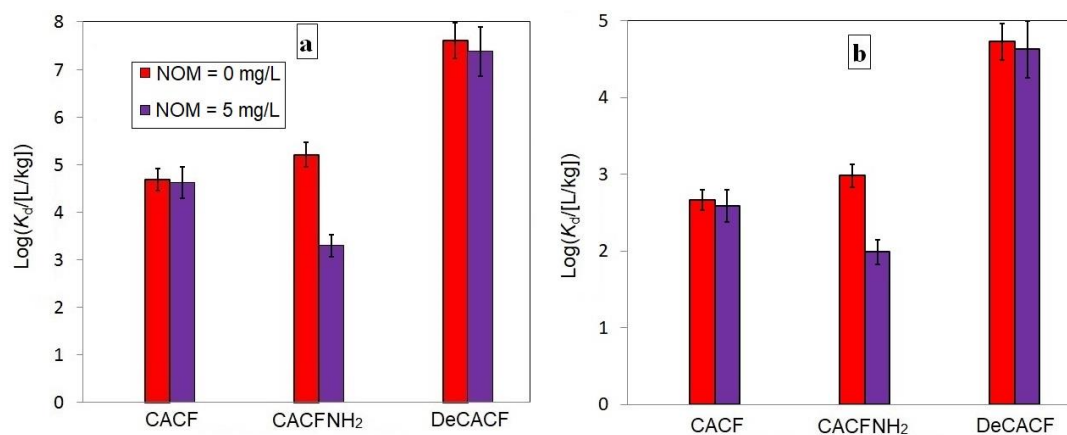


Figure 11S. Influence of NOM on sorption of PFOS (a) and PFBA (b) on the ACFs at pH 7. The experiments were performed at pH 7 with  $C_0 = 1$  mg/L PFOS or PFBA in 10 mM  $\text{Na}_2\text{SO}_4$  with and without NOM and adsorbent dosage 0.5 g/L CACF and CACFNH<sub>2</sub> and 0.1 g/L DeCACF for PFOS, 2 g/L CACF and CACFNH<sub>2</sub> and 0.5 g/L DeCACF for PFBA. The maximum deviation of single values from the mean value of the 3 experiments is reported as error bar.

### Effect of pH on adsorption of PFOA, PFOS and PFBA:

Figure 12S shows adsorption of PFOA, PFOS and PFBA on the ACFs as a function of solution pH.

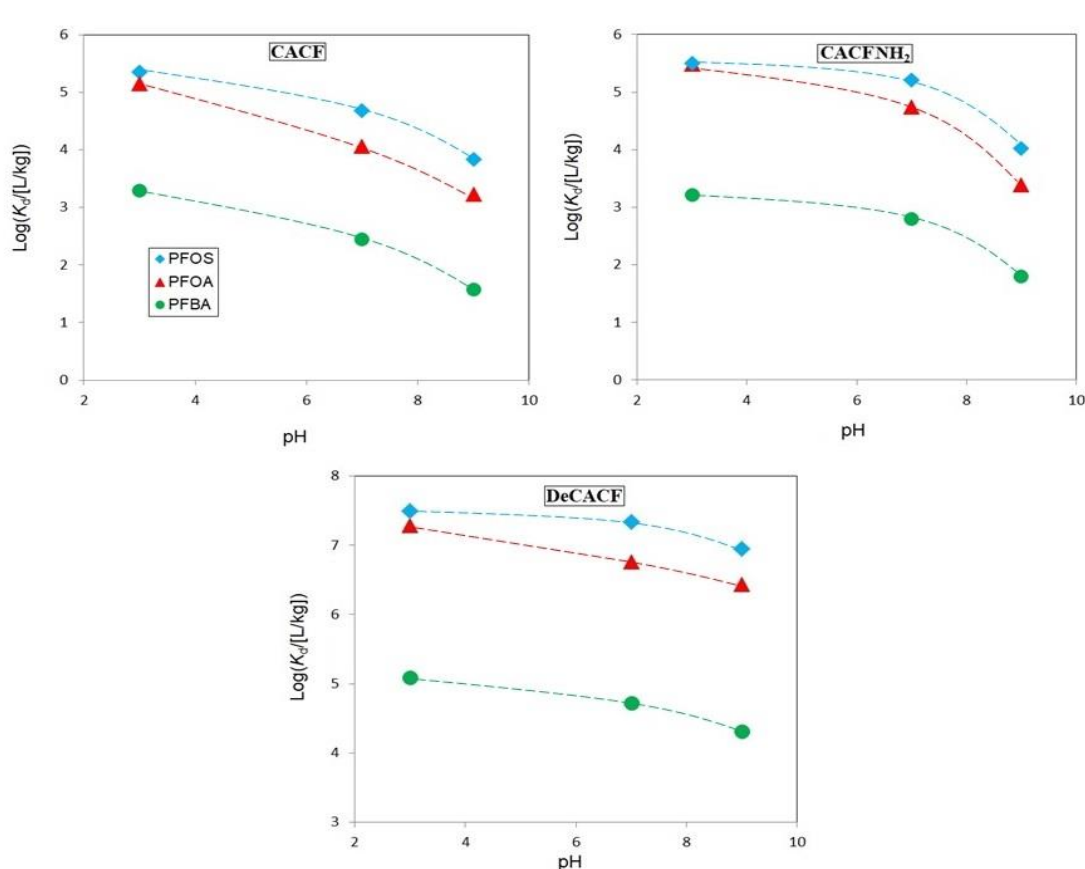


Figure 12S. Sorption of PFOA, PFOS and PFBA on DeCACF, CACF and CACF-NH<sub>2</sub> at pH 3, pH 7 and pH 9. The experiments were performed with  $C_0 = 1 \text{ mg/L}$  of adsorbate in  $10 \text{ mM Na}_2\text{SO}_4$  and adsorbent dosage  $0.02 \text{ g/L}$  for DeCACF in uptake of PFOA and PFOS;  $0.5 \text{ g/L}$  for CACF and CACF-NH<sub>2</sub> in sorption of PFOA and PFOS;  $0.5 \text{ g/L}$  for DeCACF in sorption of PFBA and  $2 \text{ g/L}$  for CACF and CACF-NH<sub>2</sub> in uptake of PFBA. Lines were added as guide to the eye.

It is obvious that changing the pH influences more significantly adsorption of the PFAAs on CACF and CACF-NH<sub>2</sub> than on DeCACF. The improvement in  $K_d$  for CACF-NH<sub>2</sub> compared to CACF mainly holds for pH 7 where aminofunctionalisation leads to a reduced density of  $-\text{COO}^-$  and presence of  $-\text{NH}_3^+$  groups. At pH 3 carboxylic groups are anyhow protonated and at pH 9 the positive charge of the amino groups is reduced. In contrast, defunctionalisation is beneficial for adsorption in the whole pH range. Also at pH 3, DeCACF is a better adsorbent than CACF even

though at this pH repulsive charges due to carboxylate groups should be minimized. This highlights the importance of charge-compensating positive charges which were introduced by the defunctionalisation. These Lewis base sites are obviously only mildly affected by an increase in pH to 9 ( $pK_a \geq 9$ ).

## References

- Ateia, M., Attia, M.F., Maroli, A., Tharayil, N., Alexis, F., Whitehead, D.C., Karanfil, T., 2018. Rapid removal of poly- and perfluorinated alkyl substances by poly(ethylenimine)-functionalized cellulose microcrystals at environmentally relevant conditions. *Environmental Science & Technology Letters* 5, 764-769.
- Bandosz, T.J., Jagiello, J., Contescu, C., Schwarz, J.A., 1993. Characterization of the surfaces of activated carbons in terms of their acidity constant distributions. *Carbon* 31, 1193-1202.
- Cai, N., Larese-Casanova, P., 2016. Application of positively-charged ethylenediamine-functionalized graphene for the sorption of anionic organic contaminants from water. *Journal of Environmental Chemical Engineering* 4, 2941-2951.
- Gómez-Bombarelli, R., Calle, E., Casado, J., 2013. Mechanisms of lactone hydrolysis in neutral and alkaline conditions. *J Org Chem* 78, 6868-6879.
- Hontoria-Lucas, C., López-Peinado, A.J., López-González, J.d.D., Rojas-Cervantes, M.L., Martín-Aranda, R.M., 1995. Study of oxygen-containing groups in a series of graphite oxides: physical and chemical characterization. *Carbon* 33, 1585-1592.
- Keen, I., Broota, P., Rintoul, L., Fredericks, P., Trau, M., Grøndahl, L., 2006. Introducing amine functionalities on a Poly(3-hydroxybutyrate-co-3-hydroxyvalerate) surface: comparing the use of ammonia plasma treatment and ethylenediamine aminolysis. *Biomacromolecules* 7, 427-434.
- Polovina, M., Babić, B., Kaluderović, B., Dekanski, A., 1997. Surface characterization of oxidized activated carbon cloth. *Carbon* 35, 1047-1052.
- Saeidi, N., Kopinke, F.-D., Georgi, A., 2020. Understanding the effect of carbon surface chemistry on adsorption of perfluorinated alkyl substances. *Chemical Engineering Journal* 381, 122689.
- Söregård, M., Östblom, E., Köhler, S., Ahrens, L., 2020. Adsorption behavior of per- and polyfluoroalkyl substances (PFASs) to 44 inorganic and organic sorbents and use of dyes as proxies for PFAS sorption. *Journal of Environmental Chemical Engineering* 8, 103744.
- Zhang, D., He, Q., Wang, M., Zhang, W., Liang, Y., 2019. Sorption of perfluoroalkylated substances (PFASs) onto granular activated carbon and biochar. *Environmental Technology*, 1-12.
- Zhang, Y., Zhi, Y., Liu, J., Ghoshal, S., 2018. Sorption of perfluoroalkyl acids to fresh and aged nanoscale zerovalent iron particles. *Environmental Science & Technology* 52, 6300-6308.



### 3.3. Controlling adsorption of perfluoroalkyl acids on activated carbon felt by means of electrical potentials

Navid Saeidi, Frank-Dieter Kopinke, Anett Georgi \*

*Helmholtz Centre for Environmental Research – UFZ, Department of Environmental Engineering,  
D-04318 Leipzig, Germany*

#### Abstract

In this work, direct electrical potentials were applied on microporous activated carbon felts (ACFs) for electroad- and -desorption of perfluorooctanoic acid (PFOA) and perfluorobutanoic acid (PFBA). Plotting adsorption affinities as single point adsorption coefficients  $K_d$  of PFOA and PFBA versus carbon electrode potentials results in bell-shaped curves with maxima located at potentials  $>$  potential of zero net charge ( $E_{PZC}$ ) of the ACFs.  $K_d$  values for electrosorption of environmentally relevant PFOA concentrations vary between 650,000 L/kg at positive potentials and 14,800 L/kg at negative potentials, i.e. a difference by a factor of 44. This difference is about a factor of 100 in case of PFBA. Based on electrosorption isotherms of PFOA, a first estimation of the concentration factor that is achievable in a fixed-bed electroadsorption/-desorption unit results in a value of about 115. The initial cyclic experiments in electroadsorption of PFOA at +500 mV and electrodesorption at -1000 mV proved that the performance of the electrosorption cell declined over prolonged polarization times. Information on  $E_{PZC}$  of the ACFs was used to select milder potential swings, e.g.  $-100 \text{ mV} < E_{PZC} = +75 \text{ mV} < +300 \text{ mV}$  which significantly improved stability in a ten cycle electroadsorption/-desorption experiment over 1000 h operation time. Competition by organic and inorganic ions as well as variable pH conditions have only minor effects on electrosorption of PFOA and PFBA. These findings indicate that this approach is not only applicable for controlling the removal of short- and long-chain perfluoroalkyl acids from contaminated water (adsorption step). It is also a promising method for on-site regeneration of carbonaceous adsorbents saturated with these compounds.

#### Keywords:

Electrosorption; PFOA; PFBA; Regeneration of activated carbon; Activated carbon felt; Surface chemistry.

---

\* Corresponding author e-mail: anett.georgi@ufz.de



## 1- Introduction

Perfluoroalkyl acids (PFAAs) are a class of fully fluorinated hydrocarbons which have been widely used for over 60 years to a wide range of industrial applications and commercial products due to their unique physical and chemical properties [1]. These compounds have been detected in various sources of water throughout the world [2, 3]. Furthermore, recent studies have addressed a rapid increase in evidence for their adverse health effects including tumor induction, hepatotoxicity, developmental toxicity, immunotoxicity, endocrine disruption, and neurotoxicity [2, 4, 5]. Therefore, the wide distribution, bioaccumulation, toxicity and chemical stability of PFAAs make it important and urgent to develop treatment methods to remove PFAAs from various sources of water.

Remediation of PFAA contaminated water is extremely challenging [6, 7]. Fixed-bed adsorption by granular activated carbon (GAC) is currently the prevailing technology at large scale [3, 7]. However, perfluorocarboxylic and sulfonic acids are a challenge even in activated carbon (AC) adsorption, as they are anionic (at all relevant pH conditions) and highly water-soluble [3, 6, 7]. The occurrence of shorter-chain PFAAs in water sources has resulted in serious problems, e.g. early breakthrough and/or no removal of perfluorobutanoic acid (PFBA) in AC filtration [3, 8, 9]. So far, on-site regeneration of AC adsorbents is not state of the art [7]. Instead, PFAA-loaded AC is incinerated or regeneration is done thermally ( $T > 800^{\circ}\text{C}$ ) in specialized plants with high-temperature post-treatment steps for exhaust gases [7, 10]. This, however, requires long-distance transportation of large amounts of adsorbent material. A recent review on the specific objectives in the removal of short- and long-chain PFAAs by adsorption addressed regeneration of PFAA exhausted adsorbents as one of the biggest challenges [7].

Adsorption coefficients ( $K_d$ ) of PFAAs on various AC materials can differ up to 4 orders of magnitude for the same adsorbate [11-14]. This large variance was attributed to different abilities for providing electrostatic interactions and charge compensation provided by positively charged surface sites (anion exchange capacity, AEC) of AC [11, 13, 15]. These results implicate that the adsorption affinity of the ACs for PFAAs can be controlled by manipulating the balance of their surface charges. One promising approach for changing the net charge on AC is the application of external electrical potentials, known as electrosorption [16]. Apart from inorganic ions, electrosorption has also been applied for manipulating the adsorption of ionic and nonionic organic compounds. As an example, the maximum adsorption capacities of aniline (in its neutral state) was

increased up to 4 times [17], of catechol and resorcinol [18] as well as benzyl alcohol [19] up to 2 times on anodically polarized AC materials. Electrosorption enhanced adsorption of various ionic aromatic compounds such as basic dyes [20] and anionic benzoate [21] up to 2 times, naphthalenesulfonate anions by 5 times [19] and by up to 5 times for some ionizable aromatic antibiotics, e.g. sulfadimethoxine, ciprofloxacin and clarithromycin [22]. The studies reviewed above observed always a clear potential dependence of electrosorption: the anionic compounds are adsorbed more strongly at more positive potentials, while cationic compounds are adsorbed more strongly at more negative potentials. Only Ban et al. [19] observed a bell-shaped curve with a maximum at zero potential (vs. Ag/AgCl as reference electrode) in electrosorption of benzyl alcohol on AC. Fischer [23] predicted that a plot of electrosorption coefficients or capacities of organic compounds on the AC materials versus applied potentials should result in bell-shaped curves with a maximum adsorption at either zero potential in electrosorption of nonionic molecules or at slightly positive and negative potentials in electrosorption of organic anions and cations, respectively. This prediction could not be validated yet for ionic organic compounds due to the lack of available experimental data from literature.

Electrosorption of PFOA and PFOS on graphene- and carbon nanotube-based electrodes has been described in three previous publications [24-26]. Li et al. [24] reported that enhanced electrostatic attractions between PFOA and PFOS anions and a polarized carbon nanotube-based electrode (+0.6 V vs. Ag/AgCl) leads to a 2-fold increase in maximum loadings (based on Langmuir isotherm fitting) compared with open circuit attempts. In these studies, various factors influencing the process, e.g., reversibility and cyclability of the process, competitive adsorption of target pollutants with non-target compounds such as inorganic and organic ions and electrosorption behaviour of the PFAAs versus potential have not been investigated. Such information are essential for practical application of electrosorption.

AC materials are the most used electrodes in electrosorption of organic compounds and/or capacitive deionization (CDI). Attrition of the AC electrodes by direct and/or indirect oxidation and reduction under electrical potentials has been posed as a serious drawback for achieving a stable performance of the process over prolonged polarization times [27-29]. In fact, it is well-known that the changes in AC properties induced by anodic and cathodic potentials may lead to performance decline of CDI cells [30-33]. Applying milder potentials on the electrodes resulted in more stable performance [34, 35]. The relation between net charge and applied potential on an

AC electrode is also determined by the fixed charges resulting from acidic and basic groups on the AC surface. This fixed charge also occurs if the electrical circuit is shorted. Applying external potentials with a sign opposite to the fixed charge first leads to charge compensation until the potential of zero net charge ( $E_{PZC}$ ) is reached. Only after crossing the  $E_{PZC}$ , electric charges can effectively accumulate net charge of the opposite sign as the fixed charge [34]. PFAA anions can adsorb favorably on a polarized AC electrode for applied potentials  $E > E_{PZC}$ . Then, electrodesorption occurs by switching potential to  $E < E_{PZC}$ . Therefore, selection of AC electrodes based on their  $E_{PZC}$  enables the user to apply milder potentials for electroadsorption and -desorption of PFAA anions. This strategy has not been applied yet for prolonging a cell performance in electrosorption of organic compounds to the best of our knowledge.

In general, due to the recalcitrance of PFAAs practically all degradation processes require harsh conditions and/or long reaction times and as such are not applicable for treatment of large volumes or flows of contaminated water with trace levels of PFAA contamination [6, 36]. Electrooxidation which is able to degrade perfluorocarboxylic and sulfonic acids using commercially available BDD electrodes faces the problems of low space-time-yield connected with high-investment costs of these electrodes [37-39]. Thus, it was applied in combination with membrane filtration as pre-step for treatment of the more concentrated PFAAs-containing retentate [39]. Another promising approach could be an electro-stimulated adsorption, i.e. treating the large volume of incoming water ( $V_{ads}$ ) containing PFAAs by favorable electroadsorption conditions and providing a low-volume PFAAs concentrate ( $V_{des}$ ) by electrodesorption of PFAAs from the saturated adsorbent electrodes. Finally, the adsorbent is regenerated and the low-volume concentrate can be processed further e.g. by electrooxidation. Reaching a low  $V_{des}/V_{ads}$  ratio or a high concentration factor is the goal of this approach.

In this study we show for the first time that by applying electric potentials to conductive activated carbon felts (ACFs), ad- and desorption of PFOA and PFBA can be effectively controlled. Based on adsorption isotherm data for PFAAs at positively and negatively charged ACFs, we provide a first estimation of the concentration factor that is achievable in a fixed-bed electrosorption unit. Special emphasis was placed on the mitigation of performance decline of an electrosorption cell over prolonged polarization times (10 electroadsorption/-desorption cycles).

## 2. Materials and Methods

### 2.1. Materials

PFOA and PFBA were purchased from Sigma-Aldrich (USA) with 96% and 98% purity, respectively. HCl (fuming 37%), NaOH, NaHCO<sub>3</sub>, KCl, NaNO<sub>3</sub>, MgSO<sub>4</sub>, CH<sub>3</sub>COONH<sub>4</sub>, Na<sub>2</sub>CO<sub>3</sub> and Na<sub>2</sub>SO<sub>4</sub> (all in highest available purity) were obtained from Merck (Germany). Methanol (99.9%) was purchased from CHEMSOLUTE (Germany). Suwannee River natural organic matter (SRNOM, reference number: 2R101N) was obtained from the International Humic Substances Society (IHSS).

### 2.2. Textural and chemical surface properties of activated carbon felts

The ACFs were purchased from Jacobi CARBONS, Sweden. The commercial names of these ACFs are ACTITEX FC 1501 (ACF1 in this study), ACTITEX FC 1001 (ACF2) and ACTITEX WK L20 (ACF3). In addition, a defunctionalised carbon felt (DeACF3, defunctionalised ACF3) was prepared by thermal treatment in N<sub>2</sub>/H<sub>2</sub> atmosphere. This procedure as well as the characterisation of the ACFs was described in detail in a previous study [40] (note that CACF in [40] = ACF3). The most important characterisation data are shown in Tables S1 and S2 in Supporting Information. Prior to use, the ACFs were washed first with methanol and then rinsed 5 times with deionized water. Finally, the ACFs were dried at 80 °C on air and kept in a desiccator for further use.

### 2.3. Electrochemical characterisation of activated carbon felts

Cyclic voltammetry (CV) experiments were carried out in three electrode cells at room temperature, using commercial Ag/AgCl reference electrodes (REs, Sensortechnik Meinsberg SE11, Germany) and platinum plates (1 cm × 4 cm) as counter electrode (CE) in 1 M Na<sub>2</sub>SO<sub>4</sub> solution. Before and after each measurement, the potential readings of the REs were verified by comparison to fresh ones. The variation was within the range of 10 mV. The electrochemical cells were made of glassware. A high resolution potentiostat/galvanostat (MSX-8, ScioSpec, Germany) was used for performing measurements of CV and electroadsorption/-desorption experiments. Electrochemical impedance spectroscopy (EIS) measurements were applied to identify relevant frequency ranges for investigating the capacitance minimum. EIS was measured from 3 mHz to 1 kHz with various potentials (from +500 mV to -500 mV) by means of a

potentiostat/galvanostat/impedancemeter (OGS100, OrigaLys, France). EIS was carried out in custom-made two-piston cells that enabled testing in a three electrode setup. Contacting of the current collectors was accomplished by titanium pistons. A piece of ACF was introduced from side to the cell and served as quasi reference electrode. It was separated from other electrodes by means of a glass-fiber separator (type GF/D, Whatman, GE healthcare life science). The reference potential of the quasi reference electrode was determined versus the commercial Ag/AgCl RE. The results were reported based on the potential of Ag/AgCl RE. Electrolyte filling was accomplished by inserting the electrolyte via filling tubes and applying a small negative pressure to ensure complete filling [41]. A schematic drawing of the cell is shown in Figure 1S in Supporting Information. For more details on the cell, we refer the readers to [41]. Open circuit potentials ( $E_0$ ) of the ACFs were also measured by means of the OGS100 instrument at pH 7.

Differential capacitance measurements were carried out in order to recognize  $E_{PZC}$  from the capacitance minimum [42]. The frequencies at which the imaginary part of  $Z$  became nearly independent of the frequency were monitored by means of Nyquist plots. These frequencies were used to calculate the capacitance  $C$  from the imaginary part ( $Z_{Im}$ ) of the impedance using Eq. 1:

$$C = - (\omega Z_{Im})^{-1} \quad (1)$$

where  $\omega$  is the angular frequency ( $\omega = 2\pi/\text{period}$ ).

#### 2.4. Analytical methods

Analysis of PFOA and PFBA was carried out by means of a liquid chromatography system coupled to a single-stage quadrupole mass spectrometer with electrospray ionization (LCMS-2020; SHIMADZU Corporation, Japan). The analytical procedure was discussed elsewhere in detail [11]. For concentrations in the range 1  $\mu\text{g/L}$  - 1  $\text{mg/L}$  the correlation coefficients ( $R^2$ ) of the linear calibration curves for PFOA and PFBA were  $> 0.99$ . The standard deviation of single values (estimated from 5 parallel measurements) was around 5%. The detection limits for PFAAs were about 0.05  $\mu\text{g/L}$ .

## 2.5. Electrosorption experiments

As mentioned earlier, all electroadsorption/-desorption experiments were carried out in a series of batch three-electrode cells connected to a potentiostat. In the cells, ACF was used as working electrode (WE), a commercial Ag/AgCl electrode as RE, and platinum plate (1 cm × 4 cm) as CE. Na<sub>2</sub>SO<sub>4</sub> solutions were used as electrolyte. The pH of the system was adjusted to the desired values by adding 0.1 M HCl or NaOH solution. After adjusting pH, certain concentrations of the target solutes were spiked from stock solutions. In electrodesorption experiments, after reaching equilibrium in electrosorption, the potential was converted to respective values.

The amount of PFOA and PFBA adsorbed by the ACFs (adsorbate loading) was calculated from Eq. 2:

$$q_e = \frac{V \times (C_0 - C_e)}{m} \quad (2)$$

here  $q_e$  (mg/g) denotes loading of adsorbate on the adsorbent at equilibrium. The initial adsorbate concentration and its concentration in solution at equilibrium are addressed by  $C_0$  and  $C_e$  (mg/L), respectively.  $V$  (L) denotes the volume of solution and  $m$  (g) is the mass of the adsorbent or WE. The single-point adsorption coefficient  $K_d$  (L/g) of the solutes on the adsorbents can be calculated by means of Eq. (3):

$$K_d = \frac{q_e}{C_e} \quad (3)$$

Equilibrium was considered to be approached after 2 d, as no significant changes in the aqueous phase solute concentrations were observed ( $\leq 5\%$ ) at further prolonged contact times.

## 2.6. Theoretical approach

### 2.6.1. Electrosorption isotherms

The experimental data were fitted with a linearised form of the empirical Freundlich equation (Eq. 4):

$$\log q_e = n \times \log C_e + \log K_F \quad (4)$$

with  $K_F$  ((mg/g)/(mg/L)<sup>n</sup>) as the Freundlich constant which denotes the adsorption affinity, while  $n$  is the dimensionless Freundlich exponent. Formally, the arguments under the logarithms have to be divided by the corresponding units.

### 2.6.2. Calculation of $V_{des}/V_{ads}$ and concentration factor

Prospectively, the batch reactor should be replaced by a continuous flow system for any practical application. In a fixed-bed flow through system the adsorbent bed is progressively loaded with the adsorbate from inflow to outflow reaching the equilibrium loading ( $q_{ads}$ ) related to the inflow concentration ( $C_{in}$ ) until breakthrough occurs. In a simplified approach, we assume a step-like breakthrough curve. Band-broadening effects due to incomplete establishment of adsorption equilibria or dispersion effects were neglected. The equilibrium loading can be described by the Freundlich isotherm parameters under adsorption conditions ( $K_{F,ads}$  and  $n_{ads}$ ), e.g. applying mild positive potentials for PFOA adsorption and breakthrough occurs after treatment of a certain volume ( $V_{ads}$ ) of inflow water:

$$q_{ads} = K_{F,ads} \times C_{in}^n \quad (5)$$

$$V_{ads} = \frac{q_{ads} \times m}{C_{in}} \quad (6)$$

For regeneration, a mild negative electrical potential is applied shifting the sorption equilibrium towards desorption, i.e. lower Freundlich coefficients  $K_{F,des} < K_{F,ads}$  and possibly different Freundlich exponents ( $n_{des} \neq n_{ads}$ ). The inflow water can be used in the desorption step, as it contains a low solute concentration ( $C_{in}$ ) compared to the following desorption step ( $C_{des}$ ). The general goal of this procedure is to reduce the volume of water which is needed for desorption ( $V_{des}$ ) compared to the cleaned water volume ( $V_{ads}$ ). The ratio  $V_{des}/V_{ads}$  can be calculated as follows, based on mass balances:

$$V_{ads} \times C_{in} = q_{ads} \times m = K_{F,ads} \times C_{in}^{n_{ads}} \times m \quad (7)$$

For the desorption step, using inflow water for regeneration, Eq. 8 can be established where the solute concentration in the effluent ( $C_{\text{des}}$ ) is determined by the loading from the adsorption step and the Freundlich parameters under desorption conditions,  $K_{\text{F,des}}$  and  $n_{\text{des}}$ . At the same time, the mass balance Eq. 9 is met with  $X_{\text{des}} = 1 - q_{\text{des}}/q_{\text{ads}}$  as the extent of adsorbent deloading:

$$V_{\text{des}} \times (C_{\text{des}} - C_{\text{in}}) = V_{\text{des}} \times \left( \left[ \frac{q_{\text{ads}}}{K_{\text{F,des}}} \right]^{\frac{1}{n_{\text{des}}}} - C_{\text{in}} \right) \quad (8)$$

$$V_{\text{des}} \times (C_{\text{des}} - C_{\text{in}}) = X_{\text{des}} \times C_{\text{in}} \times V_{\text{ads}} \quad (9)$$

where  $q_{\text{des}}$  denotes the equilibrium loading of the adsorbent under desorption conditions.

With Eqs. 8 and 9 the ratio of water volumes for desorption and adsorption is calculated (Eq. 10):

$$\frac{V_{\text{des}}}{V_{\text{ads}}} = \frac{X_{\text{des}} \times C_{\text{in}}}{\left( \frac{q_{\text{ads}}}{K_{\text{F,des}}} \right)^{\frac{1}{n_{\text{des}}}} \times C_{\text{in}}} = \frac{X_{\text{des}}}{C_{\text{in}}^a \times \left( \frac{K_{\text{F,ads}}}{K_{\text{F,des}}} \right)^{\frac{1}{n_{\text{des}}} - 1}} \quad \text{with} \quad a = \frac{n_{\text{ads}}}{n_{\text{des}}} - 1 \quad (10)$$

$X_{\text{des}}$  can be described by Eq. 11 as follows:

$$X_{\text{des}} = 1 - \frac{K_{\text{F,des}}}{K_{\text{F,ads}}} \times C_{\text{in}}^b \quad \text{with} \quad b = n_{\text{ads}} - n_{\text{des}} \quad (11)$$

If the Freundlich exponents are similar for the adsorption and desorption isotherms, i.e.  $n_{\text{ads}} \approx n_{\text{des}} \approx n$ , Eqs. 10 and 11 can be simplified to Eq. 12, which gives the reciprocal of a concentration factor  $V_{\text{des}}/V_{\text{ads}} = 1/F$ :

$$\frac{V_{\text{des}}}{V_{\text{ads}}} = \frac{X_{\text{des}}}{\left( \frac{K_{\text{F,ads}}}{K_{\text{F,des}}} \right)^{\frac{1}{n}} - 1} \quad \text{with} \quad X_{\text{des}} = 1 - \frac{K_{\text{F,des}}}{K_{\text{F,ads}}} \quad (12)$$

It is worth noting that the formulas derived above are valid for the assumed operation regime, i.e. a plug-flow regime with rectangular concentration profiles.



### 3. Results and discussion

#### 3.1. Characterisation of the ACFs

##### 3.1.2. Textural and chemical surface characteristics

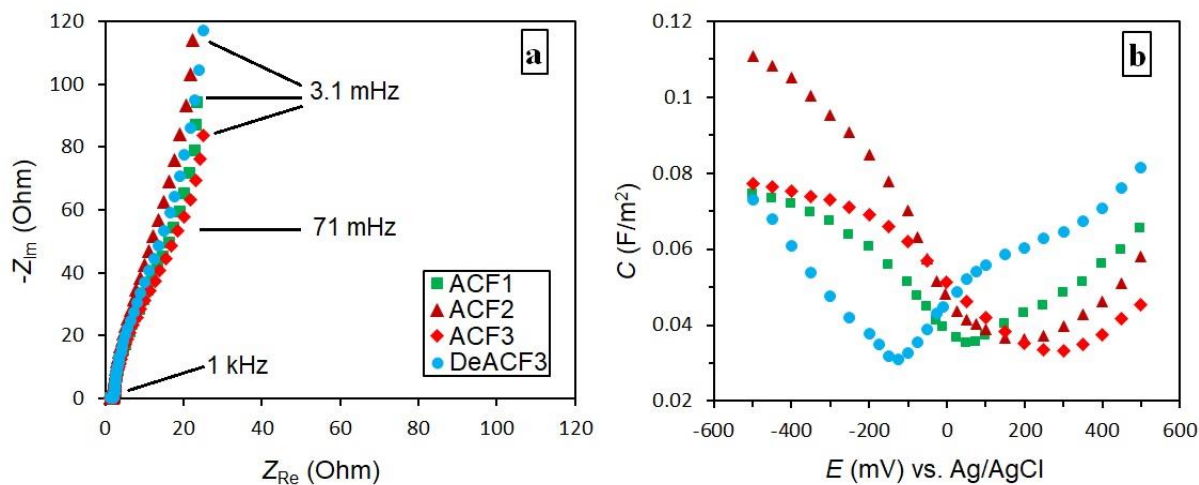
ACFs differ significantly in their pore size distributions (PSD) from common ACs. The ACFs investigated here are mostly microporous (Figure 2S) with differences in total pore volume and surface area (see Table 1S in Supporting Information). In fact, ACF1 has the highest surface area ( $1600 \text{ m}^2/\text{g}$ ) and total pore volume ( $0.74 \text{ cm}^3/\text{g}$ ), followed by ACF2, ACF3 and DeACF3. Table 2S in Supporting Information lists chemical characteristics of the surface groups of the ACFs. ACF3 has the highest concentration of acidic groups, which were largely eliminated by thermal treatment in  $\text{N}_2/\text{H}_2$  atmosphere resulting in DeACF3. Furthermore, DeACF3 contains the highest anion exchange capacity ( $\text{AEC} = 0.2 \text{ } \mu\text{mol}/\text{m}^2$ ) at pH 7, followed by ACF1, ACF2 and ACF3. The opposite order is true for cation exchange capacities (CECs). The thermal treatment also eliminated the oxygen content of ACF3 from 13.7 wt% to 1.1 wt% in DeACF3, while oxygen contents of ACF1 and ACF2 are 15.9 wt% and 3.9 wt%, respectively. Nitrogen contents of all ACFs are less than 1 wt%.

##### 3.1.3. Electrochemical characterisation

Figure 1a illustrates Nyquist plots at +100 mV obtained in 1 M  $\text{Na}_2\text{SO}_4$  solution at pH 7. The Nyquist plots are comparable with the ones of an ideally polarisable electrode, which corresponds to an Ohmic solution resistance and a double layer capacitance in series where the Nyquist plot owns a vertical line and the intercept with the real axis gives an approximate of the electrolyte resistance [43]. The results suggest a characteristic frequency of 71 mHz for all ACFs above which the imaginary part of  $Z$  becomes nearly independent of the frequency. This value was considered as the upper limit of frequency for measuring the differential capacitance as described below.

Capacitance values for the ACFs were calculated using Eq. 1 at frequencies 3.1, 7.9, 16 and 71 mHz between -500 mV and +500 mV. Figure 1b shows differential capacitance curves measured at a frequency of 3.1 mHz versus potential, while the differential capacitance curves obtained at other frequencies are shown in Figure 3S. The capacitance values were normalized to the specific surface areas of the ACFs. The minimum capacitance value is considered as  $E_{\text{PZC}}$  of the respective ACF [42]. Thus,  $E_{\text{PZC}}$  values for ACF1, ACF2, ACF3 and DeACF3 are around +75, +200, +300 and -150 mV, respectively. As can be seen in Figure 1b, when an applied potential crosses the  $E_{\text{PZC}}$

towards more positive (or more negative) potentials, anion-adsorption (or cation-adsorption) correspondingly enhances [34, 44]. A low absolute  $E_{PZC}$  value of a carbon electrode allows easy charge reversal by applying mild potentials, thus lowering carbon electrode erosion and improving long-term performance.

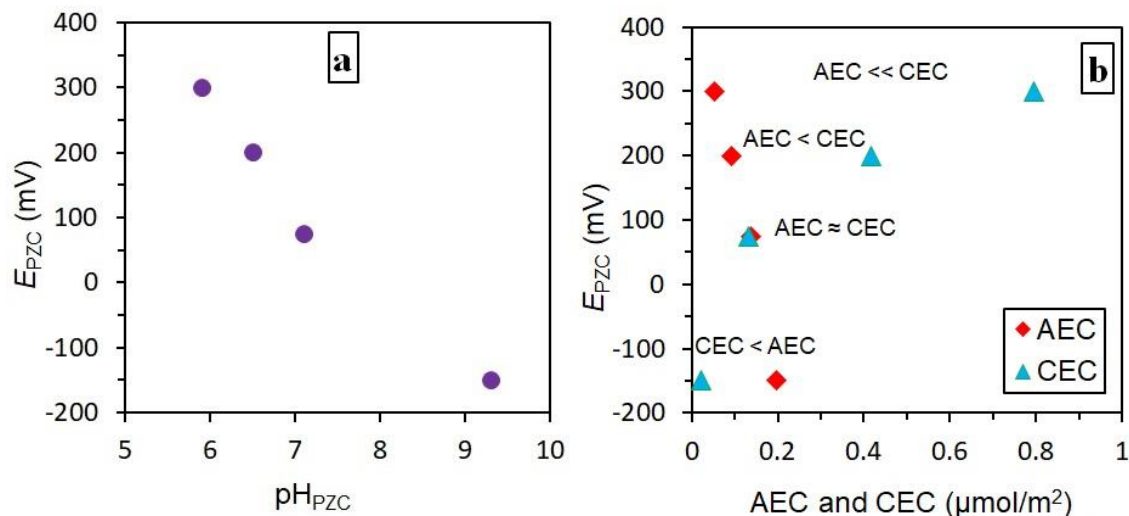


**Figure 1.** Nyquist plots of the negative imaginary part of the impedance ( $-Z_{Im}$ ) versus the real part ( $Z_{Re}$ ) measured for the ACF electrodes at +100 mV in 1 M  $Na_2SO_4$  (a). Differential capacitance ( $C$ ) of the ACFs at frequency 3.1 mHz versus the potential (b). Electrolyte was 1 M  $Na_2SO_4$  solution at pH 7. The capacitance was normalized to specific surface areas of the ACFs. The minimum capacitance values are considered as  $E_{PZC}$ .

As a consequence, DeACF3 and ACF1 were considered as more appropriate than ACF2 and ACF3 for the intended electroadsorption/-desorption approach. As mentioned earlier, the  $E_{PZC}$  of a carbon-based electrode is a transition potential region where the electrode has the least capability for ion adsorption [43].

The  $E_{PZC}$  values of the ACFs were measured under similar conditions and at pH 7. Differential capacitances in Figure 1b were normalized to the surface areas of the ACFs. Therefore, the differences in  $E_{PZC}$  of the various ACFs can be attributed to their chemical surface properties. Figure 2 shows the effect of chemical surface properties of the ACFs on  $E_{PZC}$ . The order in  $E_{PZC}$  ( $ACF3 > ACF2 > ACF1 > DeACF3$ ) is opposite to the order of  $pH_{PZC}$  of the ACFs (Figure 2a). For example,  $pH_{PZC} = 5.9$  for ACF3 means that at circumneutral pH the net charge on the surface of ACF3 without any applied electric potential is negative. Therefore, the applied positive potential firstly needs to compensate the negative charge associated to functional surface groups until a balanced net charge is reached at  $E_{PZC}$  (around +300 mV). While the applied positive potential

crosses  $E_{PZC}$  ACF3 is finally positively charged. ACF1 with  $pH_{PZC}$  close to 7, i.e. with almost balanced surface net charge at pH 7 without potential, consequently has a lower  $E_{PZC}$  value (+ 75 mV), while DeACF3 with  $pH_{PZC} = 9.3$  even has an  $E_{PZC}$  (-150 mV) in the negative potential range.

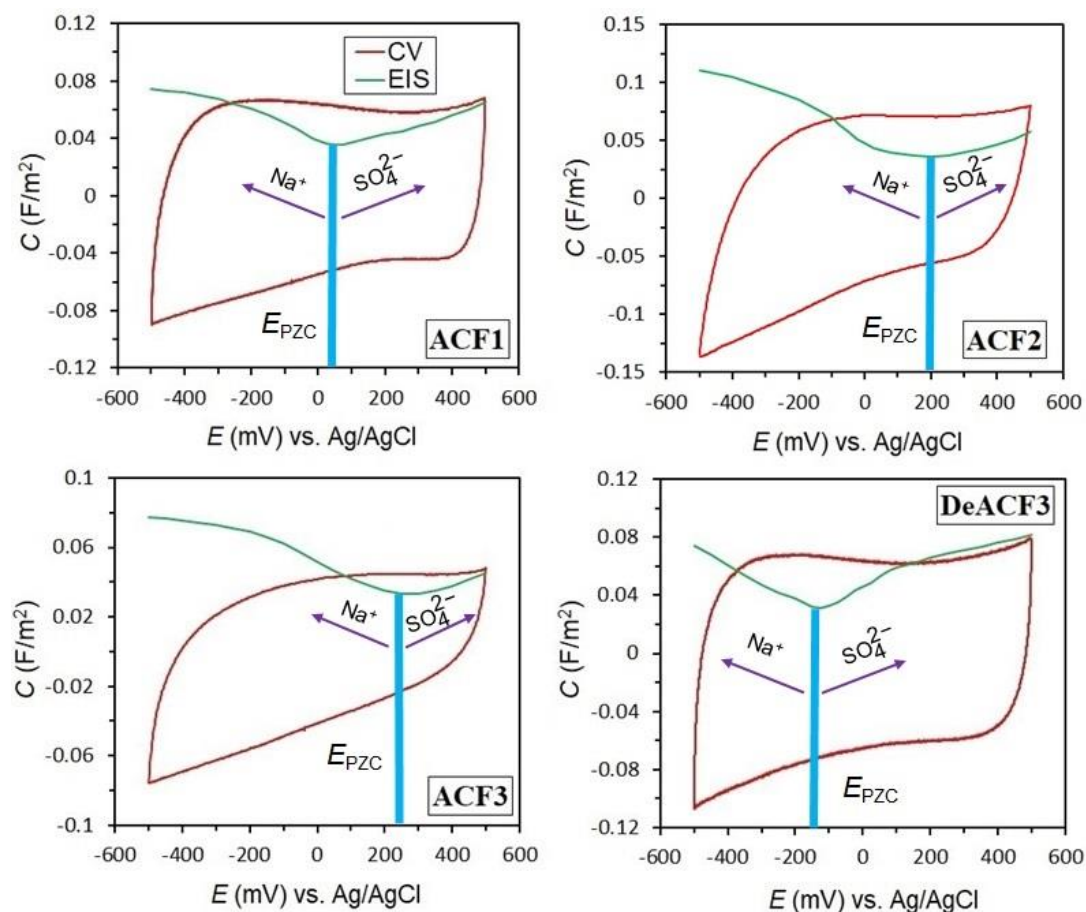


**Figure 2.** Effect of surface chemical properties of the ACFs on  $E_{PZC}$ . AEC, CEC and  $E_{PZC}$  were determined at pH 7.

As can be seen in Figure 2b, when  $CEC > AEC$ , namely in case of ACF2 and ACF3, the  $E_{PZC}$  locates in the positive potential range. However, when  $CEC < AEC$  e.g. in case of DeACF3 the  $E_{PZC}$  is in the negative range, although ACF1 with  $CEC \approx AEC$  has the lowest  $E_{PZC}$  absolute value. Note that AEC and CEC as anion and cation exchange capacity of the carbon are related to the density of positively and negatively charged surface functional groups at pH 7 (without external potential).

The study on cyclic voltammograms (CVs) of the ACFs showed quasi-rectangular curve shapes for all ACFs at the scan rate of 1 mV/s in accordance with their capacitive behaviour. Figure 3 compares capacitance values of the ACFs obtained from CVs at a scan rate of 1 mV/s with those calculated by means of EIS at a frequency of 3.1 mHz. First of all, the capacitance values obtained from both EIS and CVs are comparable. Both, EIS and CV experiments were performed in 1 M  $\text{Na}_2\text{SO}_4$  solutions at pH 7. Therefore, the capacitance is associated to adsorption of anions ( $\text{SO}_4^{2-}$ ) on the positively charged ACFs ( $E > E_{PZC}$ ). On the other hand, adsorption of cations ( $\text{Na}^+$ ) results in capacitance of the ACFs polarized with  $E < E_{PZC}$ . It can be seen from Figure 3 (EIS curves) that ACF2 has the highest total capacitance. In fact, by polarization of ACF2 to -500 mV or +500 mV,

its capacitance reaches to around 0.12 F/m<sup>2</sup> and 0.06 F/m<sup>2</sup>, respectively, resulting in a total capacitance of 0.18 F/m<sup>2</sup>.



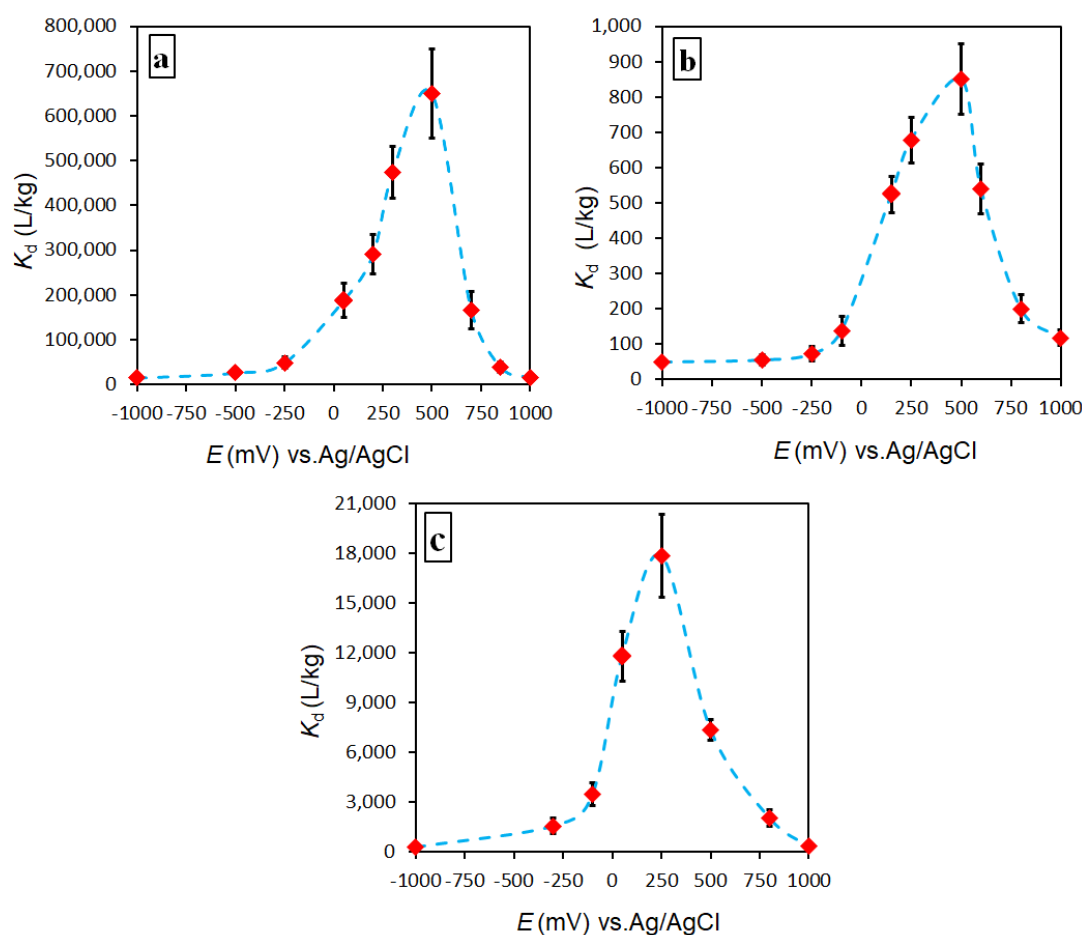
**Figure 3.** A comparison between capacitance values obtained from CV at scan rate 1 mV/s and EIS at frequency 3.1 mHz. The experiments were performed in 1 M Na<sub>2</sub>SO<sub>4</sub> at pH 7.

ACF3 shows also a higher capacitance coming from adsorption of cations (for  $E < E_{PZC} = +300$ ) than from anions (for  $E > E_{PZC} = +300$ ). In contrast, ACF1 and DeACF3 have total capacitance values around 0.16 F/m<sup>2</sup> with approximately equal contributions from adsorption of cations and anions. These results confirm our conclusion on selection of ACF1 and DeACF3 for electrosorption of PFAA anions. Nevertheless, ACF2 and ACF3 seem to be good candidates for electrosorption of organic cations. The cyclic voltammograms recorded at various scan rates can be found in Figure 4S in Supporting Information.

### 3.2. Electroadsorption/-desorption experiments

#### 3.2.1. Potential dependence and electrosorption mechanism

ACF1 and DeACF3 were applied for electrosorption experiments. Figure 4a shows adsorption coefficients ( $K_d$ ) in electrosorption of PFOA on ACF1 versus potentials. It is worth pointing out that the PFAAs are chemically stable on carbon electrodes in a wide potential range (-1000 mV to 1000 mV [24-26]). The plot of  $K_d$  (at pH 6-7) versus potential results in a bell-shaped curve with a maximum at +500 mV with respective  $K_d$  values up to  $10^6$  L/kg. This  $K_d$  value is about 50 times higher than the values at negative potentials.



**Figure 4.** Effect of electric potential on electrosorption of PFOA on ACF1 (0.04 g/L) (a) PFBA on ACF1 (1.5 g/L) (b) and PFBA on DeACF3 (0.33 g/L) (c). Experimental conditions:  $C_0 = 1$  mg/L PFOA or PFBA; electrolyte: 10 mM  $\text{Na}_2\text{SO}_4$  at pH 6-7 pH; duration of each individual experiment: 2 days. The error bars are standard deviations of 4 individual experiments. In plot (c) adsorption experiments at  $\pm 1000$  mV showed insignificant depletion of the analytes  $C_e/C_0 \geq 0.95$ . The corresponding reported  $K_d$  values ( $K_d = 160$  L/kg) were then approximated based on a 5% depletion and thus are upper limits of true  $K_d$ .

Note that the presented  $K_d$  values were measured with the same initial solute concentrations ( $C_0 = 1$  mg/L) but approaching different equilibrium states. Adsorbent loadings with PFOA range from 9 to 24 mg/g. As  $E_{PZC}$  and  $E_0$  of AFC1 are +75 mV and +225 mV, respectively, at potentials  $> +75$  mV the net charge on ACF1 is positive. Therefore, the enhancement in  $K_d$  at potentials  $> +75$  mV is most likely due to electrostatic attraction. Interestingly, increasing the potential further to +700 mV, +850 mV and +1000 mV decreases the adsorption of PFOA significantly. The reason for this counterintuitive behavior is that applying electrical potentials on the AC electrode enhances also the polarity of the surface. This affects also the hydrophobic interactions between the fluorinated tail of PFOA and the carbon surface [11].

Thus, an increasingly charged surface can have a negative effect on adsorption of PFOA as the competition by water molecules becomes more dominant [23]. Moreover, a decrease in  $K_d$  value could be caused by changing the chemical properties of the ACF from direct and indirect oxidation under positive potentials [27, 28]. These effects will be discussed in section 3.2.5. On the other hand, applying potentials more negative than the  $E_{PZC}$  (+75 mV) of ACF1 decreases significantly the adsorption affinity of PFOA. This is probably caused by electrostatic repulsion between negatively charged sites of ACF1 and PFOA as carboxylate.

Figures 4b and c show  $K_d$  values in electrosorption of PFBA on the two felts versus potential. Similar to PFOA, bell-shaped curves were obtained with PFBA as well. The potentials for maximum adsorption coefficients of PFBA are different on DeACF3 and ACF1, i.e. +250 mV versus +500 mV, respectively. The reason is probably the lower  $E_{PZC}$  (-150 mV) of DeACF3 compared with  $E_{PZC}$  of (+75 mV) ACF. In the absence of externally applied potentials, DeACF3 bears already a positive net charge at circumneutral pH due to the prevalence of basic surface groups ( $pH_{PZC} = 9.3$ ). ACF1 ( $pH_{PZC} = 7.1$ ) has an equal density of positive and negative charges under these conditions. Applying positive electric potentials improves adsorption of PFOA and PFBA anions in both cases but obviously the optimum charge density is reached at lower potential absolute values for DeACF3 which already bears positive charges related to its functional groups. At the same time, shifting electric potential to more negative values firstly has to compensate these charges on DeACF3 so that there is a shift in the declining branch of the  $K_d$  curve towards lower potentials. These results yield a general message for applying electrosorption for removal of ionized organic pollutants: surface functional and electrochemical properties of AC electrodes together must be considered for optimal design of the process.

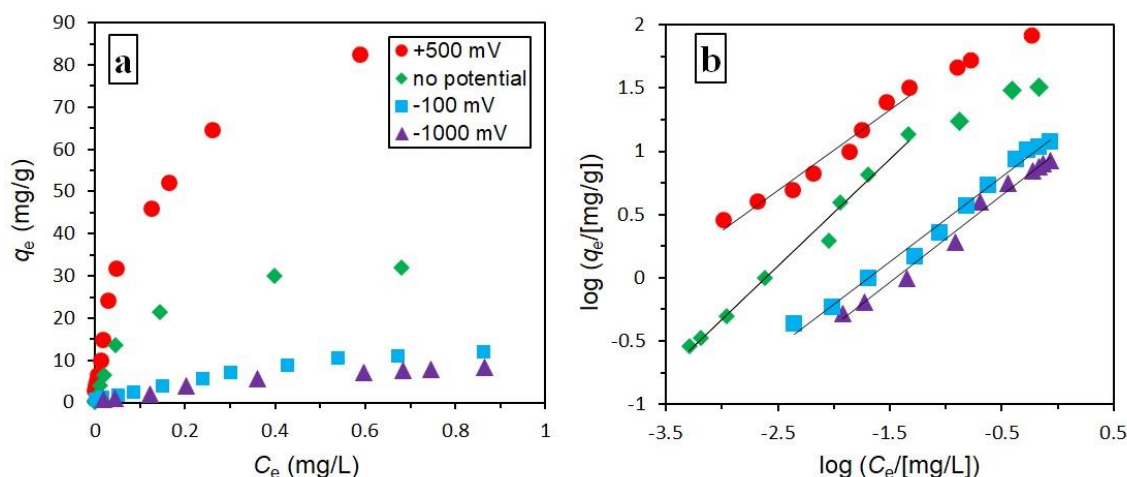
The general finding that sorption of anionic and cationic organic compounds increases or decreases by applying positive or negative potentials, respectively, was reported in previous studies as discussed in the introduction section. Our data on electrosorption of PFOA and PFBA indicate that PFAAs anions are specifically sensitive towards the charging state of the carbon surface as large differences in  $K_d$  depending on applied potential were observed (two orders of magnitude variation for PFBA compared to less than one order reported for various organic anions and cations [18-22]). Furthermore, the formation of bell-shaped curves from plotting electrosorption parameters of PFOA and PFBA versus potentials observed in the present study are in agreement with what was proposed by Fischer [23] for electrosorption of ionic and nonionic compounds. In this model, adsorption on a charged electrode is suggested to be equivalent to the moving of a slab of dielectric (adsorbate or water) in a parallel plate capacitor formed by the charged solid surface and the outer Helmholtz plane layer of counterions. Further studies are needed in order to elucidate this relevant phenomenon.

### 3.2.2. Electrosorption isotherms and concentration factor

Figure 5a shows electrosorption isotherms of PFOA on ACF1 polarized at +500 mV, -100 mV, and -1000 mV and compares these results with adsorption (no potential) isotherms. A significant effect of electrical potentials on the adsorption isotherms is obvious. The experimental data were fitted with a linearized form of the Freundlich equation (Figure 5b). Note that the Freundlich equation can only be applied within a certain solute concentration range, i.e. significantly below the maximum loadings. Table 1 lists the isotherm parameters. As described in section 2.6.2., these isotherm parameters can be used to calculate the volume of water ( $V_{des}$ ) needed for deloading of the adsorbent. As can be seen in Table 1, Freundlich exponent parameters ( $n$ ) for electrosorption at +500 mV ( $n_{ads}$ ) and at negative potentials ( $n_{des}$ ) are similar. Therefore, the simplified Eq. 12 can be applied to calculate the volume ratio of water needed for desorption related to treated water which is the reciprocal of the concentration factor ( $V_{des}/V_{ads})_{+500/-1000} = 1/F_{+500/-1000}$  for electroadsorption at +500 mV and electrodesorption at -1000 mV:

$$\frac{V_{des}}{V_{ads}} = \frac{0.95}{\left(\frac{200}{9.8}\right)^{\frac{1}{0.64}} - 1} = 0.0087 \quad \text{with} \quad X_{des} = 1 - \frac{9.8}{200} = 0.95$$

In words, by means of potential-controlled adsorption and desorption 95% of adsorbed PFOA can be released in an aqueous concentrate of about 0.9% of the treated water volume resulting in a concentration factor of  $F_{+500/-1000} = 115$ . Similarly, changing the electrodesorption potential to -100 mV yields  $F_{+500/-100} = 71$ , while  $F_{\text{no potential}/-100} = 41$  if adsorption is performed without applied external potential.



**Figure 5.** Experimental data (a) from electrosorption at +500 mV, -100 mV and -1000 mV (vs. Ag/AgCl) and adsorption (no potential) isotherms of PFOA on ACF1 fitted with Freundlich equation (b). Experimental conditions:  $C_{0,\text{PFOA}} = 1$  mg/L; electrolyte: 10 mM  $\text{Na}_2\text{SO}_4$  at pH 6-7; equilibration time in each individual experiment: 2 days.

**Table 1.** Freundlich parameters for electrosorption and adsorption without external potential of PFOA on ACF1.

Experiment	Potential <sup>a</sup> (mV)	Freundlich		
		Log ( $K_F/[(\text{mg/g})/(\text{mg/L})^n]$ )	$n$	$R^2$
PFOA on ACF1	No potential	2.20	0.84	0.985
PFOA on ACF1	+500	2.30	0.64	0.963
PFOA on ACF1	-100	1.13	0.67	0.989
PFOA on ACF1	-1000	0.99	0.69	0.987

<sup>a</sup> versus Ag/AgCl as reference electrode.

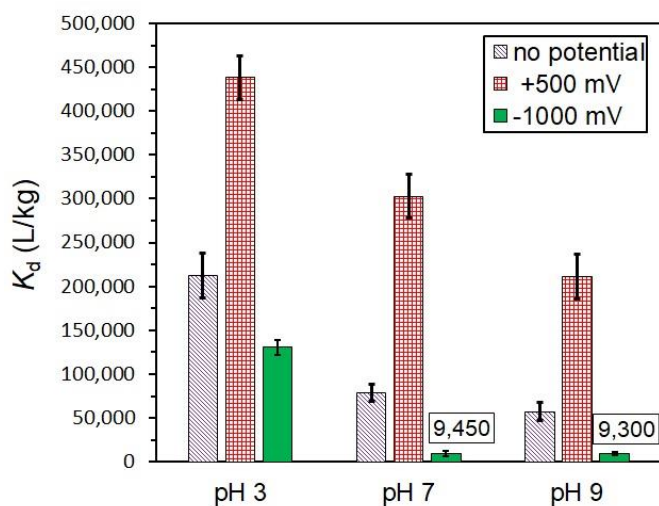
The concentration factors from electrosorption can be compared with concentration factors in other separation processes, e.g., reverse osmosis. In USA, two treatment plants for perfluoroalkyl substances-contaminated water use reverse osmosis with polyamide Hydranautics ESPA2 membranes in a three stage array with a water flux of 12 gfd (gallons per square foot per day) receiving 85% recovery (cleaned water) [45], i.e. a concentration factor of 6.7. The concentration factors calculated in the present study based on equilibrium data from batch experiments are at



least by a factor of 10 higher which illustrates the potential of the electrosorption method. Clearly, technically achievable concentration factors under application conditions can be lower and have to be determined in future studies.

### 3.2.3. Effect of electrolyte pH

The  $pH_{PZC}$  of ACF1 is around 7 (see Table 2S) and its  $E_{PZC}$  is +75 mV. It means that decreasing pH to 3 enhances the density of positive charges on ACF1, whereas an increase in pH to 9 increases the density of negative charges. In Figure 6, the pH-driven effects on adsorption of PFOA (no external potential) are compared with the potential-driven effects. The effects are as expected: charging ACF1 positively by both, decreasing pH from 7 to 3 or applying a positive potential (+500 mV at pH 7), increases adsorption affinity ( $K_d$ ) of PFOA. Charging ACF1 negatively by increasing pH to 9 or applying a negative potential (-1000 mV) decreases adsorption coefficients. It is evident from Figure 6 that the external electric potential at circumneutral pH has a stronger effect on the adsorption behaviour (about factor 30) than changing the pH (a factor of 4 with no external potential). This is in agreement with what observed by Ban et al. [19] in electrosorption of naphthoic acid and naphthalenesulfonic acid anions at different electrode potentials and electrolyte pH values on AC.

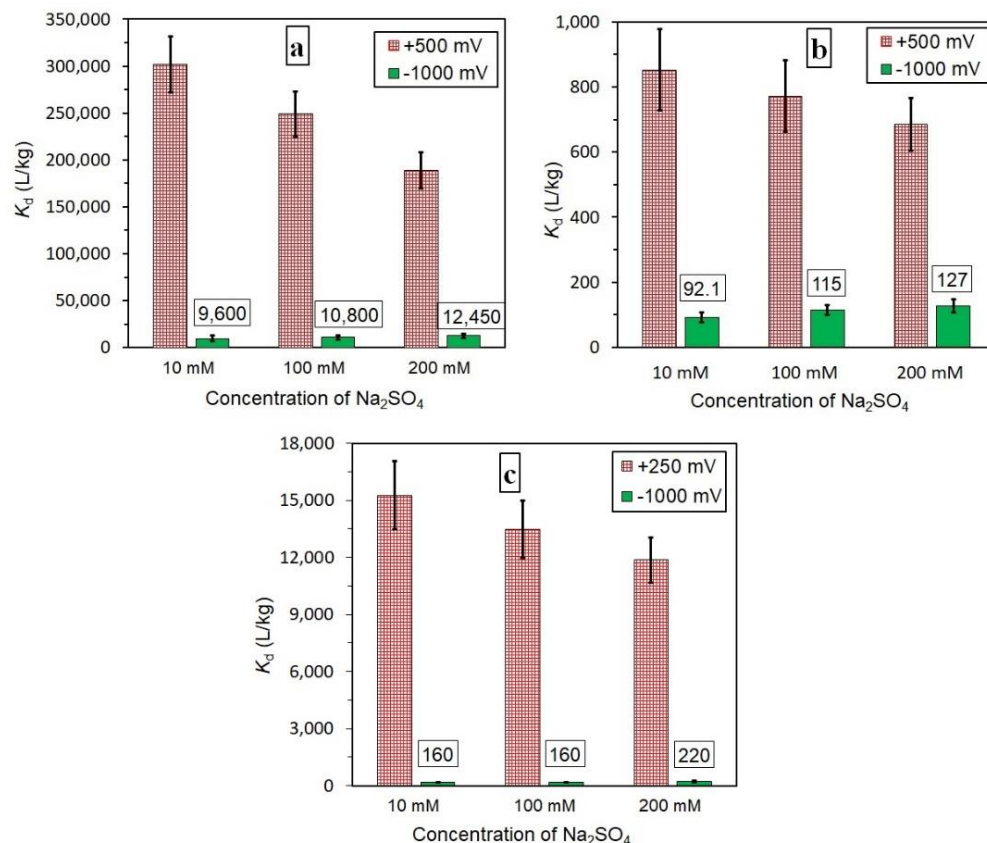


**Figure 6.** Effect of electrolyte pH on electrosorption of PFOA on ACF1 (16 mg/L). Experimental conditions:  $C_0 = 1$  mg/L in 10 mM  $Na_2SO_4$ ; equilibration time in each individual experiment: 2 days. The error bars are standard deviations from 4 individual experiments. The potentials are versus Ag/AgCl.

Another message from these results is that even at pH = 3 or 9, i.e. under conditions of prevailing positive or negative chemical surfaces charges, respectively, PFOA adsorption can be manipulated by applying external electric potentials. Nevertheless, the strongest effect of electric potential is observed at pH 7 where the chemical surface charges resulting from protonation/deprotonation equilibria are balanced and  $E_{PZC}$  has a low positive value. In contrast, Niu et al. [25] found enhanced PFOA electrosorption at a positively polarized carbon nanotube-graphene composite electrode when pH was raised from 3 to 9. This behavior is counterintuitive since PFOA must be expected to be nearly completely in the anionic state over the whole considered pH range ( $pK_a = 0-1$  [46]) and the deprotonation of the carbon surface should increase electrostatic repulsion. Our results also don't confirm this observation as shown in Figure 6. Nevertheless, there remains uncertainty whether the pH in the confined carbon pores could deviate from the measurable bulk pH so that pH effects on PFOA speciation close to adsorption sites might still occur depending on the type of carbon material applied.

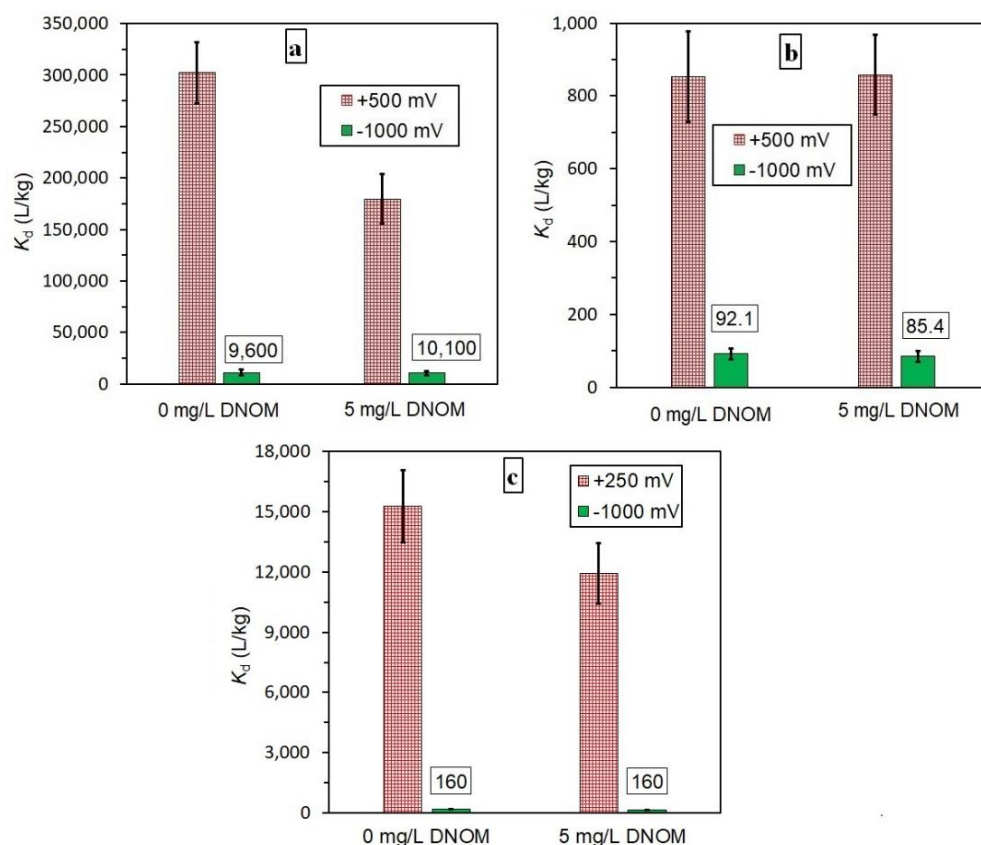
#### 3.2.4. Effects of organic and inorganic ions

It has been reported that coexisting inorganic anions and cations can affect adsorption of PFAAs on various adsorbents [3, 47]. However, their effects on electrosorption has not been studied yet. Figure 7 shows electroadsorption and subsequent electrodesorption of PFOA and PFBA by switching potential from +500 mV (+250 mV in case of PFBA on DeCACF) to -1000 mV in the presence of different concentrations of  $\text{Na}_2\text{SO}_4$ . An increase in  $\text{Na}_2\text{SO}_4$  concentration from 10 mM to 200 mM reduces  $K_d$  values in electroadsorption of both PFOA and PFBA, however, by a factor less than 2 only. The reason can be a screening of attractive positive charges at the polarized carbon surface by counterions at high ionic strength or a direct competition between  $\text{SO}_4^{2-}$  and PFAA anions for adsorption sites. Nevertheless, the superposition of hydrophobic and electrostatic interactions for PFAA anions cannot be outcompeted by inorganic anions, even in case of the dianion sulfate. Negative potential has a strong repulsive effect on the adsorbed PFAAs even in presence of 200 mM  $\text{Na}_2\text{SO}_4$ , leading to a 17-fold lower  $K_d$  at -1000 mV compared to +500 mV for PFOA and 70-fold lower for PFBA on DeACF3. This means that the electroadsorption/-desorption concept for PFAAs is applicable for water containing even high concentrations of inorganic ions.



**Figure 7.** Effect of inorganic ions on electroadsorption/-desorption of PFOA and PFBA. a) PFOA on ACF1 (16 mg/L), b) PFBA on ACF1 (1.5 g/L) and c) PFBA on DeACF3 (0.33 g/L). Experimental conditions:  $C_0 = 1$  mg/L PFOA or PFBA in  $x$  mM  $\text{Na}_2\text{SO}_4$  at pH = 7; equilibration time in each individual experiment: 2 days. The error bars are standard deviations from 4 individual experiments. In plot c, the experiments at -1000 mV in 10 and 100 mM  $\text{Na}_2\text{SO}_4$  showed insignificant depletion of the analytes  $C_e/C_0 \geq 0.95$ . The corresponding reported  $K_d$  values ( $K_d = 160$  L/kg) were then approximated based on a 5% depletion and thus are upper limits of true  $K_d$ . The potentials are versus Ag/AgCl.

Dissolved natural organic matter (DNOM) as ubiquitous component of surface and groundwater comprises refractory macromolecules with aromatic and aliphatic regions bearing acidic functional groups such as carboxylic acid groups [48] and thus carries negative charges at pH 7. DNOM often plays a competitive role in the adsorption process [49, 50]. The effect of DNOM on electrosorption of PFAAs has not been studied yet. Figure 8 shows electrosorption results for PFOA and PFBA in water containing 5 mg/L DNOM at pH 7. The presence of DNOM in solution reduces electroadsorption of the PFAAs only moderately by a factor  $< 2$ . This effect is probably caused by competition between deprotonated DNOM molecules and the PFAA anions. Nevertheless, there is still a large difference between  $K_d$  values under electroadsorption and electrodesorption conditions, e.g. 18-fold in case of PFOA and 75-fold in case of PFBA on DeACF3.



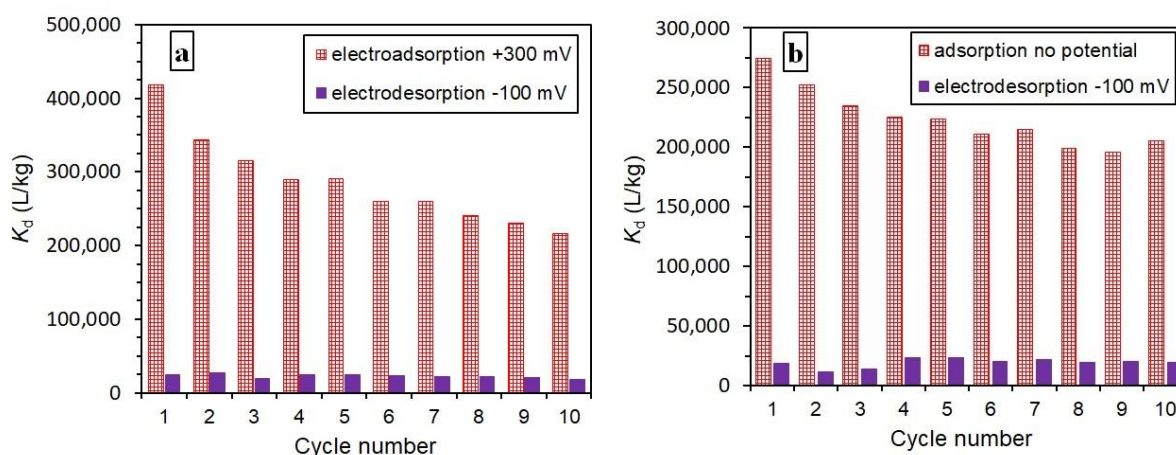
**Figure 8.** Effect of DNOM on electroadsorption/-desorption of PFOA and PFBA. a) PFOA on ACF1 (16 mg/L), b) PFBA on ACF1 (1.5 g/L) and c) PFBA on DeACF3 (0.33 g/L). Experimental conditions:  $C_0 = 1$  mg/L PFOA or PFBA in 10 mM  $\text{Na}_2\text{SO}_4$  at pH = 7; equilibration time in each individual experiment: 2 days. The error bars are standard deviations from 4 individual experiments. In plot c, the experiments at -1000 mV showed insignificant depletion of the analytes  $c/c_0 \geq 0.95$ . The corresponding reported  $K_d$  values ( $K_d = 160$  L/kg) were then approximated based on a 5% depletion and thus are upper limits of true  $K_d$ . The potentials are versus Ag/AgCl.

### 3.2.5. Long-term electroadsorption/-desorption experiments

In order to study the performance decline of the electroadsorption cell over prolonged period of time, we first run 5 cycles of electroadsorption of PFOA on ACF1 at +500 mV and electrodesorption at -1000 mV with a total time of carbon polarization of about 20 days (Figure 5Sa in Supporting Information). The results showed that the single point adsorption coefficients in electroadsorption dropped strongly from 860,000 L/kg in the first cycle to around 160,000 L/kg in the fifth cycle. Gineys et al. [27] studied the effect of positive and negative potentials on ACF in sodium sulfate solution as electrolyte. Under positive potentials  $\leq +500$  mV, the content of oxygen-containing functional groups increased with indications for formation of phenolic and carboxylic groups. Surprisingly, negative potentials on the carbon electrode lead to oxidation of the surface as well [27]. These oxidation reactions may come from secondary reactions due to reduction of dissolved

oxygen producing hydrogen peroxide. Therefore, the decrease in electroadsorption of PFOA over a number of potential cycles is probably caused by advancing surface oxidation of the carbon surface, induced by the applied harsh electrosorption conditions (from +500 mV to -1000 mV).

In order to minimize carbon electrode erosion, we followed two strategies. We first tried to avoid the secondary reactions coming from the reduction of dissolved oxygen in the solution. Therefore, we repeated the above mentioned 5 cycle electrosorption experiment, while this time nitrogen was purged in the solution during the experiment. Again a significant drop as high as 670,000 L/kg was observed in the electroadsorption coefficient of the first cycle compared to that of the fifth cycle (Figure 5Sb). Afterwards, the electrosorption experiment was performed with milder electric potentials, e.g.  $-100 \text{ mV} < E_{\text{PZC}} = +75 \text{ mV} < +300 \text{ mV}$  (Figure 9a). The decline in the corresponding  $K_d$  values along 10 cycles of electroadsorption is still observable but less significant (less than a factor of 2).



**Figure 9.** Electroadsorption and electrodesorption of PFOA ( $C_0 = 1 \text{ mg/L}$ ) on/from ACF1 (66.7 mg/L) in 10 mM  $\text{Na}_2\text{SO}_4$  at pH 7. a) 10 cycles electroadsorption at +300 mV and electrodesorption at -100 mV. b) 10 cycles adsorption without potential and electrodesorption at -100 mV. Each cycle covers 4 days, 2 days electroadsorption and 2 days electrodesorption. The potentials are versus Ag/AgCl.

Anodic polarization can be seen as more critical in terms of carbon oxidation than cathodic polarization. Bayram and Ayrancı reported that cathodic polarization of ACF (by -1500 mV vs. Ag/AgCl) affected slightly the surface chemical properties [28], whereas polarization with +500 mV [28] and +300 mV (vs.  $\text{Hg}/\text{Hg}_2\text{SO}_4$ ) [27] led to a significant surface oxidation. Note that ACF1 has a high affinity towards PFOA even without applying external potentials. Thus, in

order to better protect ACF1 against attrition induced by positive potentials, PFOA adsorption can be carried out without applying an external positive potential, while a mild negative potential of -100 mV can be applied for electrodesorption. Figure 9b illustrates the results from 10 cycles of adsorption with no external potential and electrodesorption at -100 mV over a prolonged operation time of at least 1000 h. The result is a rather stable adsorption performance of the electrosorption cell. After an initial loss of about 20% in  $K_d$  (cycle 1-5) the ACF1 electrode kept its performance almost constant (<10% decline in cycle 5-10).

#### 4. Conclusions

External potentials were successfully used for controlling adsorption of PFOA and PFBA on microporous activated carbon felts (ACFs) with various surface chemistries. The electrosorption of both anionic compounds was influenced by the net charge on the non-polarized ACFs (studied by potential of zero charge,  $E_{PZC}$ ) as well as the applied external potentials. Electrosorption of PFOA and PFBA resulted in bell-shaped curves of  $K_d$  values versus potential with maxima in  $K_d$  at potentials  $> E_{PZC}$ . These results indicate that for selection of appropriate carbon electrode materials, their surface chemistry and in particular their  $E_{PZC}$  should be taken into account.

The large differences between maximum  $K_d$  in electroadsorption at positive potential and  $K_d$  obtained at negative potential, e.g. 650,000 L/kg at +500 mV vs. 14,800 L/kg at -1000 mV in case of PFOA, enables one to remove the compound from a high volume of water by electroadsorption and to release it in a low volume concentrate by means of electrodesorption. An estimation of the concentration factor in an electroadsorption/-desorption unit for PFOA removal was calculated as 115 for the conditions given above. It is lower for milder potential swings, e.g. 71 for electrosorption at +500 mV vs. -100 mV and 41 for no potential vs. -100 mV. These numbers are much higher than the reported concentration factor for PFAA removal (6.7) in a reverse osmosis process [45].

Information on  $E_{PZC}$  of carbon electrodes is also useful for protecting them against attrition caused by applying harsh potentials. Electroadsorption of PFOA at +500 mV and electrodesorption at -1000 mV showed a significant decline in electroadsorption of PFOA over 5 electroadsorption/-desorption cycles. Selection of milder potentials based on  $E_{PZC}$  of the ACF used as adsorbent (electrodesorption at -100 mV  $< E_{PZC} = +75$  mV  $<$  electroadsorption at +300 mV) resulted in only small losses of performance after 10 cycles (1000 h). An almost stable performance of the

electrosorption cell was achieved without external potential for adsorption and -100 mV for electrodesorption.

The weak impact of competitive inorganic and organic ions on electrosorption of PFBA and PFOA and a small effect of variable pH values indicate that this concept is applicable for remediation of various sources of water contaminated with both short- and long-chain perfluoroalkyl acids.

## References

- [1] O.S. Arvaniti, A.S. Stasinakis, Review on the occurrence, fate and removal of perfluorinated compounds during wastewater treatment, *Science of The Total Environment* 524-525 (2015) 81-92.
- [2] K. Sznajder-Katarzyńska, M. Surma, I. Cieřlik, A review of perfluoroalkyl acids (PFAAs) in terms of sources, applications, human exposure, dietary intake, toxicity, legal regulation, and methods of determination, *Journal of Chemistry* 2019 (2019) 2717528.
- [3] H.N. Phong Vo, H.H. Ngo, W. Guo, T.M. Hong Nguyen, J. Li, H. Liang, L. Deng, Z. Chen, T.A. Hang Nguyen, Poly-and perfluoroalkyl substances in water and wastewater: a comprehensive review from sources to remediation, *Journal of Water Process Engineering* 36 (2020) 101393.
- [4] S. Hurley, E. Houtz, D. Goldberg, M. Wang, J.-S. Park, D.O. Nelson, P. Reynolds, L. Bernstein, H. Anton-Culver, P. Horn-Ross, M. Petreas, Preliminary associations between the detection of perfluoroalkyl acids (PFAAs) in drinking water and serum concentrations in a sample of california women, *Environmental Science & Technology Letters* 3 (2016) 264-269.
- [5] G.B. Post, J.A. Gleason, K.R. Cooper, Key scientific issues in developing drinking water guidelines for perfluoroalkyl acids: contaminants of emerging concern, *PLOS Biology* 15 (2017) e2002855.
- [6] V.A. Arias Espana, M. Mallavarapu, R. Naidu, Treatment technologies for aqueous perfluorooctanesulfonate (PFOS) and perfluorooctanoate (PFOA): a critical review with an emphasis on field testing, *Environmental Technology & Innovation* 4 (2015) 168-181.
- [7] E. Gagliano, M. Sgroi, P.P. Falciglia, F.G.A. Vagliasindi, P. Roccaro, Removal of poly- and perfluoroalkyl substances (PFAS) from water by adsorption: Role of PFAS chain length, effect of organic matter and challenges in adsorbent regeneration, *Water Research* 171 (2020) 115381.
- [8] C.P. Higgins, J.A. Field, Our stainfree future? a virtual issue on poly- and perfluoroalkyl substances, *Environmental Science & Technology* 51 (2017) 5859-5860.
- [9] P. McCleaf, S. Englund, A. Östlund, K. Lindegren, K. Wiberg, L. Ahrens, Removal efficiency of multiple poly- and perfluoroalkyl substances (PFASs) in drinking water using granular activated carbon (GAC) and anion exchange (AE) column tests, *Water Research* 120 (2017) 77-87.
- [10] M.M. Schultz, D.F. Barofsky, J.A. Field, Fluorinated alkyl surfactants, *Environmental Engineering Science* 20 (2003) 487-501.
- [11] N. Saeidi, F.-D. Kopinke, A. Georgi, Understanding the effect of carbon surface chemistry on adsorption of perfluorinated alkyl substances, *Chemical Engineering Journal* 381 (2020) 122689.
- [12] S. Deng, Y. Nie, Z. Du, Q. Huang, P. Meng, B. Wang, J. Huang, G. Yu, Enhanced adsorption of perfluorooctane sulfonate and perfluorooctanoate by bamboo-derived granular activated carbon, *Journal of Hazardous Materials* 282 (2015) 150-157.
- [13] Y. Zhi, J. Liu, Surface modification of activated carbon for enhanced adsorption of perfluoroalkyl acids from aqueous solutions, *Chemosphere* 144 (2016) 1224-1232.
- [14] M. Söregård, E. Östblom, S. Köhler, L. Ahrens, Adsorption behavior of per- and polyfluoroalkyl substances (PFASs) to 44 inorganic and organic sorbents and use of dyes as proxies for PFAS sorption, *Journal of Environmental Chemical Engineering* 8 (2020) 103744.
- [15] Y. Zhi, J. Liu, Adsorption of perfluoroalkyl acids by carbonaceous adsorbents: effect of carbon surface chemistry, *Environmental Pollution* 202 (2015) 168-176.
- [16] K.Y. Foo, B.H. Hameed, A short review of activated carbon assisted electrosorption process: an overview, current stage and future prospects, *Journal of Hazardous Materials* 170 (2009) 552-559.
- [17] Y. Han, X. Quan, S. Chen, H. Zhao, C. Cui, Y. Zhao, Electrochemically enhanced adsorption of aniline on activated carbon fibers, *Separation and Purification Technology* 50 (2006) 365-372.



- [18] E. Bayram, N. Hoda, E. Ayranci, Adsorption/electrosorption of catechol and resorcinol onto high area activated carbon cloth, *Journal of Hazardous Materials* 168 (2009) 1459-1466.
- [19] A. Bán, A. Schafer, H. Wendt, Fundamentals of electrosorption on activated carbon for wastewater treatment of industrial effluents, *Journal of Applied Electrochemistry* 28 (1998) 227-236.
- [20] E. Bayram, E. Ayranci, Electrochemically enhanced removal of polycyclic aromatic basic dyes from dilute aqueous solutions by activated carbon cloth electrodes, *Environmental Science & Technology* 44 (2010) 6331-6336.
- [21] C.O. Ania, F. Béguin, Mechanism of adsorption and electrosorption of bentazone on activated carbon cloth in aqueous solutions, *Water Research* 41 (2007) 3372-3380.
- [22] S. Wang, X. Li, H. Zhao, X. Quan, S. Chen, H. Yu, Enhanced adsorption of ionizable antibiotics on activated carbon fiber under electrochemical assistance in continuous-flow modes, *Water Research* 134 (2018) 162-169.
- [23] V.M. Fischer, In situ electrochemical regeneration of activated carbon, University of Groningen, Netherlands, 2001.
- [24] X. Li, S. Chen, X. Quan, Y. Zhang, Enhanced adsorption of PFOA and PFOS on multiwalled carbon nanotubes under electrochemical assistance, *Environmental Science & Technology* 45 (2011) 8498-8505.
- [25] Z. Niu, Y. Wang, H. Lin, F. Jin, Y. Li, J. Niu, Electrochemically enhanced removal of perfluorinated compounds (PFCs) from aqueous solution by CNTs-graphene composite electrode, *Chemical Engineering Journal* 328 (2017) 228-235.
- [26] S. Wang, X. Li, Y. Zhang, X. Quan, S. Chen, H. Yu, H. Zhao, Electrochemically enhanced adsorption of PFOA and PFOS on multiwalled carbon nanotubes in continuous flow mode, *Chinese Science Bulletin* 59 (2014) 2890-2897.
- [27] M. Gineys, R. Benoit, N. Cohaut, F. Béguin, S. Delpeux-Ouldriane, Behavior of activated carbon cloths used as electrode in electrochemical processes, *Chemical Engineering Journal* 310 (2017) 1-12.
- [28] E. Bayram, E. Ayranci, A systematic study on the changes in properties of an activated carbon cloth upon polarization, *Electrochimica Acta* 56 (2011) 2184-2189.
- [29] Z. Tabti, R. Ruiz-Rosas, C. Quijada, D. Cazorla-Amorós, E. Morallón, Tailoring the surface chemistry of activated carbon cloth by electrochemical methods, *ACS Applied Materials & Interfaces* 6 (2014) 11682-11691.
- [30] P.M. Biesheuvel, S. Porada, M. Levi, M.Z. Bazant, Attractive forces in microporous carbon electrodes for capacitive deionization, *Journal of Solid State Electrochemistry* 18 (2014) 1365-1376.
- [31] G. Wang, B. Qian, Q. Dong, J. Yang, Z. Zhao, J. Qiu, Highly mesoporous activated carbon electrode for capacitive deionization, *Separation and Purification Technology* 103 (2013) 216-221.
- [32] I. Villar, S. Roldan, V. Ruiz, M. Granda, C. Blanco, R. Menéndez, R. Santamaría, Capacitive deionization of NaCl solutions with modified activated carbon electrodes, *Energy & Fuels* 24 (2010) 3329-3333.
- [33] M.A. Anderson, A.L. Cudero, J. Palma, Capacitive deionization as an electrochemical means of saving energy and delivering clean water. Comparison to present desalination practices: will it compete?, *Electrochimica Acta* 55 (2010) 3845-3856.
- [34] X. Gao, A. Omosibi, J. Landon, K. Liu, Surface charge enhanced carbon electrodes for stable and efficient capacitive deionization using inverted adsorption-desorption behavior, *Energy & Environmental Science* 8 (2015) 897-909.
- [35] I. Cohen, E. Avraham, Y. Bouhadana, A. Soffer, D. Aurbach, Long term stability of capacitive de-ionization processes for water desalination: The challenge of positive electrodes corrosion, *Electrochimica Acta* 106 (2013) 91-100.
- [36] L. Qian, A. Georgi, R. Gonzalez-Olmos, F.-D. Kopinke, Degradation of perfluorooctanoic acid adsorbed on Fe-zeolites with molecular oxygen as oxidant under UV-A irradiation, *Applied Catalysis B: Environmental* 278 (2020) 119283.
- [37] Á. Soriano, D. Gorri, L.T. Biegler, A. Urtiaga, An optimization model for the treatment of perfluorocarboxylic acids considering membrane preconcentration and BDD electrooxidation, *Water Research* 164 (2019) 114954.
- [38] D. Huang, K. Wang, J. Niu, C. Chu, S. Weon, Q. Zhu, J. Lu, E. Stavitski, J.-H. Kim, Amorphous Pd-loaded  $\text{Ti}_4\text{O}_7$  electrode for direct anodic destruction of perfluorooctanoic acid, *Environmental Science & Technology* 54 (2020) 10954-10963.
- [39] Á. Soriano, D. Gorri, A. Urtiaga, Membrane preconcentration as an efficient tool to reduce the energy consumption of perfluorohexanoic acid electrochemical treatment, *Separation and Purification Technology* 208 (2019) 160-168.
- [40] N. Saeidi, F.-D. Kopinke, A. Georgi, What is specific in adsorption of perfluoroalkyl acids on carbon materials?, *Chemosphere* (2020) 128520.
- [41] D. Weingarh, M. Zeiger, N. Jäckel, M. Aslan, G. Feng, V. Presser, Graphitization as a universal tool to tailor the potential-dependent capacitance of carbon supercapacitors, *Advanced Energy Materials* 4 (2014) 1400316.



- [42] L.-H. Shao, J. Biener, D. Kramer, R.N. Viswanath, T.F. Baumann, A.V. Hamza, J. Weissmüller, Electrocapillary maximum and potential of zero charge of carbon aerogel, *Physical Chemistry Chemical Physics* 12 (2010) 7580-7587.
- [43] J. Heinze, Allen J. Bard and Larry F. Faulkner: *Electrochemical methods – fundamentals and applications*. Wiley, New York 1980, 718 + XVIII S., Preis: £ 14.70, *Berichte der Bunsengesellschaft für physikalische Chemie* 85 (1981) 1085-1086.
- [44] M.D. Levi, S. Sigalov, D. Aurbach, L. Daikhin, In situ electrochemical quartz crystal admittance methodology for tracking compositional and mechanical changes in porous carbon electrodes, *The Journal of Physical Chemistry C* 117 (2013) 14876-14889.
- [45] T.D. Appleman, C.P. Higgins, O. Quiñones, B.J. Vanderford, C. Kolstad, J.C. Zeigler-Holady, E.R.V. Dickenson, Treatment of poly- and perfluoroalkyl substances in U.S. full-scale water treatment systems, *Water Research* 51 (2014) 246-255.
- [46] K.-U. Goss, The  $pK_a$  values of PFOA and other highly fluorinated carboxylic acids, *Environmental Science & Technology* 42 (2008) 456-458.
- [47] M.F. Rahman, S. Peldszus, W.B. Anderson, Behaviour and fate of perfluoroalkyl and polyfluoroalkyl substances (PFASs) in drinking water treatment: a review, *Water Research* 50 (2014) 318-340.
- [48] S.J. Driver, E.M. Perdue, Acidic functional groups of suwannee river natural organic matter, humic acids, and fulvic acids, advances in the physicochemical characterization of dissolved organic matter: impact on natural and engineered systems, *American Chemical Society* 2014, pp. 75-86.
- [49] T.D. Appleman, E.R.V. Dickenson, C. Bellona, C.P. Higgins, Nanofiltration and granular activated carbon treatment of perfluoroalkyl acids, *Journal of Hazardous Materials* 260 (2013) 740-746.
- [50] D.N. Kothawala, S.J. Köhler, A. Östlund, K. Wiberg, L. Ahrens, Influence of dissolved organic matter concentration and composition on the removal efficiency of perfluoroalkyl substances (PFASs) during drinking water treatment, *Water Research* 121 (2017) 320-328.

Appendix: supporting information to

**Controlling adsorption of perfluoroalkyl acids on activated carbon felt by means of electrical potentials**

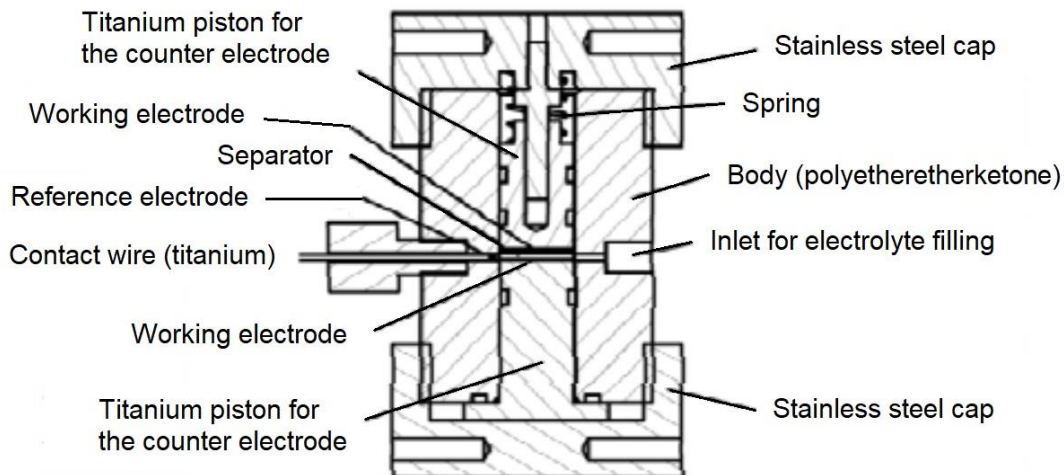
Navid Saeidi, Frank-Dieter Kopinke, Anett Georgi\*

*Helmholtz Centre for Environmental Research – UFZ, Department of Environmental Engineering,  
D-04318 Leipzig, Germany*

Corresponding author e-mail: anett.georgi@ufz.de

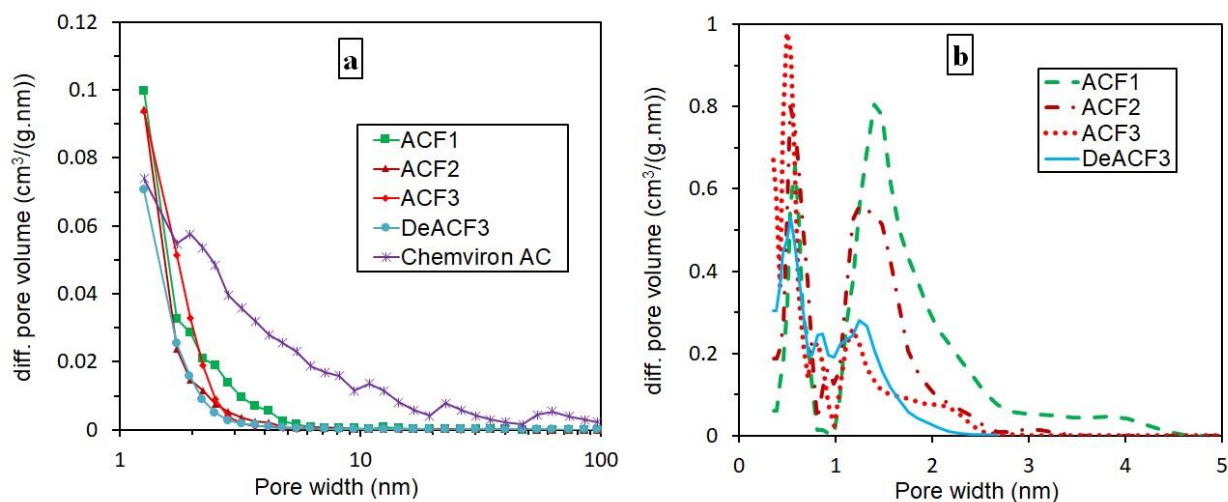
(6 Pages, 2 Tables and 5 Figures)

**Figure 1S** shows the configuration of the three electrode cell which was used for EIS measurements [1].



**Figure 1S.** Schematic drawing of the three electrode cell used for EIS measurements [1].

**Figure 2S** illustrates a comparison of pore size distributions of the activated carbon felts (ACFs) used here.



**Figure 2S.** Pore size distributions of the ACFs and a commercial powder AC (Chemvicon): a) mesopores analyzed by means of N<sub>2</sub> adsorption/desorption data and BJH method; b) micropores obtained by CO<sub>2</sub> adsorption results and NLDFT analysis.

**Tables 1S** and **2S** list textural properties and chemical surface characteristics of the ACFs, respectively.

**Table 1S.** Textural properties of the activated carbon felts used in this work.

Sample	BET surface area (m <sup>2</sup> /g) <sup>a</sup>	Total pore volume (cm <sup>3</sup> /g) <sup>a</sup>	Pore volume for 1-2 nm pore width <sup>b</sup>	Pore volume for < 1 nm pore width <sup>b</sup>	Fiber Diameter (μm) <sup>c</sup>
ACF1	1600	0.74	0.47	0.13	10 ± 2
ACF2	1400	0.62	0.34	0.21	12 ± 1
ACF3	1100	0.53	0.14	0.23	12 ± 1
DeACF3	1000	0.46	0.16	0.15	6.5 ± 1

<sup>a</sup> obtained using N<sub>2</sub> adsorption/desorption, <sup>b</sup> obtained using CO<sub>2</sub> adsorption,

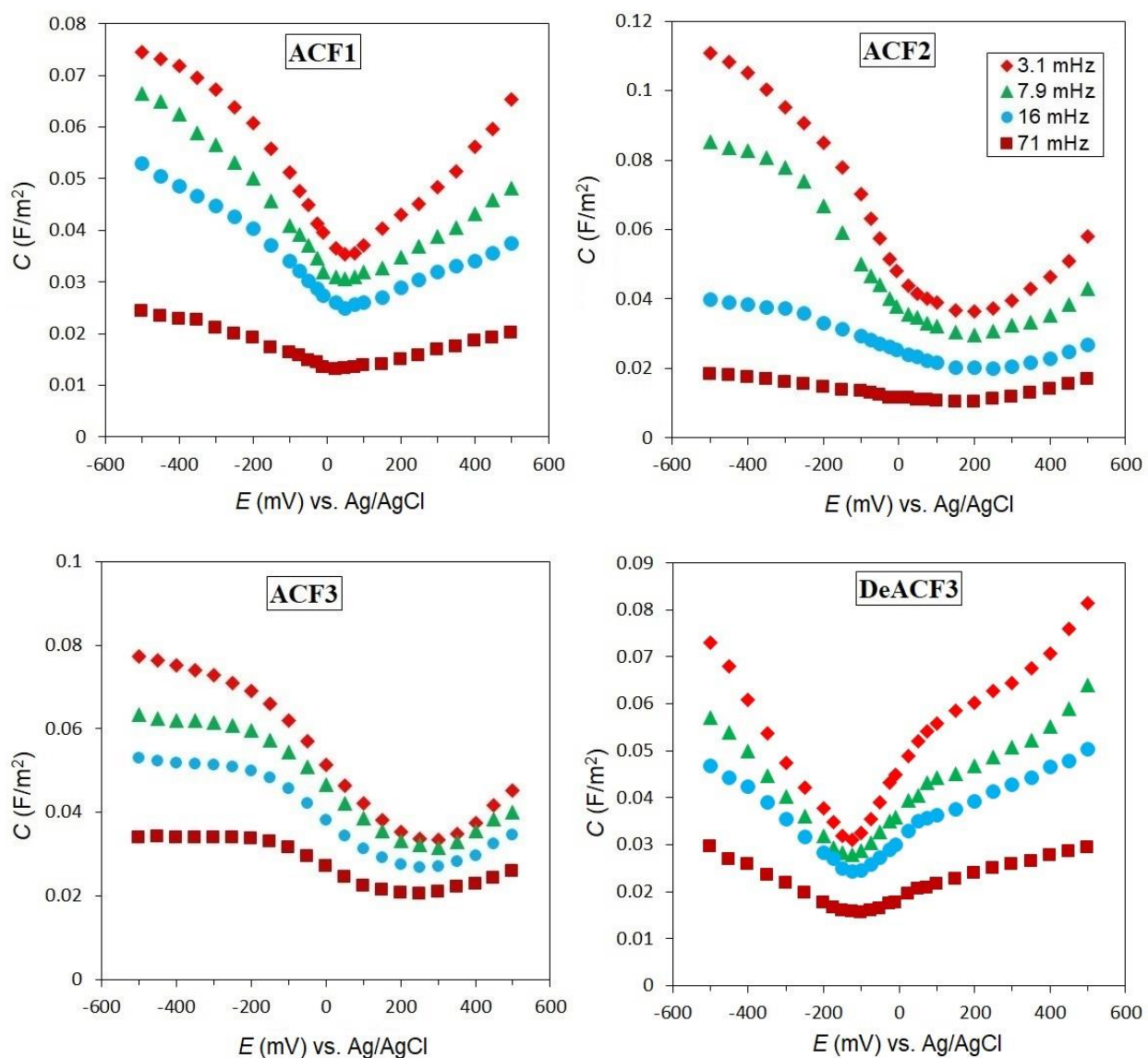
<sup>c</sup> an average of 10 measurements was reported.

**Table 2S.** Surface chemical properties of the activated carbon felts used here.

Sample	Boehm Titration				TPD <sup>c</sup>			N- content <sup>b</sup>	pH <sub>PZC</sub>	AEC	CEC
	pK <sub>a</sub> ~ 3-6	pK <sub>a</sub> ~ 6-10	pK <sub>a</sub> ~ 10-13	pK <sub>a</sub> ~ 3-13							
	Carboxyli c acids	Lactons and lactols	Phenols	Total acidity	CO	CO <sub>2</sub>	O- content <sup>a</sup>				
	(μmol/m <sup>2</sup> )						(wt%)			(μmol/m <sup>2</sup> )	
ACF1	0.0687	0.0750	0.287	0.431	1.19	0.169	3.9	0.5	7.1	0.137	0.131
ACF2	0.298	0.0992	0.695	1.09	4.22	1.13	15.9	0.6	6.5	0.0922	0.418
ACF3	1.12	0.321	0.643	2.08	3.39	2.14	13.7	0.5	5.9	0.054	0.79
DeACF3	0.0233	0.130	0.0670	0.22	0.55	0.084	1.1	0.3	9.3	0.20	0.021

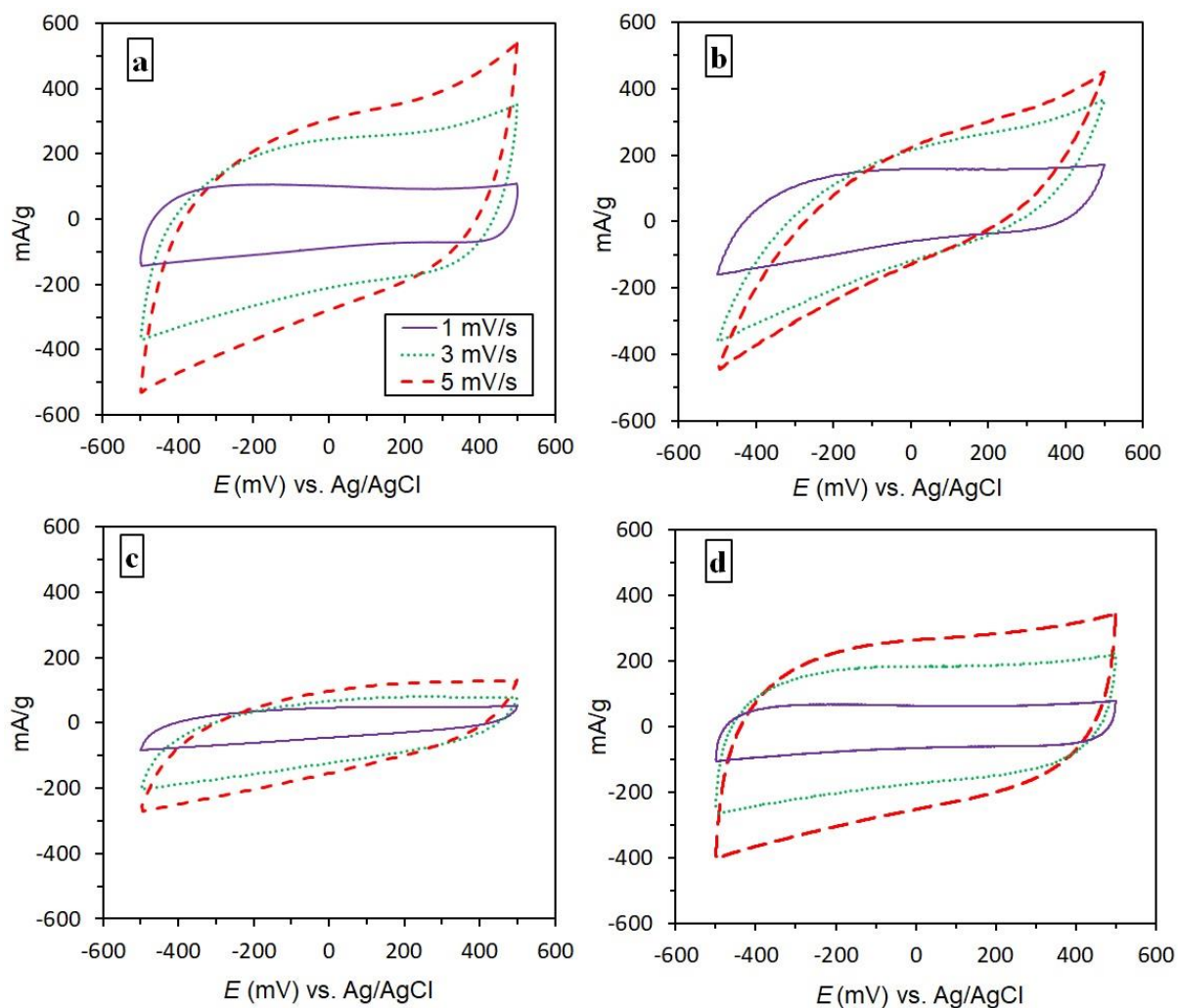
<sup>a</sup> calculated from released CO and CO<sub>2</sub>, <sup>b</sup> analysed by means of XPS, <sup>c</sup> temperature programmed decomposition.

**Figure 3S** shows differential capacitance of the ACFs versus potential at 4 different frequencies, namely 3.1, 7.9, 16 and 71 mHz.



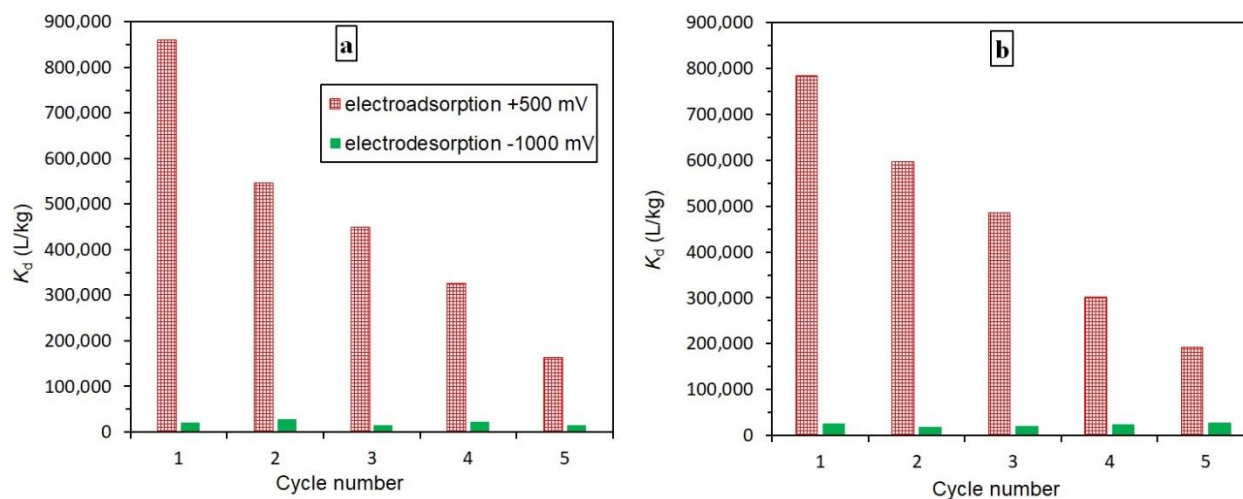
**Figure 3S.** Differential capacitance ( $C$ ) of the ACFs at frequencies 3.1, 7.9, 16 and 71 mHz versus potential ( $E$ , against Ag/AgCl as reference electrode). Electrolyte was 1 M  $\text{Na}_2\text{SO}_4$  solution at pH 7. The capacitance values were normalized to specific surface areas of the ACFs. The minimum capacitance values are considered as  $E_{PZC}$ .

**Figure 4S** shows cyclic voltammograms of the ACFs in 1 M Na<sub>2</sub>SO<sub>4</sub> at scan rates of 1 mV/s, 3 mV/s and 5 mV/s after reaching stabilization (steady state current) which takes place after several cycles. Shape of CVs depends on properties of the ACFs as well as mobility of Na<sup>+</sup> and SO<sub>4</sub><sup>2-</sup> ions in the hydrated state [2]. The quasi-rectangular shape of curves for all ACFs at the scan rate of 1 mV/s discloses the capacitive behavior of them. When the scan rate is increased the shape of CVs are distorted due to rising *iR*-drop which comes principally from the complex internal distribution of electrolyte resistance in porous electrodes [2].



**Figure 4S.** Cyclic voltammograms (CVs) of the ACFs obtained in 1 M Na<sub>2</sub>SO<sub>4</sub> solution (pH 7) at various scan rates.

**Figure 5Sa** shows electroadsorption of PFOA on ACF1 at +500 mV and electrodesorption of it at -1000 mV in 5 cycle. **Figure 5Sb** shows the electrosorption experiment with purging nitrogen in solution.



**Figure 5S.** Electroadsorption and electrodesorption of PFOA ( $C_0 = 1$  mg/L) on/from ACF1 (66.7 mg/L) in 10 mM  $\text{Na}_2\text{SO}_4$  at pH 7. 5 cycles electroadsorption at +500 mV and electrodesorption at -1000 mV without (a) and with (b) purging nitrogen in the solution. Each cycle covers 4 days, 2 days electroadsorption and 2 days electrodesorption. The potentials are versus Ag/AgCl.

## Reference

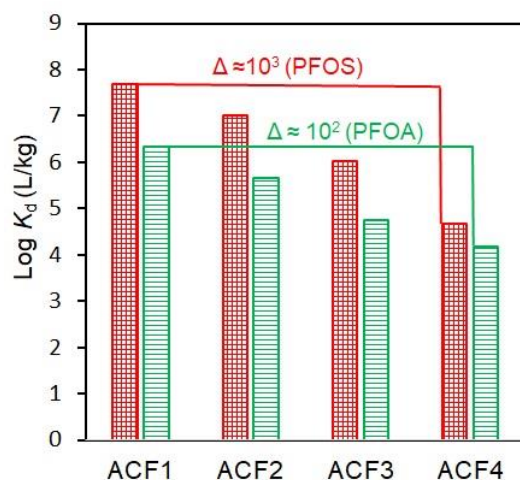
- [1] D. Weingarth, M. Zeiger, N. Jäckel, M. Aslan, G. Feng, V. Presser, Graphitization as a universal tool to tailor the potential-dependent capacitance of carbon supercapacitors, *Advanced Energy Materials* 4 (2014) 1400316.
- [2] E. Bayram, E. Ayranci, A systematic study on the changes in properties of an activated carbon cloth upon polarization, *Electrochimica Acta* 56 (2011) 2184-2189.

#### 4. Summary

The present thesis contributes to the enhancement of perfluoroalkyl acids (PFAAs) removal from water by means of adsorption on activated carbon (AC) and development of an approach for on-site regeneration of the AC saturated with the compounds. PFAAs have been detected in various sources of water throughout the world (Phong Vo et al., 2020). The published studies have been indicating the serious adverse effects of these compounds on health of human beings and wildlife (Sznajder-Katarzyńska et al., 2019). Therefore, it is necessary to remove them from various sources of water, although the conventional wastewater treatment methods are not able to remediate the water sources contaminated with PFAAs (Phong Vo et al., 2020). Among all remediation technologies, adsorption on AC is the most widely applied technique for removal of PFAAs from water (Zhang et al., 2019). However, various AC materials showed diverse performances towards PFAAs (Zhang et al., 2019). In addition, AC and other adsorbents have generally very low adsorption affinities toward short-chain PFAAs (Zhang et al., 2019; Phong Vo et al., 2020). Varying adsorption behaviour of PFAAs on AC in presence of competitive organic and inorganic ions is an additional problem. More importantly, there is no efficient on-site regeneration technology for AC saturated with the compounds (Gagliano et al., 2020; Phong Vo et al., 2020). The objective of this thesis is to enhance the adsorption technique for removal of PFAAs from water by mitigating the above mentioned problems. To this end, priority research lines were identified and three main goals were set: (1) to investigate the effect of AC textural and chemical surface properties on adsorption of PFAAs and to study deeply the adsorption mechanism of these compounds, (2) to develop targeted functional groups on AC and tailor its surface chemistry for preparing an adsorbent with exceptionally high adsorption affinity and capacity towards both short- and long-chain PFAAs, and (3) to develop an electrochemical-based approach for controlling adsorption of PFAAs on AC for a long-term electroadsorption/electrodesorption process that allows on-site regeneration of AC.



**Understanding the effect of carbon surface chemistry on adsorption of perfluorinated alkyl substances** (published in *Chemical Engineering Journal*, Vol (381) 122689 (2020))



**Graphical abstract**

In this part, it was observed that adsorption coefficients of perfluorooctanoic acid (PFOA) and perfluorosulfonic acid (PFOS) on four commercial activated carbon felts (ACFs) vary significantly under similar experimental conditions (graphical abstract). To address the reasons for these differences, the adsorption affinities and capacities of PFOA and PFOS were successfully correlated to textural and chemical surface properties of AC materials. For the first time, the favorable active sites of AC for exceptionally high adsorption of the compounds were identified, while the reasons for very low adsorption affinity of PFAAs on some ACs were reported. For this purpose, 4 commercial ACFs were characterised by various techniques. A set of batch experiments were carried out under well-defined conditions. The effect of competitive organic and inorganic ions as well as solution pH on adsorption of PFAAs on the ACFs were studied.

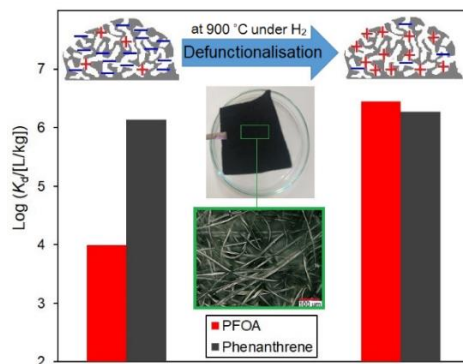
- **Surface chemistry controls PFAAs adsorption on microporous activated carbon.** The adsorption coefficients of the PFAAs normalized to the available surface area of the applied ACFs revealed strong differences. On the one hand, these ACFs owned different available pore volumes in the 1-2 nm range (i.e. by a factor < 5). However, these differences by far cannot explain the differences in adsorption capacities (up to a factor of 30 between the best adsorbent and the worst one). Furthermore, one can estimate the degree of pore filling reached at the highest maximum loading achieved, i.e. for PFOS on the best adsorbent.

Based on a molar volume of PFOS of about 270 mL/mol, the maximum volumetric loading of mL PFOS/g resulted in a filling degree of 1-2 nm pores of only 15%. It means the *volume* of this micropore fraction will most likely not be the limiting factor in PFAAs adsorption. In conclusion, the availability of pores in a certain size range cannot explain the vastly different adsorption properties of the ACFs. Surface chemistry obviously plays a major role.

- **Anion exchange capacity (AEC) of AC is a good indicator of adsorption performance toward PFAAs.** The adsorption behaviour of PFOA and PFOS on the ACFs was correlated to the parameters characterising surface chemistry (anion exchange capacity (AEC), cation exchange capacity (CEC), point of zero net proton charge (PZC) and oxygen content) of the ACFs. The maximum loading of PFOA and PFOS on the ACFs at pH = 7 correlates well and positively with AEC, meaning the higher the AEC, the higher the adsorption capacity. CEC has an inverse correlation with the maximum loading of PFOA and PFOS on the ACFs. CEC of the ACFs determined at pH = 7 originates mainly from deprotonated oxygen-containing acidic groups, e.g. carboxylic groups, causing electrostatic repulsion with PFAA anions. The correlation with oxygen content, however, was not strong. Oxygen content can be considered as a general measure for surface polarity and thus as an inverse measure of hydrophobicity. Thus, the ACF with high AEC and low CEC at pH 7 is an optimal adsorbent for PFAAs at pH values  $\leq 7$ .
- **Basic sites in  $\pi$ -electron-rich regions of AC are important for PFAAs adsorption.** In general surface basicity of AC can be related to O- or N-containing basic groups as well as basic groups and electron-rich sites of the carbon backbone. The ACFs studied in this part of work contain very low and comparable nitrogen contents. It means that their different basicity is caused by oxygen-free  $\pi$ -electron rich regions and/or oxygen-containing basic groups. Thermal-programmed decomposition (TPD) results revealed that the two ACFs with the highest adsorption of PFAAs not only show a low surface acidity (related to CO<sub>2</sub> releasing groups) but also own lower concentrations of CO-releasing functional groups compared to the other ACFs. Thus, their basicity is most likely resulting from oxygen-free  $\pi$ -electron regions in the graphene layers which behave as Lewis base and are positively charged at circumneutral pH due to binding protons.

- **Maximum loadings of PFAAs are in any case equal to or lower than AEC of the ACF.** The correlation between maximum loadings in adsorption of PFAAs on the ACFs revealed that the maximum loading is in any case equal to or lower than the AEC of the ACF. This indicates that the anions of these molecules can be adsorbed favorably by a combination of hydrophobic and electrostatic interactions if sufficient charge-balancing cationic sites are available at the ACF surface. These results give clear indications on the optimal surface chemistry of ACs for achieving high performance in removal of PFOA and PFOS: basic sites in  $\pi$ -electron rich regions on AC are important for adsorption of PFAAs.
- **Effect of inorganic ions on PFAAs adsorption depends on the surface chemistry of the AC.** Inorganic ions have diverse effects on adsorption of PFAAs on various adsorbents. However, the possible reasons for such a diversity haven't been clearly discussed yet. In the present work, adsorption of PFOA and PFOS on the ACFs at circumneutral pH from water containing various concentrations of  $\text{Na}_2\text{SO}_4$  (from 10 mM to 200 mM) disclosed that adsorption is only slightly suppresses by inorganic ions for ACFs with  $\text{PZC} > 7$  and  $\text{CEC} < \text{AEC}$  due to minor competition effects for anion binding. In contrast, ACFs with  $\text{PZC} < 7$  and  $\text{CEC} > \text{AEC}$  benefit from high ionic strength due to suppression of electrostatic repulsion.
- **High adsorption affinity was achieved in adsorption of PFOS from real ground water on the second best adsorbent.** The effect of dissolved natural organic matter (DNOM) on adsorption of PFAAs on the ACF was studied. It was expected that DNOM containing organic anionic molecules would compete with adsorption of PFOA and PFOS anions. However, no considerable decrease was observed in adsorption affinity of PFOA and PFOS on all ACFs in presence of 5 to 20 mg/L DNOM at pH 7 as well as at pH 3. The reason is probably a size exclusion effect on DNOM from microporous ACF. Consequently, a very good performance was also observed in adsorption experiments with a real groundwater containing 4.6  $\mu\text{g/L}$  PFOS.

**What is specific in adsorption of PFAAs on carbon materials?** (published in *Chemosphere*, Vol (271) 128520 (2021))



Graphical abstract

The results from the previous part deliver two main messages: (i) there is a big difference between adsorption affinities and capacities of PFAAs on various AC materials and (ii) there are clear indications on the optimal surface chemistry of ACs for achieving high performance in removal of PFAAs. In fact,  $\pi$ -electron basicity of the graphene layers is favorable for adsorption of PFAAs. In this part, the commercial ACF with the lowest affinity for PFAAs (named WK in previous work) was modified to develop very stable oxygen-free basic sites on it. In addition, nitrogen-containing functional groups, e.g. amines, can create basic sites on AC. To develop the above mentioned functional groups on AC, the following approaches were followed:

- Development of Lewis-base  $\pi$ -electron-rich regions on the ACF at 900 °C under nitrogen/hydrogen atmosphere.
- Creation of basic amine groups on the ACF by reaction with ethylenediamine under mild conditions.

The modified ACFs and the original one were applied for adsorption of long-chain PFAAs (PFOA and PFOS), a short-chain PFAA (perfluorobutanoic acid, PFBA), phenanthrene (as nonionic compound) and octanoic acid (as PFOA fluorine-free analogon) from water with various salt matrices and DNOM.

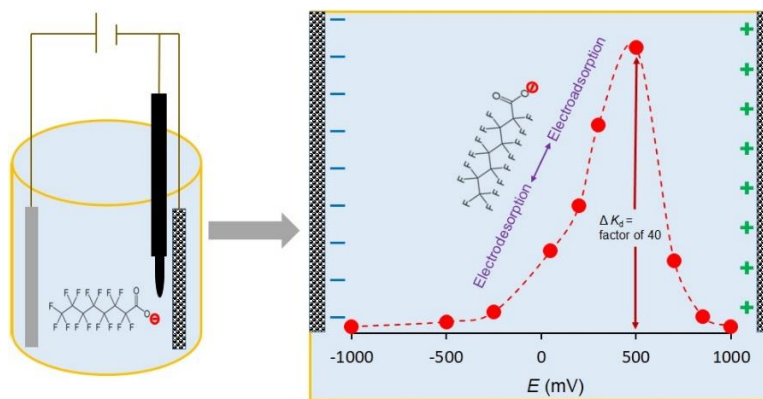
- **Amino-functionalisation of ACF without any pretreatment but using its native content of carboxylic groups directly for amidation.** The amino-functionalisation usually involves a two-step procedure, i.e. acyl-chlorination followed by an amidation process under mild conditions. In this work, this method was used for preparing amino-functionalised ACF ( $-\text{CONH}-\text{CH}_2-\text{CH}_2-\text{NH}_2$ ) without any pretreatment of the original ACF but using its native content of carboxylic groups directly for amidation. The targeted

functional group was characterised by XPS and TPD techniques. Amidation of the ACF increased the anion exchange capacity by a factor of two.

- **Thermally defunctionalised ACF has exceptionally high affinity to short- and long-chain PFAAs, although amidation has minor effect on adsorption affinities of the compounds.** The commercial ACF (CACF), defunctionalised ACF (DeCACF) and amino-functionalised ACF (CACFNH<sub>2</sub>) were applied for adsorption of PFOA, PFOS and PFBA from water. The results showed the three ACFs have various affinities towards the compounds. Defunctionalisation enhanced adsorption affinity for the compounds by up to 3 orders of magnitude, while improvement by amino-functionalisation was minor. This high adsorption affinity is especially important for PFBA ( $K_d$  up to 10<sup>5</sup> L/kg at equilibrium aqueous phase concentrations  $C_e = 3 \mu\text{g/L}$ ), as it is much higher compared to the affinities published elsewhere.
- **Stable basic sites were developed on DeCACF.** DeCACF was applied in five adsorption-desorption cycles (around 500 h) with intermittent extractive regeneration using methanol. DeCACF kept its high affinity towards PFOA ( $K_d$  up to 10<sup>7</sup> L/kg) and PFBA ( $K_d$  up to 10<sup>5</sup> L/kg) within the adsorption cycles. Therefore, the procedure used here results in an adsorbent with stable favourable basic sites for a strong uptake of short- and long-chain PFAAs.
- **Low impact of pH, inorganic and organic competitive ions on adsorption performance of the defunctionalised ACF.** The results showed that adsorption of PFAAs on DeCACF is fairly insensitive to competition by background electrolyte, e.g. Na<sub>2</sub>SO<sub>4</sub>. In fact, in adsorption from solutions containing from 10 to 200 mM Na<sub>2</sub>SO<sub>4</sub> the adsorption affinities ( $K_d$ ) of PFOA, PFOS and PFBA on DeCACF are up to 10<sup>7</sup> L/kg, 10<sup>8</sup> L/kg and 10<sup>5</sup> L/kg, respectively. Furthermore, the adsorption affinities of the compounds in presence of 5 mg/L DNOM are comparable with the values above mentioned. Increasing pH to even 9 had negligible negative impact on adsorption of PFAAs. Therefore, DeCACF has very high performance in adsorption of PFAAs from water with various salt matrices and DNOM at a wide range of pH, e.g. 3 to 9.
- **Sensitivity of adsorption towards AC surface chemistry: PFAAs >> octanoic acid > phenanthrene.** The adsorption results of octanoic acid (OCA, as PFOA F-free analogon) and phenanthrene (PHE, as nonionic organic compound) were correlated with surface

chemistry parameters of three ACFs, e.g. CACF, CACFNH<sub>2</sub> and DeCACF. The three adsorbates reacted with different sensitivity to the changes in AC surface chemistry. PHE was rather insensitive as it shows only a slight increase in Langmuir maximum adsorption capacity ( $q_m$ ) for the defunctionalised carbon and nearly no change in  $K_d$ . PFOA and OCA were much more sensitive. In fact, PFOA reacted most strongly, i.e. with an increase in  $K_d$  by 3 orders of magnitude after the defunctionalisation of the ACF, whereas for OCA this enhancement was only by a factor of 4. The specific importance of activated carbon surface chemistry for adsorption of PFAAs might result from their extremely low  $pK_a$  values ( $< 1$ ) which strongly limits charge neutralization options in adsorption. In this case, positively charged surface groups in a rather non-polar environment are detrimental for providing both, charge-balancing for PFAA anionic head groups and hydrophobic interactions of the tail.

**Controlling adsorption of perfluoroalkyl acids on activated carbon felt by means of electrical potentials** (published in *Chemical Engineering Journal*, Vol (406) 129070 (2021))



**Graphical abstract**

In this part, an electrochemical-based approach was developed for controlling adsorption of PFAAs on ACF. In fact, in this part it was tried to not only enhance adsorption of PFAAs on the adsorbent by means of external potential, but also regenerate the saturated adsorbent with PFAAs. This approach can be used as an on-site regeneration technique. Three steps were considered for developing this method:

- Selection of suitable ACFs as working electrode based on characterization by electrical impedance spectroscopy (EIS) and cyclic voltammetry (CV) and correlations to textural and chemical surface properties of the ACFs.
  - Electrosorption experiments in conventional three-electrode cells (Ag/AgCl reference and Pt counter electrode): electrosorption mechanism of PFAAs, electroadsorption and electrode desorption isotherms, effect of competitive inorganic and organic ions as well as solution pH on electrosorption.
  - Sustaining the electrosorption cell for a long-term adsorption/desorption cycle.
- **Before using an AC in electrosorption, its potential of zero charge ( $E_{PZC}$ ) should be considered.** The general approach in controlling adsorption of PFAAs on AC is enhancing its adsorption on AC by charging the AC positively by means of external electric potential and then switching potential to negative values for desorption. In this respect there is an important criterion. It is related to the surface chemical properties of the ACF and determines which potential has to be applied in order to obtain a positive ( $E > E_{PZC}$ ) or negative ( $E < E_{PZC}$ ) net charge of the surface. A problem for using carbon-based materials, in particular AC, as electrodes in electroadsorption/-desorption of organic and inorganic compounds is its attrition by direct and/or indirect oxidation and reduction under high potentials (Gineys et al., 2017). Therefore, an ACF with a low absolute value of  $E_{PZC}$  is able to be charged positively and negatively under mild potentials (i.e. sufficiently far from critical oxidation/reduction potentials of the carbon) and can be a good selection for a long-term electroadsorption/-desorption of PFAAs.
- **Electrosorption of PFOA and PFBA on ACF versus potential results in bell-shaped curves.** A plot of adsorption affinities ( $K_d$ ) of PFOA on ACF1 ( $E_{PZC} = +75$  mV) versus potential resulted in a bell-shaped curve with a peak at +500 mV with respective  $K_d$  value up to  $10^6$  L/kg. This  $K_d$  value is more than forty-times the values at negative potentials. As  $E_{PZC}$  of ACF1 is +75 mV, the net charge on ACF1 at potentials  $> +75$  mV is positive, i.e. electrostatic attractions between PFOA anions and positively charged sites exist at these potentials. In contrast, at potentials  $< +75$  mV, the net charge is negative, resulting in electrostatic repulsion toward PFOA. By applying potentials  $> +500$  mV on ACF1, electroadsorption of PFOA dropped. In contrast to inorganic anions, adsorption of PFOA is influenced to some extent by hydrophobic interactions of the carbon tail of PFOA and

the surface of AC (Zhang et al., 2019; Phong Vo et al., 2020). Thus, an increasingly charged surface can have a negative effect on adsorption of PFOA as the water adsorption becomes more dominant (Fischer, 2001). Moreover, the decrease in  $K_d$  values could be caused by changing chemical properties of the ACF from direct and indirect oxidations. Similar to PFOA, bell-shaped curves were obtained from electrosorption of PFBA on ACF1 and DeACF3 ( $E_{PZC} = -150$  mV) versus potential. The general finding that sorption of anionic and cationic organic compounds increases or decreases by applying positive or negative potentials, respectively, was reported in previous studies (Wang et al., 2018). However, PFAA anions are specifically sensitive towards the charging state of the carbon surface as large differences in  $K_d$  depending on applied potential were observed (up to two orders of magnitude variation compared to less than one order reported for various organic anions and cations (Wang et al., 2018)).

- **Electroadsorption of PFOA from a large volume of water and its electrodesorption into a low volume of PFOA concentrate: concentration factor ( $F$ ) = 115.** Prospectively, the batch reactors should be replaced by a continuous flow system for practical application. The general goal of this procedure is to reduce the volume of water which is needed for desorption ( $V_{des}$ ) related to the volume of treated water in the adsorption step, i.e. increasing the concentration factor. A step-like breakthrough curve was assumed for the adsorption and desorption steps and a simplified approach based on Freundlich isotherms was used for calculating the volume of desorption water and the resulting concentration factors. They are  $F_{+500/-1000} = 115$  (for electroadsorption at +500 mV and electrodesorption at -1000 mV),  $F_{+500/-100} = 71$  and  $F_{no\ potential/-100} = 41$ . These numbers are much higher than the concentration factor reported in reverse osmosis retaining PFAAs in a concentrate, which is typically below 10.
- **Effect of external potential on electrosorption of PFOA is much stronger than the effect of changing solution pH.** ACF1 with point of zero net proton charge  $pH_{PZC} = 7.1$  and  $E_{PZC} = +75$  mV was used to compare the effects of solution pH and external potential on (electro)sorption of PFOA. Charging ACF1 positively by either decreasing pH to 3 or applying a positive potential (+500 mV) positively influences adsorption affinity of PFOA. Charging ACF1 negatively by increasing pH to 9 and applying a negative potential (-1000 mV) on ACF1 had a negative effect on adsorption affinity of PFOA. The results



revealed that manipulating the surface charges of ACF1 by external electric potential has stronger effects on the adsorption behaviour of PFOA than changing pH in a moderate range. Furthermore, it was realized that applying positive and negative potentials significantly influences adsorption behaviour of PFOA even at pH values 3 and 9.

- **Competitive inorganic and organic ions have negligible effect on electrosorption of PFOA and PFBA.** Electroadsorption and electrodesorption of PFOA and PFBA were performed in water with various salt matrices and 5 mg/L DNOM. The results showed negligible effect of inorganic ions on electroadsorption and electrodesorption of compounds even in water with up to 200 mM Na<sub>2</sub>SO<sub>4</sub>. Furthermore, the presence of 5 mg/L of DNOM didn't influence strongly electroadsorption and electrodesorption of the fluorinated adsorbates. The results from this part indicate that this technique has a great potential in remediation of various water resources, e.g. groundwater and sea water.
- **A long-term electroadsorption/-desorption process of PFOA (10 cycles in 1000 h).** 5 cycles of alternating electroadsorption (at +500 mV) and electrodesorption (at -1000 mV) of PFOA on ACF1 revealed that single point adsorption coefficients in electroadsorption dropped significantly from 860,000 L/kg in the first cycle to around 160,000 L/kg in the fifth cycle. The decrease was probably caused by attrition of ACF under the harsh anodic potential (in electroadsorption) and the harsh cathodic potential (in electrodesorption). By selecting milder potentials, e.g.  $-100 \text{ mV} < E_{\text{PZC}} < +300 \text{ mV}$ , the decline in performance of the ACF1 cell was mitigated over 10 cycles (around 1000 h), although a drop in electroadsorption of PFOA was still observed. Anodic polarization influences ACFs' properties stronger than cathodic polarization (Gineys et al., 2017). With the knowledge of high adsorption affinity of ACF1 towards PFOA even without applying positive potentials, adsorption was carried out without potential, while a mild negative potential ( $-100 \text{ mV} < E_{\text{PZC}}$  of ACF1) was applied for desorption. The results revealed a quiet stable performance of the ACF1 cell over 10 cycles (1000 h). After an initial loss of about 20% in  $K_d$  (cycle 1-5) the ACF1 electrode kept its performance almost constant (<10% decline in cycle 5-10).

## 5. Conclusion and outlook

**Technical implications.** In order to develop suitable methods for remediation of various sources of water contaminated with perfluoroalkyl acids (PFAAs), the achievements of this thesis can be discussed in light of enhancement performance of adsorption technologies. A good selection of activated carbon (AC) having high affinity towards PFAAs has been problematic. The adsorption coefficient based on  $K_d$  in adsorption of PFAAs on AC materials can differ by 3 orders of magnitude (Du et al., 2014; Deng et al., 2015).

*Regarding diverse adsorption performances among various ACs*, in this thesis a good correlation was observed between adsorption behaviour of PFAAs with chemical surface characteristics of 4 commercial and 2 chemically modified activated carbon felts (ACFs). High specific surface area of activated carbon materials is a prerequisite for adsorption performance, however, adsorption of PFAAs on AC is to a large extent also governed by its surface chemical properties. A correlation of adsorption affinities and capacities of PFOA, PFOS and perfluorobutanoic acid (PFBA) with anion exchange capacity (AEC), cation exchange capacity (CEC), point of zero net proton charge (PZC) and oxygen content of 4 commercial and 2 chemically modified ACFs revealed the following information: 1) AEC and PZC are good indicators for adsorption performance of AC for PFAAs, i.e. the higher the AEC and PZC the higher adsorption affinity and capacity of PFAAs. 2) Maximum loading of PFAAs on AC is in any case lower than or equal to AEC of the AC. 3) A superposition of hydrophobic interactions and electrostatic attractions results in exceptionally high adsorption affinities of PFOS (up to  $10^8$  L/kg), PFOA (up to  $10^7$  L/kg) and PFBA (up to  $10^5$  L/kg). 4)  $\pi$ -electron rich sites on AC expose such superposition and are probably more important than nitrogen- and oxygen-containing basic groups for adsorption of PFAAs. Defunctionalisation of AC at high temperature (900 °C) and under hydrogen resulted in an ACF with stable basicity and very high adsorption affinity towards both short-chain and long-chain PFAAs. Application of such modified ACF in a flow cell for adsorption of a mixture of PFAAs is recommendable. The same modification procedure can be also performed for a granular AC. Studying its adsorption performance in a pilot fixed-bed unit is worth to do. In addition, this modification procedure can be further optimized in future studies in terms of the balance between targeted surface modification and carbon consumption as well as the usage of forming gas (5 vol-%  $H_2$  in  $N_2$ ) for safety reasons.

*Regarding specific adsorption behaviour of PFAAs on AC*, a comparison between adsorption affinities and capacities of PFOA with octanoic acid (as F-free analogon of PFOA) and

phenanthrene (as nonionic compound) revealed that adsorption of PFAAs on AC is much more sensitive to changing surface properties of AC, followed by octanoic acid, while phenanthrene is almost independent of. This observation is very important for a deeper understanding of the fate of ionic organic compounds in the environment. The results presented here clarify that adsorption behaviour of PFAAs is different from ‘common’ ionic organic compounds possibly due to their strong acidity ( $pK_a < 1$ ). It seems necessary to perform a comprehensive study on the adsorption behaviour of various ionic organic compounds. Sigmund et al. (Sigmund et al., 2020) have very recently reported a model to predict Freundlich isotherm parameters for adsorption of ionic compounds to carbonaceous adsorbents using a deep learning neural network approach. However, PFAAs were not included in their training data set.

Strong competitive effects of organic and inorganic ions on adsorption of PFAAs influence negatively adsorption efficiency of AC towards these compounds (Du et al., 2014; Rahman et al., 2014; Kothawala et al., 2017). *Regarding diverse effects of inorganic and organic ions on adsorption of PFAAs on AC*, the results of this thesis disclosed that a good selection of AC based on its textural and chemical surface properties can significantly mitigate this problem. In fact, effect of inorganic ions on adsorption of PFOS, PFOA and PFBA on AC depends on the surface chemical properties of the AC. The adsorption affinities of ACFs which have a higher density of positively charged sites at pH 7 (according to  $PZC \geq 7$  and  $AEC > CEC$  at pH 7), slightly decrease with an increase of  $Na_2SO_4$  concentration up to 200 mM. A stronger and opposite trend is observed for the ACFs which have a higher density of negative surface charges ( $PZC \leq 7$ ,  $CEC > AEC$  at pH 7). It is recommended to study the effects of bivalent cations such as  $Mg^{+2}$  and  $Ca^{+2}$  on adsorption of PFAAs on well-characterised ACs. In general, competitive adsorption of dissolved natural organic matter (DNOM, 5 mg/L) is reduced in case of microporous ACFs by size exclusion, while the presence of nitrogen-containing functional groups on ACF obtained by amino-functionalization exposed favorable sites for adsorption of the anionic DNOM molecules. In the present study, Suwannee River natural organic matter (SRNOM, reference number: 2R101N), which is a reference material of the International Humic Substances Society (IHSS), was used as DNOM. SRNOM has an average molar mass of about 24,000 g/mol (24 kDa) (Driver and Perdue, 2014). It is recommended to use other types of DNOM with lower molar mass for studying more deeply effects of DNOM on adsorption of PFAAs on microporous AC.

*Regarding regeneration of AC saturated with PFAAs*, difficult regeneration of AC saturated with the compounds has been addressed in previous studies as one of the biggest challenges in efficient remediation of various water sources contaminated with PFAAs (Schultz et al., 2003; Gagliano et al., 2020). In addition to the discussions above, the results of sections 3.1 and 3.2 deliver an important message: state of net charge on AC is determining for adsorption of PFAAs. Surface charge of ACs can be manipulated for controlling adsorption of PFAAs. An approach for controlling surface charges is applying electrical potentials. AC materials carry various surface functional groups. Accordingly, they respond differently towards external potentials. To have a high performance electrosorption cell with a long term applicability, a good selection of AC is very important. In this thesis, it was proposed that the potential in which the surface charges of an AC are balanced (potential of zero charge,  $E_{PZC}$ ) can be a good indicator for an appropriate selection of AC for this purpose. In fact, when  $E_{PZC}$  of an AC has a low absolute value, it can be charged positively and negatively already at mild anodic and cathodic potentials, relevant for electroadsorption and electrodesorption, respectively. This is especially important for protecting AC against possible direct and indirect oxidation and reduction under high positive and negative potentials.  $E_{PZC}$  values of ACFs range from -150 mV to +300 mV and correlate well with chemical surface properties of the ACFs. The ACF with  $AEC > CEC$  has negative  $E_{PZC}$  (-300 mV), while the ACF with  $AEC < CEC$  has  $E_{PZC} = +300$  mV and another ACF with  $AEC \approx CEC$  has very low positive  $E_{PZC}$ . Adsorption affinities (or capacities) of PFOA (on ACF1 with  $E_{PZC} = +75$  mV) and PFBA (on ACF1 and defunctionalised ACF with  $E_{PZC} = -150$  mV) versus potential in batch reactors result in bell-shape curves with corresponding peaks at potentials more positive than the respective  $E_{PZC}$  values. Decreasing potentials to values  $< E_{PZC}$  create negatively charged sites on the ACFs and reduce significantly the adsorption coefficients, i.e. from  $10^6$  L/kg down to  $10^4$  L/kg in case of PFOA, from  $10^5$  L/kg down to  $10^3$  L/kg in case of PFBA. Interestingly, rising the potential to values above the adsorption peak potential has a decreasing effect on adsorption of both PFOA and PFBA as well. Fischer (Fischer, 2001) has already predicted such a behaviour for electrosorption of organic compounds on AC, although he couldn't validate his model with experimental data due to lack of suitable experimental data in the literature. Working on a predictive model for electrosorption of ionic organic compounds is recommendable. A two-dimensional porous electrode modified Donnan model was already developed and successfully used for prediction of desalination performance (Porada et al., 2013a). However, the superposition

of electrostatic and non-electrostatic e.g. hydrophobic interactions between adsorbate and sorbent surface need to be taken into account in case of electrosorption of organic ions.

*Regarding pre-concentration of water containing PFAAs*, the high difference in adsorption affinities under positive and negative electrical potentials, i.e. a difference in  $K_d$  values up to 2 orders of magnitude, enables electroadsorption of PFOA and PFBA from a high volume of water ( $V_{ads}$ ) and their electrodesorption into a low-volume concentrate of the adsorbates ( $V_{des}$ ). Based on electroadsorption and electrodesorption isotherms of PFOA a first estimation of the concentration factor is as high as 115. This is much higher than concentration factors in reverse osmosis of PFAAs, e.g. 6.7 in (Appleman et al., 2014). Thus, it is worth to continue technology development for applying this procedure in continuous processes. Effect of inorganic and organic competitive ions on electroadsorption and electrodesorption of PFAAs were also studied, revealing minor effects in electrosorption of PFOA and PFBA on the ACFs. It means that this process is applicable in various sources of water, largely independent of their salt content.

*Regarding protection of ACF against attrition induced by external potentials within a long term electrosorption process*, the results of section 3.3. open up research opportunities for pilot continuous processes for adsorption and desorption of PFAAs.

**Potential applications.** Although ACFs were used in this thesis, it is very likely that the reported results can be extended to all types of AC materials. It is highly recommended that before applying AC for removal of PFAAs from water, the chemical surface properties of the AC is evaluated. Ideal AC adsorbents for removal of short- and long-chain PFAAs should have a low heteroatom content, leading to a low surface polarity and sufficient density of carbon-based positive charges at circumneutral pH. Such AC can postpone breakthrough of the PFAAs in a fixed-bed adsorber significantly. For instance, it was shown in section 3.2 that a targeted modification of microporous AC for developing the above mentioned surface properties on the AC can enhance single point adsorption coefficients of even short-chain PFAAs (PFBA) at its environmentally relevant concentrations up to 3 orders of magnitude (from  $10^2$  L/kg to up to  $10^5$  L/kg). In addition, the modified microporous AC is not sensitive to the presence of inorganic ions, organic ions and pH of water. The results on adsorption of PFOS from real ground water (section 3.1) proved the fact that the adsorbents identified in this thesis as most suitable ones for removal of PFAAs have as high affinity as predicted.

The electrochemical-based regeneration approach proposed in this thesis can be adopted for on-site regeneration of AC materials saturated with PFAAs. In addition, the results obtained here can be used for designing a flow cell for a practical electroadsorption/electrodesorption unit.

In conclusion, this study has significantly extended the scientific knowledge regarding remediation of water contaminated with perfluoroalkyl acids by means of adsorption on AC. At this stage, the characteristics of AC with exceptionally high adsorption affinity towards PFAAs were addressed, targeted modification approaches for developing such properties on AC were proposed and a deeper mechanistic insight on adsorption of the compounds on AC was discussed. Furthermore, for the first time an electrochemical-based approach for on-site regeneration of AC materials saturated with PFAAs was proposed and developed for a long term (1000 h) adsorption-desorption process.



## References

- Ahrens, L., 2011. Polyfluoroalkyl compounds in the aquatic environment: a review of their occurrence and fate. *Journal of Environmental Monitoring* 13, 20-31.
- Ahrens, L., Felizeter, S., Sturm, R., Xie, Z., Ebinghaus, R., 2009. Polyfluorinated compounds in waste water treatment plant effluents and surface waters along the River Elbe, Germany. *Marine Pollution Bulletin* 58, 1326-1333.
- Ahrens, L., Shoeib, M., Harner, T., Lee, S.C., Guo, R., Reiner, E.J., 2011. Wastewater treatment plant and landfills as sources of polyfluoroalkyl compounds to the atmosphere. *Environmental Science & Technology* 45, 8098-8105.
- Ahrens, L., Xie, Z., Ebinghaus, R., 2010. Distribution of perfluoroalkyl compounds in seawater from Northern Europe, Atlantic Ocean, and Southern Ocean. *Chemosphere* 78, 1011-1016.
- Anderson, M.A., Cudero, A.L., Palma, J., 2010. Capacitive deionization as an electrochemical means of saving energy and delivering clean water. Comparison to present desalination practices: Will it compete? *Electrochimica Acta* 55, 3845-3856.
- Andreozzi, R., Caprio, V., Insola, A., Marotta, R., 1999. Advanced oxidation processes (AOP) for water purification and recovery. *Catalysis Today* 53, 51-59.
- Ania, C.O., Béguin, F., 2007. Mechanism of adsorption and electrosorption of bentazone on activated carbon cloth in aqueous solutions. *Water Research* 41, 3372-3380.
- Appleman, T.D., Dickenson, E.R.V., Bellona, C., Higgins, C.P., 2013. Nanofiltration and granular activated carbon treatment of perfluoroalkyl acids. *Journal of Hazardous Materials* 260, 740-746.
- Appleman, T.D., Higgins, C.P., Quiñones, O., Vanderford, B.J., Kolstad, C., Zeigler-Holady, J.C., Dickenson, E.R.V., 2014. Treatment of poly- and perfluoroalkyl substances in U.S. full-scale water treatment systems. *Water Research* 51, 246-255.
- Arias Espana, V.A., Mallavarapu, M., Naidu, R., 2015. Treatment technologies for aqueous perfluorooctanesulfonate (PFOS) and perfluorooctanoate (PFOA): a critical review with an emphasis on field testing. *Environmental Technology & Innovation* 4, 168-181.
- Arp, H.P.H., Niederer, C., Goss, K.-U., 2006. Predicting the partitioning behavior of various highly fluorinated compounds. *Environmental Science & Technology* 40, 7298-7304.
- Arvaniti, O.S., Stasinakis, A.S., 2015. Review on the occurrence, fate and removal of perfluorinated compounds during wastewater treatment. *Science of The Total Environment* 524-525, 81-92.
- Ateia, M., Alsaiee, A., Karanfil, T., Dichtel, W., 2019. Efficient PFAS removal by amine-functionalized Sorbents: critical review of the current literature. *Environmental Science & Technology Letters* 6, 688-695.
- Ateia, M., Attia, M.F., Maroli, A., Tharayil, N., Alexis, F., Whitehead, D.C., Karanfil, T., 2018. Rapid removal of poly- and perfluorinated alkyl substances by poly(ethylenimine)-functionalized cellulose microcrystals at environmentally relevant conditions. *Environmental Science & Technology Letters* 5, 764-769.
- Ayranci, E., Duman, O., 2006. Adsorption of aromatic organic acids onto high area activated carbon cloth in relation to wastewater purification. *Journal of Hazardous Materials* 136, 542-552.
- Ayranci, E., Hoda, N., Bayram, E., 2005. Adsorption of benzoic acid onto high specific area activated carbon cloth. *Journal of Colloid and Interface Science* 284, 83-88.
- Babić, B.M., Milonjić, S.K., Polovina, M.J., Kaludierović, B.V., 1999. Point of zero charge and intrinsic equilibrium constants of activated carbon cloth. *Carbon* 37, 477-481.
- Baggioli, A., Sansotera, M., Navarrini, W., 2018. Thermodynamics of aqueous perfluorooctanoic acid (PFOA) and 4,8-dioxo-3H-perfluorononanoic acid (DONA) from DFT calculations: Insights into degradation initiation. *Chemosphere* 193, 1063-1070.
- Ban, A., Schafer, A., Wendt, H., 1998. Fundamentals of electrosorption on activated carbon for wastewater treatment of industrial effluents. *Journal of Applied Electrochemistry* 28, 227-236.
- Bán, A., Schafer, A., Wendt, H., 1998. Fundamentals of electrosorption on activated carbon for wastewater treatment of industrial effluents. *Journal of Applied Electrochemistry* 28, 227-236.
- Bandosz, T.J., Jagiello, J., Contescu, C., Schwarz, J.A., 1993. Characterization of the surfaces of activated carbons in terms of their acidity constant distributions. *Carbon* 31, 1193-1202.
- Banks, R., Smart, B., Tatlow, J., 1994. *Organofluorine chemistry: principles and commercial applications*. New York (NY): Plenum. 670 p.
- Bansal, R., Goyal, M., 2005. *Activated carbon adsorption*. Boca Raton: CRC Press, <https://doi.org/10.1201/9781420028812>.
- Baudequin, C., Couallier, E., Rakib, M., Deguerry, I., Severac, R., Pabon, M., 2011. Purification of firefighting water containing a fluorinated surfactant by reverse osmosis coupled to electrocoagulation–filtration. *Separation and Purification Technology* 76, 275-282.



Bayram, E., Ayranci, E., 2010. Electrochemically enhanced removal of polycyclic aromatic basic dyes from dilute aqueous solutions by activated carbon cloth electrodes. *Environmental Science & Technology* 44, 6331-6336.

Bayram, E., Ayranci, E., 2011. A systematic study on the changes in properties of an activated carbon cloth upon polarization. *Electrochimica Acta* 56, 2184-2189.

Bayram, E., Hoda, N., Ayranci, E., 2009. Adsorption/electrosorption of catechol and resorcinol onto high area activated carbon cloth. *Journal of Hazardous Materials* 168, 1459-1466.

Bhhatrai, B., Gramatica, P., 2011. Prediction of aqueous solubility, vapor pressure and critical micelle concentration for aquatic partitioning of perfluorinated chemicals. *Environmental Science & Technology* 45, 8120-8128.

Biesheuvel, P.M., 2015. Activated carbon is an electron-conducting amphoteric ion adsorbent. [arXiv preprint arXiv:1509.06354](https://arxiv.org/abs/1509.06354).

Biesheuvel, P.M., Porada, S., Levi, M., Bazant, M.Z., 2014. Attractive forces in microporous carbon electrodes for capacitive deionization. *Journal of Solid State Electrochemistry* 18, 1365-1376.

Biesheuvel, P.M., van Limpt, B., van der Wal, A., 2009. Dynamic adsorption/desorption process model for capacitive deionization. *The Journal of Physical Chemistry C* 113, 5636-5640.

Boehm, H.P., 1966. Chemical identification of surface groups. in: Eley, D.D., Pines, H., Weisz, P.B. (Eds.). *Advances in Catalysis*. Academic Press, pp. 179-274.

Boehm, H.P., 1994. Some aspects of the surface chemistry of carbon blacks and other carbons. *Carbon* 32, 759-769.

Bossi, R., Strand, J., Sortkjaer, O., Larsen, M.M., 2008. Perfluoroalkyl compounds in Danish wastewater treatment plants and aquatic environments. *Environment International* 34, 443-450.

Boulanger, B., Vargo, J.D., Schnoor, J.L., Hornbuckle, K.C., 2005. Evaluation of perfluorooctane surfactants in a wastewater treatment system and in a commercial surface protection product. *Environmental Science & Technology* 39, 5524-5530.

Brendel, S., Fetter, É., Staude, C., Vierke, L., Biegel-Engler, A., 2018. Short-chain perfluoroalkyl acids: environmental concerns and a regulatory strategy under REACH. *Environmental Sciences Europe* 30, 9.

Brooke, D., Footitt, A.J., Nwaogu, T.A., 2004. Environmental risk evaluation report: perfluorooctane sulfonate (PFOS). UK Environment Agency.

Buck, R.C., Franklin, J., Berger, U., Conder, J.M., Cousins, I.T., de Voogt, P., Jensen, A.A., Kannan, K., Mabury, S.A., van Leeuwen, S.P., 2011. Perfluoroalkyl and polyfluoroalkyl substances in the environment: Terminology, classification, and origins. *Integrated Environmental Assessment and Management* 7, 513-541.

C. Hansch, A.L., and D. Hoek-man, 1995. Exploring QSAR, hydrophobic, electronic, and steric constants. American Chemical Society, Washington, DC.

Cai, N., Larese-Casanova, P., 2016. Application of positively-charged ethylenediamine-functionalized graphene for the sorption of anionic organic contaminants from water. *Journal of Environmental Chemical Engineering* 4, 2941-2951.

Calvete, T., Lima, E.C., Cardoso, N.F., Dias, S.L.P., Pavan, F.A., 2009. Application of carbon adsorbents prepared from the Brazilian pine-fruit-shell for the removal of Procion Red MX 3B from aqueous solution—kinetic, equilibrium, and thermodynamic studies. *Chemical Engineering Journal* 155, 627-636.

Campo, J., Masiá, A., Picó, Y., Farré, M., Barceló, D., 2014. Distribution and fate of perfluoroalkyl substances in Mediterranean Spanish sewage treatment plants. *Science of The Total Environment* 472, 912-922.

Carrott, P.J.M., Nabais, J.M.V., Ribeiro Carrott, M.M.L., Pajares, J.A., 2001. Preparation of activated carbon fibres from acrylic textile fibres. *Carbon* 39, 1543-1555.

Carter, K.E., Farrell, J., 2008. Oxidative destruction of perfluorooctane sulfonate using boron-doped diamond film electrodes. *Environmental Science & Technology* 42, 6111-6115.

Carter, K.E., Farrell, J., 2010. Removal of perfluorooctane and perfluorobutane sulfonate from water via carbon adsorption and ion exchange. *Separation Science and Technology* 45, 762-767.

Chen, H., Chen, S., Quan, X., Zhao, Y., Zhao, H., 2009. Sorption of perfluorooctane sulfonate (PFOS) on oil and oil-derived black carbon: influence of solution pH and  $[Ca^{2+}]$ . *Chemosphere* 77, 1406-1411.

Chen, J., Zhang, P., 2006. Photodegradation of perfluorooctanoic acid in water under irradiation of 254 nm and 185 nm light by use of persulfate. *Water Science and Technology* 54, 317-325.

Chen, W., Zhang, X., Mamadiev, M., Wang, Z., 2017. Sorption of perfluorooctane sulfonate and perfluorooctanoate on polyacrylonitrile fiber-derived activated carbon fibers: in comparison with activated carbon. *RSC Advances* 7, 927-938.

Chen, X., Xia, X., Wang, X., Qiao, J., Chen, H., 2011. A comparative study on sorption of perfluorooctane sulfonate (PFOS) by chars, ash and carbon nanotubes. *Chemosphere* 83, 1313-1319.

Cheng, J., Psillakis, E., Hoffmann, M.R., Colussi, A.J., 2009. Acid dissociation versus molecular association of perfluoroalkyl oxoacids: environmental implications. *The Journal of Physical Chemistry A* 113, 8152-8156.

Chularueangakorn, P., Tanaka, S., Fujii, S., Kunacheva, C., 2014. Adsorption of perfluorooctanoic acid (PFOA) onto anion exchange resin, non-ion exchange resin, and granular-activated carbon by batch and column. *Desalination and Water Treatment* 52, 6542-6548.

Cohen, I., Avraham, E., Bouhadana, Y., Soffer, A., Aurbach, D., 2013. Long term stability of capacitive de-ionization processes for water desalination: the challenge of positive electrodes corrosion. *Electrochimica Acta* 106, 91-100.

Conte, L., Falletti, L., Zaggia, A., Milan, M., 2015. - Polyfluorinated organic micropollutants removal from water by ion exchange and adsorption.

Cornelissen, G., Gustafsson, Ö., Bucheli, T.D., Jonker, M.T.O., Koelmans, A.A., van Noort, P.C.M., 2005. Extensive sorption of organic compounds to black carbon, coal, and kerogen in sediments and soils: mechanisms and consequences for distribution, bioaccumulation, and biodegradation. *Environmental Science & Technology* 39, 6881-6895.

D'eon, J.C., Crozier, P.W., Furdui, V.I., Reiner, E.J., Libelo, E.L., Mabury, S.A., 2009. Perfluorinated phosphonic acids in Canadian surface waters and wastewater treatment plant effluent: discovery of a new class of perfluorinated acids. *Environmental Toxicology and Chemistry* 28, 2101-2107.

da Silva-Rackov, C.K.O., Lawal, W.A., Nfodzo, P.A., Vianna, M.M.G.R., do Nascimento, C.A.O., Choi, H., 2016. Degradation of PFOA by hydrogen peroxide and persulfate activated by iron-modified diatomite. *Applied Catalysis B: Environmental* 192, 253-259.

Deng, S., Nie, Y., Du, Z., Huang, Q., Meng, P., Wang, B., Huang, J., Yu, G., 2015. Enhanced adsorption of perfluorooctane sulfonate and perfluorooctanoate by bamboo-derived granular activated carbon. *Journal of Hazardous Materials* 282, 150-157.

Deng, S., Niu, L., Bei, Y., Wang, B., Huang, J., Yu, G., 2013. Adsorption of perfluorinated compounds on aminated rice husk prepared by atom transfer radical polymerization. *Chemosphere* 91, 124-130.

Deng, S., Yu, Q., Huang, J., Yu, G., 2010. Removal of perfluorooctane sulfonate from wastewater by anion exchange resins: Effects of resin properties and solution chemistry. *Water Research* 44, 5188-5195.

Dobbs, R.A., Cohen, J. M., 1980. Carbon adsorption isotherms for toxic organics. U.S. EPA Cincinnati, OH.

Driver, S.J., Perdue, E.M., 2014. Acidic functional groups of suwannee river natural organic matter, humic acids, and fulvic acids. *Advances in the physicochemical characterization of dissolved organic matter: impact on natural and engineered systems*. American Chemical Society, pp. 75-86.

Du, Z., Deng, S., Bei, Y., Huang, Q., Wang, B., Huang, J., Yu, G., 2014. Adsorption behavior and mechanism of perfluorinated compounds on various adsorbents—a review. *Journal of Hazardous Materials* 274, 443-454.

Du, Z., Deng, S., Chen, Y., Wang, B., Huang, J., Wang, Y., Yu, G., 2015. Removal of perfluorinated carboxylates from washing wastewater of perfluorooctanesulfonyl fluoride using activated carbons and resins. *Journal of Hazardous Materials* 286, 136-143.

Emmett, E.A., Shofer, F.S., Zhang, H., Freeman, D., Desai, C., Shaw, L.M., 2006. Community exposure to perfluorooctanoate: relationships between serum concentrations and exposure sources. *Journal of Occupational and Environmental Medicine* 48.

Endo, S., Goss, K.-U., 2014. Applications of polyparameter linear free energy relationships in environmental chemistry. *Environmental Science & Technology* 48, 12477-12491.

Eschauzier, C., Beerendonk, E., Scholte-Veenendaal, P., De Voogt, P., 2012. Impact of treatment processes on the removal of perfluoroalkyl acids from the drinking water production chain. *Environmental Science & Technology* 46, 1708-1715.

Exner, M., Färber, H., 2006. Perfluorinated surfactants in surface and drinking waters (9 pp). *Environmental Science and Pollution Research* 13, 299-307.

Fidel, R.B., Laird, D.A., Thompson, M.L., 2013. Evaluation of modified boehm titration methods for use with biochars. *Journal of Environmental Quality* 42, 1771-1778.

Fischer, V.M., 2001. In situ electrochemical regeneration of activated carbon. University of Groningen, Netherlands.

Foo, K.Y., Hameed, B.H., 2009. A short review of activated carbon assisted electrosorption process: An overview, current stage and future prospects. *Journal of Hazardous Materials* 170, 552-559.

Fujii, S., Polprasert, C., Tanaka, S., Hong Lien, N.P., Qiu, Y., 2007. New POPs in the water environment: distribution, bioaccumulation and treatment of perfluorinated compounds – a review paper. *Journal of Water Supply: Research and Technology-Aqua* 56, 313-326.

Gagliano, E., Sgroi, M., Falciglia, P.P., Vagliasindi, F.G.A., Roccaro, P., 2020. Removal of poly- and perfluoroalkyl substances (PFAS) from water by adsorption: Role of PFAS chain length, effect of organic matter and challenges in adsorbent regeneration. *Water Research* 171, 115381.

Gao, X., Omosebi, A., Landon, J., Liu, K., 2015. Surface charge enhanced carbon electrodes for stable and efficient capacitive deionization using inverted adsorption–desorption behavior. *Energy & Environmental Science* 8, 897-909.

Gao, X., Porada, S., Omosebi, A., Liu, K.L., Biesheuvel, P.M., Landon, J., 2016. Complementary surface charge for enhanced capacitive deionization. *Water Research* 92, 275-282.

Gellrich, V., Brunn, H., Stahl, T., 2013. Perfluoroalkyl and polyfluoroalkyl substances (PFASs) in mineral water and tap water. *Journal of Environmental Science and Health, Part A* 48, 129-135.

Giesy, J.P., Kannan, K., 2001. Global distribution of perfluorooctane sulfonate in wildlife. *Environmental Science & Technology* 35, 1339-1342.

Gilli, G., Gilli, P., 2000. Towards an unified hydrogen-bond theory. *Journal of Molecular Structure* 552, 1-15.

Gilli, P., Pretto, L., Bertolasi, V., Gilli, G., 2009. Predicting hydrogen-bond strengths from acid–base molecular properties. The  $pK_a$  slide rule: toward the solution of a long-lasting problem. *Accounts of Chemical Research* 42, 33-44.

Gineys, M., Benoit, R., Cohaut, N., Béguin, F., Delpeux-Ouldriane, S., 2017. Behavior of activated carbon cloths used as electrode in electrochemical processes. *Chemical Engineering Journal* 310, 1-12.

Gómez-Bombarelli, R., Calle, E., Casado, J., 2013a. Mechanisms of lactone hydrolysis in acidic conditions. *The Journal of Organic Chemistry* 78, 6880-6889.

Goss, K.-U., 2008. The  $pK_a$  values of PFOA and other highly fluorinated carboxylic acids. *Environmental Science & Technology* 42, 456-458.

Han, Y., Quan, X., Chen, S., Zhao, H., Cui, C., Zhao, Y., 2006a. Electrochemically enhanced adsorption of aniline on activated carbon fibers. *Separation and Purification Technology* 50, 365-372.

Han, Y., Quan, X., Chen, S., Zhao, H., Cui, C., Zhao, Y., 2006b. Electrochemically enhanced adsorption of phenol on activated carbon fibers in basic aqueous solution. *Journal of Colloid and Interface Science* 299, 766-771.

Hassan, M., Liu, Y., Naidu, R., Du, J., Qi, F., 2020. Adsorption of perfluorooctane sulfonate (PFOS) onto metal oxides modified biochar. *Environmental Technology & Innovation* 19, 100816.

Heinze, J., 1981. Allen J. Bard and Larry F. Faulkner: *Electrochemical methods – fundamentals and applications*. Wiley, New York 1980, 718 + XVIII S., Preis: £ 14.70. *Berichte der Bunsengesellschaft für physikalische Chemie* 85, 1085-1086.

Higgins, C.P., Field, J.A., 2017. Our stainfree future? a virtual issue on poly- and perfluoroalkyl substances. *Environmental Science & Technology* 51, 5859-5860.

Higgins, C.P., Luthy, R.G., 2006. Sorption of perfluorinated surfactants on sediments. *Environmental Science & Technology* 40, 7251-7256.

Hilber, I., Bucheli, T., 2010. Activated carbon amendment to remediate contaminated sediments and soil: a review. *Global Nest Journal* 12, 305-317.

Hoffman, K., Webster, T.F., Bartell, S.M., Weisskopf, M.G., Fletcher, T., Vieira, V.M., 2011. Private drinking water wells as a source of exposure to perfluorooctanoic acid (PFOA) in communities surrounding a fluoropolymer production facility. *Environmental Health Perspectives* 119, 92-97.

Hollingsworth, J., Sierra-Alvarez, R., Zhou, M., Ogden, K.L., Field, J.A., 2005. Anaerobic biodegradability and methanogenic toxicity of key constituents in copper chemical mechanical planarization effluents of the semiconductor industry. *Chemosphere* 59, 1219-1228.

Hölzer, J., Midasch, O., Rauchfuss, K., Kraft, M., Reupert, R., Angerer, J., Kleeschulte, P., Marschall, N., Wilhelm, M., 2008. Biomonitoring of perfluorinated compounds in children and adults exposed to perfluorooctanoate-contaminated drinking water. *Environmental Health Perspectives* 116, 651-657.

Hontoria-Lucas, C., López-Peinado, A.J., López-González, J.d.D., Rojas-Cervantes, M.L., Martín-Aranda, R.M., 1995. Study of oxygen-containing groups in a series of graphite oxides: physical and chemical characterization. *Carbon* 33, 1585-1592.

Hori, H., Nagaoka, Y., Murayama, M., Kutsuna, S., 2008. Efficient decomposition of perfluorocarboxylic acids and alternative fluorochemical surfactants in hot water. *Environmental Science & Technology* 42, 7438-7443.

Hori, H., Nagaoka, Y., Yamamoto, A., Sano, T., Yamashita, N., Taniyasu, S., Kutsuna, S., Osaka, I., Arakawa, R., 2006. Efficient decomposition of environmentally persistent perfluorooctanesulfonate and related fluorochemicals using zerovalent iron in subcritical water. *Environmental Science & Technology* 40, 1049-1054.

Hsieh, H.-S., Pignatello, J.J., 2017. Activated carbon-mediated base hydrolysis of alkyl bromides. *Applied Catalysis B: Environmental* 211, 68-78.

Hu, X.C., Andrews, D.Q., Lindstrom, A.B., Bruton, T.A., Schaidt, L.A., Grandjean, P., Lohmann, R., Carignan, C.C., Blum, A., Balan, S.A., Higgins, C.P., Sunderland, E.M., 2016. Detection of poly- and perfluoroalkyl substances (PFASs) in U.S. drinking water linked to industrial sites, military fire training areas, and wastewater treatment plants. *Environmental Science & Technology Letters* 3, 344-350.

Huang, D., Wang, K., Niu, J., Chu, C., Weon, S., Zhu, Q., Lu, J., Stavitski, E., Kim, J.-H., 2020. Amorphous Pd-loaded  $\text{Ti}_4\text{O}_7$  electrode for direct anodic destruction of perfluorooctanoic acid. *Environmental Science & Technology* 54, 10954-10963.

Hurley, S., Houtz, E., Goldberg, D., Wang, M., Park, J.-S., Nelson, D.O., Reynolds, P., Bernstein, L., Anton-Culver, H., Horn-Ross, P., Petreas, M., 2016. Preliminary associations between the detection of perfluoroalkyl acids (PFAAs) in drinking water and serum concentrations in a sample of california women. *Environmental Science & Technology Letters* 3, 264-269.

Huset, C.A., Chiaia, A.C., Barofsky, D.F., Jonkers, N., Kohler, H.-P.E., Ort, C., Giger, W., Field, J.A., 2008. Occurrence and mass flows of fluorochemicals in the glatt valley watershed, Switzerland. *Environmental Science & Technology* 42, 6369-6377.

Inyang, M., Dickenson, E.R.V., 2017. The use of carbon adsorbents for the removal of perfluoroalkyl acids from potable reuse systems. *Chemosphere* 184, 168-175.

ISMI, S.a., 2019. Use of PFAS/PFOA compounds by US SIA Members. Semiconductor industry association and international SEMATECH manufacrung initiative, INC. US, December 2019.

Jacquesy, J.-C., Gesson, J.-P., Jouannetaud, M.-P., 1988. Protonated phenol derivatives as reactive species. *Reviews of Chemical Intermediates* 9, 1-26.

Ji, W., Xiao, L., Ling, Y., Ching, C., Matsumoto, M., Bisbey, R.P., Helbling, D.E., Dichtel, W.R., 2018. Removal of GenX and perfluorinated alkyl substances from water by amine-functionalized covalent organic frameworks. *Journal of the American Chemical Society* 140, 12677-12681.

Jia, B., Zhang, W., 2016. Preparation and application of electrodes in capacitive deionization (CDI): a state-of-art review. *Nanoscale Research Letters* 11, 64.

Jing, P., Rodgers, P.J., Amemiya, S., 2009. High lipophilicity of perfluoroalkyl carboxylate and sulfonate: implications for their membrane permeability. *Journal of the American Chemical Society* 131, 2290-2296.

Kah, M., Brown, C.D., 2008. LogD: Lipophilicity for ionisable compounds. *Chemosphere* 72, 1401-1408.

Kah, M., Sigmund, G., Xiao, F., Hofmann, T., 2017. Sorption of ionizable and ionic organic compounds to biochar, activated carbon and other carbonaceous materials. *Water Research* 124, 673-692.

Kaiser, M.A., Barton, C.A., Botelho, M., Buck, R.C., Buxton, L.W., Gannon, J., Kao, C.C., Larsen, B.S., Russel, M.H., Wang, N., Waterland, R.L., 2006. Understanding the transport of anthropogenic fluorinated compounds in the environment. *Organohalogen Compounds* 68, 675-678.

Karickhoff, S.W., 1981. Semi-empirical estimation of sorption of hydrophobic pollutants on natural sediments and soils. *Chemosphere* 10, 833-846.

Karoyo, A.H., Wilson, L.D., 2013. Tunable macromolecular-based materials for the adsorption of perfluorooctanoic and octanoic acid anions. *Journal of Colloid and Interface Science* 402, 196-203.

Keen, I., Broota, P., Rintoul, L., Fredericks, P., Trau, M., Grøndahl, L., 2006. Introducing amine functionalities on a poly(3-hydroxybutyrate-co-3-hydroxyvalerate) surface: comparing the use of ammonia plasma treatment and ethylenediamine aminolysis. *Biomacromolecules* 7, 427-434.

Keller, A.A., Sirivithayapakorn, S., Kram, M., 1999. Remediation of MTBE-contaminated water and soil. *Remediation Journal* 10, 55-68.

Key, B.D., Howell, R.D., Criddle, C.S., 1998. Defluorination of organofluorine sulfur compounds by pseudomonas Sp. strain D2. *Environmental Science & Technology* 32, 2283-2287.

Kim, S.-K., Im, J.-K., Kang, Y.-M., Jung, S.-Y., Kho, Y.L., Zoh, K.-D., 2012. Wastewater treatment plants (WWTPs)-derived national discharge loads of perfluorinated compounds (PFCs). *Journal of Hazardous Materials* 201-202, 82.

Kishi, T., Arai, M., 2008. Study on the generation of perfluorooctane sulfonate from the aqueous film-forming foam. *Journal of hazardous materials* 159, 81-86.

Kissa, E., 2001. Fluorinated surfactants and repellents, second ed. Marcel Dekker,, second edition ed. Marcel Dekker, New York.

Koelmans, A.A., Jonker, M.T.O., Cornelissen, G., Bucheli, T.D., Van Noort, P.C.M., Gustafsson, Ö., 2006. Black carbon: the reverse of its dark side. *Chemosphere* 63, 365-377.

Kothawala, D.N., Köhler, S.J., Östlund, A., Wiberg, K., Ahrens, L., 2017. Influence of dissolved organic matter concentration and composition on the removal efficiency of perfluoroalkyl substances (PFASs) during drinking water treatment. *Water Research* 121, 320-328.

Kratochvil, D., Volesky, B., 1998. Advances in the biosorption of heavy metals. *Trends in Biotechnology* 16, 291-300.

Krusic, P.J., Marchione, A.A., Roe, D.C., 2005. Gas-phase NMR studies of the thermolysis of perfluorooctanoic acid. *Journal of Fluorine Chemistry* 126, 1510-1516.

Kumarasamy, E., Manning, I.M., Collins, L.B., Coronell, O., Leibfarth, F.A., 2020. Ionic fluorogels for remediation of per- and polyfluorinated alkyl substances from water. *ACS Central Science* 6, 487-492.

Kunacheva, C., Tanaka, S., Fujii, S., Boontanon, S.K., Musirat, C., Wongwattana, T., Shivakoti, B.R., 2011. Mass flows of perfluorinated compounds (PFCs) in central wastewater treatment plants of industrial zones in Thailand. *Chemosphere* 83, 737-744.

Kwadijk, C.J.A.F., Korytár, P., Koelmans, A.A., 2010. Distribution of perfluorinated compounds in aquatic systems in the Netherlands. *Environmental Science & Technology* 44, 3746-3751.

Kwon, Y.-N., Shih, K., Tang, C., Leckie, J.O., 2012. Adsorption of perfluorinated compounds on thin-film composite polyamide membranes. *Journal of Applied Polymer Science* 124, 1042-1049.

Lampert, D.J., Frisch, M.A., Speitel, G.E., 2007. Removal of perfluorooctanoic acid and perfluorooctane sulfonate from wastewater by ion exchange. *Practice Periodical of Hazardous, Toxic, and Radioactive Waste Management* 11, 60-68.

Langmuir, I., 1918. The adsorption of gases on plane surfaces of glass, mica and platinum. *Journal of the American Chemical Society* 40, 1361-1403.

Lau, C., 2012. Perfluorinated Compounds. in: Luch, A. (Ed.). *Molecular, clinical and environmental toxicology: volume 3: environmental toxicology*. Springer Basel, Basel, pp. 47-86.

Lee, Y.-C., Lo, S.-L., Chiueh, P.-T., Liou, Y.-H., Chen, M.-L., 2010. Microwave-hydrothermal decomposition of perfluorooctanoic acid in water by iron-activated persulfate oxidation. *Water Research* 44, 886-892.

Lee, Y.-C., Lo, S.-L., Kuo, J., Lin, Y.-L., 2012. Persulfate oxidation of perfluorooctanoic acid under the temperatures of 20–40°C. *Chemical Engineering Journal* 198-199, 27-32.

Levi, M.D., Sigalov, S., Aurbach, D., Daikhin, L., 2013. In situ electrochemical quartz crystal admittance methodology for tracking compositional and mechanical changes in porous carbon electrodes. *The Journal of Physical Chemistry C* 117, 14876-14889.

Li, F., Wei, W., Gao, D., Xia, Z., 2017. The adsorption behavior and mechanism of perfluorochemicals on oxidized fluorinated graphene sheets supported on silica. *Analytical Methods* 9, 6645-6652.

Li, X., Chen, S., Quan, X., Zhang, Y., 2011a. Enhanced adsorption of PFOA and PFOS on multiwalled carbon nanotubes under electrochemical assistance. *Environmental Science & Technology* 45, 8498-8505.

Li, X., Pignatello, J.J., Wang, Y., Xing, B., 2013. New insight into adsorption mechanism of ionizable compounds on carbon nanotubes. *Environmental Science & Technology* 47, 8334-8341.

Li, X., Zhao, H., Quan, X., Chen, S., Zhang, Y., Yu, H., 2011b. Adsorption of ionizable organic contaminants on multi-walled carbon nanotubes with different oxygen contents. *Journal of Hazardous Materials* 186, 407-415.

Lin, A.Y.-C., Panchangam, S.C., Ciou, P.-S., 2010. High levels of perfluorochemicals in Taiwan's wastewater treatment plants and downstream rivers pose great risk to local aquatic ecosystems. *Chemosphere* 80, 1167-1174.

Lindstrom, A.B., Strynar, M.J., Libelo, E.L., 2011. Polyfluorinated compounds: past, present, and future. *Environmental Science & Technology* 45, 7954-7961.

Liu, K., Zhang, S., Hu, X., Zhang, K., Roy, A., Yu, G., 2015. Understanding the adsorption of PFOA on MIL-101(Cr)-based anionic-exchange metal-organic frameworks: comparing DFT calculations with aqueous sorption experiments. *Environmental Science & Technology* 49, 8657-8665.

Llorca, M., Farré, M., Picó, Y., Müller, J., Knepper, T.P., Barceló, D., 2012. Analysis of perfluoroalkyl substances in waters from Germany and Spain. *Science of The Total Environment* 431, 139-150.

Long, L., Hu, X., Yan, J., Zeng, Y., Zhang, J., Xue, Y., 2019. Novel chitosan-ethylene glycol hydrogel for the removal of aqueous perfluorooctanoic acid. *Journal of Environmental Sciences* 84, 21-28.

Lorenzo, M., Campo, J., Farré, M., Pérez, F., Picó, Y., Barceló, D., 2016. Perfluoroalkyl substances in the Ebro and Guadalquivir river basins (Spain). *Science of The Total Environment* 540, 191-199.

Ma, R., Shih, K., 2010. Perfluorochemicals in wastewater treatment plants and sediments in Hong Kong. *Environmental Pollution* 158, 1354-1362.

Machado, F.M., Bergmann, C.P., Fernandes, T.H.M., Lima, E.C., Royer, B., Calvete, T., Fagan, S.B., 2011. Adsorption of reactive red M-2BE dye from water solutions by multi-walled carbon nanotubes and activated carbon. *Journal of Hazardous Materials* 192, 1122-1131.

Marsh, H., Rodríguez-Reinoso, F., 2006a. CHAPTER 8 - Applicability of activated carbon. in: Marsh, H., Rodríguez-Reinoso, F. (Eds.). *Activated carbon*. Elsevier Science Ltd, Oxford, pp. 383-453.

Marsh, H., Rodríguez-Reinoso, F., 2006b. CHAPTER 9 - Production and reference material. in: Marsh, H., Rodríguez-Reinoso, F. (Eds.). *Activated Carbon*. Elsevier Science Ltd, Oxford, pp. 454-508.

McCleaf, P., Englund, S., Östlund, A., Lindegren, K., Wiberg, K., Ahrens, L., 2017. Removal efficiency of multiple poly- and perfluoroalkyl substances (PFASs) in drinking water using granular activated carbon (GAC) and anion exchange (AE) column tests. *Water Research* 120, 77-87.

Menéndez, J.A., Phillips, J., Xia, B., Radovic, L.R., 1996. On the Modification and characterization of chemical surface properties of activated carbon: in the search of carbons with stable basic properties. *Langmuir* 12, 4404-4410.

Moriwaki, H., Takagi, Y., Tanaka, M., Tsuruho, K., Okitsu, K., Maeda, Y., 2005. Sonochemical decomposition of perfluorooctane sulfonate and perfluorooctanoic acid. *Environmental Science & Technology* 39, 3388-3392.

Niu, J., Conway, B.E., 2002. Development of techniques for purification of waste waters: removal of pyridine from aqueous solution by adsorption at high-area C-cloth electrodes using in situ optical spectrometry. *Journal of Electroanalytical Chemistry* 521, 16-28.

Niu, J., Li, Y., Shang, E., Xu, Z., Liu, J., 2016. Electrochemical oxidation of perfluorinated compounds in water. *Chemosphere* 146, 526-538.

Niu, Z., Wang, Y., Lin, H., Jin, F., Li, Y., Niu, J., 2017. Electrochemically enhanced removal of perfluorinated compounds (PFCs) from aqueous solution by CNTs-graphene composite electrode. *Chemical Engineering Journal* 328, 228-235.

Ochoa-Herrera, V., Sierra-Alvarez, R., 2008. Removal of perfluorinated surfactants by sorption onto granular activated carbon, zeolite and sludge. *Chemosphere* 72, 1588-1593.

Oen, A.M.P., Beckingham, B., Ghosh, U., Kruså, M.E., Luthy, R.G., Hartnik, T., Henriksen, T., Cornelissen, G., 2012. Sorption of organic compounds to fresh and field-aged activated carbons in soils and sediments. *Environmental Science & Technology* 46, 810-817.

Olah, G.A., Ku, A.T., 1970. Stable carbonium ions. CVIII. Protonated lactones and their cleavage reactions in fluorosulfuric acid-antimony pentafluoride solution. *The Journal of Organic Chemistry* 35, 3916-3922.

Oren, Y., 2008. Capacitive deionization (CDI) for desalination and water treatment — past, present and future (a review). *Desalination* 228, 10-29.

Pan, B., Xing, B., 2008. Adsorption mechanisms of organic chemicals on carbon nanotubes. *Environmental Science & Technology* 42, 9005-9013.

Pan, Y., Shi, Y., Wang, J., Cai, Y., 2011. Evaluation of perfluorinated compounds in seven wastewater treatment plants in Beijing urban areas. *Science China Chemistry* 54, 552-558.

Papirer, E., Dentzer, J., Li, S., Donnet, J.B., 1991. Surface groups on nitric acid oxidized carbon black samples determined by chemical and thermodesorption analyses. *Carbon* 29, 69-72.

Papirer, E., Li, S., Donnet, J.-B., 1987. Contribution to the study of basic surface groups on carbons. *Carbon* 25, 243-247.

Petrie, B., Barden, R., Kasprzyk-Hordern, B., 2015. A review on emerging contaminants in wastewaters and the environment: current knowledge, understudied areas and recommendations for future monitoring. *Water Research* 72, 3-27.

Phong Vo, H.N., Ngo, H.H., Guo, W., Hong Nguyen, T.M., Li, J., Liang, H., Deng, L., Chen, Z., Hang Nguyen, T.A., 2020. Poly-and perfluoroalkyl substances in water and wastewater: a comprehensive review from sources to remediation. *Journal of Water Process Engineering* 36, 101393.

Pignatello, J.J., Mitch, W.A., Xu, W., 2017. Activity and reactivity of pyrogenic carbonaceous matter toward organic compounds. *Environmental Science & Technology* 51, 8893-8908.

Pikaar, I., Koelmans, A.A., van Noort, P.C.M., 2006. Sorption of organic compounds to activated carbons. Evaluation of isotherm models. *Chemosphere* 65, 2343-2351.

Pittman, C.U., He, G.R., Wu, B., Gardner, S.D., 1997. Chemical modification of carbon fiber surfaces by nitric acid oxidation followed by reaction with tetraethylenepentamine. *Carbon* 35, 317-331.

Polovina, M., Babić, B., Kaluderović, B., Dekanski, A., 1997. Surface characterization of oxidized activated carbon cloth. *Carbon* 35, 1047-1052.

Porada, S., Borchardt, L., Oschatz, M., Bryjak, M., Atchison, J.S., Keesman, K.J., Kaskel, S., Biesheuvel, P.M., Presser, V., 2013a. Direct prediction of the desalination performance of porous carbon electrodes for capacitive deionization. *Energy & Environmental Science* 6, 3700-3712.

Porada, S., Zhao, R., van der Wal, A., Presser, V., Biesheuvel, P.M., 2013b. Review on the science and technology of water desalination by capacitive deionization. *Progress in Materials Science* 58, 1388-1442.

Post, G.B., Gleason, J.A., Cooper, K.R., 2017. Key scientific issues in developing drinking water guidelines for perfluoroalkyl acids: Contaminants of emerging concern. *PLOS Biology* 15, e2002855.

Post, G.B., Louis, J.B., Lippincott, R.L., Procopio, N.A., 2013. Occurrence of perfluorinated compounds in raw water from new jersey public drinking water systems. *Environmental Science & Technology* 47, 13266-13275.

Punyapalakul, P., Suksumboon, K., Prarat, P., Khaodhiar, S., 2013. Effects of surface functional groups and porous structures on adsorption and recovery of perfluorinated compounds by inorganic porous silicas. *Separation Science and Technology* 48, 775-788.

Qian, L., Georgi, A., Gonzalez-Olmos, R., Kopinke, F.-D., 2020. Degradation of perfluorooctanoic acid adsorbed on Fe-zeolites with molecular oxygen as oxidant under UV-A irradiation. *Applied Catalysis B: Environmental* 278, 119283.

Qiu, L., Chen, Y., Yang, Y., Xu, L., Liu, X., 2013. A study of surface modifications of carbon nanotubes on the properties of polyamide 66/multiwalled carbon nanotube composites. *Journal of Nanomaterials* 2013, 8.

Qu, Y., Zhang, C., Li, F., Bo, X., Liu, G., Zhou, Q., 2009. Equilibrium and kinetics study on the adsorption of perfluorooctanoic acid from aqueous solution onto powdered activated carbon. *Journal of Hazardous Materials* 169, 146-152.

Radjenovic, J., Sedlak, D.L., 2015. Challenges and opportunities for electrochemical processes as next-generation technologies for the treatment of contaminated water. *Environmental Science & Technology* 49, 11292-11302.

Rahman, M.F., Peldszus, S., Anderson, W.B., 2014. Behaviour and fate of perfluoroalkyl and polyfluoroalkyl substances (PFASs) in drinking water treatment: a review. *Water Research* 50, 318-340.

Rosario-Ortiz, F. (Ed.), 2014. *Advances in the physicochemical characterization of dissolved organic matter: impact on natural and engineered systems*. American Chemical Society.

Rumsby, P.C., McLaughlin, C.L., Hall, T., 2009. Perfluorooctane sulphonate and perfluorooctanoic acid in drinking and environmental waters. *Philosophical Transactions of the Royal Society A: Mathematical, Physical and Engineering Sciences* 367, 4119-4136.

Saeidi, N., Kopinke, F.-D., Georgi, A., 2020a. Understanding the effect of carbon surface chemistry on adsorption of perfluorinated alkyl substances. *Chemical Engineering Journal* 381, 122689.

Saeidi, N., Kopinke, F.-D., Georgi, A., 2020b. What is specific in adsorption of perfluoroalkyl acids on carbon materials? *Chemosphere*, 128520.

Saeidi, N., Kopinke, F.-D., Georgi, A., 2021. Controlling adsorption of perfluoroalkyl acids on activated carbon by means of electrical potentials. *Chemical Engineering Journal* 416, 129070.

Saha, D., Grappe, H.A., 2017. 5 - Adsorption properties of activated carbon fibers. in: Chen, J.Y. (Ed.). *Activated carbon fiber and textiles*. Woodhead Publishing, Oxford, pp. 143-165.

Sangster, J., 1989. Octanol-water partition coefficients of simple organic compounds. *Journal of Physical and Chemical Reference Data* 18, 1111-1229.

Santos, A., Rodríguez, S., Pardo, F., Romero, A., 2016. Use of fenton reagent combined with humic acids for the removal of PFOA from contaminated water. *Science of The Total Environment* 563-564, 657-663.

Sauvé, S., Desrosiers, M., 2014. A review of what is an emerging contaminant. *Chemistry Central Journal* 8, 15.

Scheringer, M., Trier, X., Cousins, I.T., de Voogt, P., Fletcher, T., Wang, Z., Webster, T.F., 2014. Helsingør Statement on poly- and perfluorinated alkyl substances (PFASs). *Chemosphere* 114, 337-339.

Schröder, H.F., Meesters, R.J.W., 2005. Stability of fluorinated surfactants in advanced oxidation processes—a follow up of degradation products using flow injection–mass spectrometry, liquid chromatography–mass spectrometry and liquid chromatography–multiple stage mass spectrometry. *Journal of Chromatography A* 1082, 110-119.

Schultz, M.M., Barofsky, D.F., Field, J.A., 2003. Fluorinated alkyl surfactants. *Environmental Engineering Science* 20, 487-501.

Schultz, M.M., Higgins, C.P., Huset, C.A., Luthy, R.G., Barofsky, D.F., Field, J.A., 2006. Fluorochemical mass flows in a municipal wastewater treatment facility. *Environmental Science & Technology* 40, 7350-7357.

Schuricht, F., Borovinskaya, E.S., Reschetilowski, W., 2017. Removal of perfluorinated surfactants from wastewater by adsorption and ion exchange — influence of material properties, sorption mechanism and modeling. *Journal of Environmental Sciences* 54, 160-170.

Schwanz, T.G., Llorca, M., Farré, M., Barceló, D., 2016. Perfluoroalkyl substances assessment in drinking waters from Brazil, France and Spain. *Science of The Total Environment* 539, 143-152.

Shafeeyan, M.S., Daud, W.M.A.W., Houshmand, A., Shamiri, A., 2010. A review on surface modification of activated carbon for carbon dioxide adsorption. *Journal of Analytical and Applied Pyrolysis* 89, 143-151.

Shafique, U., Schulze, S., Slawik, C., Böhme, A., Paschke, A., Schüürmann, G., 2017. Perfluoroalkyl acids in aqueous samples from Germany and Kenya. *Environmental Science and Pollution Research* 24, 11031-11043.

Shao, L.-H., Biener, J., Kramer, D., Viswanath, R.N., Baumann, T.F., Hamza, A.V., Weissmüller, J., 2010. Electrocapillary maximum and potential of zero charge of carbon aerogel. *Physical Chemistry Chemical Physics* 12, 7580-7587.

Shivakoti, B.R., Fujii, S., Nozoe, M., Tanaka, S., Kunacheva, C., 2010. Perfluorinated chemicals (PFCs) in water purification plants (WPPs) with advanced treatment processes. *Water Supply* 10, 87-95.

Sigmund, G., Gharasoo, M., Hüffer, T., Hofmann, T., 2020. Deep learning neural network approach for predicting the sorption of ionizable and polar organic pollutants to a wide range of carbonaceous materials. *Environmental Science & Technology* 54, 4583-4591.

Sinclair, E., Kannan, K., 2006. Mass loading and fate of perfluoroalkyl surfactants in wastewater treatment plants. *Environmental Science & Technology* 40, 1408-1414.

Söregård, M., Östblom, E., Köhler, S., Ahrens, L., 2020. Adsorption behavior of per- and polyfluoroalkyl substances (PFASs) to 44 inorganic and organic sorbents and use of dyes as proxies for PFAS sorption. *Journal of Environmental Chemical Engineering* 8, 103744.

Soriano, Á., Gorri, D., Biegler, L.T., Urtiaga, A., 2019a. An optimization model for the treatment of perfluorocarboxylic acids considering membrane preconcentration and BDD electrooxidation. *Water Research* 164, 114954.

Soriano, Á., Gorri, D., Urtiaga, A., 2019b. Membrane preconcentration as an efficient tool to reduce the energy consumption of perfluorohexanoic acid electrochemical treatment. *Separation and Purification Technology* 208, 160-168.

Stasinakis, A.S., Thomaidis, N.S., Arvaniti, O.S., Asimakopoulos, A.G., Samaras, V.G., Ajibola, A., Mamais, D., Lekkas, T.D., 2013. Contribution of primary and secondary treatment on the removal of benzothiazoles, benzotriazoles, endocrine disruptors, pharmaceuticals and perfluorinated compounds in a sewage treatment plant. *Science of The Total Environment* 463-464, 1067-1075.

Steinle-Darling, E., Reinhard, M., 2008. Nanofiltration for trace organic contaminant removal: structure, solution, and membrane fouling effects on the rejection of perfluorochemicals. *Environmental Science & Technology* 42, 5292-5297.

Stock, N.L., Muir, D.C.G., Mabury, S., 2009. Perfluoroalkyl compounds. In: Harrad, S. (Ed.), *persistent organic pollutants*. John Wiley and Sons, Ltd., Chichester, UK, pp. 25-69.

Streat, M., Patrick, J.W., Perez, M.J.C., 1995. Sorption of phenol and para-chlorophenol from water using conventional and novel activated carbons. *Water Research* 29, 467-472.

Strelko, V., Malik, D.J., Streat, M., 2002. Characterisation of the surface of oxidised carbon adsorbents. *Carbon* 40, 95-104.

Sznajder-Katarzyńska, K., Surma, M., Cieřlik, I., 2019. A review of perfluoroalkyl acids (PFAAs) in terms of sources, applications, human exposure, dietary intake, toxicity, legal regulation, and methods of determination. *Journal of Chemistry* 2019, 2717528.

T. Pancras, G.S., T. Held, K. Baker, I. Ross, H. Slenders, M.J. Spence, 2016. Environmental fate and effects of polyand perfluoroalkyl substances (PFAS). ARCADIS, Brussels.

Tabti, Z., Ruiz-Rosas, R., Quijada, C., Cazorla-Amorós, D., Morallón, E., 2014. Tailoring the surface chemistry of activated carbon cloth by electrochemical methods. *ACS Applied Materials & Interfaces* 6, 11682-11691.

Tang, C.Y., Fu, Q.S., Robertson, A.P., Criddle, C.S., Leckie, J.O., 2006. Use of reverse osmosis membranes to remove perfluorooctane sulfonate (PFOS) from semiconductor wastewater. *Environmental Science & Technology* 40, 7343-7349.

Tang, H., Xiang, Q., Lei, M., Yan, J., Zhu, L., Zou, J., 2012. Efficient degradation of perfluorooctanoic acid by UV–Fenton process. *Chemical Engineering Journal* 184, 156-162.

Teaf, C.M., Garber, M.M., Covert, D.J., Tuovila, B.J., 2019. Perfluorooctanoic acid (PFOA): environmental sources, chemistry, toxicology, and potential risks. *Soil and Sediment Contamination: An International Journal* 28, 258-273.

Teixidó, M., Pignatello, J.J., Beltrán, J.L., Granados, M., Peccia, J., 2011. Speciation of the ionizable antibiotic sulfamethazine on black carbon (biochar). *Environmental Science & Technology* 45, 10020-10027.

Thompson, J., Eaglesham, G., Mueller, J., 2011a. Concentrations of PFOS, PFOA and other perfluorinated alkyl acids in Australian drinking water. *Chemosphere* 83, 1320-1325.

Thompson, J., Eaglesham, G., Reungoat, J., Poussade, Y., Bartkow, M., Lawrence, M., Mueller, J.F., 2011b. Removal of PFOS, PFOA and other perfluoroalkyl acids at water reclamation plants in South East Queensland Australia. *Chemosphere* 82, 9-17.

Tran, H.N., You, S.-J., Hosseini-Bandegharai, A., Chao, H.-P., 2017. Mistakes and inconsistencies regarding adsorption of contaminants from aqueous solutions: a critical review. *Water Research* 120, 88-116.

Vecitis, C.D., Park, H., Cheng, J., Mader, B.T., Hoffmann, M.R., 2009. Treatment technologies for aqueous perfluorooctanesulfonate (PFOS) and perfluorooctanoate (PFOA). *Frontiers of Environmental Science & Engineering in China* 3, 129-151.

Villar, I., Roldan, S., Ruiz, V., Granda, M., Blanco, C., Menéndez, R., Santamaría, R., 2010. Capacitive deionization of NaCl solutions with modified activated carbon electrodes. *Energy & Fuels* 24, 3329-3333.

W., G.N., Daniel, M., Norbert, H., A., M.P., Michael, P.E., 2015. Suwannee River Natural Organic Matter: isolation of the 2R101N reference sample by reverse osmosis. *Environmental Engineering Science* 32, 38-44.

Wagoner, D.B., Christman, R.F., Cauchon, G., Paulson, R., 1997. Molar mass and size of suwannee river natural organic matter using multi-angle laser light scattering. *Environmental Science & Technology* 31, 937-941.



Walters, R.W., Luthy, R.G., 1984. Equilibrium adsorption of polycyclic aromatic hydrocarbons from water onto activated carbon. *Environmental Science & Technology* 18, 395-403.

Wang, F., Shih, K., 2011. Adsorption of perfluorooctanesulfonate (PFOS) and perfluorooctanoate (PFOA) on alumina: influence of solution pH and cations. *Water Research* 45, 2925-2930.

Wang, G., Qian, B., Dong, Q., Yang, J., Zhao, Z., Qiu, J., 2013. Highly mesoporous activated carbon electrode for capacitive deionization. *Separation and Purification Technology* 103, 216-221.

Wang, S., Li, X., Zhang, Y., Quan, X., Chen, S., Yu, H., Zhao, H., 2014. Electrochemically enhanced adsorption of PFOA and PFOS on multiwalled carbon nanotubes in continuous flow mode. *Chinese Science Bulletin* 59, 2890-2897.

Wang, S., Li, X., Zhao, H., Quan, X., Chen, S., Yu, H., 2018. Enhanced adsorption of ionizable antibiotics on activated carbon fiber under electrochemical assistance in continuous-flow modes. *Water Research* 134, 162-169.

Wang, T., Zhao, C., Li, P., Li, Y., Wang, J., 2015. Fabrication of novel poly(m-phenylene isophthalamide) hollow fiber nanofiltration membrane for effective removal of trace amount perfluorooctane sulfonate from water. *Journal of Membrane Science* 477, 74-85.

Wardman, P., 1989. Reduction potentials of one-electron couples involving free radicals in aqueous solution. *Journal of Physical and Chemical Reference Data* 18, 1637-1755.

Weingarth, D., Zeiger, M., Jäckel, N., Aslan, M., Feng, G., Presser, V., 2014. Graphitization as a universal tool to tailor the potential-dependent capacitance of carbon supercapacitors. *Advanced Energy Materials* 4, 1400316.

Wellen, B.A., Lach, E.A., Allen, H.C., 2017. Surface  $pK_a$  of octanoic, nonanoic, and decanoic fatty acids at the air-water interface: applications to atmospheric aerosol chemistry. *Physical Chemistry Chemical Physics* 19, 26551.

Xiao, F., Halbach, T.R., Simcik, M.F., Gulliver, J.S., 2012. Input characterization of perfluoroalkyl substances in wastewater treatment plants: source discrimination by exploratory data analysis. *Water Research* 46, 3101-3109.

Xu, C., Chen, H., Jiang, F., 2015. Adsorption of perfluorooctane sulfonate (PFOS) and perfluorooctanoate (PFOA) on polyaniline nanotubes. *Colloids and Surfaces A: Physicochemical and Engineering Aspects* 479, 60-67.

Yu, J., Lv, L., Lan, P., Zhang, S., Pan, B., Zhang, W., 2012. Effect of effluent organic matter on the adsorption of perfluorinated compounds onto activated carbon. *Journal of Hazardous Materials* 225-226, 99-106.

Yu, Q., Deng, S., Yu, G., 2008. Selective removal of perfluorooctane sulfonate from aqueous solution using chitosan-based molecularly imprinted polymer adsorbents. *Water Research* 42, 3089-3097.

Yu, Q., Zhang, R., Deng, S., Huang, J., Yu, G., 2009. Sorption of perfluorooctane sulfonate and perfluorooctanoate on activated carbons and resin: kinetic and isotherm study. *Water Research* 43, 1150-1158.

Zhang, D., He, Q., Wang, M., Zhang, W., Liang, Y., 2019. Sorption of perfluoroalkylated substances (PFASs) onto granular activated carbon and biochar. *Environmental Technology*, 1-12.

Zhang, D., Luo, Q., Gao, B., Chiang, S.-Y.D., Woodward, D., Huang, Q., 2016a. Sorption of perfluorooctanoic acid, perfluorooctane sulfonate and perfluoroheptanoic acid on granular activated carbon. *Chemosphere* 144, 2336-2342.

Zhang, J., Zhang, Y., Yu, S., Tang, Y., 2016b. Sorption characteristics of tetrabromobisphenol A by oxidized and ethylenediamine-functionalized multi-walled carbon nanotubes. *Desalination and Water Treatment* 57, 17343-17354.

Zhang, Q., Deng, S., Yu, G., Huang, J., 2011. Removal of perfluorooctane sulfonate from aqueous solution by crosslinked chitosan beads: sorption kinetics and uptake mechanism. *Bioresource Technology* 102, 2265-2271.

Zhang, Y., Zhi, Y., Liu, J., Ghoshal, S., 2018. Sorption of perfluoroalkyl acids to fresh and aged nanoscale zerovalent iron particles. *Environmental Science & Technology* 52, 6300-6308.

Zhi, Y., Liu, J., 2015. Adsorption of perfluoroalkyl acids by carbonaceous adsorbents: effect of carbon surface chemistry. *Environmental Pollution* 202, 168-176.

Zhi, Y., Liu, J., 2016. Surface modification of activated carbon for enhanced adsorption of perfluoroalkyl acids from aqueous solutions. *Chemosphere* 144, 1224-1232.

Zhou, Q., Deng, S., Yu, Q., Zhang, Q., Yu, G., Huang, J., He, H., 2010. Sorption of perfluorooctane sulfonate on organo-montmorillonites. *Chemosphere* 78, 688-694.

Zhou, Q., Pan, G., Shen, W., 2013. Enhanced sorption of perfluorooctane sulfonate and Cr(VI) on organo montmorillonite: influence of solution pH and uptake mechanism. *Adsorption* 19, 709-715.

Zhuo, Q., Deng, S., Yang, B., Huang, J., Wang, B., Zhang, T., Yu, G., 2012. Degradation of perfluorinated compounds on a boron-doped diamond electrode. *Electrochimica Acta* 77, 17-22.

Zhuo, Q., Deng, S., Yang, B., Huang, J., Yu, G., 2011. Efficient electrochemical oxidation of perfluorooctanoate using a Ti/SnO<sub>2</sub>-Sb-Bi anode. *Environmental science & technology* 45, 2973-2979.

Zielke, U., Hüttinger, K.J., Hoffman, W.P., 1996. Surface-oxidized carbon fibers: I. surface structure and chemistry. *Carbon* 34, 983-998.

Zou, L., Morris, G., Qi, D., 2008. Using activated carbon electrode in electrosorptive deionisation of brackish water. *Desalination* 225, 329-340.

## **Acknowledgements**

I spent 4 amazing years, from December 2016 to November 2020, at the UFZ in Leipzig working on my PhD. I experienced here happy days and sometimes stressful moments. But after these 4 years, I would like to thank all the people whose help was crucial in completing my PhD. First of all, I would like to thank my supervisors at UFZ, Prof. Dr. Frank-Dieter Kopinke and Dr. Anett Georgi, for their great support, guidelines and helpfulness during these years. In particular, I would like to thank Anett Georgi who replied my e-mail 5 years ago and introduced me to Prof. Kopinke as a potential applicant for DAAD scholarship. Furthermore, she spent not only a lot of time on reading and correcting my writings and discussing my results, but also she supported me always outside the workplace by helping me to live better in a foreign land. I would like to thank my wonderful colleagues of the department of Environmental Engineering, for explanations, the teachings, helps and for patiently trying to speak German with me. I want to particularly thank to Silke Woszidlo, Jieying Zhou and Merle Scherf because of their helps and supports for running my experiments. I am grateful for DAAD because of funding my PhD. Then, I would like to thank my mother Maryam, my father Ata and my brothers and sister for their support and for encouraging me to complete this chapter of my life. Last but not least, I thank my lovely wife Felor whose love, support, patience, and company have been fundamental not only for my life but also for completing my PhD.

I also want to mention that during my PhD I had the chance to meet visiting scientists and students. I want to thank all of them. In particular, meeting Lionel Domergue during 2018 FIFA World Cup was a wonderful experience for me.



## Curriculum vitae

### Navid Saeidi

Date of birth: 02.04.1985

Place of birth: Teheran, Iran

Nationality: Iran

E-mail addresses: [navid.saeidi@ufz.de](mailto:navid.saeidi@ufz.de); [navid\\_saeidi13@yahoo.com](mailto:navid_saeidi13@yahoo.com)

Phone number: +491791265739

Address: Merseburger Str. 37, 04177 Leipzig

Professional webpages: [Linkedin](#) [Google scholar](#) [UFZ graduate school HIGRADE](#)

### Education

---

**PhD candidate**, Department of Environmental Engineering, Helmholtz Center for Environmental Research – UFZ, Leipzig. Thesis title: “**Improving adsorption of perfluoroalkyl acids by tailoring surface chemistry of activated carbon and electric potentials.**” (Dec 2016-present), supervisors: Prof. Frank-Dieter Kopinke and Dr. Anett Georgi.

**Master of Chemical Eng.** (Separation), Semnan University, Semnan, Iran; GPA: 18.04/20. Thesis title: “**Preparation of granular activated carbon from powder sample.**” (2009-2012), supervisor: Prof. Mohammad Nader Lotfollahi.

**Bachelor of Chemical Eng.** (Mining Industries), Semnan University, Semnan, Iran. Thesis title: “**Separation of benzene from hexane.**” (2004-2009), supervisor: Prof. Mohammad Nader Lotfollahi.



## List of publications

### *Publications from this thesis*

**Saeidi, N.**, Kopinke, F.-D., Georgi, A. “Understanding the effect of carbon surface chemistry on adsorption of perfluorinated alkyl substances.” *Chemical Engineering Journal*, Vol (381) 122689 (2020).

**Saeidi, N.**, Kopinke, F.-D., Georgi, A. “What is specific in adsorption of perfluoroalkyl acids on carbon materials.” *Chemosphere*, Vol (273) 128520 (2021).

**Saeidi, N.**, Kopinke, F.-D., Georgi, A. “Controlling adsorption of perfluoroalkyl acids on activated carbon felt by means of electrical potentials.” *Chemical Engineering Journal*, Vol (406) 129070 (2021).

### *Conference contributions*

**Saeidi, N.**, Kopinke, F.-D., Georgi, A. “Adsorption of perfluorinated surfactants on activated carbon: role of surface chemistry.” Oral presentation in 2<sup>nd</sup> Global Conference on Catalyst, Chemical Engineering and Technology, Sep. 2018, Rome, Italy.

**Saeidi, N.**, Kopinke, F.-D., Georgi, A. “Tuning activated carbon adsorption by surface chemistry and electric potentials: perfluorinated alkyl surfactants as target pollutants.” Oral presentation in 15<sup>th</sup> international conference on Sustainable Use and Management of Soil, Sediment and Water Resources (AquaConSoil), May 2019, Antwerp, Belgium.

**Saeidi, N.**, Kopinke, F.-D., Georgi, A. “Electrosorption/-desorption for removal of perfluoroalkyl acids.” An International Conference on Characterization and Remediation of Per and Polyfluoroalkyl Substances and Other Emerging Contaminants, May 2021, Leipzig, Germany (online).

**Saeidi, N.**, Kopinke, F.-D., Georgi, A. “Electrosorption of perfluoroalkyl acids on activated carbon: accumulation of the compounds and on-site regeneration of activated carbon. ” Oral presentation in 16<sup>th</sup> AquaConSoil, June 2021 (online).



Kurzfassung der wissenschaftlichen Ergebnisse  
zur Dissertation

**Improving adsorption of perfluoroalkyl acids by  
tailoring surface chemistry of activated carbon and  
electric potentials**

Der Fakultät für Chemie und Mineralogie der Universität Leipzig  
vorgelegt von

M. Sc. (Chemieingenieur) Navid Saeidi  
geboren am 02.04.1985 in Teheran (Iran)

Angefertigt am Helmholtz-Zentrum für Umweltforschung GmbH –  
UFZ, Department für Technische Umweltchemie



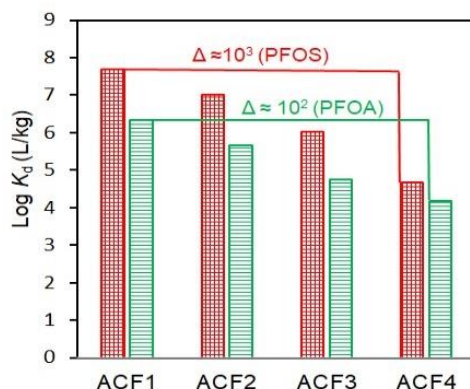
## **1. Introduction**

The present thesis contributes to the enhancement of perfluoroalkyl acids (PFAAs) removal from water by means of adsorption on activated carbon (AC) and development of an approach for on-site regeneration of the AC saturated with the compounds. PFAAs have been detected in various sources of water throughout the world (Phong Vo et al., 2020). The published studies have been indicating the serious adverse effects of these compounds on health of human beings and wildlife (Sznajder-Katarzyńska et al., 2019). Therefore, it is necessary to remove them from various sources of water, although the conventional wastewater treatment methods are not able to remediate the water sources contaminated with PFAAs (Phong Vo et al., 2020). Among all remediation technologies, adsorption on AC is the most widely applied technique for removal of PFAAs from water (Phong Vo et al., 2020). However, various AC materials showed diverse performances towards PFAAs (Phong Vo et al., 2020). In addition, AC and other adsorbents have generally very low adsorption affinities toward short-chain PFAAs (Phong Vo et al., 2020). Varying adsorption behaviour of PFAAs on AC in presence of competitive organic and inorganic ions is an additional problem. More importantly, there is no efficient on-site regeneration technology for AC saturated with the compounds (Gagliano et al., 2020). The objective of this thesis is to enhance the adsorption technique for removal of PFAAs from water by mitigating the above mentioned problems. To this end, priority research lines were identified and three main goals were set: (1) to investigate the effect of AC textural and chemical surface properties on adsorption of PFAAs and to study deeply the adsorption mechanism of these compounds, (2) to develop targeted functional groups on AC and tailor its surface chemistry for preparing an adsorbent with exceptionally high adsorption affinity and capacity towards both short- and long-chain PFAAs, and (3) to develop an electrochemical-based approach for controlling adsorption of PFAAs on AC for a long-term electroadsorption/electrodesorption process that allows on-site regeneration of AC.

## **2. Results and discussion**

### **2.1. Understanding the effect of carbon surface chemistry on adsorption of perfluorinated alkyl substances**

It was observed that adsorption coefficients of perfluorooctanoic acid (PFOA) and perfluorosulfonic acid (PFOS) on four commercial activated carbon felts (ACFs) vary significantly under similar experimental conditions (graphical abstract).



**Graphical abstract**

To address the reasons for these differences, the adsorption affinities and capacities of PFOA and PFOS were successfully correlated to textural and chemical surface properties of AC materials. For the first time, the favorable active sites of AC for exceptionally high adsorption of the compounds were identified, while the reasons for very low adsorption affinity of PFAAs on some ACs were reported. A set of batch experiments were carried out under well-defined conditions.

**- Surface chemistry controls PFAAs adsorption on microporous activated carbon.** The ACFs owned different available pore volumes in the 1-2 nm range (i.e. by a factor < 5). However, these differences by far cannot explain the differences in adsorption capacities (up to a factor of 30 between the best adsorbent and the worst one). Furthermore, for adsorption of PFOS on the best adsorbent and based on a molar volume of PFOS of about 270 mL/mol, the maximum volumetric loading of mL PFOS/g resulted in a filling degree of 1-2 nm pores of only 15%. Surface chemistry obviously plays a major role.

**- Anion exchange capacity (AEC) of AC is a good indicator of adsorption performance.** The adsorption behaviour of PFOA and PFOS on the ACFs was correlated to the parameters characterising surface chemistry (anion exchange capacity (AEC), cation exchange capacity (CEC), point of zero net proton charge (PZC) and oxygen content) of the ACFs. The maximum loading of PFOA and PFOS on the ACFs at pH = 7 correlates well and positively with AEC. CEC has an inverse correlation with the maximum loading of PFOA and PFOS on the ACFs. The correlation with oxygen content, however, was not strong. Oxygen content can be considered as a general measure for surface polarity and thus as an inverse measure of hydrophobicity. Therefore, the ACF with high AEC and low CEC at pH 7 is an optimal adsorbent for PFAAs at pH values  $\leq$  7.

**- Basic sites in  $\pi$ -electron-rich regions of AC are important for PFAAs adsorption.** In general surface basicity of AC can be related to O- or N-containing basic groups as well as basic groups and electron-rich sites of the carbon backbone. The ACFs studied in this part of work contain very low and comparable nitrogen contents. It means that their different basicity is caused by oxygen-free  $\pi$ -electron rich regions and/or oxygen-containing basic groups. Thermal-programmed decomposition (TPD) results revealed that the two ACFs with the highest adsorption of PFAAs not only show a low surface acidity (related to CO<sub>2</sub> releasing groups) but also own lower concentrations of CO-releasing functional groups compared to the other ACFs. Thus, their basicity is most likely resulting from oxygen-free  $\pi$ -electron regions in the graphene layers which behave as Lewis base and are positively charged at circumneutral pH due to binding protons.

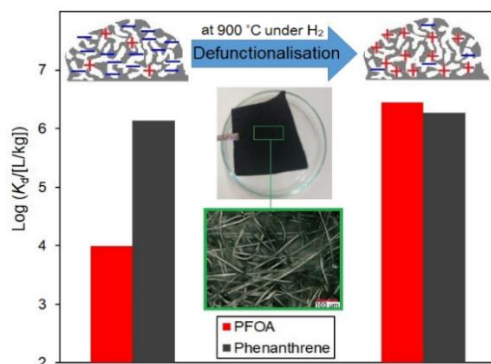
**- Maximum loadings of PFAAs are in any case equal to or lower than AEC of the ACF.** The correlation between maximum loadings in adsorption of PFAAs on the ACFs revealed that the maximum loading is in any case equal to or lower than the AEC of the ACF. This indicates that the anions of these molecules can be adsorbed favorably by a combination of hydrophobic and electrostatic interactions if sufficient charge-balancing cationic sites are available at the ACF surface. These results give clear indications on the optimal surface chemistry of ACs for achieving high performance in removal of PFOA and PFOS: basic sites in  $\pi$ -electron rich regions on AC are important for adsorption of PFAAs.

**- Effect of inorganic ions on PFAAs adsorption depends on the surface chemistry of the AC.** Inorganic ions have diverse effects on adsorption of PFAAs on various adsorbents. However, the possible reasons for such a diversity haven't been clearly discussed yet. In the present work, it was disclosed that adsorption of the compounds is only slightly suppresses by inorganic ions (10 mM to 200 mM of Na<sub>2</sub>SO<sub>4</sub>) for ACFs with PZC > 7 and CEC < AEC due to minor competition effects for anion binding. In contrast, ACFs with PZC < 7 and CEC > AEC benefit from high ionic strength due to suppression of electrostatic repulsion.

**- High adsorption affinity was achieved in adsorption of PFOS from real ground water on the second best adsorbent.** Adsorption affinities of PFOA and PFOS on all ACFs in presence of 5 to 20 mg/L natural organic matter (DNOM) at pH 7 as well as at pH 3 was influenced slightly. The reason is probably a size exclusion effect on DNOM from microporous ACF. Consequently, a very good performance was also observed in adsorption experiments with a real groundwater containing 4.6  $\mu$ g/L PFOS.

## 2.2. What is specific in adsorption of PFAAs on carbon materials?

The results from the previous part deliver two main messages: (i) there is a big difference between adsorption affinities and capacities of PFAAs on various AC materials and (ii) there are clear indications on the optimal surface chemistry of ACs for achieving high performance in removal of PFAAs.



Graphical abstract

In fact,  $\pi$ -electron basicity of the graphene layers is favorable for adsorption of PFAAs. In this part, the commercial ACF with the lowest affinity for PFAAs (named WK in previous work) was modified to develop very stable oxygen-free basic sites on it. In addition, nitrogen-containing functional groups, e.g. amines, can create basic sites on AC. To develop the above mentioned functional groups on AC, the following approaches were followed:

- Development of Lewis-base  $\pi$ -electron-rich regions on the ACF at 900 °C under nitrogen/hydrogen atmosphere.
- Creation of basic amine groups on the ACF by reaction with ethylenediamine under mild conditions.

The modified ACFs and the original one were applied for adsorption of long-chain PFAAs (PFOA and PFOS), a short-chain PFAA (perfluorobutanoic acid, PFBA), phenanthrene (PHE, as nonionic compound) and octanoic acid (OCA, as PFOA fluorine-free analogon) from water.

**- Amino-functionalisation of ACF without any pretreatment but using its native content of carboxylic groups directly for amidation.** The amino-functionalisation usually involves a two-step procedure, i.e. acyl-chlorination followed by an amidation process under mild conditions. In this work, this method was used for preparing amino-functionalised ACF ( $-\text{CONH}-\text{CH}_2-\text{CH}_2-\text{NH}_2$ ) without any pretreatment of the original ACF but using its native content of carboxylic groups directly for amidation. The targeted functional group was characterised by X-ray Photoelectron

Spectroscopy (XPS) and TPD techniques. Amidation of the ACF increased the anion exchange capacity by a factor of two.

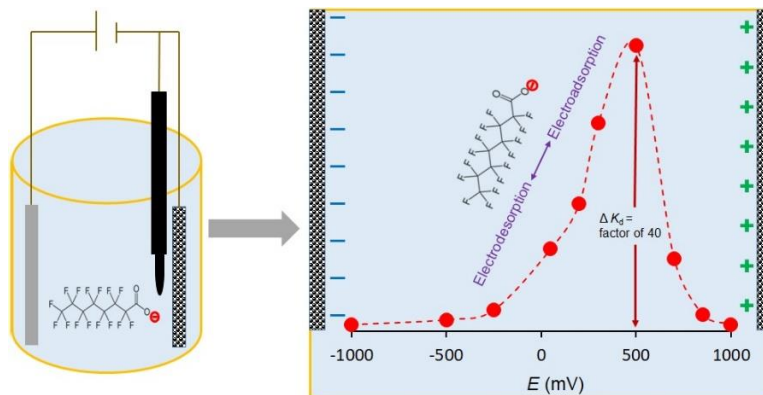
**- Thermally defunctionalised ACF has exceptionally high affinity to short- and long-chain PFAAs, although amidation has minor effect on adsorption affinities of the compounds.** The commercial ACF (CACF), defunctionalised ACF (DeCACF) and amino-functionalised ACF (CACFNH<sub>2</sub>) were applied for adsorption of PFOA, PFOS and PFBA from water. Defunctionalisation enhanced adsorption affinity for the compounds by up to 3 orders of magnitude, while improvement by amino-functionalisation was minor. This high adsorption affinity is especially important for PFBA ( $K_d$  up to  $10^5$  L/kg at equilibrium aqueous phase concentrations  $C_e = 3 \mu\text{g/L}$ ), as it is much higher compared to the affinities published elsewhere.

**- Stable basic sites were developed on DeCACF.** DeCACF was applied in five adsorption-desorption cycles (around 500 h) with intermittent extractive regeneration using methanol. DeCACF kept its high affinity towards PFOA ( $K_d$  up to  $10^7$  L/kg) and PFBA ( $K_d$  up to  $10^5$  L/kg) within the adsorption cycles. Therefore, the procedure used here results in an adsorbent with stable favourable basic sites for a strong uptake of short- and long-chain PFAAs.

**- Low impact of pH, inorganic and organic competitive ions on adsorption performance of the defunctionalised ACF.** The results showed that DeCACF has high performance in adsorption of PFAAs from water with various salt matrices and DNOM at a wide range of pH, e.g. 3 to 9.

**- Sensitivity of adsorption towards AC surface chemistry: PFAAs >> octanoic acid > phenanthrene.** The adsorption results of OCA and PHE were correlated with surface chemistry parameters of three ACFs, e.g. CACF, CACFNH<sub>2</sub> and DeCACF. The three adsorbates reacted with different sensitivities to the changes in AC surface chemistry. PHE was rather insensitive as it shows only a slight increase in Langmuir maximum adsorption capacity ( $q_m$ ) for the defunctionalised carbon and nearly no change in  $K_d$ . PFOA and OCA were much more sensitive. In fact, PFOA reacted most strongly, i.e. with an increase in  $K_d$  by 3 orders of magnitude after the defunctionalisation of the ACF, whereas for OCA this enhancement was only by a factor of 4. The specific importance of AC surface chemistry for adsorption of PFAAs might result from their extremely low  $pK_a$  values ( $< 1$ ) which strongly limits charge neutralization options in adsorption. In this case, positively charged surface groups in a rather non-polar environment are detrimental for providing both, charge-balancing for PFAA anionic head groups and hydrophobic interactions of the tail.

### 2.3. Controlling adsorption of perfluoroalkyl acids on activated carbon felt by means of electrical potentials



Graphical abstract

In fact, in this part it was tried to not only enhance adsorption of PFAAs on the adsorbent by means of external potential ( $E$ ), but also regenerate the saturated adsorbent with PFAAs. This approach can be used as an on-site regeneration technique. Three steps were considered for developing this method:

- Selection of suitable ACFs as working electrode based on characterisation by electrical impedance spectroscopy (EIS) and cyclic voltammetry (CV) and correlations to textural and chemical surface properties of the ACFs.
- Electrosorption experiments in conventional three-electrode cells (Ag/AgCl reference and Pt counter electrode): electrosorption mechanism of PFAAs, electroadsorption and electrodesorption isotherms, effect of competitive inorganic and organic ions as well as solution pH on electrosorption.
- Sustaining the electrosorption cell for a long-term adsorption/desorption cycle.

**- Before using an AC in electrosorption, its potential of zero charge ( $E_{PZC}$ ) should be considered.** The general approach in controlling adsorption of PFAAs on AC is enhancing its adsorption on AC by charging the AC positively by means of external electric potential and then switching potential to negative values for desorption. In this respect there is an important criterion. It is related to the surface chemical properties of the ACF and determines which potential has to be applied in order to obtain a positive ( $E > E_{PZC}$ ) or negative ( $E < E_{PZC}$ ) net charge of the surface. A problem for using carbon-based materials, in particular AC, as electrodes in electroadsorption/-desorption of organic and inorganic compounds is its attrition by direct and/or indirect oxidation and reduction under high potentials. Therefore, an ACF with a low absolute value of  $E_{PZC}$  is able

to be charged positively and negatively under mild potentials (i.e. sufficiently far from critical oxidation/reduction potentials of the carbon).

**- Electrosorption of PFOA and PFBA on ACF versus potential results in bell-shaped curves.**

A plot of adsorption affinities ( $K_d$ ) of PFOA on ACF1 ( $E_{PZC} = +75$  mV) versus potential resulted in a bell shape curve with a peak at +500 mV with respective  $K_d$  value up to  $10^6$  L/kg. This  $K_d$  value is more than forty-times the values at negative potentials. As  $E_{PZC}$  of ACF1 is +75 mV, the net charge on ACF1 at potentials  $> +75$  mV is positive, i.e. electrostatic attractions between PFOA anions and positively charged sites exist at these potentials. In contrast, at potentials  $< +75$  mV, the net charge is negative, resulting in electrostatic repulsion toward PFOA. By applying potentials  $> +500$  mV on ACF1, electroadsorption of PFOA dropped. In contrast to inorganic anions, adsorption of PFOA is influenced to some extent by hydrophobic interactions of the carbon tail of PFOA and the surface of AC (Phong Vo et al., 2020). Thus, an increasingly charged surface can have a negative effect on adsorption of PFOA as the water adsorption becomes more dominant. Similar to PFOA, bell-shaped curves were obtained from electrosorption of PFBA on ACF1 and DeACF3 ( $E_{PZC} = -150$  mV) versus potential. The general finding that sorption of anionic and cationic organic compounds increases or decreases by applying positive or negative potentials, respectively, was reported in previous studies (Wang et al., 2018). However, PFAA anions are specifically sensitive towards the charging state of the carbon surface as large differences in  $K_d$  depending on applied potential were observed (up to two orders of magnitude variation compared to less than one order reported for various organic anions and cations (Wang et al., 2018)).

**- Electroadsorption of PFOA from a large volume of water and its electrodesorption into a low volume of PFOA concentrate: concentration factor ( $F$ ) = 115.** Prospectively, the batch reactors should be replaced by a continuous flow system for practical application. The general goal of this procedure is to reduce the volume of water which is needed for desorption ( $V_{des}$ ) related to the volume of treated water in the adsorption step, i.e. increasing the concentration factor. A step-like breakthrough curve was assumed for the adsorption and desorption steps and a simplified approach based on Freundlich isotherms was used for calculating the volume of desorption water and the resulting concentration factors. They are  $F_{+500/-1000} = 115$  (for electroadsorption at +500 mV and electrodesorption at -1000 mV),  $F_{+500/-100} = 71$  and  $F_{no\ potential/-100} = 41$ . These numbers are much higher than the concentration factor reported in reverse osmosis retaining PFAAs in a concentrate, which is typically below 10.

**- Effect of external potential on electrosorption of PFOA is much stronger than the effect of changing solution pH.** ACF1 with point of zero net proton charge  $pH_{PZC} = 7.1$  and  $E_{PZC} = +75$  mV was used to compare the effects of solution pH and external potential on (electro)sorption of PFOA. The results revealed that manipulating the surface charges of ACF1 by external electric potential has stronger effects on the adsorption behaviour of PFOA than changing pH in a moderate range. Furthermore, it was realized that applying positive and negative potentials significantly influences adsorption behaviour of PFOA even at pH values 3 and 9.

**- Competitive inorganic and organic ions have negligible effect on electrosorption of PFOA and PFBA.** Electroadsorption and electrodesorption of PFOA and PFBA were performed in water with various salt matrices and 5 mg/L DNOM. The results showed negligible effect of inorganic ions (up to 200 mM  $Na_2SO_4$ ) and DNOM on electroadsorption and electrodesorption of compounds. Thus, this technique has a great potential in remediation of various water resources, e.g. groundwater and sea water.

**- A long-term electroadsorption/-desorption process of PFOA (10 cycles in 1000 h).** 5 cycles of alternating electroadsorption (at +500 mV) and electrodesorption (at -1000 mV) of PFOA on ACF1 revealed that single point adsorption coefficients in electroadsorption dropped significantly from 860,000 L/kg in the first cycle to around 160,000 L/kg in the fifth cycle. The decrease was probably caused by attrition of ACF under the harsh anodic potential (in electroadsorption) and the harsh cathodic potential (in electrodesorption). By selecting milder potentials, e.g.  $-100 \text{ mV} < E_{PZC} < +300 \text{ mV}$ , the decline in performance of the ACF1 cell was mitigated over 10 cycles (around 1000 h), although a drop in electroadsorption of PFOA was still observed. It is known that anodic polarization influences ACFs' properties stronger than cathodic polarization. Adsorption was then carried out without potential, while a mild negative potential ( $-100 \text{ mV} < E_{PZC}$  of ACF1) was applied for desorption. The results revealed a quiet stable performance of the ACF1 cell over 10 cycles (1000 h). After an initial loss of about 20% in  $K_d$  (cycle 1-5) the ACF1 electrode kept its performance almost constant (<10% decline in cycle 5-10).

### 3. Conclusion

Technical implications. This study has significantly extended the scientific knowledge regarding remediation of water contaminated with perfluoroalkyl acids (PFAAs) by means of adsorption on activated carbon (AC). At this stage, the characteristics of AC with exceptionally high adsorption



affinity towards PFAAs were addressed, targeted modification approaches for developing such properties on AC were proposed and a deeper mechanistic insight on adsorption of the compounds on AC was discussed. Furthermore, for the first time an electrochemical-based approach for on-site regeneration of AC materials saturated with PFAAs was proposed and developed for a long term (1000 h) adsorption-desorption process. The results on adsorption of perfluorosulfonic acid from real ground water proved the fact that the adsorbents identified in this thesis as most suitable ones for removal of PFAAs have as high affinity as predicted. Therefore, it is highly recommended that before applying AC for removal of PFAAs from water, the chemical surface properties of the AC is evaluated.

Potential applications. Ideal AC adsorbents for removal of short- and long-chain PFAAs should have a low heteroatom content, leading to a low surface polarity and sufficient density of carbon-based positive charges at circumneutral pH. Such AC can postpone breakthrough of the PFAAs in a fixed-bed adsorber significantly. The electrochemical-based regeneration approach proposed in this thesis can be adopted for on-site regeneration of AC materials saturated with PFAAs.

## References

- Gagliano, E., Sgroi, M., Falciglia, P.P., Vagliasindi, F.G.A., Roccaro, P., 2020. Removal of poly- and perfluoroalkyl substances (PFAS) from water by adsorption: Role of PFAS chain length, effect of organic matter and challenges in adsorbent regeneration. *Water Research* 171, 115381.
- Phong Vo, H.N., Ngo, H.H., Guo, W., Hong Nguyen, T.M., Li, J., Liang, H., Deng, L., Chen, Z., Hang Nguyen, T.A., 2020. Poly-and perfluoroalkyl substances in water and wastewater: A comprehensive review from sources to remediation. *Journal of Water Process Engineering* 36, 101393.
- Sznajder-Katarzyńska, K., Surma, M., Cieślak, I., 2019. A review of perfluoroalkyl acids (PFAAs) in terms of sources, applications, human exposure, dietary intake, toxicity, legal regulation, and methods of determination. *Journal of Chemistry* 2019, 2717528.
- Wang, S., Li, X., Zhao, H., Quan, X., Chen, S., Yu, H., 2018. Enhanced adsorption of ionizable antibiotics on activated carbon fiber under electrochemical assistance in continuous-flow modes. *Water Research* 134, 162-169.

## Own publications

- Saeidi, N.,** Kopinke, F.-D., Georgi, A. “Understanding the effect of carbon surface chemistry on adsorption of perfluorinated alkyl substances.” *Chemical Engineering Journal*, Vol (381) 122689 (2020).
- Saeidi, N.,** Kopinke, F.-D., Georgi, A. “What is specific in adsorption of perfluoroalkyl acids on carbon materials.” *Chemosphere*, Vol (273) 128520 (2021).
- Saeidi, N.,** Kopinke, F.-D., Georgi, A. “Controlling adsorption of perfluoroalkyl acids on activated carbon felt by means of electrical potentials.” *Chemical Engineering Journal*, Vol (406) 129070 (2021).

ISSN 1860-0387

Helmholtz Centre for  
Environmental Research – UFZ  
Permoserstraße 15  
04318 Leipzig | Germany  
**[www.ufz.de](http://www.ufz.de)**

NOT FOR SALE.